This work is protected by copyright and other intellectual property rights and duplication or sale of all or part is not permitted, except that material may be duplicated by you for research, private study, criticism/review or educational purposes. Electronic or print copies are for your own personal, non-commercial use and shall not be passed to any other individual. No quotation may be published without proper acknowledgement. For any other use, or to quote extensively from the work, permission must be obtained from the copyright holder/s.

The potential of umbilical cord cells, autologous bone marrow stromal cells and autologous chondrocytes for bone and cartilage repair

Atanu Bhattacharjee

Submitted for Doctor of Philosophy (PhD)

March 2018

Keele University

Acknowledgements

I thank my supervisors Prof JB Richardson and Prof S Roberts for mentoring and guiding me through this PhD. I am grateful for their patience, constant support and encouragement during my research. I am indebted to Dr JH Kuiper for his time and effort which allowed me to develop scientific skills to analyse and interpret data. I thank Dr K Wright for her valuable advice during my *In vitro* research, Dr C Mennan for her support during my work in the laboratory, Dr HS McCarthy, Dr B Tins and Dr VC Pullicino for their advice and contributions during my research.

I would like to take this opportunity to acknowledge the funding support from the Institute of Orthopaedics, Oswestry and Arthritis Research, UK. I remain thankful to the authority of The Robert Jones and Agnes Hunt Orthopaedic Hospital Foundation Trust, Oswestry for providing me with the opportunity to undertake the research.

Lastly, I thank my wife Debanjali and our sons Aaruni and Jishnu for their encouragement and constant support during the entire course of this research.

Dedication

This thesis is dedicated to the memory of my mother, Late Mrs Santi Bhattacharjee and my father, Late Dr S M Bhattacharjee.

List of Abbreviations

ACI-Autologous Chondrocyte Implantation

ALP-Alkaline Phosphatase

ANOVA-Analysis of Variance

BMSC-Bone Marrow-derived Mesenchymal Stromal Cells

BMMSC- Bone Marrow-derived Mesenchymal Stem Cells

BMP-Bone Morphogenic Protein

BCMT-Bilayer Collagen Membrane Technique

BSA-Bovine Serum Albumin

BMI-Body Mass Index

CCE-Counterflow centrifugal elutriation

CL-Cord Lining

CD-Cluster of Differentiation

CSF-Colony Stimulating Factor

CFU-F-Colony Forming Unit-Fibroblast

COMP-Cartilage Oligomeric Matrix Protein

CONSORT-Consolidated Standards of Reporting Trial

CT-Scan-Computed Tomography Scan

CI-Confidence Interval

DMEM-Dulbecco's Modified Eagle's Medium

DT-Doubling Time

DMMB-Dimethyl Methylene Blue Assay

DAPI-4,6 Diamino-2-Phenylidone 2Hydrochloride

DFVO-Distal Femoral Varus Osteotomy

DMSO-Dimethylsulphoxide

DESS-Double Echo Steady State

EDTA-Ethylene Diamine Tetra Acetic Acid

FITC-Fluorescein isothiocyanate

FU-Follow-up

FMOD-Fibromodulin

FGF- Fibroblast Growth Factor

FBS-Foetal Bovine Serum

FCS-Foetal Calf Serum

FSC-Forward scatter

FACS-Fluorescence Activated Cell Sorting

FLASH-Fast Low Angle Shot

GVHD-Graft Versus Host Disease

GAG-Glycosaminoglycans

GLAD-Generative Model of Labels and Difficulties

GMP-Good Manufacturing Practice

HUCMSC-Human Umbilical Cord Matrix-Stromal Cells

HUCPV-Human Umbilical Cord Perivascular cells

hUVEC-Human Umbilical Vascular Endothelial Cells

HLA-Human Leucocyte Antigen

HIF-Hypoxia Inducible Factor

H&E-Haematoxylin & Eosin

HSCT-Haematopoeitic Stem Cell Transplantation

HTO-High Tibial Osteotomy

HT/HA-Hydroxyapatite

Ig-Immunoglobulin

ISCT-International Society of Cellular Therapy

ICRS-International Cartilage Repair Society

IDO-Indoleamine dioxide

i NOS-inducible Nitric Oxide Synthase

ITS-Insulin Transferrin Selenium

IL-Interleukin

IGF-Insulin Like Growth Factor

IQR-Inter Quartile Range

IKDC-International Knee Documentation Society

KOOS-Knee injury and Osteoarthritis Outcome Score

MRI-Magnetic Resonance Imaging

MOCART-Magnetic Resonance Observation of Cartilage Repair Tissue

MSC-Mesenchymal Stem Cells

MHC-Major Histocompatibility Complex

MLR-Mixed Lymphocyte Reaction

MFC-Medial Femoral Condyle

MF-Microfracture

MACI-Matrix induced Autologous Chondrocyte Implantation

NEAA-Non Essential Amino Acids

OA-Osteoarthritis

OD-Osteochondritis Dissecans

OR-Odds Ratio

OCD-Osteochondral Defect

OAT-Osteochondral Autologous Transplantation

OAS-Oswestry Arthroscopy Score

P-Passage

PBS-Phosphate Buffered Saline

P&S-Penicillin & Streptomycin

PA-Peri-arterial tissue

PV- Peri-venous tissue

PCR- Polymerase Chain Reaction

PE-Phycoerythrin

qRT-PCR- quantitative Reverse Transcription Polymerase Chain Reaction

REACT-Retrospective Assessment of Autologous Chondrocyte Transplantation

RCT-Randomised control trial

RANKL-Receptor Activator of Factor Kappa B Ligand

SOX-9- Sex Determining Region Box-9

SD-Standard Deviation

SC-Stromal Cells

SCB-Subchondral bone

SPRINT-Study to Prospectively Evaluate Reamed Intramedullary Nails in Patients with Tibial Fracture

SE-Standard Error

TRA-Tumour Repressor Antigen

TNF-Tumour Necrosis Factor

TGF-Transforming Growth Factor

TCP-Tri Calcium Phosphate

TTO-Tibial Tubercle Osteotomy

TKR-Total Knee Replacement

UC-Umbilical Cord

UCA- Umbilical Cord Artery

UCV- Umbilical Cord Vein

USFDA-United States Federal Drug Agency

VEGF-Vascular Endothelial Growth Factor

VAS-Visual Analogue Score

WJ- Wharton's Jelly

WOMAC- Western Ontario & McMaster Universities Osteoarthritis Index

Wnt-Wingless-related integration site

List of Figures

List of Tables

Appendices

List of publications

Bhattacharjee A., McCarthry H.S., Tins B., Roberts S., Kuiper J.H., Harrison P.E., Richardson J.B. 2016. Autologous Bone Plug supplemented with Autologous Chondrocyte Implantation in osteochondral defects of the knee. *American Journal of Sports Medicine* (Epub ahead of print).

Mennan C., Wright K., Bhattacharjee A., Balain B., Richardson J.B., Roberts S. 2013. Isolation and characterisation of mesenchymal stem cells from different regions of the human umbilical cord. *Biomed Research International (open access electronic publication).*

Abstract

Aims

To evaluate the *in vitro* potential of umbilical cord(UC)-derived cells as an allogeneic cell source that could be used 'off-the-shelf' in orthopaedics for bone and cartilage regeneration. The study also assesses the *in-vivo* efficacy of cell therapy in orthopaedics for the formation of *de novo* bone, cartilage and integration of both.

Methods

- *In vitro* potential of cells isolated from the four structural layers of the umbilical cord were characterised according to the criteria of the International Society for Cellular Therapy (ISCT). The differentiation potentials of these cell preparations, particularly for bone and cartilage formation, were also evaluated to ascertain their efficacy as potential cell sources for orthopaedic regenerative medicine.
- Efficacy of autologous bone marrow-derived mesenchymal stromal cells (BMSC) for new bone formation *in vivo* for patients with lower limb long bone nonunions were assessed with a self-controlled randomised trial.
- Efficacy and structural outcome of simultaneous autologous bone plug graft to restore subchondral bone with Autologous Chondrocyte Implantation (ACI) were evaluated to identify the quality and integration of the repair cartilage with the subchondral bone, described as the 'Osplug' technique.
- Efficacy of concurrent realignment with ACI in patients with underlying chondral defects and idiopathic varus or valgus malalignments of the knee joint were studied to ascertain the outcome of simultaneous correction of the mechanical axis in patients receiving biological repair of the cartilage.

Results

- Potential of UC-derived cells in bone and cartilage formation: Cell preparations from four structural regions of umbilical cord were isolated via an *in vitro* explant culture technique. Osteogenic differentiation in these cell preparations correlated with a significant rise in alkaline phosphatase activity in the culture medium of the differentiated cells, in comparison to their respective controls. Following chondrogenic differentiation, a considerable variation in metachromasia was noted with toluidine blue staining, although type II collagen immunostaining was

predominantly absent except in one sample of cells from Wharton's Jelly. Cells from all the four layers of UC also expressed surface markers according to the ISCT criteria for Mesenchymal Stem Cells (MSC). However, it did not conform to the recommended standards quantitatively on fluorometric analysis.

- New bone formation in nonunion: There was absence of significant increase in new bone formation on the side of BMSC insertion in cases with nonunion of fracture. Four predictors of successful fracture union in this study were shorter *in-vitro* cell doubling times of patient's BMSC, the absence of diabetes, younger age and fewer operative procedures to treat the nonunion before the trial intervention.
- Bone and cartilage healing in osteochondral defects: Significant improvement in clinical and functional outcome was found at mid-term follow-up after concurrent bone graft and ACI to restore subchondral bone and cartilage. Integration of the grafted bone had a direct correlation with the clinical outcome in these patients.
- Cartilage repair with realignment: Simultaneous ACI with correction of malalignment led to significant improvement in clinical outcome, particularly in patients with varus deformity. Patients with valgus deformity were noted to fail relatively early with poor outcome.

Conclusion

The current thesis extends from exploring the *in vitro* potential of UC to the clinical application of autologous chondrocytes and BMSC for cartilage and bone regeneration. UC-derived cells were noted to have properties akin to MSC with trilineage differentiation capacity. However, regeneration of new bone with BMSC in nonunions remains challenging. Nonetheless,significant clinical improvement was noted in patients receiving ACI with underlying malalignment and subchondral bone defect when treated with concurrent realignment and bone graft respectively. Further work on the immunomodulatory effect of UC-derived cells in addition to longer-term follow-up of the patients receiving cell-based therapy is required to consolidate our understanding of future cell therapy in orthopaedics.

Chapter 1: Introduction

1.1 Background

Arthritis and trauma have been identified as emerging challenges for the current and future generations of musculoskeletal health care providers (Speerin et al., 2014). Both these conditions are predicted to create significant social and financial liabilities over the coming years (Busija et al., 2013, Tecic et al., 2013). Conventional orthopaedic surgical procedures currently dominate the choice of treatment for both these conditions.

A total of 620,400 primary hip replacements and 676,082 primary knee replacements were carried out predominantly for osteoarthritis (OA) in England and Wales during 2003-2013, with approximately 15,000 in each group being revised at least once within this period (NJR, 2014). The median age of patients for a cemented total knee replacement is 70 years. The median age of patients receiving a partial knee replacement, however, is 7-11 years younger than those receiving total knee replacements, and there has been an increasing requirement for revision surgeries among this group (NJR, 2014). The survivorship of primary hip and knee replacements additionally showed a steady decline among young patients, representing the high physical demands of such patients (NJR, 2014). Moreover, the financial implications of revision knee replacements can vary from £9,655 to £30,111 within the National Health Service in the UK (Kallala et al., 2015).

The incidence of nonunions following a new fracture has been reported to range from 0.02%-10% (Court-Brown et al., 2010, Mills and Simpson, 2013). Such nonunions of lower limb fractures have been observed in 6.7 per 100,000 people with an estimated cost of £7500 to £85,000 per person to the NHS, excluding morbidity and loss of earnings (Mills and Simpson, 2013).

While early arthritis from cartilage defects and fractures continue to evolve as a significant economic and social burden, complementary treatment options need to be developed to curtail the complications and address the above conditions from a biological perspective. Treating fractures and focal cartilage defects with pertinent cells to regenerate bone and repair cartilage, respectively, can evolve as a useful alternative. Such a cell-based therapy for treatment of cartilage defects can potentially prolong the survival of the natural joint reducing the risk of primary joint replacement surgeries and also of revision surgeries. Similarly, regenerating bone with appropriate cells can potentially promote bone healing in fracture nonunions by forming new bones.

In the present work, the prospect of cells derived from the human umbilical cord for the generation of cartilage and bone has been assessed *in vitro* to identify the allogeneic potential of these cells for 'off-the-shelf' use in bone and cartilage repair. The work also evaluates the outcome of clinical applications of autologous cell therapy in the regeneration of bone in fracture nonunions and repair of cartilage for focal cartilage defects.

1.2 Scope of umbilical cord-derived cells in bone and cartilage regeneration in orthopaedics

1.2.1 Overview

In 1966 Freidenstein et al. demonstrated progenitor cells with fibroblastoid morphology from bone marrow with the capacity of osteogenic differentiation (Freidenstein et al., 1966). In 1991, Caplan defined them as mesenchymal stem cells (MSCs) because of their mesodermal location and multi-lineage differentiation potential triggered by environmental cues and their genetic potential (Caplan, 1991). In the same year, fibroblast-like cells from Wharton's Jelly (WJ) of the umbilical cord (UC) were also isolated (McElreavey et al., 1991). In 1999 Pittenger et al. performed monolayer culture of undifferentiated bone marrow derived cells and induced *in vitro* tri-lineage mesodermal differentiation (bone, fat & cartilage) of these particular cells (Pittenger et al., 1999). These cells had a uniform absence of haematopoietic surface antigen but the presence of SH2, SH3, CD24, CD70, CD90, CD106, CD120, CD120a and CD124 surface antigens (Pittenger et al., 1999). Subsequently, three position statements have been published by the International Society for Cellular Therapy (ISCT), proposing criteria for defining MSCs irrespective of their isolation and culture expansion strategy (Pittenger et al., 1999, Dominici et al., 2006, Krampera et al., 2013, Horwitz et al., 2005).

1.2.2 Definition of Mesenchymal Stem Cell

The initial definition of MSC was laid by Pittenger et al. based on cells isolated from bone marrow and cultured in monolayer with trilineage differentiation capacity at a controlled *in vitro* condition. Additionally, these cells from bone marrow had a stable phenotype with retention of their characteristics inclusive of their differentiation potential following *in vitro*

expansion (Pittenger et al., 1999). Horwitz et al.(2005) proposed a formal approach to classifying MSC by advocating the use of the term 'Mesenchymal Stem Cell (MSC)' for long-term self-renewing cells with *in vivo* differentiation capacity to multiple cell types. The unfractionated fibroblastoid and plastic adherent cells originating from supporting mesodermal stromal tissue regardless of the source (e.g., bone marrow, umbilical cord blood) may contain a subset of the MSC. However, often this cell population are heterogeneous and should be identified as multipotent 'Mesenchymal Stromal Cells ' until their particular biologic potential is demonstrated (Horwitz et al., 2005). A further structured and objective approach was laid by Dominici et al. (2006) clearly defining MSC with three criteria-

- Plastic adherence at the culture
- Specific surface phenotype
    - ≥ 95% positive expression of CD105, CD73 and CD90
    - ≤ 2% negative expression of CD45, CD34, CD14(or CD11b), CD79α(CD19) and HLA-DR
- *In vitro* differentiation to osteoblasts, adipocytes and chondroblasts (demonstrated *in vitro* cell culture) (Dominici et al., 2006).

However, the definition by Dominici et al. had very little focus on immunological properties of these cells. A recent working proposal by ISCT has highlighted the importance of specific areas including immunological properties of these cells while defining the characteristics of MSCs (Krampera et al., 2013). The following areas highlighted by Krampera et al. (2013) will allow methodological standardisation and improve comparability of results amongst different published reports:

- MSC are specific to tissues from which they are isolated and their distinct embryological origin, which also predicts the pool of endogenous progenitors.
- Functional assay of both resting and primed MSC to demonstrate the immune regulatory properties is clinically more pertinent, regardless of the species or tissue source.
- Variables of cell culture influencing the immune properties of the cells, e.g., cell density at passage, culture medium, growth factors, population doublings (along with number of passages) should be accounted before generalisability of the features present in these cells
- Properties of MSC drawn from animal models should be cautiously interpreted because of the distinct mechanistic pathways between species for, e.g.,- the activation of indoleamine dioxide (IDO) pathway in humans in contrast to inducible Nitric Oxide Synthase (iNOS) pathway in murine for immunosuppression (Krampera et al., 2013).

In the current work, bone marrow mesenchymal stromal cells (BMSC) has been used to identify cells which were not formally characterised in vitro but derived from the bone marrow. Whereas bone marrow derived mesenchymal stem cells (BMMSC) or mesenchymal stem cells(MSC) are limited to cells which fulfil the criteria laid by the ISCT (Dominici et al., 2006).

1.2.3 Rationale for using umbilical cord as cell source

Several studies have now confirmed that cells derived from UC share the surface properties of MSC and their *in vitro* capacity of trilineage differentiation (Mennan et al., 2013, Secco et al., 2008). Isolation of MSCs derived from whole UCs or specific anatomical locations has

been described by enzymatic digestion, explant or a combination of mechanical disassociation followed by enzymatic digestion (Sarugaser et al., 2005, Seshareddy et al., 2008, Pereira et al., 2008, Kadam et al., 2009, La Rocca et al., 2009, Gonzalez et al., 2010, Arufe et al., 2011, Bode et al., 2013, Yoon et al., 2013). Despite BMMSCs being the gold-standard, using UC as a source of MSCs has the advantage of being a medical waste with minimal ethical concern. Moreover, these cells can be obtained without subjecting patients to an additional procedure and have a shorter culture time with a faster proliferation rate in comparison to BMMSC (Mennan et al., 2013).

Additionally, these cells were found to be immune-privileged with a potential for allogeneic use in regenerative medicine (Deuse et al., 2011, Sarugaser et al., 2005). The potential for allogeneic transplantation of UC-derived MSCs is supported by their role in ameliorating immune responses both *in vitro* and *in vivo* animal models (Weiss et al., 2008, LeMaoult et al., 2005, Kim et al., 2015). Human UC matrix-stromal cells (hUCMSC) from WJ inhibit the proliferation of stimulated T-cells in two-way Mixed Lymphocyte Reactions (MLR); similarly, these cells do not elicit an appreciable T-cell proliferative response in a one-way MLR (Weiss et al., 2008). Also, these cells do not produce co-stimulatory molecules CD40, CD80 and CD86 (Weiss et al., 2008). The human leukocyte antigen (HLA)-DR expression in WJ cells treated with TNF-α and IFN- γ is absent with a marked reduction in expression of the same antigen in cord lining (CL) cells following priming with high dose IFN- γ (Kita et al., 2010, Prasanna et al., 2010) .

To summarise, UC-derived cells have multipotent differentiation capacities with immunomodulatory properties rendering them to be a suitable cell source for regenerative medicine.

1.2.4 Functional anatomy of UC

Human UC is a foetal-maternal communication developed in the fifth week of gestation and exists until parturition (Cunningham and Williams, 2010). The full length of UC is usually equal to the length of the foetus (approximately 50 cm), but variation in size commonly exists (Standring, 2005).The UC connects the foetus to the developing placenta implanted into the myometrium of the uterine wall. The UC is usually inserted near the centre of the placenta; in 7% of cases it is inserted near the margin of the placenta ('marginal insertion'), while in 1% it is inserted outside the placenta and within the membranes ('velamentous insertion') (Cunningham and Williams, 2010). It carries and protects one umbilical cord vein (UCV) and two umbilical cord arteries (UCA). These play a critical role in foeto-maternal gaseous and metabolite exchanges. The single UCV is a broad calibre vessel, and the two UCAs are intertwined along the axis of the UCV. The supporting stromal tissue surrounding these vessels is a loose proteoglycan-rich matrix constituting WJ (Cunningham and Williams, 2010). The WJ and the three vessels are encased in the CL (Cord lining) membrane which is continuous with the amnion of the placenta (Figure 1.1). The CL membrane has important fluid exchange functions. The UC is twisted due to foetal movements. However, the WJ matrix protects the cord vessels and prevents them from being strangulated.

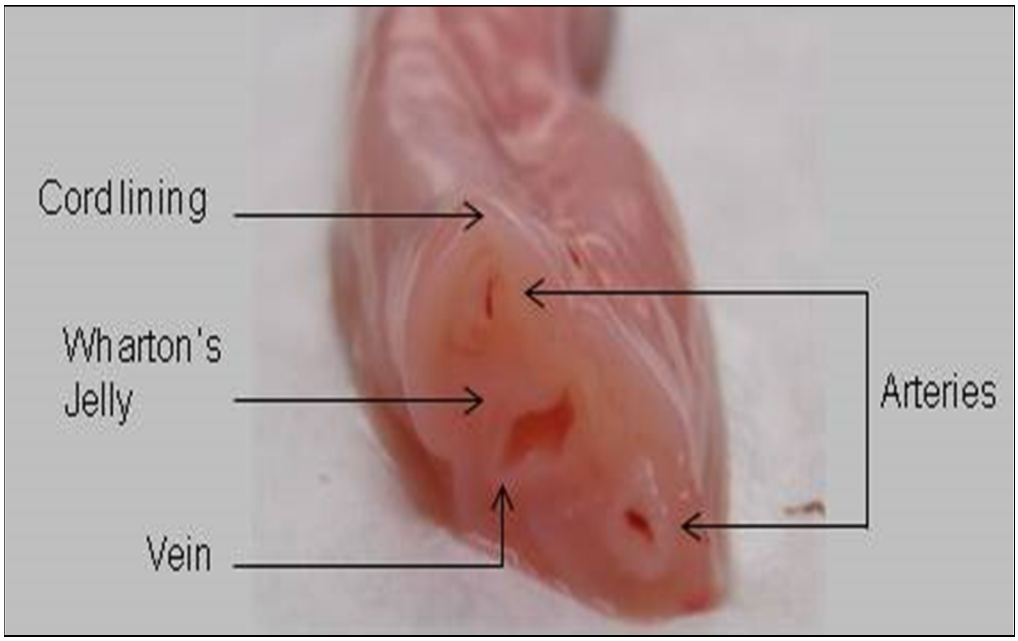

Figure 1.1 Cross-section of umbilical cord showing the four anatomical regions with two umbilical cord arteries and one umbilical cord vein surrounded in the supporting matrix, Wharton's Jelly, all encased by the cord lining membrane

In the following section, an overview of the literature is undertaken to ascertain the potential of cells from UC and specific anatomical locations of UC in orthopaedic regenerative medicine, in particular on bone and cartilage formation.

1.2.5 Literature search results

The results of the search are chronologically presented below in Table 1.1. Abstracts of the available literature were reviewed to include relevant articles. Original articles describing isolation strategy of cells from human UC and different anatomical locations of the UC, culture methods and results that have potential implications for bone and cartilage regeneration were typically included. The review also highlights the variety of acronyms that have been used for cells derived from the UC (and different anatomical areas of the cord) which is further complicated by differences in isolation strategy, culture medium, differentiation potential and surface phenotype.

Authors	Isolation strategy	Culture medium	Differentiation	Surface phenotype
Subramaniam et al., 2015	Cells from five compartments of the cord-Aminion, Sub-Amnion, Peri-venous(PV) isolated enzymatically , WJ(aspirated and centrifuged), mixed cord(details not reported)	DMEM-low glucose+L-glutamine+ Antibiotics&Antimycotics	Osteogenesis +ve, Adipogenesis +ve, Chondrogenesis +ve	Flow cytometry +ve to CD90, CD105, HLA-ABC(>97%) and –ve to CD14, CD19, CD34, CD45, CD117, HLA-DR(3.7-22.4%)
Chang et al., 2014	Explant with microdissection of the vessel and cord lining to isolate WJ and subsequently centrifuged (cells termed as human umbilical cord WJ-MSC-hUCMSC)	DMEMF12 +10%FBS+P&S	Osteogenesis +ve from P1-P3 with no difference between cell passage, Adipogenesis +ve, Chondrogenesis +ve. In vivo osteogenesis in a mouse model(BALB/Cnu/nu) after 56 days.	Flow cytometry from (P1 to P3) CD73, CD90, CD105 and -ve CD45,
Mennan et al., 2013	Whole cord treated with 1mg/ml of Collagenase I for 1 h at 37 deg C (cells termed 'mixed cord cells')/Explant of dissected artery, vein, WJ, cord lining	DMEM F12+10% FCS+P&S(1%)	Osteogenesis +ve, Adipogenesis +ve, Chondrogenesis +ve	Flow cytometry of all cell preparations at P2-3 were +ve (>95%) CD73, CD90, CD105 and -ve (<2%) CD14, CD19, CD31, CD34, CD45, HLA-DR
Han et al., 2013	WJ isolated after removing the vessels and aventitia from the cord and then minced 1mm pieces. Explant/0.1% Collagenase IV for 16-18 hrs at 37 deg C/0.2% Collagenase II for 16-20 hrs at 37 deg C	DMEM + 10%(v/v) FBS+Penicillin(1000U)+Streptomycin(100µg)	Chondrogenic-not reported, Adipogenic +ve, osteogenic-Von Kossa +ve	Immuno- fluorescence with +ve CD44 and CD90 but -ve CD31 and CD45

Authors	Isolation strategy	Culture medium	Differentiation	Surface phenotype
Yoon et al., 2013	WJ isolated after vessels are removed from the cord and minced into 2-3mm pieces. Explant/0.1% Collagenase II for 30 mins at 37 deg C for isolation	Low glucose DMEM+10%(v/v)FBS+P&S	Not reported	Flow cytometry(P2) +ve to CD105, CD13, CD 73, HLA Class I and -ve for CD34, CD45, CD31 and HLA Class II
Salehinejad et al., 2012	WJ isolated by careful dissection from the vessels and the cord lining and cells isolated by the following technique- Explant/Collagenase+Trypsin/Trypsin+EDTA/Collagenase+Hyaluronidase+Trypsin (Collagenase Type-B was used) Incubation time was 2-3h at 37 deg C (termed human umbilical cord derived mesenchymal(HUCM) cells)	DMEMF12+10%(v/v)FBS+P&S&Amphotericin	Osteogeneic differentiation +ve, Adipogenic differentiation +ve, Chondrogenic differentiation not reported	Flow cytometry -ve CD34, CD45 and +ve CD44, CD105 but CD73 & CD90 expression was higher in explant group i.e 72.23± 3.6 and 74.47± 0.67
Marmotti et al., 2012	Explant from minced whole cord for isolation of cells (termed UC-Mesenchymal Stem Cells)	DMEMF12+5%human platelet lysate+105FBS+NEAA+Sodium pyruvate+ Heparin(500IU)+P&S	Osteogenesis +ve, Adipogenesis+ve , Chondrogenesis +ve	Flow cytometry(P1)+ve for C73, C90, CD105, CD44, CD29 and -ve to CD34. Noted 40% cell s were absent to HLA-ABC and HLA-DR

Authors	Isolation strategy	Culture medium	Differentiation	Surface phenotype
Fong et al., 2012	Each cord was divided into 2cm pieces and the blood gently teased out, the cord is subsequently opened longitudinally to face the inner surface on a 60mm Petri dish containing 2mg/ml of Collagenase I and II (each) in addition to 100IU/ml of Hyaluronidase contained in high glucose DMEM for 45mins at 37ºC. The cord pieces are then transferred o fresh DMEM, and WJ separated from the vessels and the cord lining and centrifuged 300g for five mins (Fong et al., 2007) and the pellets suspended in the respective media.	**Simple medium**-DMEM-high glucose+20% FBS+1% NEAA+2mM L-glutamine+0.1mMβ-mercaptoethanol+antibiotics; **Complex medium** is simple medium+1%ITS +16ng/ml FGF2; **Supercomplex medium** is DMEM low glucose+MCDB 201 medium+2% FBS+1%ITS+0.5g/ml albumax+ dexamethasone(10nmol/l)+Ascorbic acid 2-phosphate(100umol/L)+10M β Glycerophosphate +EGF(10ng/ml) +PDGF(10ng/ml)	Chondrogenesis-cells cultured in complex medium and subsequently grown in the chondrogenic medium has the best *in vitro* chondrogenesis amongst the three culture conditions. Adipogenesis and osteogenesis not reported.	Flow cytometry-+ve C29, CD44, CD13, CD105, CD146, CD10 and -ve CD117, CD14. Consistent for all three media but CD105 ranged from 81.07% to 98.40% in three culture condition.
Tsagias et al., 2011	Whole cord treated with 2.7mg/ml of collagenase type-I+0.7mg/ml of hyaluronidase for 3 hrs at 37 deg C followed by 2.5% Trypsin for 30 mins	α - modification of Eagles medium+10%FCS+100µ m of L-ascorbic acid-2-phosphate+P&S	Osteogenic +ve, Chondrogenic not reported, Adipogenic +ve	Flow cytometry +ve for CD29, CD90, CD105, CD44 and -ve for CD34, CD45

Authors	Isolation strategy	Culture medium	Differentiation	Surface phenotype
Tong et al., 2007	Blood vessels are dissected from the whole cord and then used for explant or enzyme(0.4% Collagenase II and 0.01% DNAse I for 30 mins at 37 deg C) or enzymatic mechanical dissociation(same enzymatic treatment followed by homogenisation of the tissue after the enzyme activity is inhibited)	DMEM F12+Glutamax I+10%FBS+40ng/ml of bFGF+ P&S&A+ Gentamicin	Osteogenic +ve, Adipogenic +ve, Chondrogenic not reported	Flow cytometry +ve to CD105, CD73, CD90, C29 and -ve to CD34, CD45, HLA-DR
Majore et al, 2010	Explant from whole cord with α- MEM +15% allogeneic serum + 50µg/ml gentamicin(termed Mesenchymal Stromal Cells from UC)	α- MEM +10% allologous serum + 50µg/ml gentamicin	Chondrogenesis +ve, Adipogenesis +ve, Osteogenesis-weak noted at appox 6 weeks	Flow cytometry +ve CD44(99.9%), CD73(98.9%), CD90(99.9), CD105(98.8), and -ve CD31(0.9%), C34(1.4%), HLA-I(2.5%)
Hartman n et al, 2010	Whole cord with artery removed treated with collagenase(300U/l)+hyaluronidase(1mg/ml) for 1 h than with 0.1%trypsin EDTA for 30 mins(cells termed umbilical cord derived mesenchymal stem cells-UCMSC)	MesenCult ACF/StemProMSC SFM/FBS containing Grwith Medium(#1)	Osteogenesis +ve,Adipogenesis +ve	Flow cytometry +ve to CD73, CD90, CD105(nearly 100% all) and -ve to CD34, CD45, HLA-DR(for all types of media)
Reza e al, 2010	Explant of dissected cord lining membrane in Medium 171(Cascade Biologics, OR) to isolate MUCIN expressing Cord Lining Epithelial Cells-CLEC-MUC)	PTTe-1 medium+2.5% FBS+50µ g of IGF-1+50µ g Platelet Derived Growth Factor BB+5µ g/ml of transforming growth factor-β 1+ 5µ g/ml of Insulin	Not reported	Flow cytometry moderate positivity to CD105, weak expression of CD73 with relatively low CD34 and C45 expression, MHC Class I was positive and MHC Class II was consistently negative.

Authors	Isolation strategy	Culture medium	Differentiation	Surface phenotype
Majore et al., 2009	Explant from whole cord with α- MEM +15% allologous serum+5g/l glucose + 50µg/ml gentamicin + Amphotericin +P&S	α- MEM +10% allologous serum + 50µg/ml gentamicin	Not reported	Flow cytometry-Smaller cells were more +ve to CD73, and CD90 in comparison to relatively larger cells but all cell types were +ve to CD73, CD90, CD105 and -ve to CD34, CD45
Ishige et al., 2009	Explant technique after dissection of Umbilical cord artery (UCA), Umbilical cord vein (UCV) & Umbilical cord Wharton's Jelly (UCWJ) (termed as UCA cells, UCV cells and UCWJ cells)	α- MEM +10% FBS serum + P&S & Amphotericin	UCWJ cells ha weakest osteogenicity in comparison to UCA and UCV. Chondrogenesis +ve but -ve to Type-2collagen, Adipogenesis +ve	Flow cytometry +ve for CD13, CD29, CD73, CD90, CD105, HLA-ABC and -ve to CD31, CD34, CD45, CD133, CD271, HLA-DR
Gonzalez et al., 2009	Explants of cord lining with gelatinous part up with sterile coverslips on the top after the vessels and WJ is dissected at 37 deg C(termed umbilical cord lining stem cells-ULSCs)	DMEM Glutamax+15%FBS+NEAA+Vitamins+P&S	Chondrogenesis +ve, Adipogenesis +ve, Osteogenesis +ve	Flow cytometry +ve to CD44, C73, C105, CD90, CD106, CD166, HLA-ABC and -ve to C19, CD34, CD45, C117, CD133, HLA-DR

Authors	Isolation strategy	Culture medium	Differentiation	Surface phenotype
La-Rocca et al., 2009	Explant of whole UC being longitudinally opened but vessels not removed to isolate cells (termed human extraembryonic mesoderm stem cells-HEMSC)	DMEM low glucose+10%FCS+NEAA+2mML-glutamine +antibiotics	Osteogenesis +ve, Adipogenesis +ve, Chondrogenesis -not reported	Immunocytochemistry -ve to CD31, C33, CD34, CD38, CD45 CD79 and +ve to CD10, CD13. RT-PCR +ve for C73, CD90, CD105, HLA-A, HLA-G and -ve for HLA-DR
Qiao et al., 2008	Explant culture of the whole cord after cord blood is removed.	DMEM-LG+10% FBS+5% Horse serum+P&S	Osteogenesis +ve, Adipogenesis +ve but chondrogenesis not reported	Flow cytometry -ve to CD34, CD38, CD71, HLA-DR and +ve to CD13, CD29, CD44, CD105 and HLA class I
Jo et al., 2008	Enzymatic isolation from the whole cord with 0.1% collagenase for 2h followed by 0.25% trypsin for 1h in DMEM-LG with P&S	DMEM-LG+10% FBS+10ng/ml basic fibroblast growth factor +P&S	Osteogenesis+ve, Adipogenesis +ve, Chondrogenesis +ve (RT-PCR +ve for Type-2 Collagen)	Flow cytometry (upto P9) showed >75% positivity to CD73, CD90 CD105, CD117, CD166 and -ve to CD34, CD45, HLA-DR

Authors	Isolation strategy	Culture medium	Differentiation	Surface phenotype
Kadam et al., 2008	Enzymatic isolation of human umbilical cord vascular endothelial cells (termed hUVEC)(exposure time 30 mins at 37 degC) and human umbilical cord matrix-stromal stem cells(hUCMSC) with dispase type II and collagenase type IV(exposure time one hr followed by EDTA and trypsin for 30 min at 37 deg C).	M199+20%umbilical cord blood serum(UCBS)+2mM L-glutamine+5ng/ml Vascular endothelial growth factor +10µg/ml heparin+P&S for hUVEC; DMEM with Ham's F12(1:1 v/v)+ 10% UCBS for hUCMSC	Chondrogenesis +, Osteogenic +ve, Adipogenesis +ve	Flow cytometry +ve for CD44(66.7%),CD90(96.6%), CD73(33%), CD117(48.98%) and -ve for CD33, CD34, CD45 and CD105
Secco et al., 2008	UC filled with 0.1% Collagenase for 20mins at 37deg C	DMEM LG+10%FBS+P&S	OSteogenesis +ve, Chondrogenesis +ve, Adipogenesis +ve and not different from cord blood	Flow cytometry –ve to CD31, CD3, CD45, HLA-DR and +ve to CD90, CD29, HLA-ABC

Authors	Isolation strategy	Culture medium	Differentiation	Surface phenotype
Karahuseyinoglu et al., 2007	Minced UC with artery and vein removed is treated with Collagenase B (1µg/ml) in DMEM-Ham's F12 +10%(v/v)FBS +P&S &Amphotericin at 37 deg C for 4 hrs in gentle orbital shaker(termed Human Umbilical Cord Stromal cells)	DMEM-Ham's F12(1:1v/v) +10%(v/v)FBS +P&S &Amphotericin	Chondrogenic differentiation +ve with +ve Type-2 Collagen, Osteogenic differentiation +ve, adipogenic differentiatio +ve at 40 days	Flow cytometry(P2) +ve to CD105, CD44, CD73 and -ve for CD34, CD45, CD14 and HLA-DR
Baksh et al., 2007	Dissected vessels the three vessels (two arteries and one vein) with surrounding WJ looped and treated with 1mg/ml of Collagenase for 18-24h-CD45 +ve cells removed with magnetic bead(termed human umbilical cord peri-vascular cells-HUCPV) (According to Sarugaser et al., 2005)	DMEM F12+10%FBS	More osteogenic and adipogenic capacity than BMMSC; comparable chondrogenic properties including GAG content at ay 14 and 21	Flow cytometry(P3) –ve CD31, CD34, CD45 and +ve to C90, CD49e, CD146(endothelial marker)
Sarugaser et al., 2005	Dissected vessels(x3) with surrounding WJ looped and treated with 1mg/ml of Collagenase for 18-24h-CD45 +ve cells removed with magnetic bead(termed human umbilical cord peri-vascular cells-HUCPV)	75% α- MEM+15% FBS+ antibiotics	Osteogenesis +ve, Adipogenesis and chondrogenesis not reported	Flow cytometry +ve (>95%) CD44, CD73, CD90, CD105 and MHC Class I and -ve to HLA-DR, CD34, CD45

Authors	Isolation strategy	Culture medium	Differentiation	Surface phenotype
Wang et al., 2004	Dissected WJ from the vessels and the cord linings treated with collagenase(2mg/ml) for 16 hrs and then 2.5% of Trypsin for 30 mins at 37 deg C(termed as Wharton's Jelly MSC-**WJ MSC**)	DMEM+10%FBS+glucose(4.5g/l)	Chondrogenesis +ve(+ve type-2 collagen), osteogenic differentiation +ve, adipogenic differentiation +ve	Flow cytometry +ve to CD105, CD44, C29, CD51 and -ve toCD34, CD45
Panepucci et al., 2004	Cord vein cannulated and filled with 1% Collagenase-this was clamped for 20mins at 37deg C	α- MEM+20% FCS+antibiotics+20mML-glutamine+P&S	Osteogenesis+ve, Adipogenesis +ve, Chondrogenesis +ve (Type-2 Collagen +ve)	Flow cytometry +ve to CD13 (93.9%), CD29(97.9%), CD44 (85.6%), CD54(72.5%), CD90(98.2%), HLA-Class I(94.6%) and –ve to CD34(1.1%), CD45(0.006%), CD14(0.006%), HLA-DR(1.6%)
Romanov et al., 2003	UC vein was cannulated and filled with 0.1%collagenase +Medium 199 for 15 mins at 37 deg C; the endothelial and subendothelial cells were retrieved	DMEM-LG+20mM HEPES+ 2mMl L-glutamine+1mM Sodium pyruvate +P&S	Osteogenesis +ve, Adipogenesis +ve but Chondrogenesis not reported	Flow cytometry initially(P1) revealed ASMA+ve MSC-like cells and vWF and PECAM+ve endothelial cells but -ve to CD34
Covas et al., 2003	UC vein was isolated and catheterised to treat the lumen with 1% collagenase for 20 mins at 37 deg C	α- MEM+20% FCS+antibiotics+20mML-glutamine+P&S	Osteogenesis +ve, Adipogenesis +ve but Chondrogenesis not reported	Flow cytometry +ve to CD29, CD13, CD44, CD49e, CD54, CD90, HLA class I and -ve to CD45, CD14, CD106, CD51/61, HLA-DR

Table 1.1 Summary of literature review for cells derived from the umbilical cord with potential for orthopaedic application

1.2.5.1 Isolation Strategy: Several methods of isolation of cells from the UC and specific anatomical parts of UC were noted. These can be broadly classified into three groups: explant technique (Chang et al., 2014, Ishige et al., 2009, La Rocca et al., 2009, Majore et al., 2009), enzymatic isolation technique (Chang et al., 2014, Hartmann et al., 2010, Jo et al., 2008, Kadam et al., 2009, Karahuseyinoglu et al., 2007) and combined mechanical disassociation with enzymatic isolation technique (Tong et al., 2011, Subramanian et al., 2015). All these methods are reported with the successful isolation of cells, but each has intricate protocols.

The UC tissue used for the explant technique can include a whole cord *in-situ* (Majore et al., 2009, Qiao et al., 2008), dissected tissue from one particular anatomical location such as WJ (Yoon et al., 2013, Salehinejad et al., 2012) or CL (Reza et al., 2011) (Gonzalez et al., 2010). Furthermore, different UC tissues used include a longitudinally opened UC with vessels retained (La Rocca et al., 2009), a UC with only the vessels removed (Tong et al., 2011, Chang et al., 2014) or distinct anatomical compartments separated from each cord for concurrent isolation from different locations (Mennan et al., 2013, Ishige et al., 2009, Marmotti et al., 2012). Use of a high magnification operating microscope has also been reported recently to improve the precision of dissection in separating the anatomical compartments for the explant technique (Subramanian et al., 2015, Chang et al., 2014).

The method developed by Subramanian et al. (2015) describes WJ being precisely separated by dissection, followed by aspiration with a syringe under high magnification with a microscope; the amnion, sub-amnion and perivascular cells from the same cord were released by enzymatic digestion. Another protocol for using combined enzymatic mechanical disassociation describes the removal of the cord vessels followed by mincing and subsequent enzyme treatment of the tissue for 30 minutes with further mechanical

homogenisation and filtration was undertaken before cell seeding (Tong et al., 2011). The above technique was reported to yield a higher number of nucleated cells in comparison to explant or enzymatic isolation methods alone, but the time to attain cell confluence in culture remained comparable to the explant method in the same study.

Similarly, enzymatic isolation technique was used to isolate cells from a whole cord (Mennan et al., 2013, Tsagias et al., 2011, Jo et al., 2008), the endothelial compartment of an umbilical cord vein after it being cannulated and filled with enzyme (Romanov et al., 2003, Covas et al., 2003). Methods describing vessels being ligated and dissected with surrounding cord matrix (Baksh et al., 2007, Sarugaser et al., 2005), a cord with only blood vessels being removed (Tong et al., 2011) (Karahuseyinoglu et al., 2007) or a cord with only umbilical cord artery being removed (Hartmann et al., 2010, Seshareddy et al., 2008) are also noted in the literature. Separate areas of the cord region such as the WJ (Han et al., 2013, Salehinejad et al., 2012, Yoon et al., 2000, Wang et al., 2004) and concurrent isolation from the endothelial cells by cannulating the vein followed by enzymatic treatment of the remnant cord are few other techniques of tissue preparation before enzymatic isolation of cells (Kadam et al., 2009).

The enzyme used for isolating cells varied in type and concentration from 0.1% collagenase-IV (Han et al., 2013), 0.2% collagenase II (Han et al., 2013), 0.1% collagenase II (Yoon et al., 2013), 1% collagenase (Panepucci et al., 2004), combined collagenase I (2.7mg/ml) with hyaluronidase (0.7mg/ml), collagenase (1mg/ml) (Sarugaser et al., 2005), collagenase-I(1mg/ml) (Mennan et al., 2013), combined collagenase & EDTA/collagenase Type-B (Salehinejad et al., 2012), collagenase (300U/l) with hyaluronidase (1mg/ml) followed by 2.5% trypsin (Tsagias et al., 2011), 0.4% collagenase with 0.01% DNAse (Tong et al., 2011), collagenase (2mg/ml) followed by trypsin (2.5%) and dispase type-II with collagenase type-

IV (Kadam et al., 2009). Incubation period with the enzyme isolation techniques ranged from 20 minutes (Secco et al., 2008, Covas et al., 2003), 1hour (Mennan et al., 2013, Jo et al., 2008), 2-3 hours (Salehinejad et al., 2012), 16-20 hours (Han et al., 2013) up to a maximum of 18-24 hours (Sarugaser et al., 2005).

1.2.5.2 Differentiation potential of the cells

Osteogenic differentiation pathway of progenitor cells: The orchestration of specific growth factors involved in differentiation MSC *in vitro* although complex is explored to underpin the stages of osteogenic differentiation of a progenitor cell. Broadly *in vitro* osteogenic differentiation consists of three phases-

Phase of cell proliferation: This phase is marked by a significant early increase in the DNA content of the cells (first four days) followed by a gradual decrease over a period of 2 weeks due to confluence dependent apoptosis (Brezden and Rauth, 1996). This phase is also marked by upregulation VEGF which is shown to increase the number of osteoblasts and osteoid volume (Hiltunen et al., 2003). VEGF also acts with BMP-4 at a critical ratio for cell recruitment, survival and promotion of early stages of endochondral ossification (Peng et al., 2002). Similarly, IGF-1 (Manduca et al., 1997) and PDGF (Gruber et al., 2002) is also upregulated during this phase which leads to proliferation of osteoprogenitors.

Phase of cell differentiation: PDGF and TGF-β show a peak in this period. TGF-β is ascribed to have an encouraging role in osteoprogenitor differentiation during the early stages of differentiation however it can be inhibitory at later stages by inhibiting BMP-2 induced osteocalcin gene expression and ALP activity (Spinella-Jaegle et al., 2001b). The other two key factors promoting differentiation at this stage are FGF2 and BMP-2. FGF2 positively stimulates osteogenic differentiation of the progenitor cells by mitogen-activated protein

kinase (Mansukhani et al., 2000); additionally it also simultaneously stimulates osteocalcin acting in conjunction with cyclic adenosine monophosphate (Schedlich et al., 1994). The BMP-2, on the other hand, stimulates upregulation RUNX2 (Lee et al., 2003) and Osterix(Osx) (Celil and Campbell, 2005) both at mRNA and protein level at this stage promoting cell differentiation.

Phase of maturation: BMP-2 and FGF-2 are maintained at a high level of both mRNA and protein expression at this stage suggesting their role in the maturation of osteoblasts. FGF signalling at this stage is also prevention of cell death at this stage which can be due to serum starvation (Hill et al., 1997) or peroxynitrite (Kelpke et al., 2001). It has also been proposed that FGF-2 inhibit apoptosis of immature osteocytes, however, promotes apoptosis of mature osteocytes and hence renews the osteoblast pool (Marie, 2003)

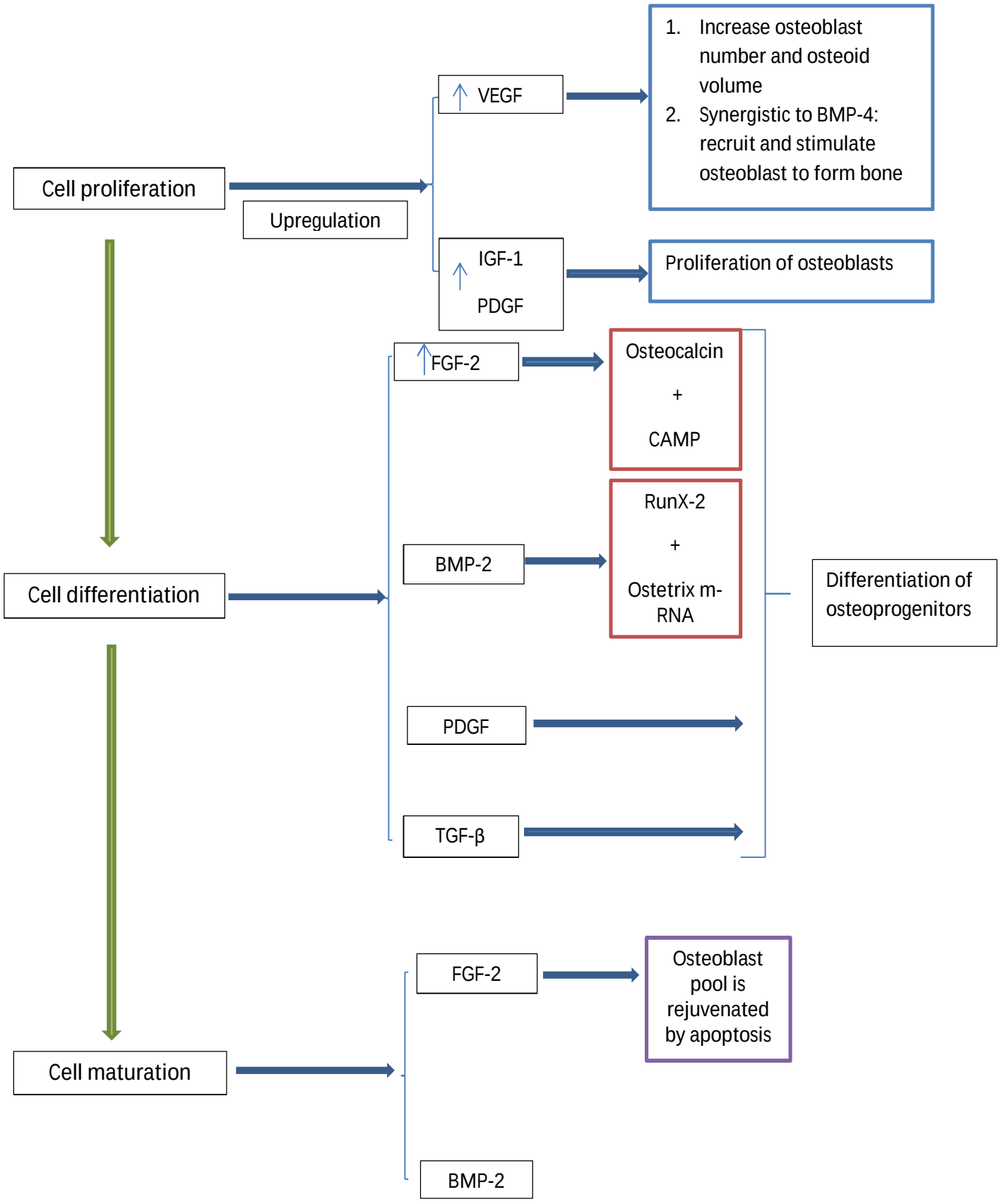

Figure 1.2: Schematic representation of the osteogenic differentiation pathway

Osteogenic potential of UC derived cells: Cells from the whole cord, in addition to separate anatomical compartments, have been reported to have varying osteogenic potential. The first report of explant culture comparing the differentiation potential of cells from different cord locations concluded that WJ cells were the least osteogenic, even after prolonged culture, followed by cells from UCAs, whereas highest osteogenic capability was noted in cells grown from UCVs (Ishige et al., 2009). A comparative study has also confirmed that peri-vascular cells isolated enzymatically had greater osteogenicity than BMMSCs (Baksh et al., 2007). Cells isolated from the whole cord using the explant technique (La Rocca et al., 2009) or enzymatic isolation technique (Qiao et al., 2008, Jo et al., 2008) were also reported to have an upregulation of osteogenic markers on RT-PCR after being osteogenically induced. Moreover, cells isolated enzymatically from the whole cord after the vessels being removed and cultured in three types of media (MesenCultACF, StemPro MSC SFM), showed no difference in their osteogenicity after being induced *in vitro* (Hartmann et al., 2010). However, explant culture of the whole cord grown in allogenic serum reported weak osteogenicity even after six weeks of culture in differentiation medium, despite the addition of 1,25-dihydroxy vitamin D3 (Majore et al., 2011).

A further report of cells from four locations of the UC (UCA, UCV, WJ and CL) by the explant technique along with enzymatic isolation of cells from the whole cord demonstrated cells from WJ and whole cords had better osteogenic differentiation in comparison to those from UCA, UCV and CL tissue assessed subjectively by cellular alkaline phosphatase (Mennan et al., 2013). Recent reports of cells from different anatomical locations separated meticulously also showed WJ cells had high expression of genomic markers, namely osteocalcin, osteopontin, bone sialoprotein and alkaline phosphatase significantly, in comparison to cells from perivascular, sub-amnion, amnion and mixed cord regions

(Subramanian et al., 2015). A separate study also demonstrated that the osteogenic potential of WJ cells was consistent from P1 to P3 with evidence of new bone formation in tissue-engineered demineralised bone matrix inserted into a periosteal defect created in a mouse model (BALB/Cnu/nu) at 56 days (Chang et al., 2014).

Chondrogenic differentiation pathway: Chondrogenic differentiation of an MSC involves complex coordination of different signalling pathways, the key players are briefly described in this section.

FGF signalling pathway:

FGF2 promotes chondrocyte proliferation by enhancing TGF-β1 expression (Stevens et al., 2004). Chondrocyte differentiation, on the other hand, is due to FGF2 mediated downregulation of TGF-b2 expression which is led by an increase in basal expression of Sox-9 and inhibition of IGF-1 and TGF-β signalling (Handorf and Li, 2011).

TGF-b/BMP signalling pathway:

TGF-b/BMP signalling activates Smad-dependent signal transduction in target cells through two receptors (type1 and type2) (Cleary et al., 2015). The TGF-B-mediated Smad 2/3 and Smad 1/5/8 signalling is essential for initial chondrogenic differentiation (Cleary et al., 2015). TGF-beta also activates mitogen-activated protein kinase (MAPK) proteins p38, ERK and JNK in MSC leading to downregulation of N-cadherin expression by blocking Wnt-mediated-b-catenin nuclear translocation (Tuli et al., 2003). This reduces N-cadherin expression and promotes progression from cell condensation to chondrogenic differentiation (Tufan and Tuan, 2001, Tufan et al., 2002).BMP signalling also plays a key role in condensation,

promoting coalesce of chondroprogenitor cells into clusters in vitro, an essential step before differentiation (Pizette and Niswander, 2000).

Wnt/b-catenin signalling pathway:

The canonical Wnt/b-catenin is most studied with respect to chondrogenesis. The Wnt proteins(Wnt 5a and Wnt 5b) has been ascribed to play a central role in chondrogenic cell migration and condensation (Bradley and Drissi, 2011).The chondrogenic effect of Wnt is also observed to occur through a canonical pathway involving downstream stabilisation of cytoplasmic b-catenin and formation of lymphoid enhancing factor(LEF)/T-cell factor-induced gene transcription (Kirton et al., 2007).

Hedgehog signalling pathways:

a. Sonic Hedgehog(Shh) signalling pathway:

   BMP and Shh work in conjunction to establish a positive regulatory loop with Sox9 and Nkx3.2 (a transcription factor that increases Sox9 expression) (Zeng et al., 2002). It also increases target cellular response to BMP (Murtaugh et al., 1999). Shh is traditionally observed to synergistically enhance chondrogenesis in the presence of FGF2 and FGF8 (Abzhanov and Tabin, 2004).

b. Indian Hedgehog (Ihh) signalling pathway:

   Ihh promotes chondrogenic differentiation by the expansion of Sox-9 expression in addition to upregulation of FGF8 expression in MSC (Zhou et al., 2007). In growth plate, Ihh produced by hypertrophic and pre-hypertrophic chondrocytes increases expression of Pthrp which antagonises differentiation by protein-kinase-A mediated

mechanism, this feedback loop coordinates chondrocyte proliferation and differentiation (Deckelbaum et al., 2002).

Notch signalling pathway:

The Notch Intracellular Domain (NICD) is central to the Notch-mediated regulation of chondrogenesis. The NICD induces HES gene family that encodes for basic helix- loop- helix (bHLH) nuclear proteins which are suppressors of transcription (Kageyama et al., 2007). The Hes-1 and Hey-1, members of the HES gene family, binds to the Sox9 binding site for Col 2a1 enhancer and inhibits Sox-9 mediated transcriptional activation of col2a1 (Grogan et al., 2008).

Hypoxia signalling:

Hypoxia-inducible factors(HIF) are transcription factors that respond to the hypoxia in the cellular environment and forms key factors in the differentiation pathway as chondrocytes reside in a hypoxic environment (Brighton and Heppenstall, 1971b, Brighton and Heppenstall, 1971a). Specifically, HIF's promotes chondrocyte expression of extracellular matrix and also enhance expression of col2a1, Sox9 and aggrecan and inhibit col1a1 and col1a2 (Adesida et al., 2012, Lafont et al., 2007, Koay and Athanasiou, 2008).There are six members of HIF family with HIF-1α and HIF-2α are shown to be linked with chondrogenesis. HIF-1α plays a key role in the survival of chondrocytes in the hypoxic environment by cAMP response element-binding protein/p300 (Ke and Costa, 2006) and upregulation of heat shock protein (HSP) 90 and HSP 70 (Genin et al., 2008). HIF-2α promotes chondrocyte differentiation through transcription of Sox trio, aggrecan, Col2a1 and Col10a1 genes (Khan et al., 2007).

Vascular endothelial growth factor signalling (VEGF):

Hypertrophic chondrocytes secrete VEGF promoting angiogenesis thereby reducing the severity of hypoxia required to maintain chondrocyte phenotype and promote differentiation to bone (Carlevaro et al., 2000, Gerber et al., 1999). Hence, regulating VEGF signalling is of prime importance to maintain cartilage tissue. However, it is also observed that in vitro administration of VEGF antibodies inhibit migration of chondroprogenitor cells (Carlevaro et al., 2000) and also leads to cell death in areas of col2a1 expression (Haigh et al., 2000). These results point towards a critical regulation of VEGF for chondrogenesis of progenitor cells.

Transcription regulation of chondrogenesis:

a. SRY-box 9(SOX9):

   SOX9 regulates condensation of the chondroprogenitor cells during earlier stages of differentiation followed by chondrocyte proliferation and differentiation by controlling chondrocyte-specific genes col2a1, col9a1, col11a2 and aggrecan (Akiyama, 2008). Additionally, it induces transcription of Sox5 and Sox6, forming Sox Trio, which synergistically increases the expression of gene targets of Sox9 (Ikeda et al., 2004). Sox9 also antagonises expression of Runx2 and ostetrix preventing osteogenesis of the progenitor cells (Leung et al., 2011).

b. Runt-related transcription factor (Runx):

   Regulating Runx2 is of extreme importance for chondrogenesis of the progenitor cells which is achieved by Sox9 (Zhou et al., 2006). A direct transcriptional target of Runx2 is Col10a1, a collagen type expressed by hypertrophic chondrocytes destined for endochondral ossification (Zheng et al., 2003). It also acts with HIF to promote

angiogenesis promoting osteogeneis and threatening retention of chondrocyte phenotype (Kwon et al., 2011). However, Runx2 is also observed to regulate osteogenesis and chondrocyte proliferation through P13K-AKT signalling pathway along with simultaneous dominant control by Sox9 (Fujita et al., 2004).

Fig 1.3: Schematic representation of the different stages of chondrogenic differentiation and the signalling molecules

Chondrogenic potential of UC derived cells: Cells from the UC and particular parts of the UC are reported to have variable chondrogenic potential, which has been mostly defined by the presence of glycosaminoglycans (GAGs) in the matrix through alcian blue or toluidine blue staining. Only three studies reported the presence of type-II collagen matrix by immunocytochemistry in three tissues. These are from chondrogenically differentiated cells from the whole cord (explant isolation) (Majore et al., 2011), UCV (enzyme isolation) (Panepucci et al., 2004), WJ (separated mechanically and then enzymatically digested) (Wang et al., 2004). Another study by Jo et al. showed an increase in GAG content in cells from the whole cord (enzyme isolation) after being chondrogenically induced, with no difference from P2-P9 assessed using a 1,9 dimethyl methylene blue (DMMB) assay (Jo et al., 2008). A recent report by Subramanian et al.,(2015) used quantitative reverse transcription PCR (qRT-PCR) to compare the chondrogenic potential of cells from four anatomical regions (amnion, sub-amnion, perivascular and WJ) of UC and whole cord. This demonstrated significant upregulation of genetic markers of chondrogenesis, namely, type II collagen (COL 2A), cartilage oligomeric matrix protein (COMP), fibromodulin (FMOD) and sex determining region box-9 (SOX9) in WJ cells in comparison to other cell preparations (Subramanian et al., 2015).

Only one study compared chondrogenesis in WJ cells and human BMMSCs after being cultured in three types of media (simple media, complex media and super complex media) with subsequent chondrogenic induction of these cells with/without 3D Polycaprolactone/Collagen II nano-scaffolds (Fong et al., 2012). Both cell types showed the presence of type II collagen on immunocytochemistry, irrespective of the presence of the scaffold, but qRT-PCR showed a significantly higher expression of the genetic markers of chondrogenesis in WJ cells in comparison to BMMSCs (Fong et al., 2012). The WJ cells also

had a significantly higher production of hyaluronic acid and GAG compared to BMMCs grown in the complex media, which was shown to be related to the presence of β fibroblast growth factor (FGF2) evident on immunohistochemistry (Fong et al., 2012). It is also important to note that an earlier study by Jo et al. on cells from whole cord grown in a medium containing FGF2 showed upregulation of aggrecan, type II and type X collagen with RT-PCR following *in vitro* chondrogenic induction (Jo et al., 2008). However, a similar study comparing cells isolated from UCA, UCV, CL, WJ and whole cord demonstrated tissue metachromasia by toluidine blue staining, although variations were noted between different cords with no particular region of the UC being consistently better (Mennan et al., 2013). Likewise, the study by Ishige *et al*. demonstrated metachromasia in cells isolated concurrently from the UCV, UCA and WJ by explant technique but the presence of type II collagen was not reported (Ishige et al., 2009).

Adipogenic differentiation pathway: Adipogenic differentiation pathway is broadly divided into two major steps, first being commitment of pluripotent stem cells to preadipocyte and the second being differentiation of the preadipocyte to adipose cells (Tang and Lane, 2012). The signalling pathway involved in adipogenic differentiation of MSC to adipocytes is briefly outlined in the following section.

1. The commitment of pluripotent stem cells to preadipocyte- Four signalling pathways which influence this particular stage adipogenic differentiation are BMP (Huang et al., 2011), Wnt, Hedgehog and Retinoblastoma protein signalling.

   BMP signalling: BMP 2 and 4 are implicated for the commitment of pluripotent cells to preadipocytes. Proteomic analysis has shown three cytoskeleton-associated molecules [lysyl oxidase (Lox), translationally controlled tumour protein 1 (tpt 1), αβ

crystalline] are the three main downstream target genes of BMP signalling pathway influencing this particular stage (Huang et al., 2011). These proteins potentially determine the commitment of pluripotent cells by cell shape regulation. It has also been shown that knockout of these proteins inhibits the commitment of pluripotent cells to preadipocytes (Huang et al., 2011).

Wnt signalling: Wnts act at two points in the adipocyte differentiation programme, during the early stage it promotes the commitment of the pluripotent cells however at a later stage it inhibits differentiation to adipocytes (Bowers and Lane, 2008, Ross et al., 2000). The canonical Wnt signalling pathway performs at early the stage of differentiation leading to accumulation of β-catenin inside the nucleus and subsequent activation of transcription factors, lymphoid enhancing factors (LEFs) and/or T-cell factors(TCFs) which trigger activation of downstream genes (c-myc and cyclin-D1) (Davis and Zur Nieden, 2008). At a later stage, Wnt10 inhibit adipogenic differentiation by inhibiting transcription factors peroxisome-proliferator activator – receptor γ (PPARγ) and CCAAT enhancer binding protein α (C/EBPα) (Ross et al., 2000). It has been proposed that Wnt increases the numbers of preadipocytes during pluripotent commitment and mitotic clonal expression stage, however, it is terminated at growth arrest stage before terminal differentiation (Bowers and Lane, 2008).

Hedgehog signalling: This signalling pathway has a poorly understood mechanism of action rendering an inhibitory effect on adipogenesis (Spinella-Jaegle et al., 2001a). This is evident from the decrease in intracytoplasmic fat accumulation and reduction in expression of specific genes i.e. Smo, Gli1, Gli2 and Gli3 observed in calvarial MSC and mouse adipose derived stromal cells (James et al., 2010) .

Retinoblastoma protein signalling: The retinoblastoma protein (Rp) inhibits progression of the cell cycle by binding and inhibiting the activity of transcription factor E2F (Burkhart and Sage, 2008). During mitotic clonal expression, there is hyper-phosphorylation of Rp leading to release of E2F followed by transcriptional activation of genes required for s-phase of the cell cycle (Burkhart and Sage, 2008). However, it has also been noted the Rp can promote RUNX2 promoting osteogenesis of MSC (Thomas et al., 2001) at the same time inhibit peroxisome-proliferator activated receptor (PPARγ) c subunit, a regulator for adipogenesis (Fajas et al., 2002). So, it has been proposed that Rp has a key role in cell fate determination of an MSC by regulating both adipogenic and osteogenic differentiation pathways (Calo et al., 2010).

2. Differentiation of preadipocytes to adipocytes- The three main steps during this stage are the induction of adipogenic differentiation followed by mitotic expansion and subsequent activation of a cascade of transcription factors.

   Induction of differentiation: Preadipocytes reaches to growth arrest and enters the G1 phase of the cell cycle with induction of adipogenesis by specific differentiating medium containing high levels of insulin, dexamethasone and an agent in the serum that can increase cellular cAMP (MacDougald and Lane, 1995). These induce

   the IGF1, glucocorticoid and cAMP signalling pathways following which all the preadipocytes synchronously enter into the mitotic clonal expansion stage (s-phase of the cell cycle) (Student et al., 1980).

   Mitotic clonal expansion: Following re-entry of preadipocytes to the s-phase of the cell cycle these cells undergo two mitotic divisions and DNA replication (Tang et al.,

2003). Marked activation of C/EBPβ (Tang et al., 2005) and histone 4(H4) (Zhang et al., 2011) is also noted at the G1/S boundary of the cell cycle.

Activation of a cascade of transcription factors: The cAMP regulatory element binding protein (CREB) has been proposed to be the key molecule for adipogenic differentiation (Zhang et al., 2004). The CREB gets activated by protein kinase-A mediated phosphorylation with subsequent activation of C/EBPβ which in turn leads to increase C/EBPα and PPARγ, the overall effect being increase in expression of adipocyte genes (like cyclin B, CDC25b) (Zhang et al., 2004, Niehof et al., 1997).

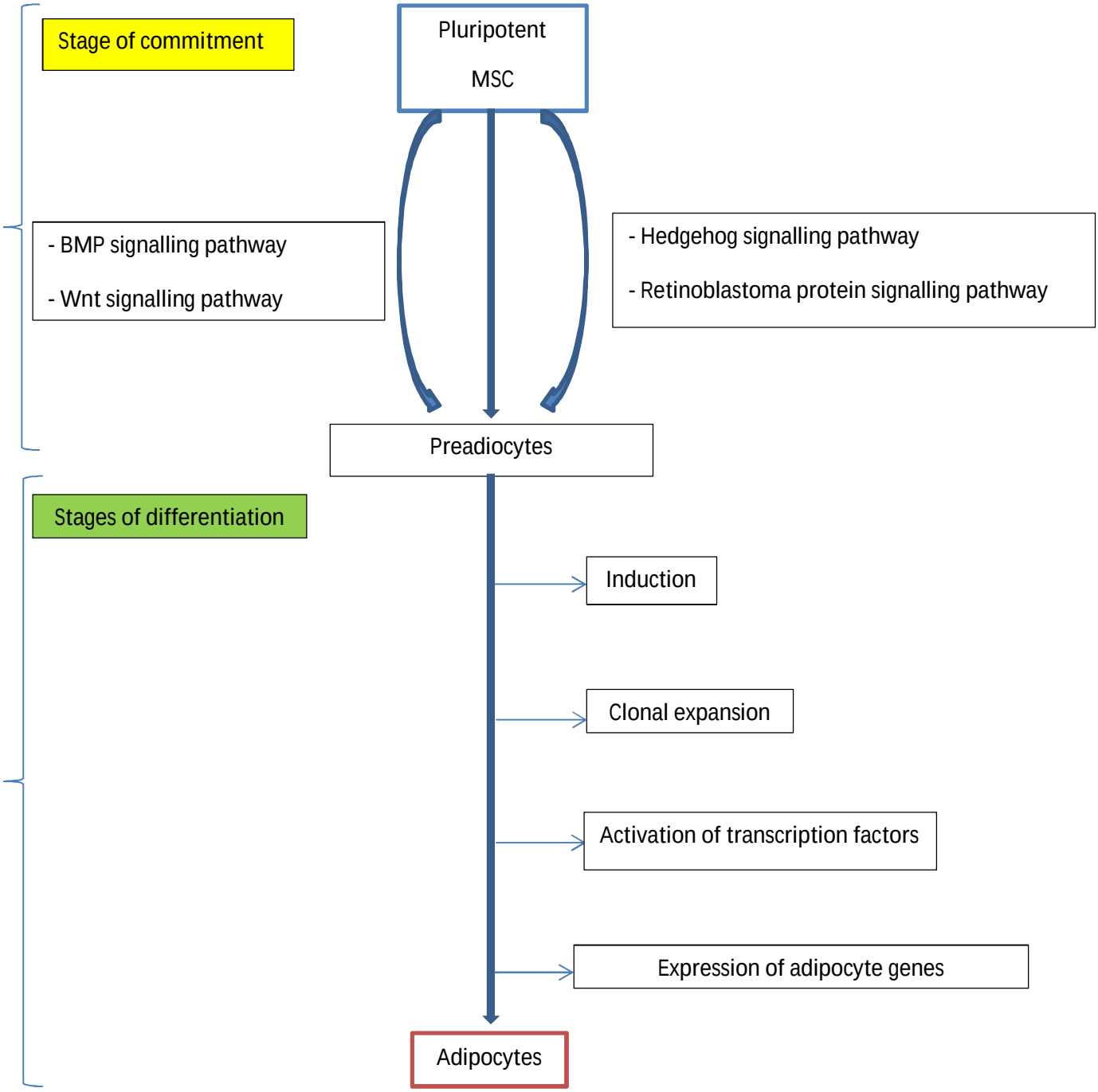

Figure 1.4: Schematic representation of adipogenic differentiation pathway

1.2.5.3 Surface phenotype: The surface phenotype of cells derived from different locations or whole UC measured with immunofluorescence was noted to be consistently positive for the recommended stem cell markers, CD73, CD90 and CD105 (Dominici et al., 2006), although these markers were not always reported in combination. The surface positivity of these antigens was also often not reported quantitatively and, if they were, considerable variations were noted, often being outside the range recommended by Dominici et al. (2006). The study by Salehinejad et al. compared the explant isolation technique with three types of combinations of enzymes, i.e., collagenase + trypsin, trypsin + EDTA and collagenase + hyaluronidase + trypsin, for isolation of cells from WJ (Salehinejad et al., 2012). Cells derived from the explant technique had the highest expression of CD73 (74.5%) and CD90 (72.2%); CD105 expression was greatest in cells isolated with collagenase + trypsin (90.3%), while cells derived with explant technique were 83% positive (Salehinejad et al., 2012). However, according to Salehinejad et al. none of the cells, irrespective of the isolation technique, quantitatively conformed to the ISCT criteria of surface phenotype for stem cells (Dominici et al., 2006, Salehinejad et al., 2012). Another study comparing the surface characteristics of WJ cells and BMMSCs grown in three types of media showed that CD105 expression can range from 81% to 98.4% in cells isolated from WJ but had a narrow range of 94.3% to 97.1% for BMMSCs (Fong et al., 2012). Furthermore, Kadam et al.,(2009) derived cells enzymatically from UCV and the whole residual cord with a combination of collagenase and dispase and cultured separately. The M199 medium (for human umbilical vascular endothelial cells, hUVECs) and DMEM with Ham'sF12 (for human umbilical cord matrix-stromal stem cells, hUCMSCs), both supplemented with cord blood serum (20%), had no surface expression of CD105 by flow cytometry analysis (Kadam et al., 2009). Moreover, Majore et al.(2009) isolated six sub-population of cells derived with the explant

technique from whole UC based on their sizes by using counterflow centrifugation elutriation. Smaller cells had a higher proliferative capacity with relatively more positivity for CD73 and CD90 in comparison to larger cells which were found to be more senescent with Senescence β-Galactosidase staining (Majore et al., 2009). Nonetheless, a comparative study of cells cultured in DMEM F12 and 10%FCS from the CL, UCA, UCV, WJ (isolated by the explant technique) and whole cord (enzymatic isolation procedure) reported no difference in CD73, CD90 and CD105 surface expression amongst the cells, with all being >95% positive on fluorometric analyses (Mennan et al., 2013). No differences in surface expression of CD73, CD90 and CD105 were also reported in cells cultured in DMEM-Low glucose with L-glutamine derived from the amnion, sub-amnion, perivascular region, whole cords and WJ, although quantification of these markers for each cell preparation was not available (Subramanian et al., 2015). Likewise, no difference was found between cells isolated from UCA, UCV and WJ cultured in α MEM and 10%FCS, with >90% being positive for the relevant surface markers, but separate comprehensive details of the surface profiles were not available in the article (Ishige et al., 2009).

The study by Subramanian et al.(2015) also reveals a wide variation in the presence of the haematopoietic markers (CD14, CD19, CD34, CD45, C117) and HLA-DR (range 3.7 to 22.4%) with no significant difference amongst each cell source (Subramanian et al., 2015). The same study also showed a significantly higher percentage of CD40-positive cells from the amnion, sub-amnion and mixed cord in comparison to perivascular cells and WJ cells. Such CD40 positive cells are suggestive of non-stem cell contamination, for instance from epithelial cells, endothelial cells or fibroblasts. Conversely, expression of markers of pericytes such as CD146 and CD271 was significantly higher in WJ and perivascular cells (Subramanian et al., 2015). Previous reports of human umbilical cord perivascular (HUCPV)

cells by Bakshi *et al.* (2008) also showed the presence of CD146 positive cells, an endothelial marker, but in the absence of CD31, these cells were noted to have tri-lineage differentiation capacity akin to MSCs (Bakhshi et al., 2008).

Nevertheless, according to Mennan *et al.* (2013) cells derived from the CL, UCA, UCV, WJ and whole cord were all <2% positive for CD14, CD19, CD34 and CD45 and HLA-DR, in line with the ISCT criteria for MSC (Dominici et al., 2006). A further study also showed the absence of CD34 and CD45 from P1 to P3 in cells isolated by the explant technique following microdissection of the WJ tissue from the whole UC and cultured in DMEM F12 with 10% FBS (Chang et al., 2014). Similarly, a previous report of simultaneous isolation of cells from the UCA, UCV and WJ of the cord found them to be <1% positive for CD31, CD34, CD45, CD133, CD271 and HLA-DR (Ishige et al., 2009). Moreover, no difference was noted in two separate reports on WJ cells (Fong et al., 2012) and UCMSC (Hartmann et al., 2010) being cultured in three different media, particularly in the absence of haematopoietic markers and MHC Class II surface molecule.

1.2.6 Summary

Several techniques have described methods of isolating MSC from UC and/or different regions of UC. These cells can have wide variations in surface phenotype and differentiation potential, and their properties do not uniformly conform to the ISCT recommended criteria (Dominici et al., 2006). This heterogeneity can be due to several factors, such as the isolation technique, the anatomical region of the UC and the culture medium used, to name but a few. This has led to an extensive literature, often with contradictory results, rendering them poorly comparable.

These cells have been observed to have consistent *in vitro* osteogenic and chondrogenic differentiation potential although few reports of conflicting results describing poor

differentiation capacity are also noted in the literature. The surface phenotype of these cells has also been variable with the quantitative parameters not always compliant with the ISCT criteria for defining an MSC (Dominici et al., 2006). Nevertheless, UC is a potential alternative source for readily isolatable cells which have properties akin to MSCs, making them a suitable candidate for *in vivo* applications in regenerative medicine. These cells were also immune privileged with encouraging results during *in vitro* and *in vivo* results in animal models.

Further, *in vitro* research on a uniform method of isolation of cells from four regions of the UC followed by characterisation need to be undertaken to identify the area with the best cell source. This will set the platform to compare the immunomodulatory and paracrine effects of these cells in the context of regeneration and hence, advance the translation of UC-derived cells in human orthopaedic regenerative medicine.

1.3 Potential of cell-based approaches for regeneration of bone in fracture nonunions

1.3.1. Overview

According to the US Federal Drug Agency, a nonunion is defined as failure to achieve bony union after nine months from the injury with no evidence of progression of healing for the last three months (USFDA, 1998). The reported incidence of nonunions following a new fracture can vary from 0.02%-10% (Court-Brown et al., 2010, Mills and Simpson, 2013). Nonunions are classified according to the presence of callus at the fracture site into hypertrophic and atrophic (Weber and Cech, 1976). Hypertrophic nonunions are hypervascular and respond to fracture healing by callus formation but fail to bridge the fractures because of instability at the fracture sites. Atrophic nonunions, on the other hand, have inert and biologically inactive fracture ends which fail to show any signs of healing with time evident by the paucity of callus formation (Weber and Cech, 1976).Although ascertaining vascularity at the fracture site can be a critical determinant of bone healing, it should not rely solely on the callus formation assessed with plain radiographs (Wu and Chen, 2000). Moreover, it has been established that blood supply to the human atrophic nonunion site is comparable to hypertrophic nonunions in the absence of infection (Reed et al., 2002). Nevertheless, animal models of atrophic nonunions have demonstrated fewer blood vessels in comparison to fracture which healed uneventfully at one week, but the difference was statistically insignificant at three weeks (Reed et al., 2003). It is also important to note that histological sections of atrophic nonunion in the study mentioned above continue to show the absence of fracture union despite restoration of interfragmentary vascularity up to 16 weeks (Reed et al., 2003). These findings are

suggestive of a strategy to enhance osteoprogenitor activity by local delivery of cells at the nonunion site to help to achieve fracture union.

1.3.2 Process of fracture union

Fracture healing has been classified broadly into two categories: direct and indirect. Direct healing occurs with complete reduction of the fracture fragment leading direct remodelling of the lamellar bone, Haversian canals and blood vessels. On the other hand, indirect healing is the commonest method of fracture repair which includes endochondral and intramembranous healing (Gerstenfeld et al., 2006). This type of repair response has been noted in fractures with some degree of micro-motion.

The five identifiable stages of the fracture healing process are:

a. Stage of inflammation This phase corresponds to the formation of a fracture haematoma with subsequent infiltration of macrophages, neutrophils and platelets. The initial pro-inflammatory response peaks at 24 hours and can extend up to 7 days with the secretion of tumour necrosis factor-α (TNF-α), interleukin-1 (IL-1), IL-6, IL-11 and IL-18, which promote migration of the inflammatory cells (Gerstenfeld et al., 2003). The TNF-α is produced by the macrophages and inflammatory cells which act as a chemotactic agent in recruiting the inflammatory cells (Kon et al., 2001). The TNF-α is also observed to induce osteogenesis of the MSCs *in vitro* (Cho et al., 2006). The IL-1 produced by macrophages corresponds with TNF-α production along with the production of cartilaginous callus, angiogenesis and further induction of IL-6 in osteoblasts. The IL-6 promotes angiogenesis by vascular endothelial growth factor (VEGF) production and also promotes differentiation of osteoblasts to osteoclasts (Marsell and Einhorn, 2011) The MSCs are recruited to the fracture site from the

surrounding tissue, periosteum and bone marrow as well as the systemic circulation (Granero-Molto et al., 2009). Different hypotheses exist with regards to homing of the MSC to the fracture site. The two most common theories are the stromal cell-derived factor 1 (SDF-1), and G-protein coupled chemokine receptor CXCR-4 axis (Granero-Molto et al., 2009) and the other being hypoxia-inducible factor-1α (HIF-1α) controlled MSC trafficking (Wan et al., 2008). The HIF-1α operates on a hypoxic gradient with concomitant induction of VEGF to promote vascularisation during fracture repair (Wan et al., 2008).

b. Endochondral ossification The generation of 'soft-callus' at this stage peaks at 7-9 days with a proteoglycan and type-II pro-collagen matrix core, in addition to subperiosteal intramembranous ossification at the fracture site (Marsell and Einhorn, 2011). This stage depends on the recruitment of MSC with a molecular cascade of collagen I and collagen II production influenced by bone morphogenic protein (BMP) 2, 5, 6 and transforming growth factor-1 (TGF-1) superfamily members respectively leading to the endochondral ossification (Cho et al., 2002).

c. Vascularisation This stage is predominantly dependent on the VEGF pathway expressed in hypertrophic chondrocytes and osteoblasts to promote blood vessel formation within the soft callus (Keramaris et al., 2008). The VEGF is also thought to promote proliferation and aggregation of the endothelial cells to support neo-angiogenesis within the callus (Kanczler and Oreffo, 2008). VEGF acts in synergy with BMP and is also promoted by mechanical stimulation during this stage of repair (Kanczler and Oreffo, 2008).

d. Mineralisation During this phase the chondrocytes at the fracture site continue to hypertrophy with resorption of the mineralised cartilage matrix by a cascade of

events linked primarily with macrophage colony stimulating factor (M-CSF), receptor activator of nuclear factor kappa B ligand (RANKL) and TNF-α (Gerstenfeld et al., 2003). These factors also promote recruitment of osteoblasts and osteoclasts to form woven bone although the primary role of TNF-α at this stage is to induce apoptosis of the chondrocytes (Gerstenfeld et al., 2003, Marsell and Einhorn, 2011). The mitochondria of the chondrocytes contain calcium which is transported to the cytoplasm and finally to the extracellular matrix where it binds with phosphates forming the nucleus of apatite crystals (Ketenjian and Arsenis, 1975).

e. Remodeling This stage consists of a balance between lamellar bone deposition by the osteoblasts and resorption by the osteoclasts. The hard callus is remodelled to a lamellar bone with a central medullary canal (Gerstenfeld et al., 2003). Biochemical harmonisation at this stage is achieved by high levels of IL-1 and TNF-α with the diminishing activity of members of the transforming growth factor (TGF)-β superfamily, such as BMPs (Marsell and Einhorn, 2011, Mountziaris and Mikos, 2008).

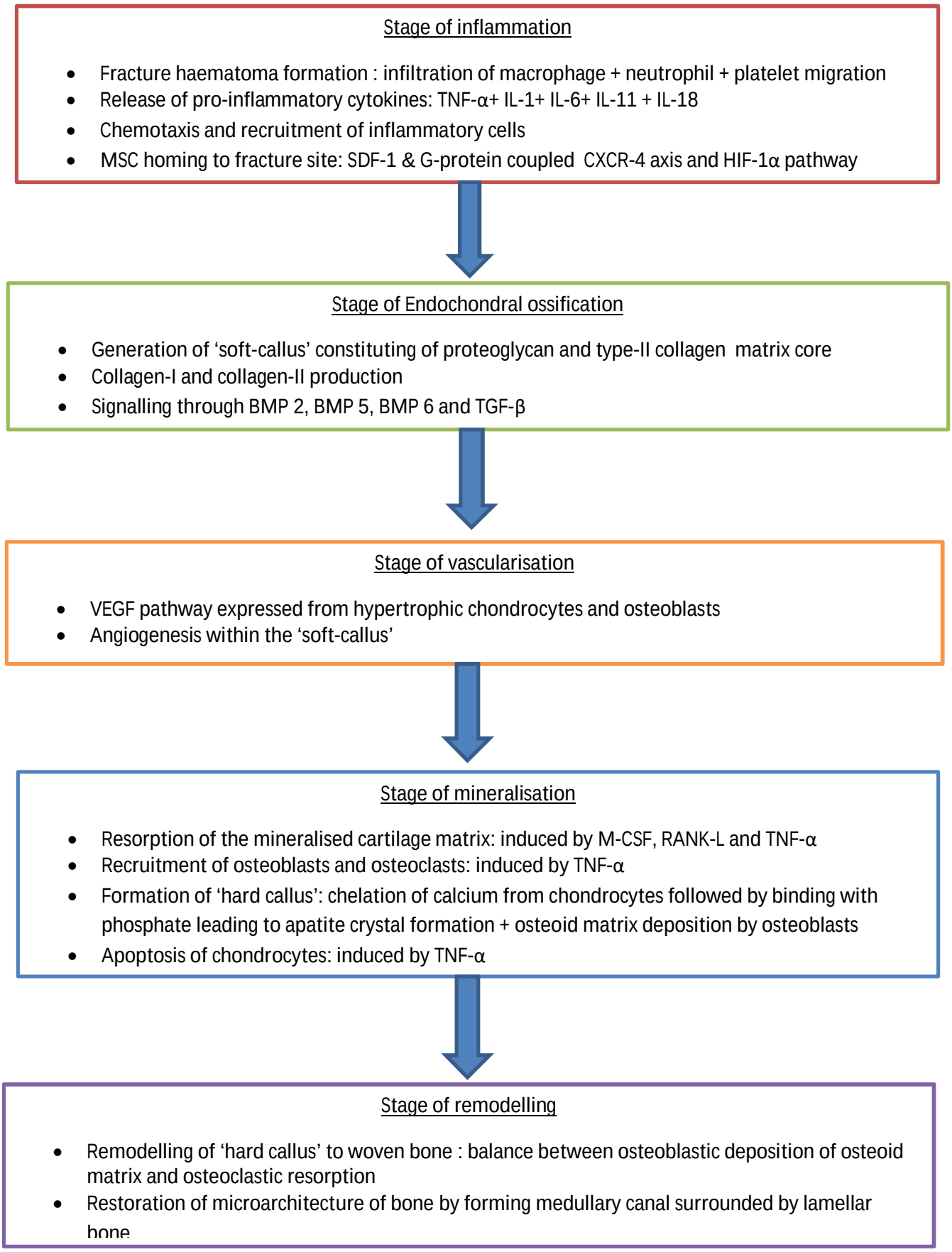

Figure 1.5: Stepwise illustration of stages of fracture healing in bone

1.3.3 Pathogenesis of fracture nonunion and the basis of cell therapy

The human fracture haematoma contains cells which have multi-lineage differentiation potential, including an osteogenic differentiation capacity, and the phenotype of these cells is similar to bone marrow derived MSCs (BMMSCs) (Jagodzinski and Krettek, 2007, Dominici et al., 2006). It has also been observed that the colony forming unit-fibroblasts (CFU-F) of such BMMSCs from patients with atrophic nonunions can be significantly lower with weak proliferative capacities in comparison to healthy volunteers and patients with multiple traumas (Seebach et al., 2007). A significant reduction in extracellular bone matrix mineralisation and proliferation, with differentially expressed factors for osteogenesis in nonunion human osteoblasts, has also been reported (Hofmann et al., 2008). The growth factors related to osteogenesis in these cells were low; such distinct properties were ascribed to alteration in wingless-related integration site (Wnt), insulin-like growth factor (IGF), TGF-β and fibroblast growth factor (FGF) signalling pathways (Hofmann et al., 2008). Nonunion stromal cells grown from the human nonunion site were noted to have slower doubling time, lower osteogenic potential and a higher rate of apoptosis in comparison to BMMSCs from healthy donors (Bajada et al., 2009). The nonunion stromal cells were found to secrete Dickkopf-1 (Dkk-1) which is an antagonist to the Wnt signalling pathway and inhibits osteogenic differentiation and fracture healing *(ibid).* A study of nonunions in rats showed that the progenitor cells from atrophic nonunion sites had impaired differentiation potential due to a sub-optimal environment and suggested reactivation of these primary cells by adding growth factors or progenitor cells to induce bone formation (Tawonsawatruk T et al., 2013). In a clinical setting, all these evidence can be converted into two fundamental principles guiding bone healing in nonunions: enhance the biological viability and provide appropriate biomechanical stability at the fracture sites (Megas, 2005).

There is evidence suggesting migration to and augmentation of the fracture repair process by transplanted MSCs in a mouse model (Granero-Molto et al., 2009). BMMSCs are also reported to have better osteogenic capacity in athymic nude rats than embryonic stem cells, with no risk of aberrant bone formation or tumorigenicity (Undale et al., 2011). In a critical-sized mouse calvarial defect, a novel tissue-engineered approach of using cultured human BMMSCs with hydroxyapatite (HT) or tricalcium phosphate (TCP) carrier successfully led to new bone formation (Mankani et al., 2006). Success in the human translation of bone tissue engineering to regenerate large bone defects by using *in vitro* expanded autologous BMSC and subsequently re-implanting them in scaffolds has also been described (Quarto et al., 2001, Marcacci et al., 2007). Similar success in treating a nonunion with autologous bone marrow derived cells has also been reported in a clinical case study (Bajada et al., 2007).

A review of the existing literature was undertaken to identify the current level of evidence for using bone marrow derived cultured cells for bone tissue regeneration in human fracture nonunion and bone defects related to trauma and limb lengthening procedures.

1.3.4. Literature Search results: The summary of the literature review is presented in Table 1.2. After reviewing the abstracts of the relevant articles generated following the search, only six articles were included and found pertinent to the topic (Table 1.2). Studies reporting the use of bone marrow aspirate to treat nonunion without being culture-expanded were excluded (Hernigou et al., 2005a, Hernigou et al., 2015). Similarly, use of culture-expanded bone marrow derived cells for calvarial defect, and mandibular defects were excluded.

The six articles found comprised of one randomised control trial with the rest being case reports, case series and retrospective cohort studies (Table 1). The randomised control trial demonstrated a significant increase in callus formation in the treatment group compared to the control group after receiving an injection of pre-differentiated bone marrow derived

cells in average eight weeks old fractures (Kim et al., 2009).). It is important to highlight that Kim et al. devised a radiological scale in this study which scored the pre- and post-treatment callus formation to account for the new bone formation after the trial intervention. The same study also showed a significant rise in callus formation in the treatment group after the injection at two months follow-up but not after one month when compared to the pre-treatment callus (*ibid).*

Only one case report highlighted the successful outcome of treating hypertrophic nonunions using cells inserted with calcium sulphate carriers(Bajada et al., 2007). A further case series of eight patients reported the use of pre-differentiated bone marrow derived MSC along with fibrin clots and bone grafts for atrophic nonunions of the upper limb leading to the successful radiological union within 5-10 months(Giannotti et al., 2013). In these series, Giannotti et al. (2013) reported insertion of culture expanded and characterised cells along with a revision of surgical fixation at the same time achieving radiological union within 12 months. Moreover, no significant adverse effects from the cell therapy were also reported at an average 76 months follow-up (*ibid*). The three other studies described successful outcome of a cell-based approach for bone regeneration in a setting of trauma with bone loss or limb lengthening procedure (Marcacci et al., 2007, Quarto et al., 2001, Kitoh et al., 2009). However, Kitoh et al. demonstrated that healing time was significantly reduced with cell therapy for femoral lengthening, although this was not significantly different to the group not receiving cell-based treatment for tibial lengthening.

Author	Cells/Carrier	Site	Treatment	Outcome
Quarto et al., 2001 (Case series)	Cultured bone marrow derived cells + HA porous bioceramic scaffolds	Three patients (one tibia, one ulna, one humerus)	Bone defect related to acute trauma and limb lengthening	Union in 6-13 months
Maracci et al., 2007 (Case series)	Cultured bone marrow derived cells + HA porous bioceramic scaffolds	Four patients (one tibia, two ulna and one humerus)	Bone defect	Union in 5-7 months
Bajada et al., 2007 (Case series)	Cultured bone marrow derived cells + Calcium Sulphate	One patient(tibia)	Hypertrophic nonunion	8 weeks
Kim et al., 2009 (Randomised control study)	Cultured pre-differentiated bone marrow derived cells+ fibrin clot	64 patients (31 patients in the treatment group and 33 patients in the control group)	Acute fractures(average eight weeks old)	Radiological union in 2 months
Kitoh et al.,2009 (Retrospective cohort)	Cultured bone marrow derived cells +Platelet Rich Plasma	51 bones(23 femur an 28 tibia) with 60 controls	Leg lengthening	Significantly quicker healing in cell therapy group in comparison to controls
Giannotti et al., 2013 (Case-series)	Cultured pre-differentiated bone marrow derived cells+ fibrin clots	Eight patients with upper limb	Atrophic nonunions	Union in 5-10 months

Table 1.2 Summary of literature review describing the human application of bone marrow derived cultured cells for bone regeneration in long bone defects and nonunions

1.3.5 Summary

Therapeutic application of bone marrow derived cells for regeneration of long bones in human fracture nonunions is a promising arena, but no randomised controlled trials have so far been reported in this area. There is only one case report of using bone marrow derived cultured cells in fracture nonunion (Bajada et al., 2007). Further reports of atrophic nonunions following fractures of the upper limb showed encouraging results with progression to the radiological union in eight cases (Giannotti et al., 2013). The only randomised control trial in this arena has shown a significant rise in the new bone formation after injection of pre-differentiated cells at the fracture site (Kim et al., 2009). Moreover, cell therapy has also been shown to produce bone healing following acute bone loss and limb lengthening procedures (Kitoh et al., 2009, Marcacci et al., 2007, Quarto et al., 2001). It is also important to identify at this stage that every fracture has unique local biology and patient-related systematic factors which can affect union despite cell-based treatment (Kitoh et al., 2009). Comparing the outcome of treatment especially in such cases may be significantly confounded by the host factors, which can, for example, include age, the presence of infection and systemic factors like diabetes.

A self-controlled randomised study of lower limb nonunions is evaluated in the present thesis to ascertain the efficacy of bone marrow derived stromal cells (BMSC) in new bone formation. A standardised isolation strategy of BMSC was established followed by a uniform method of '*in-vitro*' expansion in autologous serum. Every patient in this particular study acted as their control (i.e. self-controlled) with one side of the nonunion receiving BMSC with the carrier and the opposite side receiving carrier in isolation. The primary outcome was bone formation on serial radiographs evaluated by multiple independent assessors.

1.4 Potential of Autologous Chondrocyte Implantation in repair of chondral defects with underlying subchondral bone defects or malalignment in the knee

1.4.1 Overview

The incidence of osteochondral defects is 15-30 per 100,000 persons (Chui et al., 2015). A prospective study based on MRI in 120 patients with haemarthrosis of the knee following trauma showed acute subcortical femoral or tibial fracture in 72% patients with a substantial proportion of these progressing to an osteochondral defect at 6-12 months on further scans (Vellet et al., 1991). Such focal articular cartilage defects extending to the underlying subchondral bone can effectively generate defects which are grade 4 on the ICRS cartilage injury scale (Brittberg and Winalski, 2003). Likewise, ICRS Grade III and IV osteochondritis dissecans (OD) will also produce osteoarticular defects which extend to the subchondral bone. These cartilage defects extending to the subchondral bone may require concurrent bone graft during cartilage repair surgery (Brittberg and Winalski, 2003).

Similarly, more than 31,000 knee arthroscopies revealed approximately 53,000 hyaline cartilage lesions with Grade IV defects being commonly located on the medial femoral condyle (MFC) (Curl et al., 1997). A subsequent study of more than 25,000 knee arthroscopies confirmed this observation and highlighted the frequent association of medial meniscus tears (37%) and anterior cruciate ligament tears (36%) with such cartilage defects (Widuchowski et al., 2007). High grade focal chondral defects can progress to OA of the affected compartment with significantly higher risk for joint replacement surgery in these patients (Hernborg and Nilsson, 1977, Carnes et al., 2012). Moreover, the pain and functional impairment in patients with focal cartilage defects is not significantly different from patients awaiting total knee replacement for osteoarthritis (Heir et al., 2010). It has

also been reported that outcomes of partial knee replacement to address arthritis confined to one compartment of the knee in younger patients are not satisfactory, with poor patient-reported outcome and implant survival (Liddle et al., 2014). The treatment of symptomatic articular cartilage defects is, however, more challenging if it co-exists with malalignment of the mechanical axis in the lower limb. Techniques for the biological restoration of the joint in such cases include realignment osteotomy around the knee joint to correct the mechanical axis, alongside methods to repair the articular cartilage (Franceschi et al., 2008, Bauer et al., 2012, Sterett et al., 2010).

In the following section, we examine the structure of the articular cartilage and the types of cartilage defects. We also review the existing evidence of treating these cartilage defects, particularly when associated with subchondral bone defects or malalignment in the knee.

1.4.2 Anatomy of articular cartilage

Synovial joints are lined by extremely smooth hyaline articular cartilages bathed with synovial fluid that allows minimal friction during movement. The articular cartilage helps it bear load by withstanding shearing and compressive forces during weight-bearing and movements. The thickness of the articular cartilage varies between 1-7 mm and can alter with the geometry of the joint surface. The articular cartilage has four structural zones. Zone 1 is the superficial or tangential layer with a high collagen content and small, oval or flat relatively inactive cells aligned parallel but compact to the surface. Zone 2 is the transitional or intermediate layer with active spherical chondrocytes surrounded by oblique collagen fibres. In Zone 3, the cells are round and can be arranged in vertical columns with radial collagen fibrils; Zone 4 is the deepest, calcified zone adjacent to the subchondral bone

with reciprocal inter-digitations resisting shearing stresses between the adjacent layers. The junction between Zone 3 and Zone 4 is called the 'tide mark' (Fig 1.5).

Articular cartilage is hypocellular, aneural, avascular and alymphatic and consists mainly of water (80%). It derives nutrition from the adjacent synovial membrane, synovial fluid, vascular subchondral bone and occasional blood vessels traversing the calcified cartilage (Bora and Miller, 1987). The unique property of this cartilage is due to the interaction of the chondrocyte with the extracellular matrix, which is primarily composed of collagen, proteoglycans and non-collagenous proteins.

The type II, IX and XI collagens form a fibrillary network which renders tensile strength to the matrix, whereas Type VI collagen helps chondrocytes to attach to the matrix. The large proteoglycan, aggrecan comprises of 35% of dry cartilage weight and contributes by supporting the high compressive load on the cartilage (Izadifar et al., 2012). Aggrecans also provides swelling pressure, and small proteoglycans provide structural stability to the matrix (Buckwalter and Mankin, 1998). Structurally, the aggrecan molecule has a polypeptide core with side chains which are chondroitin sulphate and keratan sulphate polysaccharide (glycosaminoglycans). The link protein attaches the aggrecan molecules with hyaluronan polysaccharide chain creating a large proteoglycan complex embedded within the predominantly type-2 collagen fibril network. The presence of high negative charge densities of the keratan and chondroitin sulphate chains within the aggrecan monomer draws water to the extracellular matrix (Izadifar et al., 2012). A schematic representation of the articular cartilage with its structural components and different layers is illustrated in Figure 1.5.

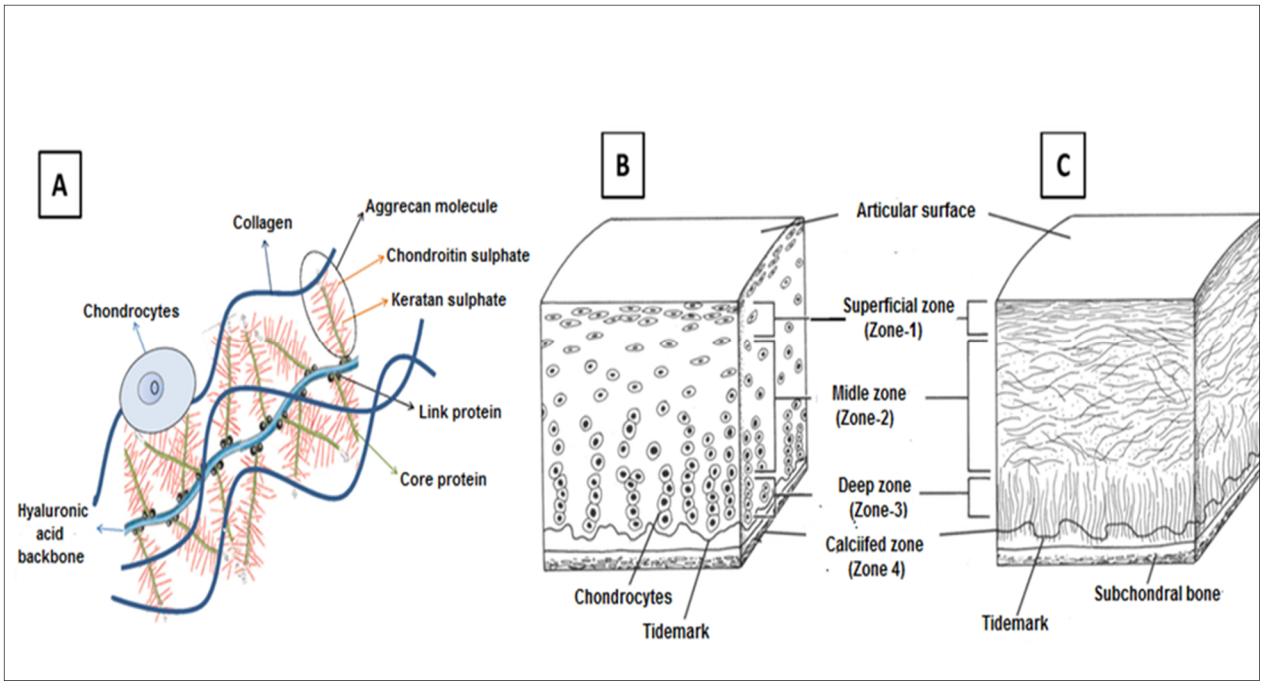

Figure 1.6 Principal components and zonal organisation of articular cartilage tissue :(A) fibrils of type II collagen, proteoglycan complexes composed of aggrecan and hyaluronan, and chondrocytes cells (reproduced from Izadafir *et al.,* 2012); (B) zonal chondrocytes; and (C) zonal collagen fibres.(Images (B) and (C) are reproduced from Buckwalter *et al.*, 1994)

1.4.3 Defects of articular cartilage

Articular cartilage defects have been classified according to the depth of the defects. These can be either full thickness, partial thickness (or flap defect) and osteochondral defects, which are full thickness defects extending into the subchondral bone (Bhosale and Richardson, 2008). The International Cartilage Repair Society (ICRS) classified hyaline cartilage lesions macroscopically into four broad grades with sub-types (Brittberg and Winalski, 2003) (Fig 1.7) -

- ICRS Grade 0- Normal hyaline cartilage
- ICRS Grade 1a- Cartilage with superficial fibrillation and or softening
- ICRS Grade 1b- Cartilage with superficial lacerations or fissures
- ICRS Grade 2- Cartilage defect extending < 50% of the thickness
- ICRS Grade 3-Cartilage defects extending >50% of the thickness
    - ICRS Grade 3a-Cartilage defects superficial to the calcified layer.
    - ICRS Grade 3b-Cartilage defects extending up to calcified layer
    - ICRS Grade 3c- Cartilage defects extending up to subchondral bone
    - ICRS Grade 3d-Cartilage defects with superficial blisters
- ICRS Grade 4-Cartilage defect extending into the subchondral bone (A) and these defects can also lead to extensive cavitation of the subchondral bone (B)

The articular cartilage defects extending up to the subchondral bone (ICRS Grade 4) are essentially osteoarticular defects with two sub-types i.e. defects associated with or without cavitation of the subchondral bone (Brittberg and Winalski, 2003). Such high-grade cartilage defects can benefit from bone graft in addition to cartilage repair to restore the underlying bone plate (Brittberg and Winalski, 2003). Joints with idiopathic malalignment can also generate localised areas of high contact stresses leading to cartilage defects (Sharma et al.,

2008). Restoration of alignment forms the basis of minimising the principal stresses on the chondral surface upon loading in such joints (Bhosale and Richardson, 2008).

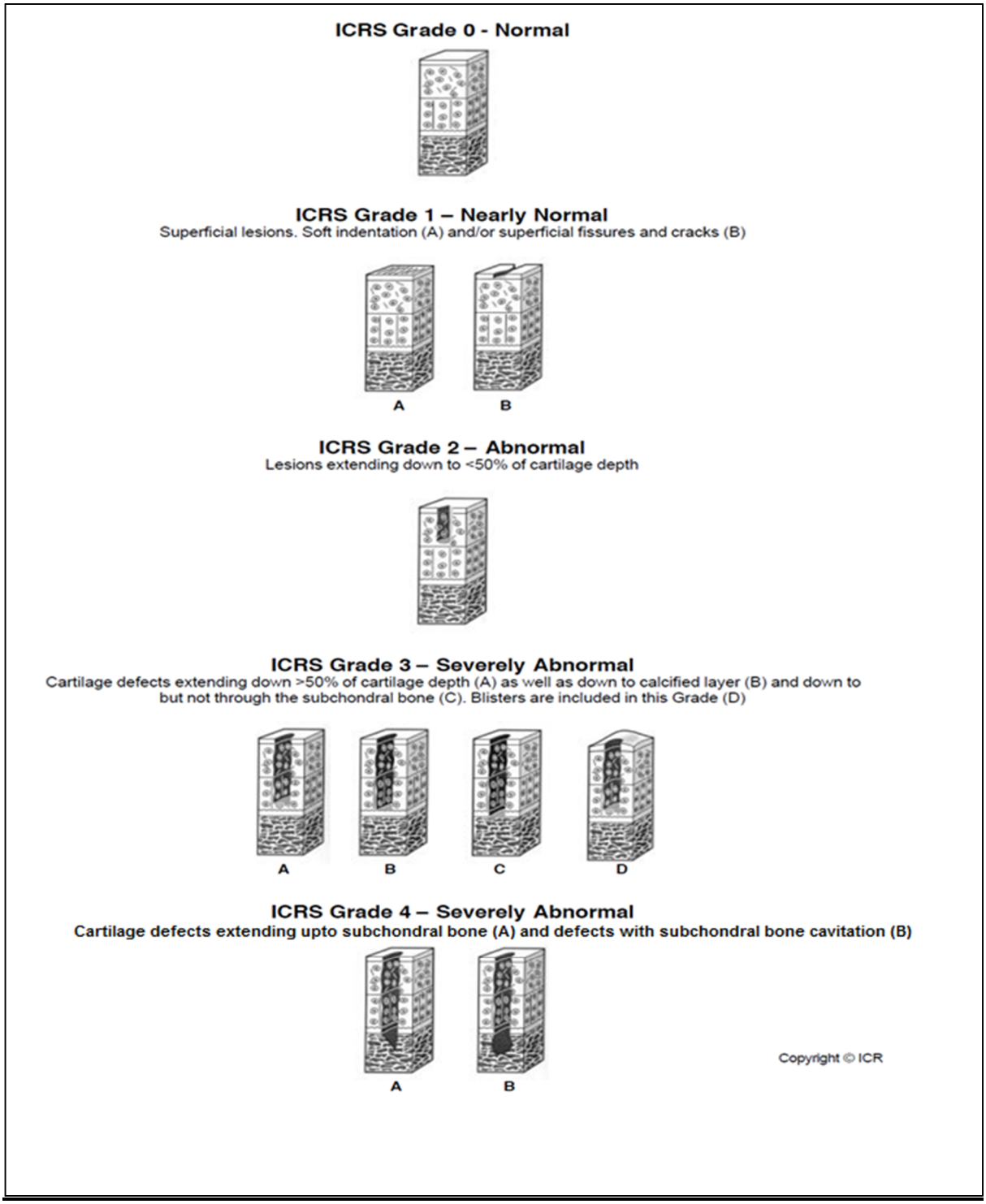

Fig 1.7 The ICRS Cartilage injury classification of four grades of cartilage defects (from the ICRS Cartilage Injury Evaluation Package [www.cartilage.org])

1.4.4 Pathogenesis and classification of Osteochondritis dissecans

The aetiology of Osteochondritis dissecans (OD) remains unclear, but it initially affects the subchondral bone and progresses to the overlying cartilage (Edmonds and Polousky, 2013). While the presence of OD has been reported in the wrist, elbow and ankle, the commonest site is the knee (Erickson et al., 2013).

There are two principles for classifying OD, based on the skeletal maturity of the patient and the stability of the lesion. According to skeletal maturity, OD can be 'juvenile' (patients with open physis) and 'adult' (skeletally mature patients) (Ochs et al., 2011).The stability of OD has been classified arthroscopically by the ICRS into four distinct types. These are stable and continuous lesion with no discontinuity but softened cartilage (ICRS type-I), a lesion which has partial discontinuity but remains stable on probing (ICRS type-II), a lesion which is completely discontinuous from the adjacent tissue but is not dislocated (ICRS type-III) and a lesion which is dislocated with a residual full-thickness cartilage and subchondral defect (ICRS type IV) (Brittberg and Winalski, 2003). The MRI scan criteria for defining the stability of OD are based on four parameters: (1) high T2 signal surrounding the OD, (2) subchondral cyst, (3) focal articular cartilage defect and (4) high T2 signal implying fracture through the cartilage (Kijowski et al., 2008). It is important to comprehend that ICRS type-III and type-IV OD are essentially osteoarticular defects comparable to ICRS Grade IV cartilage defect and hence amenable to bone graft in conjunction with cartilage repair strategy.

1.4.5 Literature review of autologous cell-based strategies for restoration of osteoarticular defects of the knee.

Different operative techniques are described for treating osteoarticular lesions, including drilling (Kocher et al., 2001, Edmonds et al., 2010), fixation (Kouzelis et al., 2006, Makino et al., 2005), excision of the fragment (Wright et al., 2004), osteochondral autografting (Laprell and Petersen, 2001), microfracture (Gudas et al., 2006, Gudas et al., 2012) and autologous chondrocyte implantation (ACI) with bone grafts (Bartlett et al., 2005), (Vijayan et al., 2012). However, the benefit of using ACI as a restorative surgery for such types of cartilage defects lies in its versatility to address defects larger than 2.5cm²(Erickson et al., 2013) and more than 8-10mm depth by concurrent autologous bone graft (Peterson et al., 2003), (Bentley et al., 2012). In the following section, a literature review has been undertaken to examine the level of current evidence in using ACI with bone graft for restoration of osteoarticular defects. We also examined the clinical and structural outcome of the repair site following use of such techniques, when available.

1.4.5.1 Literature Search results: The results of the literature review are summarised in Table 1.3. After reviewing abstracts of the relevant articles generated from the literature search, only seven articles were included and found relevant to the topic. One article was in German. Hence, only the abstract was reviewed. The articles included for review have been chronologically listed in Table 1.3.

Peterson et al. first described the use of concurrent bone graft with first-generation ACI for OD, in defects more than 1cm deep (Peterson et al., 2003). Their results demonstrated significant improvement in functional outcome in all 58 cases, but the results of 7 patients receiving concurrent bone graft with ACI (termed ‘sandwich’ technique) was not separately

reported. The first ‘sandwich’ technique had a bilayer of periosteum, one being anchored with the bone graft and the other attached to the adjacent cartilage with chondrocytes injected between these two layers (Peterson et al., 2003). This was subsequently modified with MACI to the bilayer collagen membrane technique (BCMT), with satisfactory clinical outcome in cases with OD (Bartlett et al., 2005). A further report from the same centre described the technique to be successful in cases of trauma and OD with osteoarticular defects (Vijayan et al., 2012). Two studies have drawn a correlation between the defect size and clinical outcome, stating that larger defects can potentially have the poorer outcome (Steinhagen et al., 2010, Filardo et al., 2012). Most of the studies except one (Bartlett et al., 2005) had a medium-term follow-up (mean 4-6 years) (Filardo et al., 2012, Ochs et al., 2011, Steinhagen et al., 2010, Vijayan et al., 2012). The studies found a trend of significant clinical improvement in comparison to the preoperative clinical scores for the first 12-24 months and subsequently the score was maintained at final follow-up.

Bone grafts were harvested from the distal femur (Vijayan et al., 2012, Ochs et al., 2011) (Bartlett et al., 2005), proximal tibia (Filardo et al., 2012, Steinhagen et al., 2010, Peterson et al., 2003) or iliac crest (Peterson et al., 2003, Ochs et al., 2011) but none of the studies describes donor site morbidity. The grafts were either loose cancellous bone (Bartlett et al., 2005, Filardo et al., 2012, Peterson et al., 2003, Vijayan et al., 2012) or cortico-cancellous cylinders harvested by a hollow diamond cutter (Steinhagen et al., 2010, Ochs et al., 2011). The study by Ochs et al. describes the use of glue between the bone cylinders when more than one cylinder was used. The study of Steinhagen et al. describes excising the cortical portion of the bone cylinders, actually rendering them to be cancellous bone cylinders, before impaction into the subchondral bone defect to restore the bone plate.

Vijayan et al.(2012) described the structural outcome of the BCMT in 8 out of 14 patients treated. Three samples of repair cartilage were fibrocartilage, two samples were mixed fibro and hyaline cartilage, two were fibrous tissue, and one was not defined (Vijayan et al., 2012). The study by Bartlett et al. also described histological outcome after BCMT in two patients, with one being fibrocartilage and one being hyaline. Importantly, both showed good integration of the repaired cartilage with the subchondral bone (Bartlett et al., 2005). Furthermore, radiological evidence of cartilage repair was first reported by Ochs et al. demonstrating a MOCART score of 62 out of a maximum score of 100 at a follow-up of 40 months (Ochs et al., 2011). The study by Ochs et al. also showed that filling of the defect and remodelling of the lamina formed between grafted bone and repair cartilage had a direct correlation with the clinical outcome of the patients undergoing MACI with bone graft (Ochs et al., 2011). Likewise, a subsequent observational study of 34 patients by Filardo et al. reported over 50% cartilage fill in 15 out of 17 patients. Most of these patients had no subchondral oedema and showed an isointense signal of the repair on available MRI scans (Filardo et al., 2012).

Macroscopic features of the graft site were reported by Bartlett et al. in four out of eight patients, with two being scored to be nearly normal(ICRS II) and two abnormal(ICRS II) as per the ICRS grading of cartilage repair (Bartlett et al., 2005). No further details were available for review. The report by Vijayan et al. indicates restoration of the osteoarticular height in nine patients during arthroscopic evaluation but again no objective scoring or further details were available for review (Vijayan et al., 2012).

Author & Year	Patient characteristics	Intervention	Bone graft	Clinical outcome	MRI feature	Histology	Arthroscopy
Peterson et al., 2003	58 patients (OD) mean age 26.4 years, mean defect size 5.7 sq.cm, mean depth 7.8mm (only seven patients deeper than 1cm treated with bone graft)	the sandwich technique with bilayer periosteum patch(1st generation ACI) with bone graft(only in7 patients)	Loose cancellous bone from iliac crest or proximal tibia	FU for mean 5.6 years. Modified Cincinnati score, Brittberg- Peterson score VAS, Tegner Wallgren score and Lysholm score significantly improved at two years but no sig difference from 2 years up to 10 years. No concrete results of 'sandwich' technique	13/15 patients with the appearance of normal looking cartilage at 3.5 years, deeper defects had cyst. Suggestion of bone remodelling and filling but no concrete results for 'sandwich' technique	No histology	22 patients, arthroscopic score of graft integrity mean 11.2/12 for all patients(no reports of patients requiring bone graft)
Bartlett et al., 2005	Eight patients (5 OD), mean age 26.4 years, mean defect size 5.2 sq. cm	MACI +cancellous graft (bilayer collagen membrane technique, BCMT-3rd generation ACI)	Loose cancellous bone graft from distal femur	FU for one year, Improvement in modified Cincinnati knee score, Visual analogue, Stanmore functional score(p-value-NA)	Not done	One fibrocartilage and 1 mixed fibro/hyaline cartilage with good integration	Two patients ICRS grade nearly normal and two patients abnormal
Maus et al., 2008(article in German)	13 patients with OD* (ICRS Grade 4) with mean defect size 8.1 sq.cm	MACI + cancellous bone chips or monocortical cancellous graft	autologous graft	clinical improvement in IKDC, Brittberg and ICRS score	Not available	No histology	No Arthroscopy
Steinhagen et al., 2010	22 patients with OD* (ICRS 3 and 4)mean age 29.3 years, mean defect size 6.57sq cm	MACI (Single layer)+Bone plug	proximal tibia with diamond cutter 2-3 depending	Significant improvement in Lysholm, IKDC up to 12 months which was maintained for 36 months. Defect > 6 sq.cm inferior outcome	No MRI scan	No histology	No Arthroscopy

Author & Year	Patient characteristics	Intervention	Bone graft	Clinical outcome	MRI feature	Histology	Arthroscopy
Och's et al., 2011	26 pts with OD* (ICRS 3 and 4), mean age 29.2, mean defect size 5.3 sq. cm and depth 8.7 mm,	MACI (Single layer)+Bone plug	monocortical cancellous 8mm diameter plug from the iliac crest or lateral part of the femoral condyle(for one plug)with a hollow diamond drill with glue in between the plugs	Mean FU 39.8 months with significant improvement in Lysoholm-G an IKDC score at one year which was maintained subsequently, filling of the defect and bone remodelling significantly correlated with Lysoholm-Gillquist and Tegner scores	Overall MOCART 62.4 +/- 18.9.Lamina remodelling grade increased significantly over time during follow-up	No histology	No arthroscopy
Vijayan et al,. 2012	14 patients, (6 trauma + 8 OD*), mean age 23.6 years, defect size 7.2 sq.cm, depth > 8mm	MACI + Cancellous bone graft (BCMT)	Loose cancellous bone graft from medial femoral condyle	Mean FU-5.2 years, Significant improvement in modified Cincinnati knee score, Visual analogue, Stanmore functional score (no time point)	Not reported	Eight biopsy samples (mixed 3, fibrocartilage 2, fibrous 2, non-diagnostic 1)	Nine arthroscopies at one year showed firm graft with stable margin and restored osteoarticular height (no scores)

Table 1.3 Summary of literature review for treatment of osteochondral defects or Osteochondritis dissecans using ACI and bone graft

1.4.5.4 Summary: Use of concurrent bone graft with ACI to restore osteoarticular defects has been shown to produce significant clinical improvement in mid-term follow-up studies. Larger defects are correlated with poor clinical outcome. A correlation of the filling of the defect and remodelling of the lamina with clinical outcome was also established.

Further evidence of the degree of integration of the bone graft, both histologically and from MRIs, and its correlation with clinical outcome, will be important to support full restoration of the bone defect. Assessing the surface appearance of the graft based on arthroscopic findings will also enhance the evidence base of the technique. No reports of the second generation ACI are available on this type of defects that require a concurrent bone graft. To summarise, simultaneous bone graft with ACI is a promising technique in challenging cases with loss of not only full thickness cartilage but also underlying bone. Further studies are required to study the structural outcome of such techniques.

1.4.6 Literature review of Autologous Chondrocyte Implantation with concurrent realignment for repair of articular cartilage in the malaligned knee joint

Techniques such as ACI (Minas et al., 2010, Minas et al., 2014), microfracture, abrasion arthroplasty (Matsunaga et al., 2007) and osteotomy around the knee (Saithna et al., 2014, Niinimäki et al., 2012) are commonly reported to treat cartilage defects with co-existent malalignment of the knee with variable degrees of success. However, a randomised controlled trial (RCT) established better clinical outcome in patients treated with ACI in comparison to microfracture (Saris et al., 2009). Furthermore, a mid-term report of the same group of patients at five years showed that patients receiving ACI early after the onset of symptoms (within three years) had a significantly better outcome in comparison to those receiving microfracture (Vanlauwe et al., 2011). Likewise, an RCT comparing the results of MACI with microfracture demonstrated significant clinical improvement in KOOS score after being treated with MACI and had significantly higher numbers of treatment failures in the microfracture group at two years follow-up (Saris et al., 2014). The existing evidence of treating malalignment together with cartilage defects in the knee using realignment osteotomy augmented with ACI is summarised in Table 1.4.

Authors	Patients	Technique	FU	Histology	Radiology	Predictors of failure
Ferruzi et al., 2014	56 patients with medial compartment OA + full thickness MFC cartilage loss(ICRS 3/4),	Comparison of HTO with ACI (18 patients) or MF(18 patients) and HTO alone(20 patients). All HTO's were medial opening wedge type.	11 years follow-up showed patients treated with HTO and ACI or HTO alone had significant improvement in HSS and WOMAC scores	None	Pre-op median varus in HTO 9 º, HTO +ACI is 8 º, HTO + MF is 7 º, and post-op median valgus for the whole series is 4º(range 2º varus to 7º valgus)	High BMI, Correction of varus < than 12 º and pre-op grade of OA-related to the failure. Previous meniscectomies are not linked to the failure.
Minas et al.,2014	33 patients with HTO and three patients with Distal femur varus osteotomy (DFVO) for malalignment of >3º with a concurrent cartilage defect	Mechanical axis aimed to be restored neutral except in cases with kissing lesion where overcorrection of 2º was performed with simultaneous ACI	15 years FU showed significant improvement in graft survivorship in comparison to the non-HTO group but there was no significant difference in clinical outcome at final FU	None	No data of the achieved correction	HTO improved graft survival.
Bauer et al., 2012	18 patients with full thickness cartilage loss in MFC, 15 patients with concomitant lesions of the tibia(kissing lesion)	17 lateral closing wedge HTO and one opening wedge medial HTO. All patients received MACI	FU showed significant KOOS score improvement up to 24 months which was maintained for 36 months but dropped at 60 months	One patient 20 months post HTO+MACI demonstrated hyaline-like cartilage with abundant proteoglycan matrix	Pre-op varus was median 6 º(range 5-8º), and post-op median valgus is 2º(range 6º varus to 8ºvalgus). MRI post op 12 months score 2.37(fair)	Defect size, concurrent tibial lesion,patelo-femoral OA, correction angle, BMI, previous meniscectomies, gender and age, are not significant predictors for successful MACI as evident on MRI scan

Authors	Patients	Technique	FU	Histology	Radiology	Predictors of failure
Bode et al., 2012	Retrospective study comparing only ACI(24 patients) with ACI and Osteotomy(19 patients) for 1-5º varus knees with ICRS 3-4 MFC defect; excluded patients with concomitant lesion in medial compartment, lateral compartment defect, limited range of movement, previous trauma	19 patients received medial opening wedge HTO with simultaneous ACI	FU at median 71.9 months showed no significant difference in both groups of patients evaluated with KOOS and WOMAC scores, but concurrent HTO significantly reduced reintervention	None	The pre-op varus for HTO+ACI was 3.53+/-1.09º and only ACI was 2.25+/-0.99 º, mean postoperative femorotibial angle was 8.16º+/-2.77º	Significantly high failure rates defined as requirement for further surgical intervention for patients with only ACI(10 patients) in comparison to patients with concomitant ACI(2 patients)
Minas et al., 2009	Total 155 patients: 48 patients received HTO, 44 patients received TTO, and the rest did not receive osteotomy. No further specific details on the HTO group reported.	HTO-opening wedge (36), closing wedge (11) and distal femoral osteotomy 1. These procedures were performed with concurrent ACI.	FU showed significant improvement in clinical outcome although no significant difference in patients with/without osteotomy	None	Pre-op >2º varus malalignment corrected to 2º(onto the tibial spine)	None
Franceschi et al., 2008	8 patients with 3 cm ²chondral defects(Outerbridge III or IV) on the tibial plateau in idiopathic varus knee; excluded patients >60 years, meniscal pathology, diffuse arthritis, concomitant MFC lesion or 'kissing' lesion	Arthroscopic MACI+opening wedge medial HTO	FU at 28 months(range 25-31), significant improvement of Lysholm, IKDC and VAS scores	None	pre-op varus 8.1º(range 4º-14º) and post-op valgus was 2.8º(range 1º-4º)	None

Table 1.4 Summary of existing evidence for concurrent realignment with ACI in knee for repair of cartilage defect

1.4.6.4 Summary: In summary, treating varus deformity of the knee with an underlying cartilage defect is a viable option. Successful outcome is reported for isolated MFC defects, medial tibial plateau chondral defects and also 'kissing lesions' of the medial compartment at short-term follow-up. Moreover, patients receiving HTO with ACI in the presence of underlying cartilage defects are additionally shown to have improved graft survival and decreased failure rates at long-term follow-up. However, long-term studies fail to identify a significant difference in clinical outcome scores after ACI with HTO and HTO alone statistically. There is also no consensus on the desired correction angle in this group of patients, but previous surgeries or meniscectomies do not seem to influence the outcome.

A striking absence of reports on the structural outcome of the repair site was noted in the existing literature, except in one study which described the MRI outcome in 15 patients. The report by Minas et al. describes the treatment of valgus knees with lateral compartment cartilage defect by using ACI and varus osteotomy but does not report the clinical outcome in these patients separately (Minas et al., 2014). In the present work, we evaluate the results of both varus and valgus osteotomy for lateral and medial compartment cartilage defect in the malaligned knee with reports of the structural outcome of the repair site as well as mid-term clinical follow-up in these patients.

1.5 Aims

The objectives of the present work are the following:

- To explore the potential of cartilage and bone formation by cells isolated from four anatomical parts of the umbilical cord and quantification of their surface phenotype according to the International Society for Cellular Therapy (ISCT) criteria for the definition of mesenchymal stem cells (MSC).
- To examine the efficacy of bone marrow stromal cells (BMSC) in new bone formation in a setting of nonunions in the fracture.
- To investigate the clinical, radiological and histological outcome of the concurrent bone graft with Autologous Chondrocyte Implantation in osteochondral defects of the knee.
- To assess the outcome of combined realignment and Autologous Chondrocyte Implantation in cases of idiopathic malalignment associated with an underlying cartilage defect.

Chapter 2: Cells from four regions of the Umbilical Cord by Explant Technique: A potential for Orthopaedic Regenerative Medicine

2.1 Introduction

Mesenchymal Stem Cells (MSCs) are self-renewing, plastic adherent cells with specific surface properties and immunoregulatory functions (Krampera et al., 2013, Dominici et al., 2006, Horwitz et al., 2005). First defined by Caplan in 1991, MSCs are found in tissues derived from the embryologic mesoderm; these cells have multi-lineage differentiation capacities triggered by environmental cues and their genetic potential (Caplan, 1991).

MSCs can be isolated from different developmental (adult vs foetal) or anatomical tissues, e.g. fat, bone marrow and umbilical cord (UC) (Chao et al., 2012) with standard defining characteristics (Dominici et al., 2006) and potential clinical applications. Bone marrow has been the most frequently used source of stem cells for research and clinical applications (Choudhery et al., 2013). UC-derived MSC has also been considered safe for the human clinical use with positive results in steroid-resistant graft versus host disease (GVHD) (Wu et al., 2011). Subsequently, these cells have been used as an adjunct to haematopoietic stem cell transplantation (HSCT) to enhance engraftment and leucocyte recovery without any reported adverse effects. Such applications suggest these cells have an immunomodulatory role in clinical settings (Wu et al., 2011, Chao et al., 2012, Wu et al., 2013).

The UC can be used as a readily available source of MSC and a possible alternative to bone marrow without subjecting patients to additional procedures to obtain the cells. There is minimal ethical concern in procuring cells from the UC since the cord is considered to be a biological waste, making it a globally available standardised resource for MSC- based research (Jeschke et al., 2011).

Stem cells from the UC have distinct advantages over bone marrow derived MSCs in their faster proliferation and innate immunoregulatory properties, making them an appealing donor source (Baksh et al., 2007, Mennan et al., 2013). Stem cells isolated from perinatal tissues such as the UC are intermediate between embryonic and adult stem cells in possessing pluripotent potentials and multipotent tissue maintenance properties (Taghizadeh et al., 2011). Cells from the UC have been reported to express Sox-2, Nanog and Oct-4, in addition to their capacity to transdifferentiate for tissue maintenance and homoeostasis (Carlin et al., 2006, Sarugaser et al., 2005).

UC-derived MSCs from the entire cord or particular anatomical locations have been isolated via explant cultures, enzymatic digestion or a combination of the two, with variable efficiencies (Sarugaser et al., 2005, Seshareddy et al., 2008, Pereira et al., 2008, Kadam et al., 2009, La Rocca et al., 2009, Gonzalez et al., 2010, Li and Cai, 2012, Han et al., 2013, Yoon et al., 2013). The explant culture system is based on the cellular migration potential commonly referred to as 'plate and wait' whereas in enzymatic isolation the cord extracellular matrix is digested to release the cells. A comparative review found the explant technique to be more time consuming but reliable in contrast to enzymatic isolation which was shown to be faster but more labour intense, with the risk of over-digestion of the tissue resulting in decreased cellular viability and altered function (Li and Cai, 2012).

Furthermore, explant cultures of the Wharton's Jelly (WJ) for isolation of MSCs showed high levels of FGF2 in the culture medium for 14 days in comparison to the enzymatic isolation technique which showed much smaller release for the same duration of time (Yoon et al., 2013). This is of particular importance because of the regulatory effect of FGF2 on both osteogenic and chondrogenic differentiation of MSC (Montero et al., 2000, Yoon et al.,

2013, Ng et al., 2008). Additionally, the cell yield and viability at passage 0 (P0) was noted to be significantly better in the explant group in comparison to those isolated enzymatically (Yoon et al., 2013). However, a recent study comparing cells isolated from four different regions of umbilical cords by the explant technique and enzymatic digestion of the whole cord suggested an absence of significant difference in their growth kinetics and MSC surface profile, although cells were derived more quickly and easily with the enzymatic technique (Mennan et al., 2013). Nevertheless, there are considerable variations in enzymatic isolation procedures used depending on the types of enzymes used, their concentration and the incubation time (Li and Cai, 2012). The diversity of such approaches has to be taken into account when comparing the *in vitro* and *in vivo* performance of these cells (Christodoulou et al., 2013).

The current International Society of Cellular Therapy (ISCT) working proposal has highlighted the need to characterise the immunoregulatory mechanism of MSCs fully and has outlined the multitude of experimental approaches, culture conditions, quantitative and qualitative methods and *in vitro* and *in vivo* models to assess such functions (Krampera et al., 2013). The heterogeneity in the intricacies of the methodology has led to a significant amount of scientific literature with poorly comparable results. Hence, the ISCT has recommended uniform methods of assessing the immunomodulatory effects of MSCs to obtain more consistent and reproducible data that may validate MSC-based therapeutic approaches for treating clinical conditions (Krampera et al., 2013).

This study reports the isolation of cells from four separate anatomical regions of the UC by the explant technique. These cells were culture-expanded by a uniform method and characterised according to the ISCT criteria for defining MSCs (Dominici et al., 2006);

additionally, the immunophenotype and expression of pluripotency markers in these cells were also investigated in the current work.

2.2 Materials and Methods

This study has been approved by the National Research Ethics Service, UK (Ref.no. 10/H10130/62). UCs were collected from the maternity unit at the Robert Jones and Agnes Hunt Orthopaedic Hospital, Oswestry, UK. All patients consented to the donation of the umbilical cord during an antenatal assessment in this midwife-led obstetric unit. Only umbilical cords from patients with normal deliveries were collected for this study.

2.2.1 Isolation technique and cell culture

UCs from five subjects were collected and stored in Dulbecco's phosphate buffered solution (DPBS) (Gibco, UK) at 4°C for up to 24 hours before tissue culture. The cords were divided into 5-6 cm long pieces which were longitudinally opened to expose and dissect the cord lining membrane (CL), Wharton's Jelly (WJ), umbilical cord artery and umbilical cord vein separately from within the whole cord (Figure 2.1- Illustration of the dissected UC). A histological section of the dissected umbilical cord artery and vein revealed remnants of the surrounding matrix and hence were described as umbilical cord peri-arterial (PA) tissue and umbilical cord peri-venous (PV) tissue in the present work (Figure 2.2- illustration of the histological section of the whole cord, PV and PA explant tissue).

These four types of tissues were separately dissected, minced into approximately 1-2mm^3 pieces and weighed. The minced tissues from the four layers of each cord were grown in four separate six-well plates (Starstedt, Leicester, UK). All types of explants were cultured in basal medium comprising of Dulbecco's modified Eagle's medium (DMEM) Glutamax (Gibco, UK), 15% (v/v) Foetal calf serum (FCS) (Life Sciences, UK), 1% (v/v) non-essential amino acid (Gibco, UK), 1% (v/v) Minimum Essential Medium (MEM) vitamins (Gibco, UK), 1% (v/v) penicillin and streptomycin (Life Sciences, UK) (Gonzalez et al., 2010). The plates were

incubated at 37°C and 5% (v/v) CO_2 for 21 days, and the medium was changed every 3-4 days.

During three weeks of culture, fibroblast-like adherent cells migrated from each type of explant. Extended periods of digitised images of cells migrating out of a peri-arterial explant were captured using phase contrast microscope connected to a digital video camera (TK-1280E; JVC, London, UK) kept in the tissue culture incubator. The series of digital images was converted to a video file by using Media Studio Video Editor Software (version 3.5, Ulead Systems, Karst, Germany). Adherent cells were detached using 0.25% (w/v) trypsin-EDTA solution (Invitrogen) followed by an equal volume of medium containing FCS (10%) to inhibit the activity of trypsin (passage 0 or P0). Cells were then centrifuged at 112g for 10 minutes (Harrier 18/80) to form pellets. These pellets were re-suspended in medium, and a viable cell count was performed with trypan blue exclusion on a haemocytometer. The cells were reseeded and cultured in monolayer for further expansion with the same medium. Cells were seeded at a density of 5000/cm² in 25 cm^2 tissue culture flasks (Corning Falcon, UK) for growth kinetics and 75 cm^2 tissue culture flasks (Corning Falcon, UK) for expansion. Media was changed 2-3 times per week. Cells were passaged successively at 80% confluence and reseeded. All experiments were performed at the third passage (P3) and fourth passage (P4).

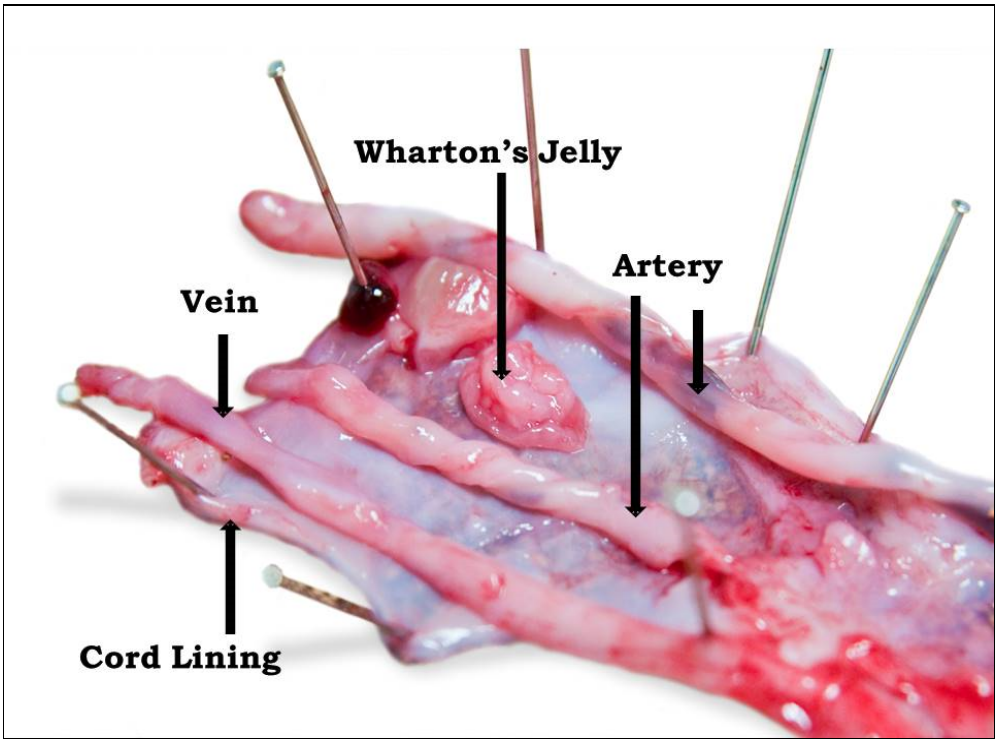

Figure 2.1 Dissection of the umbilical cord to obtain tissue from four regions for explant culture

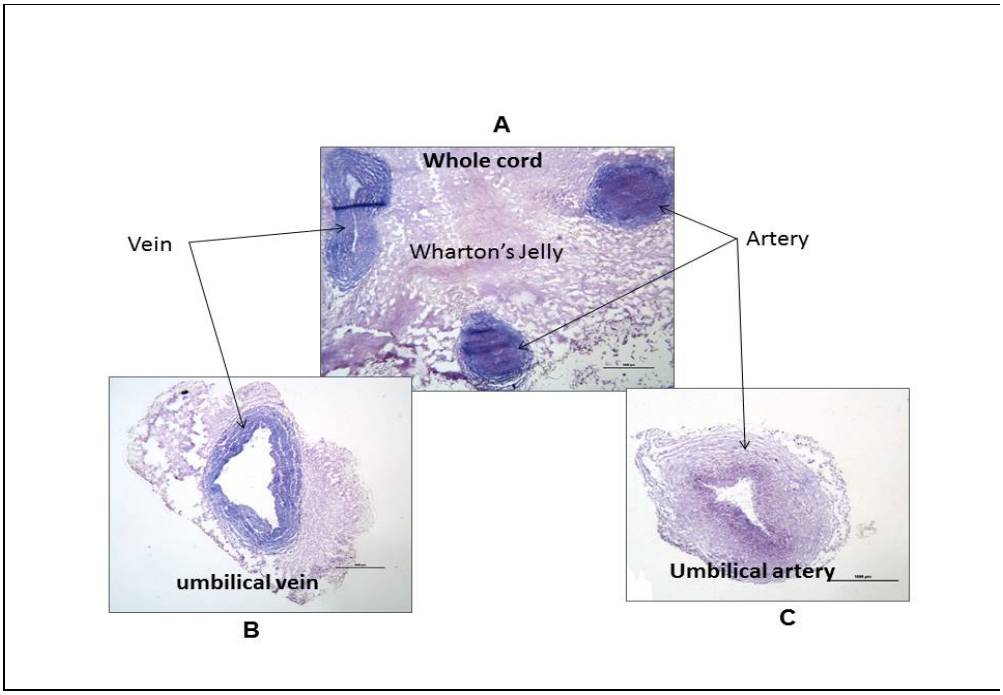

Figure 2.2 Histological section of (A) whole cord (without cord lining membrane) (B) dissected umbilical cord vein and (C) artery before explant culture. The cross-sectional image of umbilical cord artery and vein demonstrates the presence of supporting matrix (i.e. Wharton's Jelly) adherent to the outer surface following dissection of the vessels (scale bar represents 1000 µm)

2.2.2 Cell viability

At each passage cell viability was assessed by a trypan blue exclusion test. This was performed to ascertain the total number of viable cells obtained at confluence so that seeding density for further expansion and growth kinetics could be calculated. The principle of the test is based on the fact that viable cells have intact cell membranes and hence will not be stained whereas cells with disrupted cytoplasmic barriers will be stained blue from the dye.

After cells had been passaged and centrifuged to form pellets, these were resuspended in 1ml of the medium. A total of 10µl of the cell suspension was mixed thoroughly and added to an equal volume of 0.4% (w/v) trypan blue (Sigma-Aldrich) which was then loaded to a haemocytometer (Sigma-Aldrich) to calculate the number of viable cells.

2.2.3 Growth Kinetics

Cells from four separate layers of the UC (n=5) were grown to P3 in 25 cm^2 tissue culture flasks to ascertain the growth pattern of cells from different layers. The population doubling time between each passage from P0 to P3 was calculated by using the following equation:

Doubling Time (DT) = $(t_2-t_1) \times \ln(2)/\ln(n_2/n_1)$

where t_2-t_1 represents the final and initial time points, ln represents the natural logarithm, n_2 represents the final cell number harvested, and n_1 represents the initial number of cells seeded (Jordan and Smith, 2nd edition, 2000).

2.2.4 Cryopreservation of cells

Following the viable cell count described in section 2.2.2, a total of $1x10^6$ cells were re-suspended per 1ml of cold 10% (v/v) dimethyl sulphoxide (DMSO; Sigma-Aldrich) in FCS and stored in cryovials (Nunc, Fisher Scientific, Loughborough, UK). These vials were transferred to a liquid nitrogen container in designated boxes for long-term storage.

2.2.5 Cell recovery after cryopreservation

The cryovials were rapidly thawed in running hot tap water, and subsequently, 1 ml of the culture medium was added over a period of 1 minute to the thawed cell suspension. The culture medium was cooled on ice before being added by drops in the thawed cells. The cell suspension and the cold medium were left undisturbed for a further one minute. Next, 20ml of the medium was added in drops over 10 minutes. The cell suspension was then centrifuged for 10 minutes at 115g). Cell pellets were further resuspended in 20ml medium and centrifuged as described before. A trypan blue viable cell count as outlined in section 2.2.2 was undertaken before these cells were plated for monolayer culture at a density of 5000 cell/cm^2 at 37ºC with 5% CO_2 (v/v).

2.2.6 Tri-lineage mesenchymal differentiation

Differentiation potential was ascertained for cells from each of the four layers of UC (n=5) at P3. Cells were differentiated at 37°C and 5% (v/v) CO_2 with a change of media after every 3-4 days for 21 days.

2.2.6.1 Osteogenic differentiation: Cells from each layer of the cord were seeded at a density of $5x10^3$ per cm^2 into six-well plates separately and grown to 80% confluence. Osteogenic medium was prepared in DMEM F12 with 10% (v/v) FCS and antibiotics (penicillin and streptomycin, Life Sciences, UK) supplemented with 50μM ascorbate 2-phosphate, 10nM dexamethasone (Sigma) and 10mM β-glycerophosphate (Sigma-Aldrich)(Jaiswal et al., 1997a). Three wells were treated with osteogenic medium ('test wells'), and the remaining wells ('control wells') were treated with media having no osteogenic supplements for three weeks. Osteogenesis was assessed by using the following methods:

- *2.2.6.1.1 Cellular alkaline phosphatase (ALP) staining*

The alkaline phosphatase activity was determined via hydrolysis of the naphthol phosphate ester substrate (naphthol AS-BI phosphate) by the enzyme, the intermediate product then reacts with diazonium salt (fast red-TR) to form an insoluble azo dye indicating the site of its activity (Jaiswal et al., 1997b).

A solution was prepared with 25 mg naphthol AS-BI phosphate in 0.5ml of dimethylformamide (Sigma-Aldrich) which was mixed with 50ml of 0.2M hydroxymethyl hydrochloride (Tris-HCl buffer) to obtain a pH of 9 assessed with a pH metre (BDH Laboratory Supplies, Lutterworth, UK). A total of 50mg of Fast Red TR (BDH Laboratories,

UK) was added to the solution and mixed thoroughly and filtered (Whatman No.1 filter paper, Maidstone, UK) before use.

Control and test culture cells, each in three separate wells, were washed twice with PBS and fixed for 10 minutes with 4%(v/v) formalin (BDH Laboratories, UK) in PBS. Each well of the six-well plate was subsequently treated with 1ml of the staining solution and incubated for 1 hour at room temperature. The stain was thoroughly washed with PBS at room temperature. Formation of red colour indicated positive alkaline phosphatase activity (Jaiswal 1997).

- *2.2.6.1.2 Assay of ALP activity*

The culture medium from osteogenically differentiated and control cell preparations was measured in triplicate; that is culture medium from three control, and osteogenically differentiated wells for cells from four layers of the cord were collected separately. The ALP buffer was made with 50mM sodium carbonate added to 50mM Tris to pH 9.5. The buffer (45ml) was then mixed with 0.3ml of 0.5M magnesium chloride and 0.556g of para-nitrophenol phosphate (Sigma-Aldrich, UK). 50µl of the culture medium was added to 150µl of the ALP buffer and incubated for one hour at 37°C and 5% CO_2 (v/v) (Kubota et al., 2002). Colorimetric analysis of the ALP activity was measured by absorbance at 405nm wavelength using 650nm as a reference wavelength on a Bio-Tek Synergy HT plate reader.

2.2.6.2 *Chondrogenic differentiation*

A total of $5x10^5$ cells from each layer of UC were placed in a 1.5ml eppendorf (Sarstedt, UK) and centrifuged at 500g for 5 minutes in a microfuge (Henderson Biomedical, Beckenham, Kent, UK) to form pellets. These pellets were cultured in chondrogenic media containing DMEM Glutamax, 2% (v/v) FCS, 100µg/ml Gentamicin, 10µg/ml Insulin Transferrin Selenium (ITS)(Invitrogen), 0.1 mM ascorbate 2-phosphate (Sigma), 10nM dexamethasone and 10ng/ml transforming growth factor (TGF) β1 (Pepro Tech, UK). Pellets were incubated at 37°C and 5% CO_2 (v/v) and inverted after the first three days of culture (Johnstone et al., 1998, Williams et al., 2010). Media were changed every three days for 3-4 weeks.

- *2.2.6.2.1 Preparation for tissue sections*

The cell pellets were snap frozen in liquid nitrogen and stored at −80°C until use. These pellets were taken out and attached to a specimen holder kept at -20^0C with an embedding matrix (Cell Path, UK). Pellets were sectioned on a cryostat (Bright Instrument Co., Ltd., Huntingdon, UK) at 7µm thickness and collected on poly-l-lysine coated slides. These slides were labelled appropriately and stored at -20^0 C until further use.

- *2.2.6.2.2 Toluidine blue staining*

The sections were fixed for 10 minutes with 4% (v/v) formalin (BDH Laboratories, UK) in PBS. Subsequently, the slides were washed with PBS before staining with 1% aqueous toluidine blue stain to identify the presence of glycosaminoglycans (GAGs). A coverslip was finally applied on perspex mountant (Cell Path) following the staining.

- *2.2.6.2.3 Immunofluorescence for Type-II Collagen*

The poly-l-lysine coated slides were left at room temperature for 5-10 minutes to defrost, and then the sections of the pellets were delineated with a hydrophobic pen. 4800U/ml Hyaluronidase (Sigma, UK) was prepared in 0.025M sodium chloride and 0.05M sodium

acetate in distilled water at a pH of 5. This was stored in 1ml aliquots at -20^0 C. Chondroitinase ABC (MP Biomedicals, UK) was obtained at a concentration of 5 units per vial. A total of 100µl of buffer was prepared with 1.29g of TRIS and 0.8g of sodium acetate in 100µl of distilled water at pH 8. This was stored as 5µl aliquots at -20^{0}C with each vial containing 0.25U of chondroitinase ABC.

An aliquot of hyaluronidase (1ml, 4800U/ml) was combined with chondroitinase ABC (5µl, 0.25U/vial). This was added to the slides for 2 hours at room temperature and subsequently washed with PBS three times. Following washing, the slides were treated with 10% (v/v) buffered formalin in PBS for 10 minutes and washed with PBS three times. The slides were blocked with 5% (v/v) goat serum (Vector Laboratories) in PBS for 1 hour at room temperature with a further three washes in PBS. The slides were incubated overnight at 4^0 C with an antibody against type II collagen (IgG2a, CIIC1, Developmental Studies Hybridoma Bank, US) at 1:10 concentration in PBS or with mouse IgG2a at 1:500 concentrations as a control. A further negative control was treated with PBS alone. Positive controls comprised sections of human articular cartilage.

The next day the slides were washed with PBS thrice and incubated with the fluorescein-conjugated secondary antibody (Alexa Fluor, Thermo Fisher Scientific) at a concentration of 1:200 in PBS at room temperature for 1 hour in the dark. They were further washed with PBS thrice and mounted using Vectashield mountant containing 4', 6-diamidino-2-phenylindole (DAPI), followed by application of a coverslip for microscopic assessment using a fluorescent microscope (Leica) where green fluorescence indicated positivity for type-II collagen.

2.2.6.3 Adipogenic differentiation

Cells from the four regions of the UC were seeded at a density of $5x10^3$ per cm^2 into six-well plates and grown to 80% confluence. Adipogenic medium was prepared in DMEMF12 with 10% (v/v) FCS and antibiotics (penicillin and streptomycin, Life Sciences, UK) supplemented with 1μM dexamethasone (Sigma), 1% (v/v) Insulin Transferrin and Selenium (Invitrogen), 500nM 3-isobutyl -1-methylxanthine (IBMX) and 100μM Indomethacin (Sigma-Aldrich) (Pittenger et al., 1999). Three 'test' wells were treated with adipogenic medium, and the remaining three wells were 'controls' treated with a medium having no adipogenic supplements. Adipogenesis was evaluated by Oil-Red-O staining, evident as red in areas of intracellular lipid vacuoles.

- *Oil Red-O staining*

Triglycerides and cholesterol esters bind to Oil-Red-O, and hence this was used to determine intracellular lipid accumulation after adipogenic differentiation (Ramirez-Zacarias et al., 1992).The stain was freshly made by using 0.5g Oil-Red-O in 100ml of isopropyl alcohol (IPA) to prepare the stock solution. A total of 6ml of the stock was added to 4ml of distilled water to prepare the stain. This was filtered (Whatman No.1 filter paper, Maidstone, UK) before use. Control and test culture cells, each in three separate wells, were washed twice with PBS and fixed for 10 minutes with 4% (v/v) formalin (BDH Laboratories, UK) in PBS. A total of 1ml of staining solution was added to each well and then incubated for 1 hour at room temperature. The stain was then thoroughly washed with PBS at room temperature. Positive staining was evident with red staining of the intracellular lipid vacuole.

2.2.7 Mesenchymal stem cell surface markers

The BD Flow cytometer FACS scan™ was used to assess the immune profile of cell surface antigens on the cells obtained from four layers of the five UCs at P3. The surface markers tested were according to the ISCT recommendation for defining MSCs, i.e., ≥ 95% of cells must express CD105, CD90 and CD73; also, these cells should have ≤ 2% positivity for CD14, CD19, CD34, CD45 and HLA-DR (Dominici et al., 2006).

One million cells of each type were suspended in 1ml of blocking solution containing 10% (v/v) human IgG (Flebogamma DIF, Grifols UK Ltd, Cambridge, UK) made up in 2% bovine serum albumin (BSA) in DPBS. Cells were incubated on ice for 1 hour. The cells and blocking mixture were centrifuged at 500g for 5 minutes to form a pellet. This pellet was re-suspended in 2% BSA (in PBS), 100µl of this cell suspension was incubated in the dark for 30 minutes after the addition of the following phycoerythrin (PE) conjugated antibodies: CD14 (1:50), CD19 (1:50), CD31 (1:50), CD34 (1:100), CD45 (1:200), CD90 (1:200), CD105 (1:50), HLA-DR (1:200) (Immuno Tools, Germany) and CD73 (1:20) (Beckton Dickson and Company, UK). An isotype-matched control with IgG1 (1:50) and IgG2a (1:50) antibodies (Immuno Tools, Germany) was used for analysis. The cell and antibody mixture was incubated on ice placed on a gently moving platform in the dark to ensure thorough mixing. These cells were subsequently centrifuged twice with 1ml of 2% BSA in PBS to wash off the antibodies and finally were suspended in 200µl of BSA (2% in DPBS) for flow cytometry.

Computer-generated dot plots of unstained cells for each cell preparations were obtained with forward scatter on the x-axis denoting cell size and side scatter on the y-axis indicating granularity of the cells during flow cytometry (Fig 2.3). Each dot in this plot represents a cell or a cell debris fragment. The voltage and ampere setting of the viable cell population was

adjusted so that the majority of these cells appear in the middle of the dot plot. The viable cells typically had a pattern of being together, with cellular debris being the outliers. These viable cells were gated manually and cellular debris, which primarily appeared to the left of the dot plot, was excluded. The voltage and ampere setting were noted and the same procedure repeated for each type of cell preparation. Only gated cells were used for assessing the fluorescence intensity for each antigen. A collection criterion of 10,000 gated events was used for each type of antibody for analysis. Cell Quest Pro software (Beckton Dickson and Company, UK) was used to analyse the results.

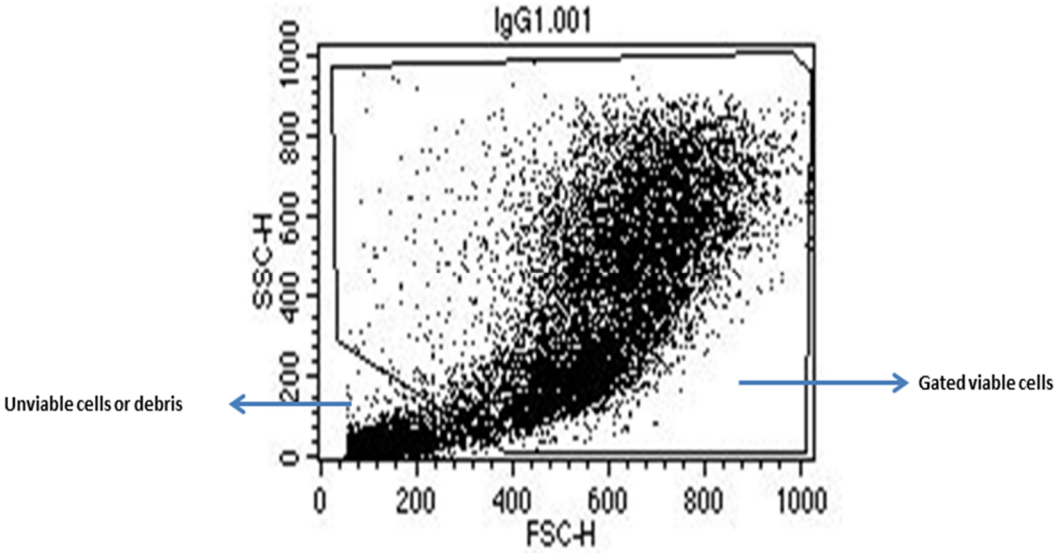

Figure 2.3 Gating of viable cells at the centre of dot-plot with the x-axis representing forward scatter (FSC) and the y-axis representing side scatter. The cell population excluded on the left-hand corner of the graph represents unviable cells or debris

2.2.8 Pluripotency markers

A list of pluripotency markers ascertained in these cells is detailed in Table 2.1. Different techniques have been improvised to identify the presence of these markers which are also elaborated in the following section.

Pluripotency markers	Characteristics features
TRA 1-60	Antigen expressed in podocalyxin, a large keratan sulphate membrane proteoglycan expressed in embryonic stem cells and embryonic cancer cells (Schopperle and DeWolf, 2007). TRA 1-60 antibody reacts with neuraminidase sensitive epitope of the proteoglycan molecule (Zhao et al., 2012)
TRA 1-81	Antigen expressed in podocalyxin, a large keratan sulphate membrane proteoglycan expressed in embryonic stem cells and embryonic cancer cells (Schopperle and DeWolf, 2007). TRA 1-81 antibody reacts with neuraminidase insensitive epitope of the proteoglycan molecule (Zhao et al., 2012)
ALP	Enzymatic marker noted to have high expression in both human and mouse embryonic stem cell (Draper and Fox, 2003, Koestenbauer et al., 2006)
SOX-2	Member of the SOX family of transcription factor regulating pluripotency, it works in conjunction with Oct3/4 and acts as a 'molecular rheostat' in embryonic cells to promote differentiation (Boer et al., 2007)
Nanog	A highly divergent homeodomain containing protein expressed in pluripotent embryonic stem cells (Silva et al., 2009)
Oct-3/4	Member of POU family transcription factor, structurally an octamer binding protein expressed in embryonic stem cells promoting differentiation and the type of cell formed depends on the level of expression of Oct3/4 (Niwa et al., 2000)
REX-1	Member of the Ying Yang (YY) subfamily of transcription factor is a marker of pluripotency independent of Oct4 which influences mitochondrial fission required for appropriate cell cycle progression required for pluripotency (Son et al., 2013)
SSEA-1	Glycolipid molecule controlling cell surface interaction during development noted in human germ cells, teratocarcinoma cells, oviduct cells and epididymis with conspicuous increase in expression following differentiation (Zhao et al., 2012)
SSEA-3	Cell surface glycoprotein noted in embryonic cells at an early-cleavage stage playing potential role in early embryogenesis (Kannagi R et al., 1983)
SSEA-4	Early embryonic glycolipid antigen used as a marker of undifferentiated pluripotent human embryonic stem cells (Gang et al., 2007)

Table 2.1: Description of the pluripotency markers ascertained on the cells from four cord regions

2.2.8.1 Immunocytochemistry: This was used to determine the expression of pluripotency markers with antibodies against Nanog (R&D Systems), REX-1 (Abcam) and OCT 3/4 (BD Biosciences) (Table 2.2) on cells derived from the four regions of UC cultured in monolayer at P4. Cells from CL, WJ, PA and PV were seeded onto chamber slides (BD Biosciences) at a density of 5000 per cm^2. Once cells had adhered (after three days), media was removed, and cells were washed twice with PBS before being fixed with 4% paraformaldehyde (w/v) for 20 min. Slides were washed twice with PBS before being blocked with buffer made up of BSA (1%), Triton X-100 (0.1% made in PBS) and either 10% donkey serum (for antibodies against Nanog) or 10% goat serum (for antibodies against REX-1 and OCT3/4) in PBS for 1 hour at room temperature. Slides were washed twice in PBS before being stained with the primary antibodies in freshly prepared respective blocking buffers. The following concentration of primary antibodies was used - Nanog (1:50), REX-1 (1:100) and Oct 3/4 (1:100) and incubated overnight in the dark at 4^oC. Primary antibody was subsequently removed, and slides were washed twice with PBS. Cells were stained with Alexa-Fluor 488 (1:250) (Invitrogen) conjugated with the respective secondary antibodies in blocking buffer and incubated for one hour at room temperature in the dark. The isotype controls for each antibody and PBS controls were also used alongside the primary antibodies (Table 2.2). Slides were washed twice with PBS before DAPI stain with Vectashield mounting medium (Vector Laboratories) was added under a coverslip, and cells were viewed under a fluorescent microscope (Leica Microsystems).

Primary antibodies	Primary antibody source	Secondary antibody	Isotype control	Isotype control, Primary & Secondary antibody conc.
Rex-1	Polyclonal rabbit IgG	Goat Anti-rabbit Polyclonal IgG	Rabbit IgG	1:100
Oct3/4	Polyclonal mouse IgG	Goat Anti-mouse Polyclonal IgG	Mouse IgG	1:100
Nanog	Polyclonal goat IgG	Donkey Anti-goat Polyclonal IgG	Goat IgG	1:50

Table 2.2 Antibodies used for pluripotency markers

2.2.8.2 Flow cytometry: Fluorometric assay was used to determine the expression of pluripotency markers TRA 1-60, TRA-1-81, SSEA-1, SSEA-3, SSEA-4 and alkaline phosphatase (ALP). A total of 9x 10^5 cells from each of the four layers of UC (n=4) were suspended in 0.9 ml of blocking solution (details in section 2.2.7). Cells were incubated on ice for one hour. The cells and blocking mixture were centrifuged at 500g for 5 minutes to form a pellet. This pellet was re-suspended in 2% BSA (in PBS). 100µl of this cell suspension (total 600µl) was incubated in the dark for 30 minutes after the addition of the pluripotency markers. The concentration of fluorescein isothiocyanate (FITC) conjugated pluripotency markers used was: TRA 1-60 (1:10), TRA-1-81(1:10), SSEA-1 (1:10), SSEA-3(1:10), SSEA-4(1:100) and alkaline phosphatase (ALP) (1:20) (all donated by Mark Jones from the Sheffield University, UK). Additionally, 100µl of this cell suspension was used for isotype-matched control with FITC IgG (1:50) antibodies (Southern Biotech). These cells were subsequently centrifuged twice with 1ml of 2% BSA in PBS to wash off the antibodies, and finally, they were suspended in 200µl of BSA (2% in PBS) for flow cytometry. The rest of the method of flow cytometry is described in section 2.2.7.

2.2.8.3 Fixation and permeabilisation followed by flow cytometry: This technique was undertaken to determine the presence of for Sox-2 antigen, another marker of a pluripotent state. The remaining 200µl of cell suspension was divided equally amongst PE-conjugated Sox-2 (1:50)(BD Bioscience), and PE-conjugated IgG2 (1:50) isotype-matched control (Immunotools, Germany) which were incubated separately for 30 minutes in ice placed on a gently moving platform to ensure thorough mixing. The cell suspension (100µl each) was fixed and permeabilised with 250µl of fixation and permeabilisation buffer (BD Cytofix/Cytoperm^{TM} plus) for 30 minutes. This was subsequently washed with 1000µl BD

Perm/Wash™ buffer and resuspended in 100µl of the same buffer before staining with the PE-conjugated Sox-2 antibody (2µl), and PE-conjugated IgG2 isotype control (2µl) for 30 minutes in the dark on ice for intracellular staining. Next, the cell suspensions with the antibody were washed twice with 1000µl BD Perm/ Wash™ buffer again and resuspended in 200µl of 2% BSA (in PBS) for flow cytometry. The Cell Quest Pro software was used to analyse the results for both FITC and PE-conjugated antibodies with their controls.

2.2.9 Immunoprofile of cells

Flow cytometry was also used to ascertain the immune profile of the cells derived from the four regions of the UC at P4. The method of flow cytometry is the same as described in section 2.2.7. The following PE-conjugated antibodies were used: HLA-ABC (ImmunoTools, Germany), CD-40 (BD Biosciences), CD-80(BD Biosciences) and CD-86 (BD Biosciences). PE-conjugated IgG1 or IgG2a (1:50) antibodies (both ImmunoTools, Germany) were used as isotype controls. The BD Flow cytometer FACS scan™ was used according to the protocol described in section 2.2.4 for flow cytometry and analysed with Cell Quest Pro software.

2.2.10 Statistical analysis

A Shapiro-Wilks test was used to ascertain the normality of the data. The relationship between the numbers of cells isolated ($x10^6$) per gram of explant tissue was determined by Pearson's correlation coefficient. A one-way ANOVA was used to determine the difference between the DT's of cells (dependent factor) derived from the four UC regions (independent factors/groups) during each passage with a *posthoc* test (Bonferroni) to identify differences in the DT's between or within groups for each cell preparation over three passages. The data for ALP activity was not normally distributed hence it was log transformed to achieve normal distribution (ascertained by Q-Q plot). A mixed model analysis was performed with the four regions of the cord and the treatment to the respective cell preparations (osteogenic differentiation and control) as fixed effects with the ALP activity as dependent variable to obtain the intercept (random effect. All analyses were done using SPSS software (Version 22.0.0.0, IBM United Kingdom Ltd, Portsmouth, UK). For all analyses, a two-tailed p-value of 0.05 or below was assumed to denote significance.

2.3 Results

2.3.1 Isolation technique and cell culture

All four layers of the UC (n=5), WJ, CL, PA and PV, produced plastic adherent fibroblast-like cells within 21 days of explant culture (Figure 2.4). Moreover, these cells had heterogeneous morphology, particularly cells derived from PA and PV tissues appeared predominantly smaller in size. A live video image of these cells emanating from the PA explant (refer to video image) showed these cells to change its shape and size constantly.

The weight of each cord region and the cell yield at P0 were found to be normally distributed (Shapiro-Wilks test $p>0.05$). There was no statistically significant correlation between explant weight and cell yield from the different layers of the UC at P0 (p-value>0.05). However, a significant correlation was noted between the numbers of cells isolated ($x10^6$) per gram of explant tissue from the PA, PV and CL, but not with cells per gram of WJ explant tissue. This implied a mutual relationship of the PA, PV and CL explant tissue weight to the number of cells retrieved from each of this region of the cord. The relationship between the cells isolated ($x10^6$) per gram of explant tissue from the PA, PV and CL and WJ are shown in Table 2.3 and 2.4.

Cord Layers (n=5)	Mean Explant Weight ± SD (in gm)	Mean Cell yield ± SD ($x10^6$)	Mean no. of cells ± SD ($x10^6$) per gram of explant tissue	p-value(between explant weight and cell yield)
CL	1.3±0.72	2.3±3.1	1.4±1.4	0.2
PA	0.74±0.9	1.4±1.7	3.01±3.4	0.8
PV	0.4±0.35	1.2±1.16	4.01±4.8	0.8
WJ	0.62±0.66	0.70±0.75	2.3±3.6	0.7

Table 2.3 Relationship between weight of explant and number of cells at P0

		PA cells per gm	PV Cells per gm	CL Cells per gm	WJ Cells per gm
PA cells per gm	Pearson Correlation	1	.957*	.937*	.563
	Sig. (2-tailed)		.011	.019	.323
	N	5	5	5	5
PV Cells per gm	Pearson Correlation	.957*	1	.994**	.306
	Sig. (2-tailed)	.011		.001	.616
	N	5	5	5	5
CL Cells per gm	Pearson Correlation	.937*	.994**	1	.258
	Sig. (2-tailed)	.019	.001		.675
	N	5	5	5	5
WJ Cells per gm	Pearson Correlation	.563	.306	.258	1
	Sig. (2-tailed)	.323	.616	.675	
	N	5	5	5	5

*. Correlation is significant at the 0.05 level (2-tailed).

**. Correlation is significant at the 0.01 level (2-tailed).

N is the number of the umbilical cord.

Table 2.4 Correlation between cell yield (in 10^6) per weight(in gm) of respective explant tissue at P0

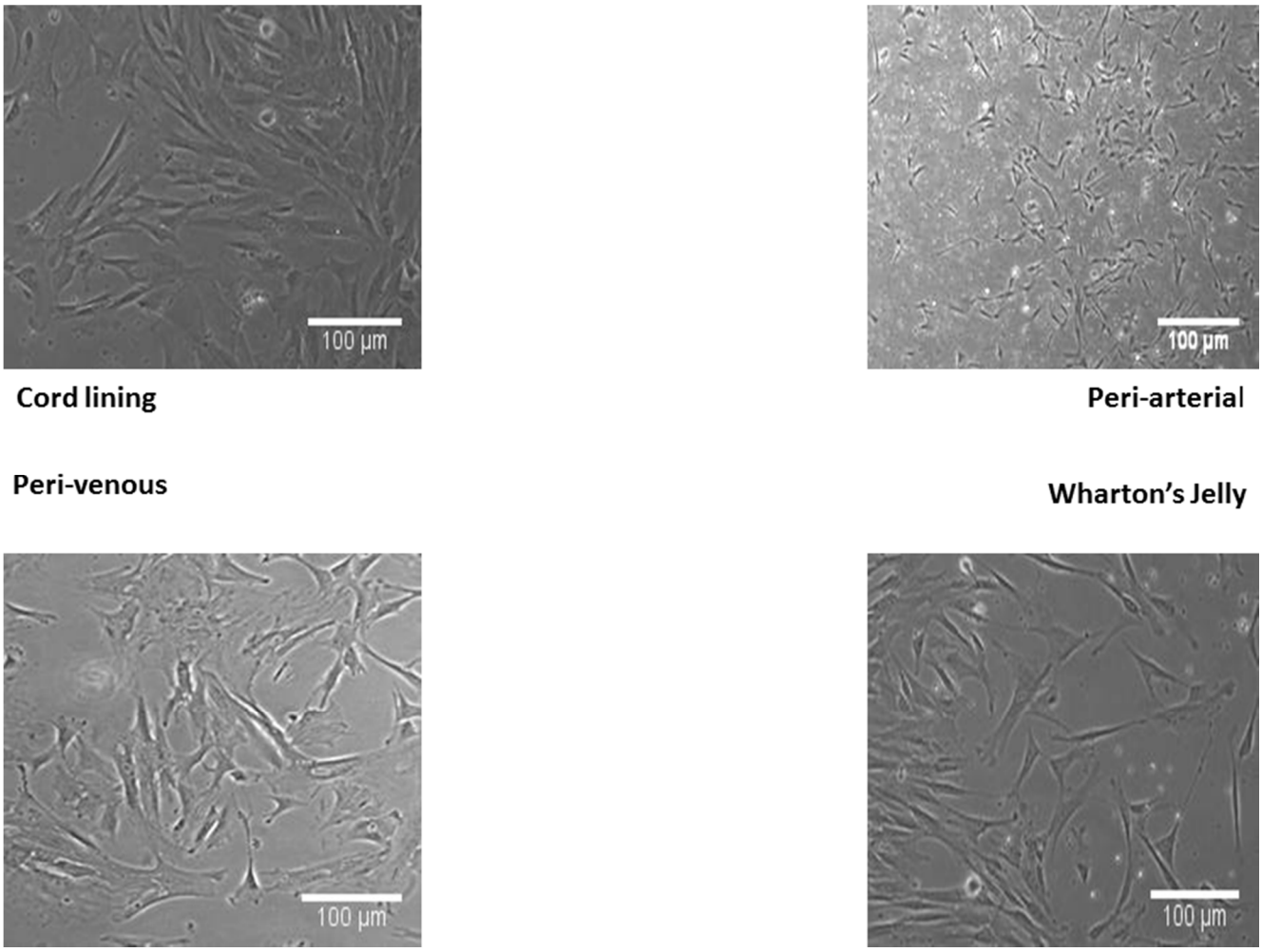

Figure 2.4 Cells at P0 isolated from four separate anatomical regions of the umbilical cord by explant culture technique

2.3.2 Growth Kinetics

The mean DT of all four types of cells was compared for three consecutive passages (P1 to P3) from four UCs. Mean DT from P1 to P3 for PA were 2.9± 0.17 (CI 1.9-3.9) days, PV cells were 3.8± 0.48(CI 2.6-5) days, CL cells were 3.5 ± 1.3 (CI 0.4-6.6) days, and WJ cells were 2.9 ±0.83 (CI 0.9-4.9) days. There was no statistically significant difference between the mean DT of cells from four UC regions (p-value < 0.05). A one-way ANOVA, with cells from all four UC regions being the independent factor (groups) and DT of cells during each passage being dependent with the *posthoc* test (Bonferroni) revealed no significant difference in cell doubling time between cells from the different regions for all three passages. The DT of cells from four anatomical regions of UC from P1 to P3 is illustrated in Figure 2.5.

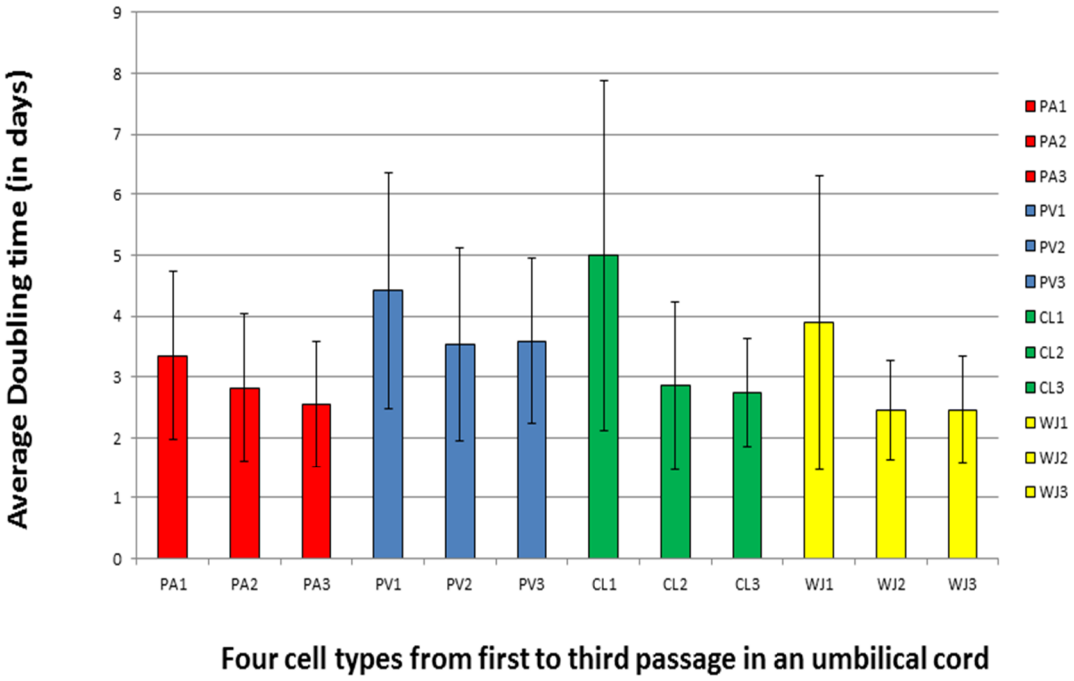

Figure 2.5 Mean doubling time of cells from four regions of the umbilical cord at three consecutive passages

(Error bar represents one standard deviation)

(PA-Peri-arterial cells, PV-Peri-venous cells, CL-Cord lining cells, WJ-Wharton's Jelly cells and the number script represent respective passages)

2.3.3Tri-lineage mesenchymal differentiation potential

2.3.3.1 Osteogenic differentiation

- *2.3.3.1.1 ALP staining*

Cellular ALP staining was positive in 'test' wells of cells from all four types of explants. Cells derived from PV tissues were noted to produce consistently better and uniform cellular staining subjectively in comparison to the other three cell preparations (Figure 2.6).

- *2.3.3.1.2 Semi-quantitative estimation of ALP activity*

The ALP activity was measured in triplicate in the culture medium for each type of cell preparations (3 wells containing control and 3 with osteogenically differentiated cells for each region from each cord). The ALP activity data was log-transformed to ensure a normal distribution which was ascertained by a Q-Q plot. ALP activity in the osteogenic medium was higher than their respective controls ($p=0.002$) for each type of cell preparation from the four distinct anatomical areas (Figure 2.7). A mixed model analysis showed osteogenic media from WJ cells had significantly less ALP activity in comparison to the osteogenic media from PA, PV and CL cells (p-value<0.05).

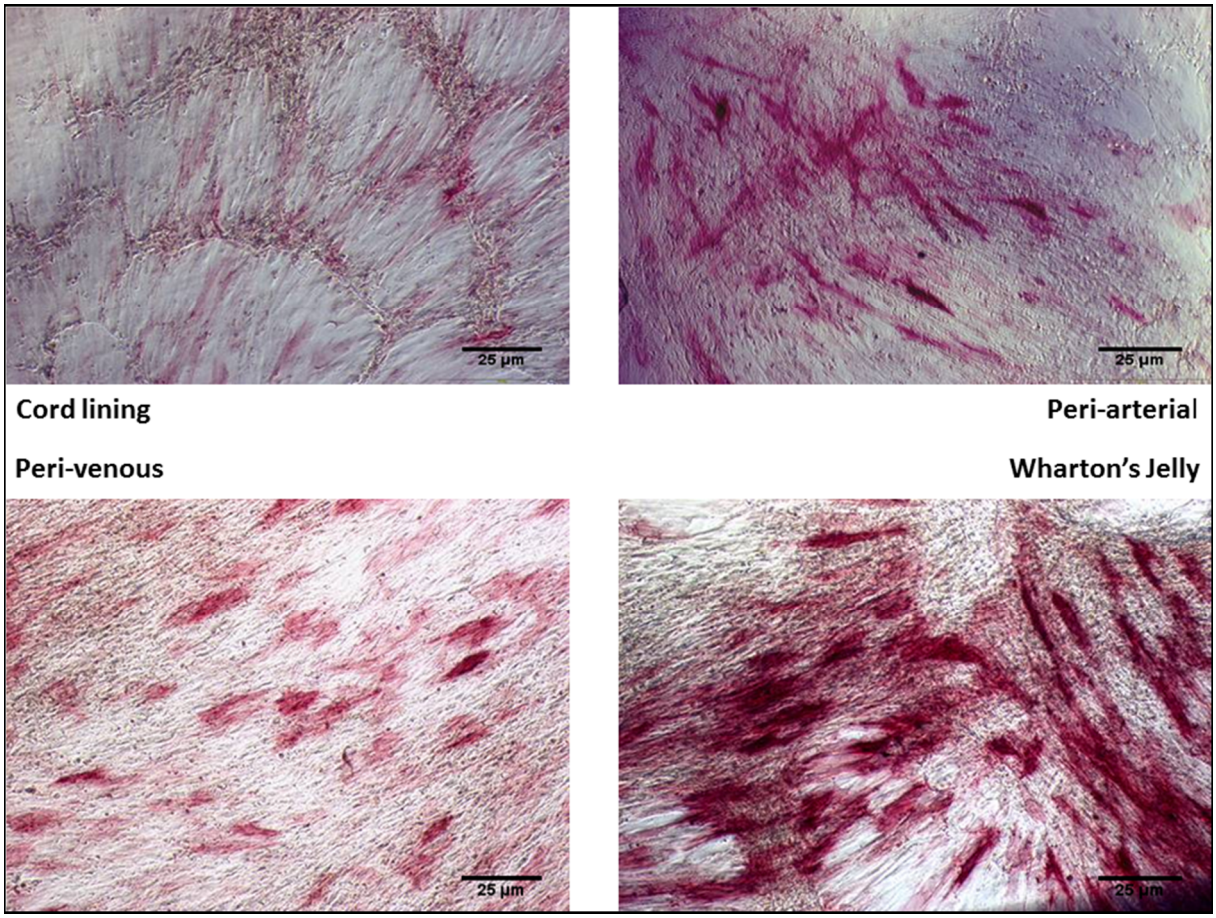

Figure 2.6 Alkaline phosphatase staining of cells from all four regions of the umbilical cord-Peri-arterial cells, Peri-venous cells, Cord lining cells and Wharton's Jelly cells at 21 days following osteogenic differentiation at P3 (scale bar represents 25 µm)

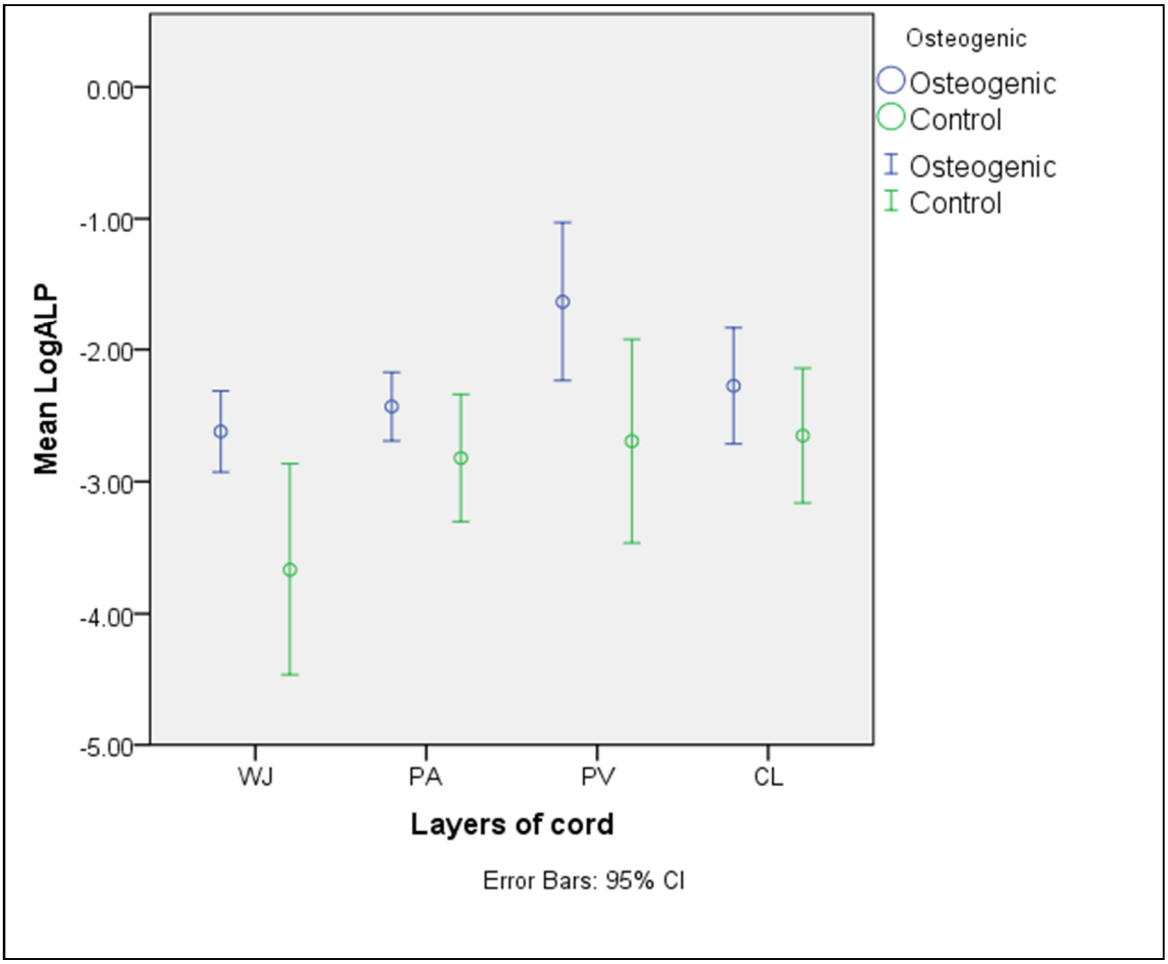

Figure 2.7 Alkaline phosphatase activity of the culture media from osteogenically differentiated cells and controls cells derived from four cord regions after 21 days at P3

(PA-Peri-arterial, PV-Peri-venous, WJ-Wharton's Jelly, CL-Cord lining)

2.3.3.2 Chondrogenic differentiation

- *2.3.3.2.1 Toluidine blue staining*

The staining for matrix metachromasia varied for different cell preparations after chondrogenic differentiation. The WJ and PV cell types showed consistently more staining in comparison to PA and CL cells, implying higher glycosaminoglycan content (Figure 2.8).

- *2.3.3.2.2 Immunofluorescence for Type-II Collagen*

All four cell preparations from the separate anatomical regions of the cord were tested for the presence of type II collagen (n=3). Only one pellet from WJ cells from one cord had a single area immunopositive for type II collagen staining. All other pellets from all four types of cell preparations were found to be negative for type II collagen following chondrogenic differentiation after 3-4 weeks.

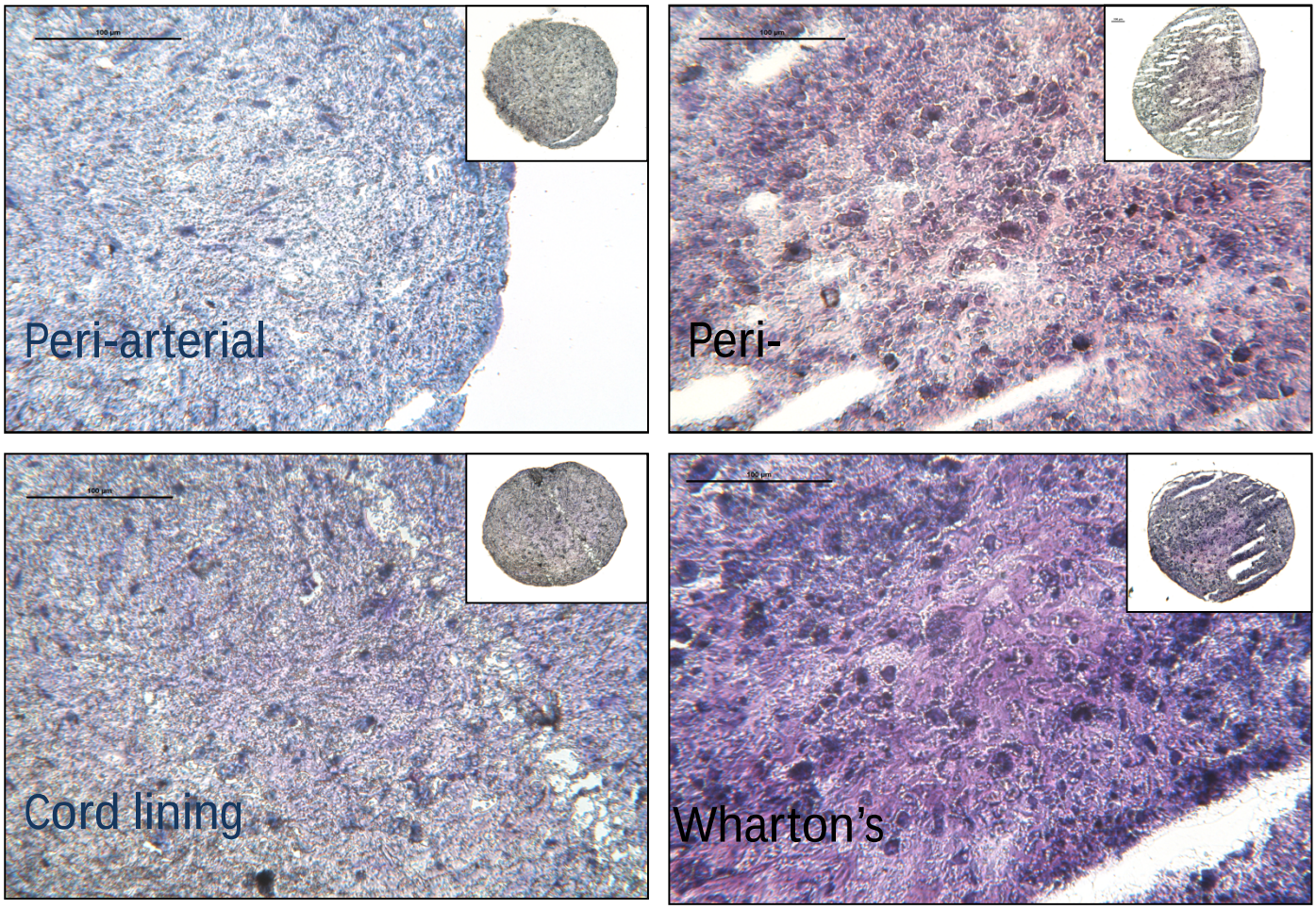

Figure 2.8 Toluidine staining following chondrogenic differentiation of Peri-venous cells, Peri-arterial cells, Cord lining cells and Wharton's Jelly cells (scale bar represents 100µm)

2.3.3.3 Adipogenic differentiation: This was observed by Oil Red-O staining of all cell preparations after culture in adipogenic differentiation medium for 21 days. Intracellular lipid accumulation was evident in all types of cell preparation although it was more pronounced in WJ cells (Figure 2.10). Spontaneous adipogenesis was not observed in any control wells.

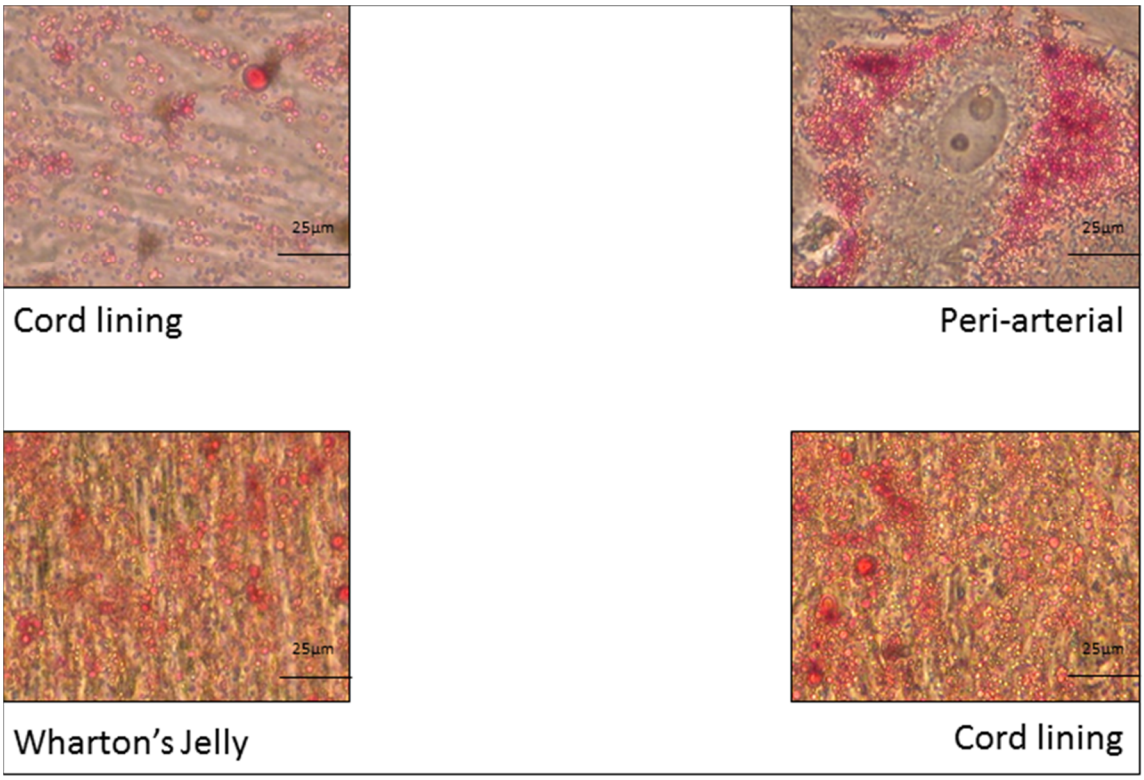

Figure 2.9 Oil Red-O staining following adipogenic differentiation of cells from the four cord regions after 21 days (scale bar represents 25 µm)

2.3.4 Mesenchymal stem cell surface markers

Cells from four regions (PA, PV, CL & WJ) of five UC were studied for characterising the surface profile of CD-antigens according to the ISCT guidelines for the definition of MSC (Dominici et al., 2006). All cell preparations showed immunopositivity for CD105, CD90 and CD73 with minimal expression of the CD14, CD19, CD34, CD45 and HLA-DR. However, quantitative analysis revealed that only two PV and one WJ cell preparation from two UC complied exactly with the limits defined by Dominici et al. (2006) to fulfil the criteria of MSC (Figure 2.11).

The frequency of cells positive for CD105 and CD73 varied widely for cells derived from all four regions with cells from PA and PV being more closely comparable. The CD90 expression was noted to have the least variability amongst these cells from all the areas of UC except WJ-derived cells. All PV cell preparations had ≤ 2% positivity for CD14, CD19, CD34, CD45 and HLA-DR rendering them compliant to the ISCT definition for these markers. Cells from all four regions of a single UC were noted to be extreme outliers (represented by *). The trend of the surface marker expressions for all the four types of cell preparations is demonstrated in Figures 2.12 and 2.13.

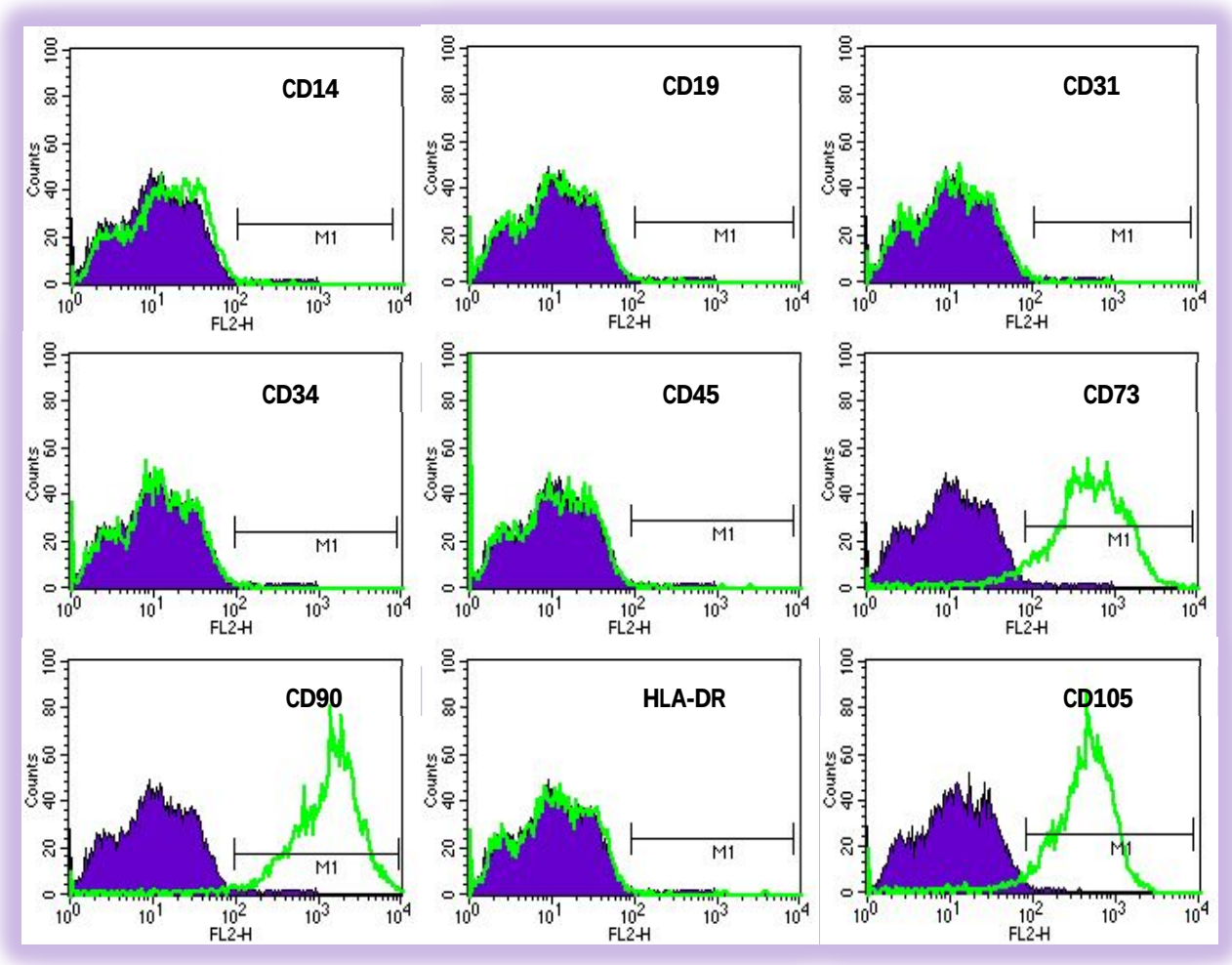

Figure 2.10 Representative flow cytometry profile of cells isolated from Wharton's Jelly complying with the criteria of ISCT for definition of MSC (Dominici et al., 2006)

(The blue shaded area represents the surface expression of isotype-matched controls, and the green line graph represents the expression of the respective surface markers on the cells)

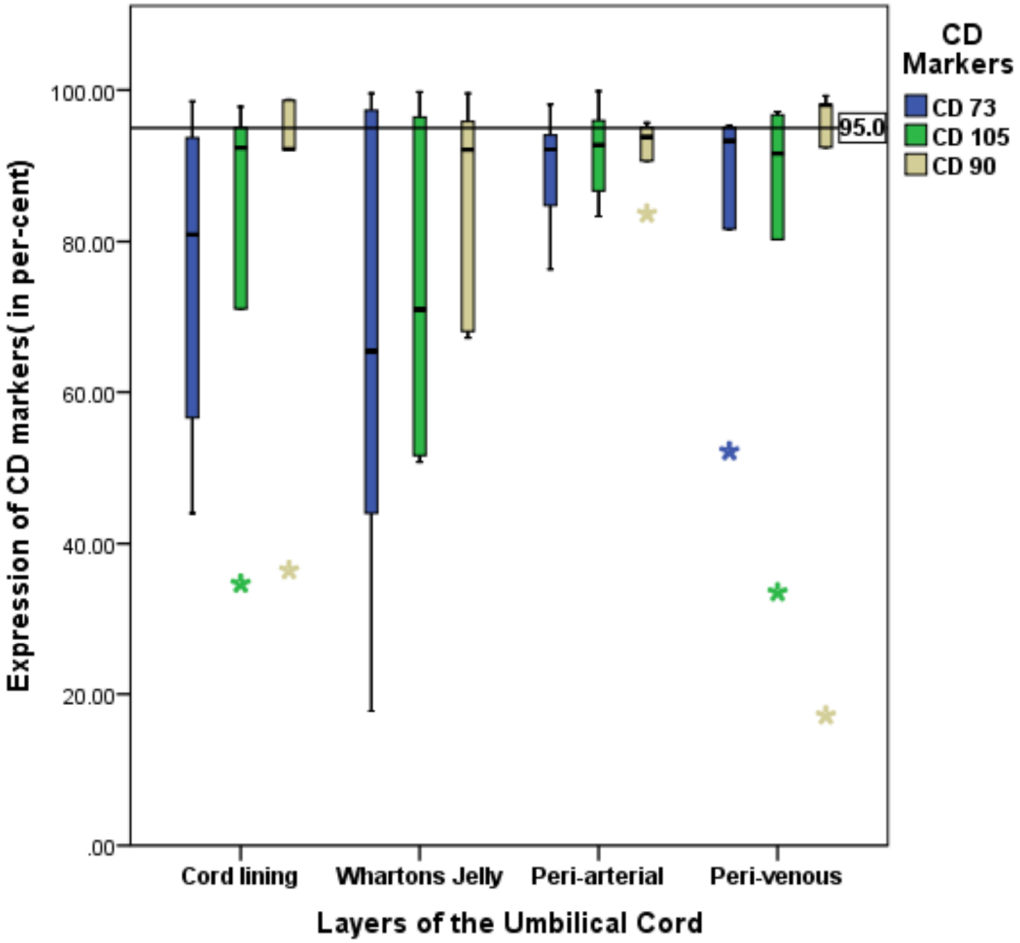

Figure 2.11 Positive CD markers on cell preparations of umbilical cords (n=5) from four regions (*shows outliers). The horizontal line denotes the defined quantitative levels according to the International Society for Cellular Therapy (Dominici et al., 2006). CD 90 was noted to have the least variability between cells derived from all the regions except Wharton's Jelly.

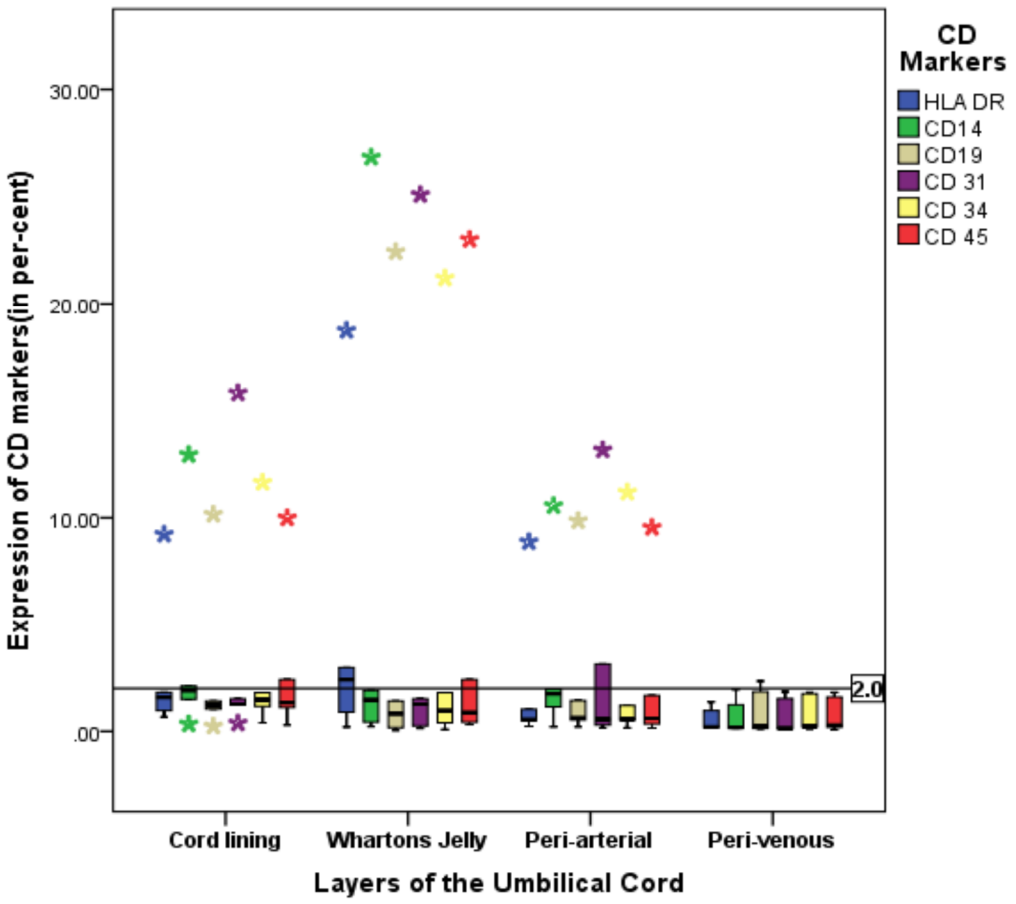

Figure 2.12 Negative CD markers on cell preparations of umbilical cords (n=5) from four regions (*shows outliers). The horizontal line denotes the defined quantitative levels according to the International Society for Cellular Therapy (Dominici et al., 2006). The cells from peri-venous regions complied with the quantitative criteria of less than 2% expression of the surface marker.

2.3.5 Pluripotency markers

Cells from all four regions of UC (n=4) were immunopositive for REX-1 (Figure 2.13), but none of the cell populations was positive for Nanog or Oct 3/4 on immunofluorescence microscopy.

Similarly, the four cell populations from the cord (n=4) had a positive surface expression of SSEA-4, ALP and SOX-2 in comparison to their isotype controls. In contrast, cells derived from all four layers lacked expression of TRA 1-60, TRA 1-81, SSEA-1 and SSEA-3.

2.3.6 Immunoprofile of cells

All cells from the four regions of the cord at P4 had a surface expression of HLA-ABC, but there was a total absence of co-stimulatory molecules of CD-40, CD-80 and CD-86.

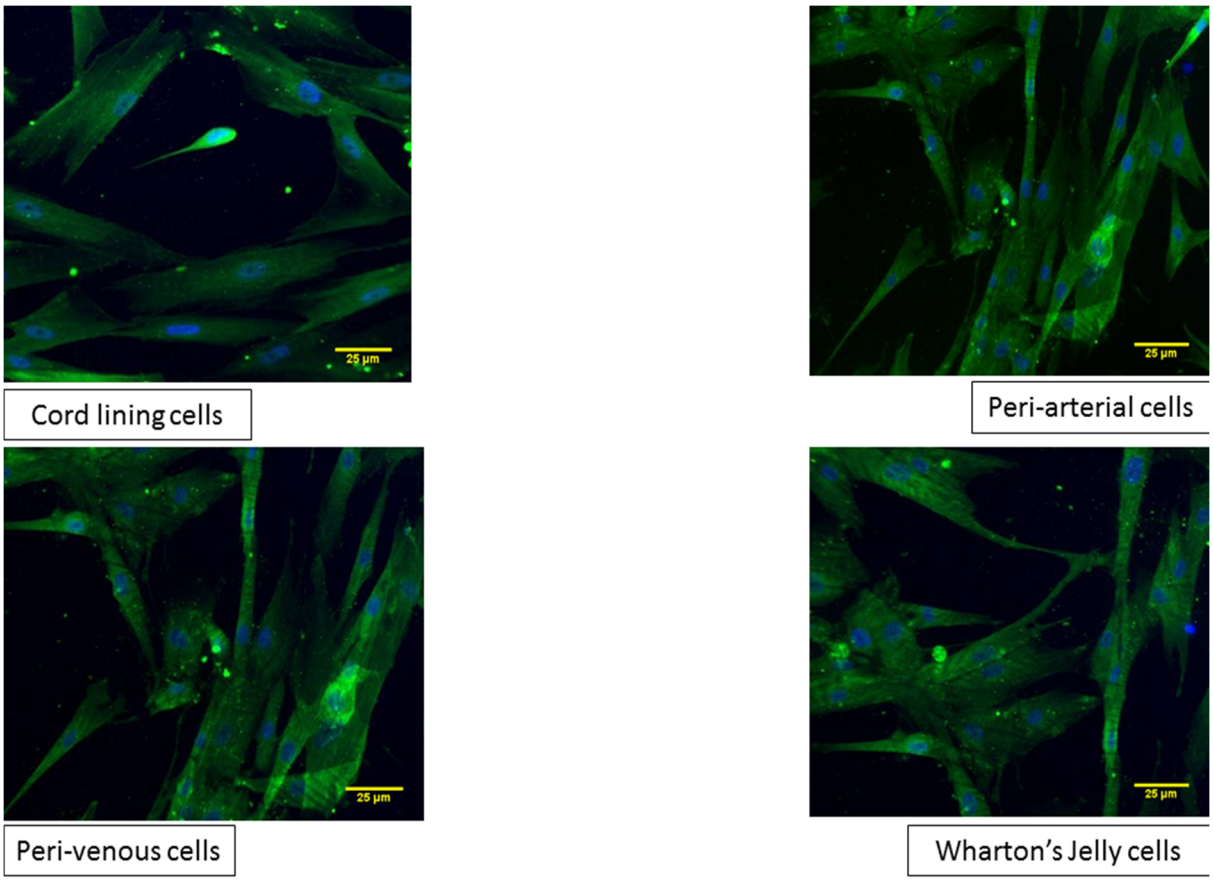

Figure 2.13 Positive immunocytochemical staining for REX-1 on cells from four layers of the umbilical cord (scale bar represents 25 µm)

2.4 Discussion

In this work the isolation of plastic-adherent cells has been reported after three weeks of explant culture. Four anatomical regions within the UCs were used as explant tissue, and a distinct culture medium previously reported to isolate cells only from cord lining membrane was used (Gonzalez et al., 2010). Cells obtained from these four regions had a different morphology but noted to be predominantly fibroblastoid in appearance with the potential for tri-lineage differentiation, and they express surface markers of stem cells according to the ISCT criteria (Dominici et al., 2006), although they do not conform uniformly to these standards quantitatively.

Consistent isolation of cells (termed human 'extraembryonic mesodermal stem cells') from a UC explant culture system with vessels *in situ* has been demonstrated, although the surface antigens on these cells were not quantified (La Rocca et al., 2009). Isolating cells from the UC by explant culture of the entire cord has also been reported (Majore et al., 2011). These cells had the same surface phenotype expression of MSCs according to the ISCT criteria but lacked evidence of osteogenic differentiation; hence, the term "multipotent mesenchymal stromal cells" was used to describe these cells (Majore et al., 2011). Isolation of cells from three anatomical regions of cord- WJ, umbilical cord artery (UCA) and umbilical cord vein (UCV) using explant culture has been described, and three distinct types of MSCs were characterised although the precise nature of the UCA and UCV explants was not histologically defined (Ishige et al., 2009). The histological presence of the supporting matrix (i.e. WJ) around the umbilical cord artery and vein explants has been demonstrated in the present work, despite meticulous dissection of the UC before isolation. Hence, it was preferred to term them peri-arterial and peri-venous explants, respectively.

For the first time, a significant correlation of the cell yields per weight of explant between CL, PA and PV has been reported in this work, but no correlation was found with WJ-derived cells of the UC. This highlights the importance of the explant weight of these three particular regions for the total cell yield, particularly during industrial-scale production of UC-derived stem cells using this technique. Direct comparisons of the doubling time (DT), although different, were not statistically significant for cells isolated from the four distinct anatomical parts of the cord. The DT from the previous study published by our group confirmed these findings, also reporting significantly shorter DTs for cells derived from different cord regions in comparison to BMMSC (Mennan et al., 2013). The present work shows PA and WJ cells have the shortest average doubling time (2.9 days), whereas the doubling time of CL and PV cells were 3.5 days and 3.8 days respectively, although there was considerable variability, however, the differences were not statistically significant. These results also conform to previous trends of a slower population doubling time for cells derived from UCV in comparison to UCA and WJ, although this group of researchers only evaluated population doubling time for nine days in culture (Ishige et al., 2009).

Cells derived from the four areas of the UC demonstrated tri-lineage differentiation in the current study. A further unique finding of the study was demonstrated by semi-quantitative estimation of the ALP activity in the culture medium of the control and osteogenically differentiated cells. At 21 days, a significant rise in ALP activity in culture medium from differentiated cells was demonstrated in comparison with their controls for cells from all four areas of the UC. Moreover, the culture medium of osteogenically differentiated WJ cells had significantly poorer ALP activity in comparison to CL, PA and PV cells. Ishge et al. (2009) noted the same findings on poor osteogenicity of WJ cells. A significant elevation of ALP activity was only reported in osteogenically differentiated UCV cells in comparison to

their respective controls but not in UCA cells for up to 28 days in addition to a complete absence of ALP activity in WJ cells till 49 days (Ishige et al., 2009). Such differences observed in our work can be caused by differences in culture conditions, including basal media and supplements used in our work during culture expansion or osteogenic differentiation.

The isolated cells from different anatomical locations in the present work differed in their expression of surface markers. Only PV cells were consistently negative for haematopoietic cell markers (<2 percent) with flow cytometry analyses. This is dissimilar to our previous report (Mennan et al., 2013) where all cells from all locations lacked surface expression of haematopoietic markers. An earlier study on MSCs from the sub-amnion of the cord lining membrane derived with the explant technique was noted to be positive for CD14, which was thought to be related to T-cell modulation, although its precise role was not established (Kita et al., 2010). Furthermore, a study on characterising CL cells showed CD34 positivity of 9.44±SD2.75% and CD45 positivity of 9.09±SD4.03%. The surface phenotypes of these cells were suggested to share epithelial and MSC properties (Reza et al., 2011).

Positive markers for stem cells were within the recommended threshold (>95%) for only three cell preparations, i.e. one WJ and two PV derived cells. For the rest of the cell preparations, it was not observed to be >95% at P3. A previous study also reports a very low CD90 (0.6%) and CD105 (1.5%) expression of enzymatically isolated WJ cells from UC at P3, which was noted to be >99% at P5 (Bakhshi et al., 2008). A similar observation was noted in WJ cells isolated with enzymes and mechanical disassociation from UCs, with a reported increase of surface expression of CD105 from 28.3% to 78.2% and CD90 expression from 90.0% to 94.9% from P2 to P10 (Fong et al., 2010).

Explant culture of the entire UC in allogenic serum has demonstrated heterogeneous cell groups which can be separated into six distinct groups by counterflow centrifugal elutriation (CCE) based on cell size (Majore et al., 2009). Quantitative flow cytometry in the same study revealed significantly higher positivity to CD73, CD90 and CD105 in smaller cells in comparison to cells with larger diameters (Majore et al., 2009). This study also reports better growth and differentiation of the fraction of cells with smaller diameters in comparison to the larger cells, which were found to be more senescent on SA-β-gal staining compared to their smaller counterparts (Majore et al., 2009). Fluorometric analyses of the CD antigens on cells from the four distinct anatomical layers of the cord grown in 10% FCS and antibiotics with no additional supplement conversely demonstrated >95% positivity of CD73, CD90 and CD105 with a uniform absence of haematopoietic markers by our group at P3 (Mennan et al., 2013).

In summary, the variation in surface expression of CD antigens noted in the current study can be multi-factorial and may be explained by different culture conditions used, which includes the basal medium of DMEM Glutamax supplemented with relatively high serum content (15% FCS) in addition to NEAA and vitamins. A different sub-population of cells can be potentially selected during isolation and culture expansion of cells from distinct anatomical parts of the UC with this media. Moreover, the surface expression of antigens alters with the passage and the present work reports only at P3, which may vary at later passage. However, all the surface antigens in the present work were precisely evaluated during fluorometric analysis and had isotype-matched control to eliminate confounding of the results due to false positivity.

A scientific control group forms an essential part of an experimental design to exclude the influence of confounding variables and bias on the results, in addition, generates a baseline data. There are extraneous variables that can influence the outcome of the experimental study - hence it is critical to identify and minimise their effects (Johnson and Besselsen, 2002). The two commonly used controls are positive and negative controls. Positive controls essentially demonstrate the response that is being sought through the experiment thereby validating the experimental design and reduces the chance of false negatives. It also can act as a standard for measurement of the outcome in the study group (Johnson and Besselsen, 2002). On the other hand, the negative control is a valuable tool in identifying a non-causal association between 'effects of exposure' and the 'outcome' (Lipsitch et al., 2010). A negative control is designed with conditions to produce no results and verified that it has indeed produced no results. This strategy underpins the possibility of confounding variables influencing the outcome if any and prevents false positives (Lipsitch et al., 2010).

All cell preparations in the present work expressed the Major Histocompatibility Complex (MHC) class-I molecule (HLA-ABC) but no MHC class II (HLA-DR) and co-stimulatory molecules, CD40, CD80 and CD86. The immunophenotype of these cells from four UC regions is a novel observation in our work. Additionally, these cells expressed SSEA-4, a surface marker for undifferentiated pluripotent embryonic stem cells (Gang et al., 2007), with positive expression of both SOX-2, a marker of self-renewal and pluripotency of embryonic MSC (Rizzino, 2013) and also REX-1, a pluripotency marker of undifferentiated embryonic stem cells. All cell types also had a positive expression of ALP, an enzymatic marker for embryonic stem cells (Zhao et al., 2012). However, none of the cell types expressed the embryonic stem cell marker Oct3/4 or Nanog (Loh et al., 2006). Nor did these

cells express the markers TRA1-60 and TRA1-81, associated with the heavily glycosylated membrane protein, podocalyxin, which is noted in embryonal carcinoma cells and pluripotent stem cells (Schopperle and DeWolf, 2007).

In conclusion, the present work has demonstrated a technique for successful isolation of cells which are akin to MSCs but unique in their surface antigen properties at early passage. These cells were noted to express some pluripotency markers indicating their self-renewal capacity, which is accompanied by their ability for tri-lineage differentiation, although the potential for WJ-derived cells to become osteogenic appears weaker than for cells from other locations of UC. These cells were also observed to uniformly exhibit MHC Class I molecule (HLA-ABC) in the absence of HLA-DR or co-stimulatory molecules, which suggests that they are suitable candidates for allogeneic transplantation. Further studies about their immunological profile after priming these cells before and after differentiation should be undertaken to ascertain their usefulness in specific locations and disorders for regenerative medicine.

Chapter 3: Bone Marrow Stromal Cells Do Not Increase New Bone Formation in Recalcitrant Nonunions: Results of a Double Blinded Randomised Controlled Trial

3.1 Introduction

A total of 850,000 new fractures are reported annually in the UK. The majority of these fractures progress to uncomplicated healing, except in 5-10% of patients whose fractures do not heal (Court-Brown et al., 2010). Recent Scottish data estimates the overall annual incidence of nonunions at 19 per 100,000 people, equivalent to the incidence of revision hip replacements (Mills and Simpson, 2013, Court-Brown et al., 2010). Lower limb nonunions make up 6.7 per 100,000 people, with a treatment cost of $11,500 to $132,000 per person to the National Health Service, excluding the morbidity and loss of earnings (Mills and Simpson, 2013).

The human fracture haematoma contains cells which have multi-lineage differentiation potential including osteogenic differentiation capacity, and the phenotype of these cells are similar to bone marrow MSCs (BMMSCs)(Jagodzinski and Krettek, 2007). Nonunion stromal cells grown from human nonunion were noted to have slower doubling time, lower osteogenic potential and a higher rate of apoptosis in comparison to BMMSCs from healthy donors(Bajada et al., 2009). These cells were found to secrete Dickkopf-1(Dkk-1) which is an antagonist to the Wnt signalling pathway and inhibits osteogenic differentiation and fracture healing *(ibid).* A study of nonunions in rats showed that the progenitor cells from the atrophic nonunion site had impaired differentiation potential due to the sub-optimal environment, nevertheless suggested reactivation of these native cells by adding growth factors or progenitor cells to induce bone formation(Tawonsawatruk T et al., 2013).

However, successful case studies of bone tissue engineering approaches to regenerate large bone defects in patients by using *in vitro* expanded autologous Bone Marrow derived Stromal Cells (BMSC) and subsequently re-implanting them in scaffolds have been reported(Quarto et al., 2001, Marcacci et al., 2007). *In vitro* studies have also demonstrated

no difference in the osteogenic capacity of BMSCs from the iliac crest in patients with atrophic nonunions and healthy volunteers (Mathieu et al., 2013). Reports of treating nonunions successfully with autologous bone marrow derived cells were also published consistent with *in vitro* studies (Bajada et al., 2007, Hernigou et al., 2005).

We report the first randomised self-controlled trial to compare new bone formation in recalcitrant nonunions treated with carrier plus *in vitro* expanded autologous BMSCs against the carrier alone (control). Secondary aims were to analyse predictors of the union in these patients and describe adverse events at final follow-up.

3.2 Methods

Patients were invited to participate in a single centre double-blinded self-controlled randomised trial by a single specialist nonunion surgeon. The trial was approved by National Research Ethics Service, South Staffordshire Local Research Ethics Committee (Ref. No. 02/42/RJH).

Patient inclusion criteria were:

a. Nonunion following fracture of tibia or femur.
b. An established nonunion according to the US Food & Drug Administration criteria(1998).

Patient exclusion criteria were:

a. Skeletal immaturity.
b. Pregnant or breastfeeding.
c. Nonunion following pathological fractures.
d. Positive to Hepatitis-B, Hepatitis-C or HIV.
e. Infection during BMSC culture.

Patients with diabetes or bone loss and smokers were not excluded.

3.2.1 *In vitro* BMSC culture

Bone marrow aspirates from the iliac crest of the patients with nonunion were harvested with aseptic precaution in the theatre. A Jamshidi needle attached to a heparanised syringe (Becton Dickson Medical Supplies, Cowley, UK) was used to aspirate bone marrow which ranged from 2-10ml. The BMSC's were isolated and cultured from the aspirate according to the previously published protocol from our centre (Wright et al., 2008).

The bone marrow aspirate was mixed with phosphate buffer solution (PBS), and the mixture was subsequently layered over two aliquots of 10ml of Lymphoprep (Fresenius Kabi Forge). The mononuclear cells were isolated by density gradient centrifugation at 900g for 20 minutes. A 'buffy coat', predominantly containing mononuclear cells was obtained; this was separated with a 19 gauge needle and 5ml syringe (Becton Dickson Medical Supplies). The harvested 'buffy-coat' layer from the two tubes was then pooled and added to 10ml of DMEM F12 (Gibco, UK), supplemented with 20% FCS, penicillin and streptomycin. The cell suspension is then centrifuged for 10 minutes at 750g. The cell pellet obtained was suspended in DMEM F12 with 20% FCS, and subsequently, a viable cell count was performed with trypan blue exclusion. These cells were plated at a density of $2x10^7$ cells per 250ml flask (Polystyrene Tissue Culture Flask, BD Biosciences, Cowley, Oxford, UK) with 20ml of the media. After 24 hours the non-adherent cells were removed by removing the media and then washing the flask with PBS. The adherent cells were continued in monolayer culture with DMEMF12 with 10%FCS and antibiotics at 37^0C, 5% (v/v) CO_2 until it reached 70% confluence. At confluence, these cells were passaged by trypsinisation and routinely re-seeded at $5x10^3$ cells/cm^2 density.

Cell numbers at the end of each passage were noted to calculate the doubling time of these cells using the following equation:

Doubling Time (DT) $=(t_2-t_1)x\ \ln(2)/\ln(n_2/n_1)$ where:

t_2-t_1 represents consecutive time points,

ln represents the linear log,

n_2 represents the final cell numbers harvested and

n_1 represents the initial number of cells(Jordan and Smith, 1997).

Autologous BMSC's were culture-expanded for three weeks. The discarded medium was sent to the microbiology department routinely for infection screening.

Following randomisation, two universal containers - one with cells in serum and the other containing serum alone- were sent out to the operating theatre for insertion at the fracture site. Each container was marked medial/ anterior and lateral/ posterior, respectively, based on the surgical approach to the nonunion site.

3.2.2 Surgical Technique

The nonunions of fractures were stabilised with internal or external fixation devices. The femoral fractures were internally fixed, and tibial fractures were predominantly fixed with external fixation systems. The nonunion site was exposed and decorticated. Depending on the surgical approach, the nonunion site was considered to have either a medial and lateral or an anterior and posterior side, although no physical partition was applied. The contents of each universal container were mixed individually with a carrier by the surgeon, who was blinded to the contents of the container. Carriers were β tricalcium phosphate (Allogran®-R, Biocomposites, Keele, UK), calcium sulphate ($CaSO_4$; Stimulan®, Biocomposites, Keele, UK), hydroxyapatite (Allogran® N, Biocomposites, Keele, UK), combination of β tricalcium phosphate and calcium sulphate or simply patient's serum (Table 3.1).

An ideal carrier material should have good biomechanical properties to withstand loading at the fracture site in conjunction with its biodegradability and porous architecture allowing implanted cells to thrive until the new bone is formed. Evidence of such osteoconductive carrier material at the outset of the trial was inconclusive with β tricalcium phosphate being easily resorbed however lacked the mechanical strength at the same time hydroxyapatite had a high strength to take the load but had poor resorption from the fracture site (Cancedda R et al., 2007). The choice of carrier in this study was guided by the degree of bone loss and the volume of pre-existing callus and differed between patients. However, each patient received the same type of carriers to preclude its influence on the 'control' and 'test' side, if any. Moreover, a total of eight patients received no carriers but autologous serum, to act as a control to the synthetic carriers used for the cells, to identify the influence of carrier material on the outcome during sub-group analysis. The two mixtures were left for 10-15 minutes to allow attachment of cells to the carrier. The operating surgeon then

inserted each mixture on the side indicated by the label on the container, thus putting the cells at their randomly allocated side. An overview of the whole method is illustrated in Figure 3.1.

Carrier type	Number of cases (%)
β tricalcium phosphate with calcium sulphate	16 (46%)
β tricalcium phosphate	6 (17%)
Calcium sulphate	4 (11%)
Hydroxyapatite	1 (3%)
Serum	8 (23%)

Table 3.1 Overview of carriers used in the trial

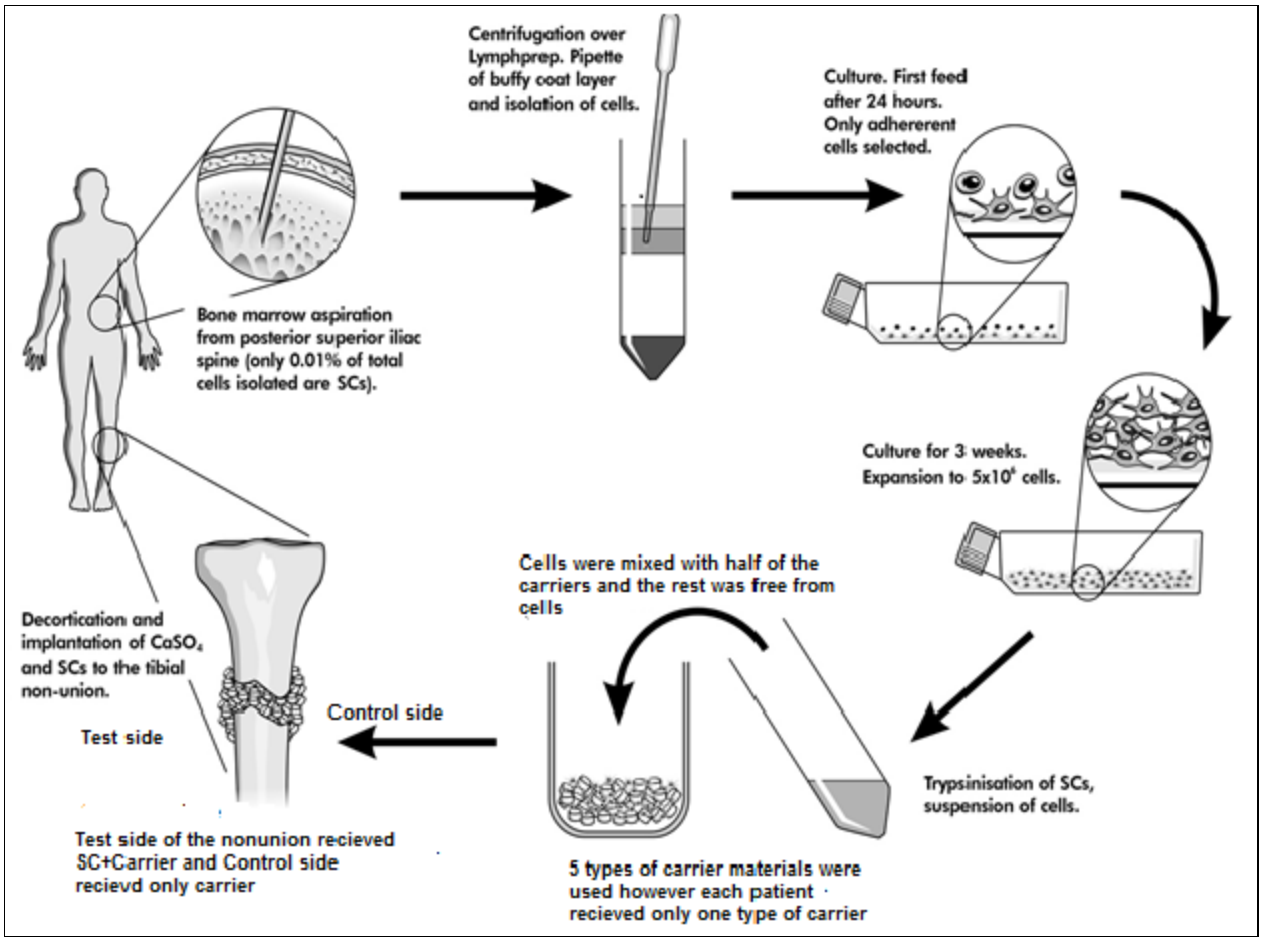

Figure 3.1 Overview of the trial methodology from bone marrow harvest to trial intervention showing separate 'test' side receiving cells with carriers and 'control' side receiving only carriers. A total of five type of carriers including serum was used in the study, however, each patient received only one type of carrier (SC-Bone marrow stromal cells; image adapted from Bajada et al., 2009)

3.2.3 Primary Outcome

The primary outcome measure was the formation of new callus and cortical bridging, assessed from preoperative and multiple postoperative radiographs and CT-scans up to 12 months. New callus was defined as new bone noted in postoperative radiographs which was adjacent to the bony cortices of the nonunion site whereas new fracture bridging was defined as new bone formation noted at the fracture gap of the nonunion site, both being compared with the immediate preoperative radiographs. These images were divided into early (3-6 months) and late (6-12 months) groups. Hence, the primary outcome was categorized as early new callus and cortical bridging (3-6 months) and late cortical bridging and new callus (6-12 months). Nonunions were assessed from anonymised slides by four reviewers (two radiologists and two orthopaedic surgeons) blinded to the side of cell insertion. None of the assessors was directly involved in recruitment or clinical care of these patients in the trial.

Each slide had a preoperative radiograph for comparison with postoperative images but no indication of time since surgery was available to the reviewer. These preoperative radiographs were to be compared with postoperative films which were marked as Image 1, Image 2 and onwards. The slides only showed a medial/ lateral or an anterior/ posterior view of the nonunion site depending on the surgical approach. A sample slide is presented in Figure 3.2.

A total of 232 postoperative images were assessed for the 35 patients by the four reviewers. At least three representative images of the CT scans were used to determine the nonunion site by the reviewers in the coronal or sagittal plane. All the preoperative images were within three months before the BMSC insertion. Every reviewer was presented with a questionnaire for assessing each image to indicate any change in callus and fracture bridging

as illustrated in Fig 3.3. If appreciable new bone formation on both sides of the fracture was noticed, as, in Fig 3.2, such observations in the assessment box of the questionnaire were also recorded. For radiographs showing both tibia and fibula fractures, only the tibia was used for assessment.

At first, each reviewer indicated the side with the largest callus and most cortical bridging preoperatively. Then each reviewer examined subsequent radiographs to indicate the side with the most substantial change in the formation of new callus and cortical bridging. This was based purely on their subjective assessment of the postoperative radiographs which was always compared with the preoperative image available in each slide. Furthermore, the second round of evaluation was undertaken by the four reviewers with at least on radiograph from each patient to assess the intra and inter-observer reliability. The second series of assessment was three months after the first to avoid recollection bias. All preoperative radiographs were also included in the same layout, as used during the first evaluation.

The primary outcome for each postoperative radiograph was assessed with a probabilistic model of labelling images termed as Generative models of Labels, Abilities and Difficulties (GLAD) (Whitehill et al., 2009a). Three parameters are taken into account in this method of assessment:

i. Expertise of the assessor
ii. Difficulty of the image
iii. Observed outcome of the image

In this probabilistic model to infer the true label of the image depends directly on the expertise of the reviewer and inversely to the difficulty of the images (Whitehill et al., 2009a). The use of a GLAD algorithm by Whitehill et al. is shown to be superior to identify

the actual label of an image and outperforms the conventional majority vote system particularly in situations where the outcome of images was split between the reviewers.

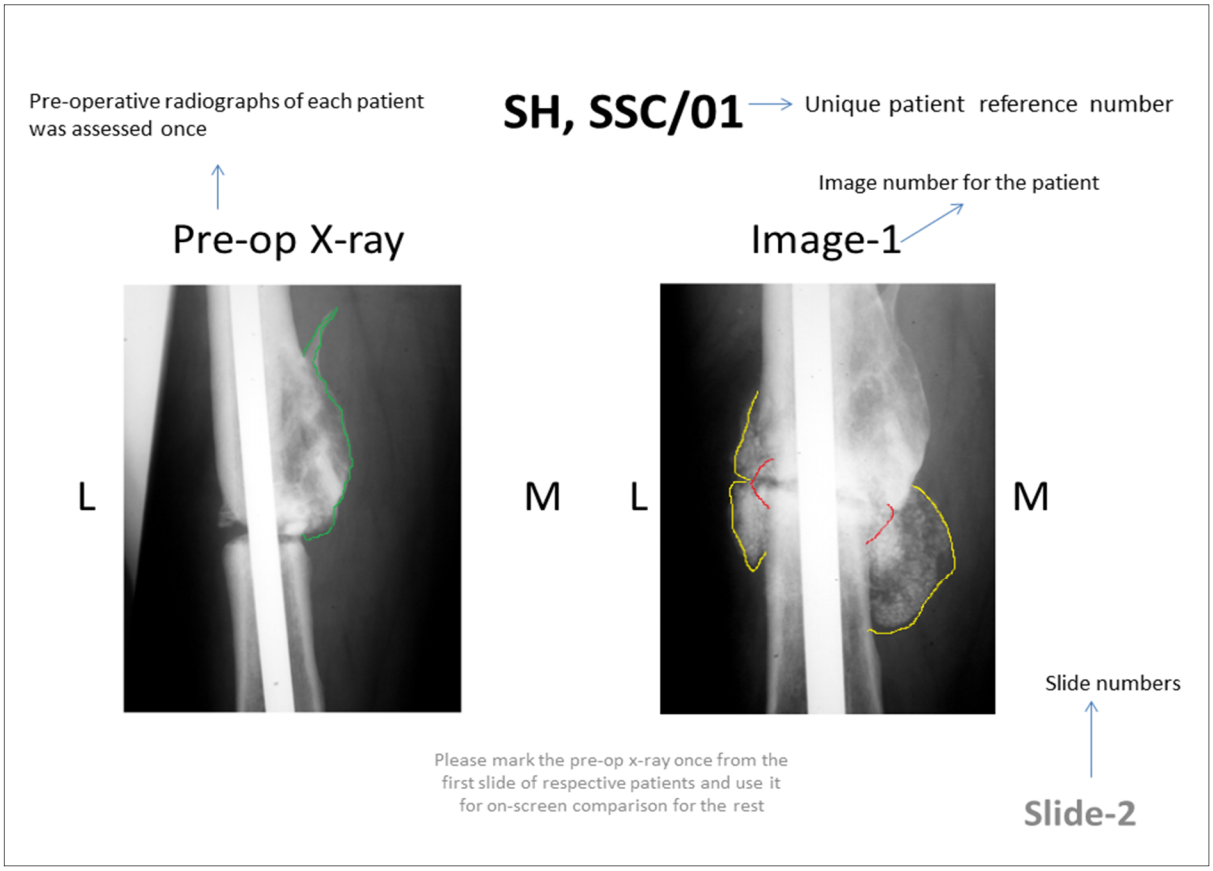

Figure 3.2 A typical slide used for assessment of new callus and cortical bridging. The image labelled pre-op radiograph (on the left) shows the outline of the callus (marked green) before cell insertion, and image one (on the right) shows the outline of new callus (marked yellow) and cortical bridging (marked red) following insertion of BMSC.

SSC-01

Slide-1: Pre-op radiographs

Which side has more callus?	Which side has more fracture bridging?
Lateral side	Lateral side
Medial side	Medial side

Slide-1: Image-1

Which side has more new callus in comparison to the pre-op radiographs?	Which side has more new fracture bridging in comparison to the pre-op radiographs?
Lateral side	Lateral side
Medial side	Medial side

Figure 3.3 A typical questionnaire for assessment of the primary outcome by independent reviewers

3.2.4 Secondary Outcomes

Radiological fracture union at final follow-up and change in the EQ-5D index at one year were used as secondary outcome measures. The radiological union was defined as cortical bridging and obliteration of the nonunion site in two perpendicular planes assessed on plain radiographs or CT scan. Safety was determined by the occurrence of any postoperative adverse events until final follow-up.

3.2.5 Power calculation

The sample size was calculated for the trial using specialised software (G*power version 2, Heinrich Heine University, Düsseldorf, Germany); it assumed a single sample binomial test to analyse the primary outcome. We hypothesised that at least three-quarters of the test sides needed to show more callus and bridging for the cells to be deemed effective, corresponding to an effect size of 0.25. Given a two-sided critical p-value of 0.05 and 80% power, the trial needed a minimum of 30 patients (Figure 3.4). A total of 35 patients were recruited to allow for drop-outs and loss to follow-up.

3.2.6 Randomisation technique

A test container with BMSCs in autologous serum and a control container with autologous serum alone were randomized using computer software (Stratos, Orthopedic Institute, Oswestry, UK) for insertion at the medial/ anterior or lateral/ posterior side of the nonunion. This created a self-controlled trial with patients serving as their own control. The cell manufacturing laboratory maintained a record of the side of cell insertion linked with a unique patient 'OsCell' number. The patients, operating surgeon and the assessors were blinded to the side of cell insertion.

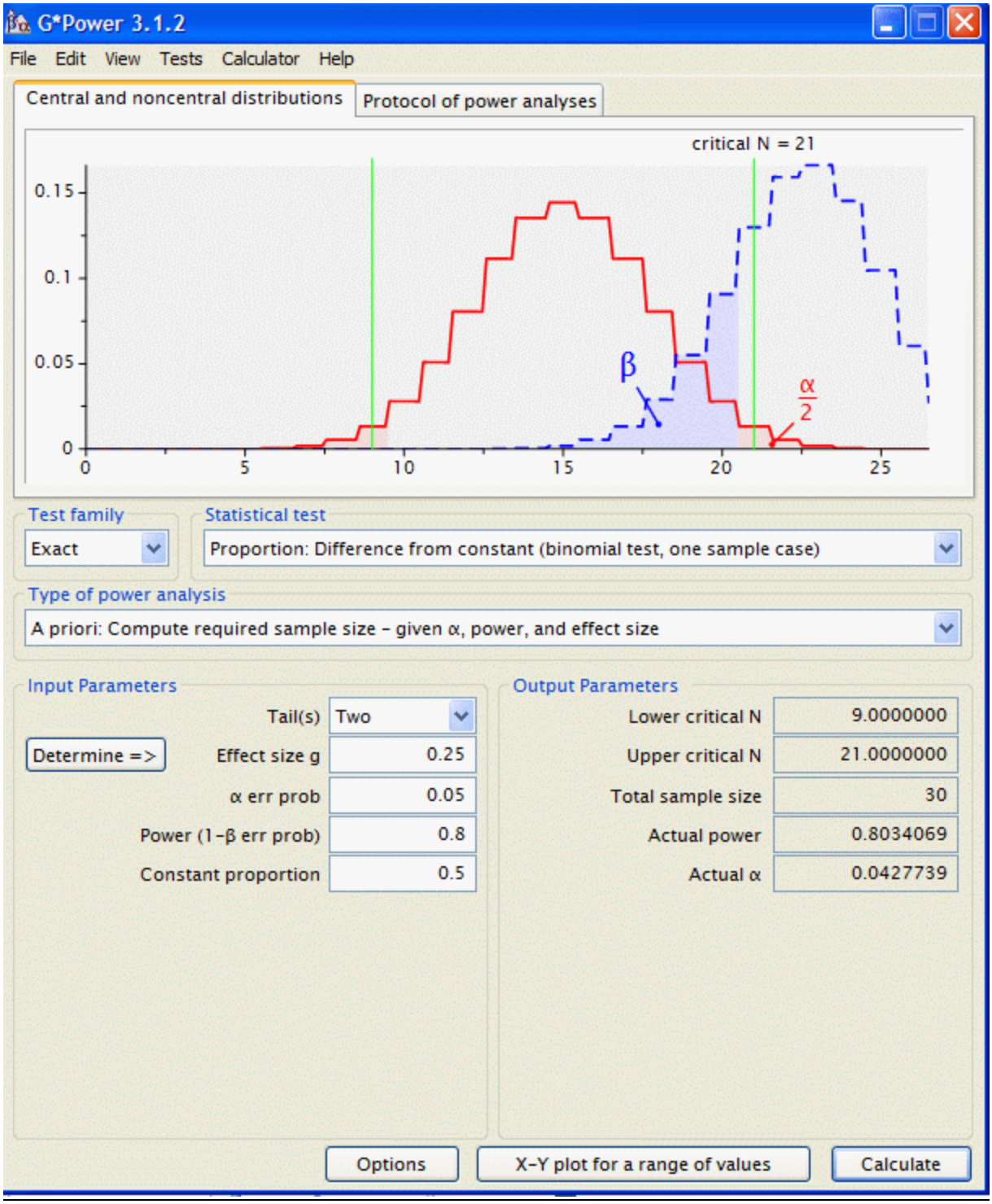

Figure 3.4 Power analysis with G*power software showing a total sample of thirty patients required to ascertain an effect size of 0.25 over a constant proportion of 0.5

3.2.7 Statistical Methods

Fleiss' kappa coefficient was used to assess the inter-observer reliability of the four reviewers, and the Spearman-Brown formula to determine their combined reliability (Kraemer, 1979). The GLAD algorithm was used to obtain the overall decision of reviewers. This method obtains a collective decision in all cases even when the vote is split and outperforms majority voting (Whitehill et al., 2009b). A single sample binomial test was used to ascertain differences in most new callus formation or bridging between test and control sides.

To find univariable predictors of fracture union, Fisher's exact test and penalized logistic regression were used to analyse categorical and continuous variables, respectively. Multiple penalized logistic regressions were used in a multivariable analysis to determine if combined independent variables gave a better prediction. For this analysis, all univariable predictors with $p<0.25$ were considered potential candidates for inclusion in the model (Hosmer and Lemeshow, 2000). Nagelkerke's R^2 was used as an overall measure of model performance (Nagelkerke, 1991).

A multilevel model with a random intercept was used to determine the difference in the EQ-5D index before and one year after treatment. This method was chosen to include all patients, even when one of their pre or postoperative EQ-5D score was missing. Statistical analyses were performed using the Optimal Label Inference Software(Whitehill et al., 2009b) and R version 3.0.2, using the packages "irr", "logistf" and "nlme". A two-sided p-value below 0.05 was assumed to denote statistical significance.

3.3 Results

3.3.1 Patient Demographics

A total of 37 patients were initially recruited for trial participation; one patient was excluded due to having a nonunion of ankle fusion undertaken for OA and hence did not meet the inclusion criteria, and one patient declined participation. Hence, 35 patients (21 males, 14 females) with a mean age of 50.6 years (range 17-75) were recruited (Table 3.2). The median duration of established nonunion was 2.9 years (range 1-33); patients had undergone a median of 4 surgical interventions (range 1-14) prior to cell insertion at the fracture site. This group of patients was defined to have 'recalcitrant' nonunions because they had an average age of more than 50 years with persistence of established nonunion for at least one year, in addition, to at least one previous failed surgery to treat the nonunion. Twenty-nine patients had atrophic nonunions, whereas six had hypertrophic nonunions; 19 patients had femoral, and 16 had tibial fracture nonunions. There was no drop-outs or loss to follow-up during the first 12 months except one death at three months. A CONSORT diagram schematically represents the patients in the trial for 12 months (Fig3.5) (Hopewell et al., 2008).

Parameter	Value
Demographics	
Sex	Male 21 (60%), female 14 (40%)
Age at accident (years)	Mean 45.2 (SD 12.4; range 16-71)
Age at trial intervention (years)	Mean 50.6 (SD 12.5; range 17-75)
Time from accident to trial intervention (months)	Mean 56.4, median 35 (range 12-396)
Fracture and nonunion characteristics	
Site	Femur 19 (54%), tibia 16 (46%)
Velocity	High 20 (57%), low 15 (43%)
Open or closed	Open 18 (52%), closed 13 (37%), Unknown 4 (11%)
Atrophic or hypertrophic	Atrophic 29 (83%), hypertrophic 6 (17%)
Number of operations before trial	Mean 2.8, median 2 (range 1-14)
Number of cases with previous autologous bone graft or BMP	Graft 10 (29%), BMP 0, Both 2 (6%)
Comorbidities	
Smoking	Yes 8 (23%), No 27 (77%)
Alcohol	Yes 16 (46%), No 13 (37%), Unknown 6 (17%)
Diabetes mellitus	Yes 5 (14%), No 30 (86%)

Table 3.2 Baseline demographics and clinical characteristics of patients included in the trial

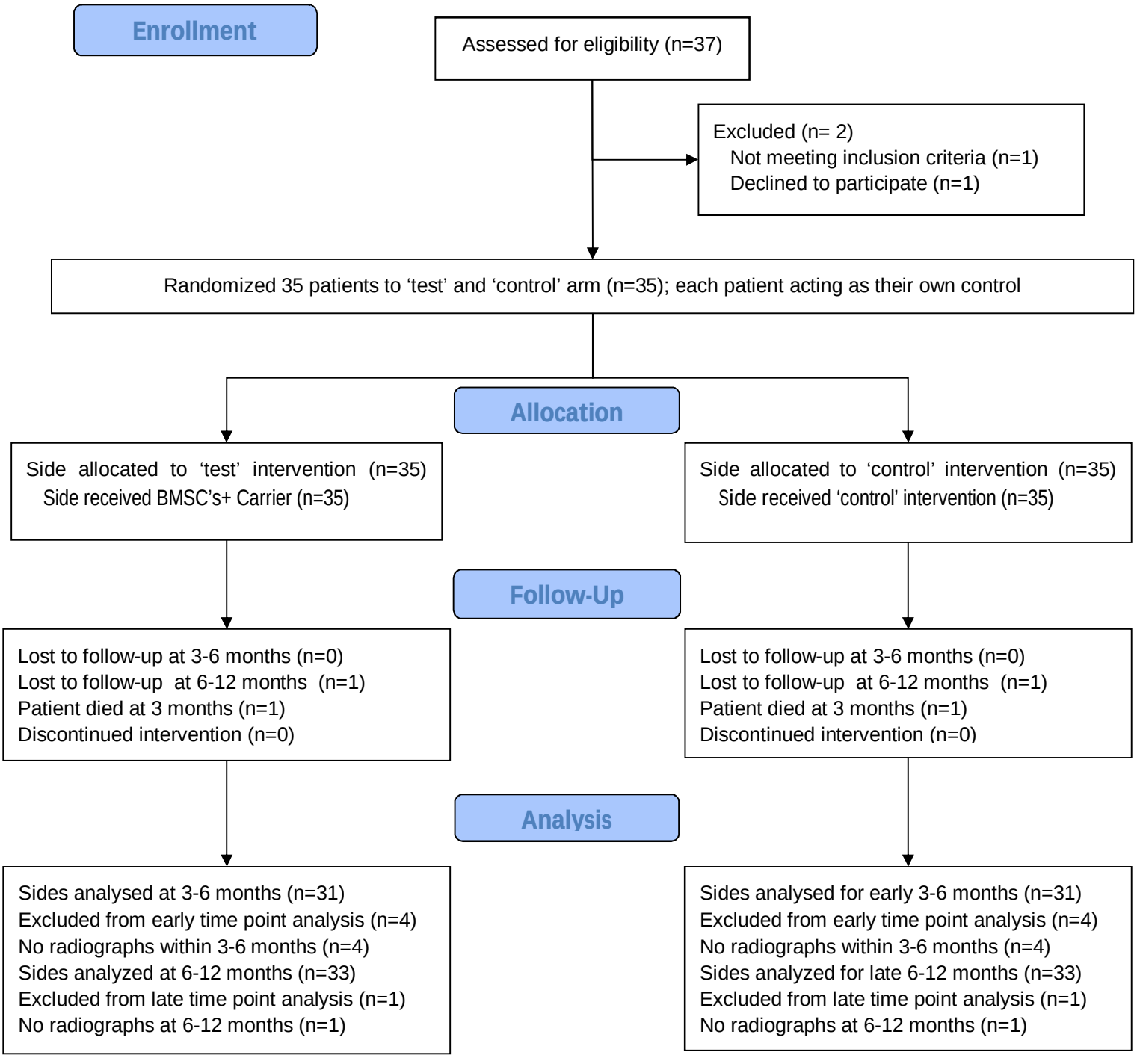

Figure-3.5 CONSORT Flow-diagram of patients in the trial

3.3.2 *In vitro* BMSC culture

Autologous BMSC's were culture-expanded for three weeks with an average cell doubling time of 7.2 days (range 2-31, SD-6.24) and without any evidence of infection in the media. A mean of $5.5x10^6$ BMSCs (range $2\text{-}10x10^6$, SD $1.99x10^6$) was inserted into the test sides of the nonunions. Twenty-seven patients (77%) received a carrier based on β-TCP, calcium sulphate or combination of both or hydroxyapatite. For eight patients (23%) autologous serum alone served as the carrier (Table 3.1).

3.3.3 Primary Outcome

Radiographs of 31 patients were available for review at early (3-6 months) time points and of 33 patients at late (6-12 months) time points. Fleiss' kappa coefficient for assessing new callus was 0.46, and new fracture bridging was 0.43. By using the combined opinion of all four assessors, their overall reliability as calculated by the Spearman-Brown formula was 0.77 for callus and 0.75 for fracture bridging, implying excellent reliability (Fleiss et al., 2003).

At 3-6 months, 12 out of 31 patients (39%; 95% CI 24-56%, p=0.28) had more new callus on the cell insertion side, whereas at 6-12 months 15 out of 33 patients (45%; 95% CI 30-62%, p=0.73) had more new callus on the cell insertion side (Fig. 4). More new fracture bridging at the cell insertion side was found in 16 out of 31 patients (52%; 95% CI 35-68%, p=1.00) at 3-6 months and in 19 out of 33 patients (58%; 95% CI 41-73%, p=0.49) at 9-12 months (Fig 3.6).

No influence of carriers were noted on the primary outcome i.e. more new callus at 3-6 months (p=0.61)/at 6-12 months (p=0.16) and more new fracture bridging at 3-6 months (p=0.77)/6-12 months (p=0.63). When restricting the analysis to the most common carrier (β-TCP with calcium sulphate; 16 patients), 4 out of 14 patients (29%; 95% CI 12-55%; p=0.18) had more callus at the cell side at 3-6 months and 4 out of 16 (25%; 95% CI 10 to 50%; p=0.08) at 6-12 months. In these patients, 6 out of 14 (43%; 95% CI 22-68%; p=0.79) had more bridging at the cell side at 3-6 months and 7 out of 16 (44%; 95% CI 23 to 67%; p=0.80) at 6-12 months.

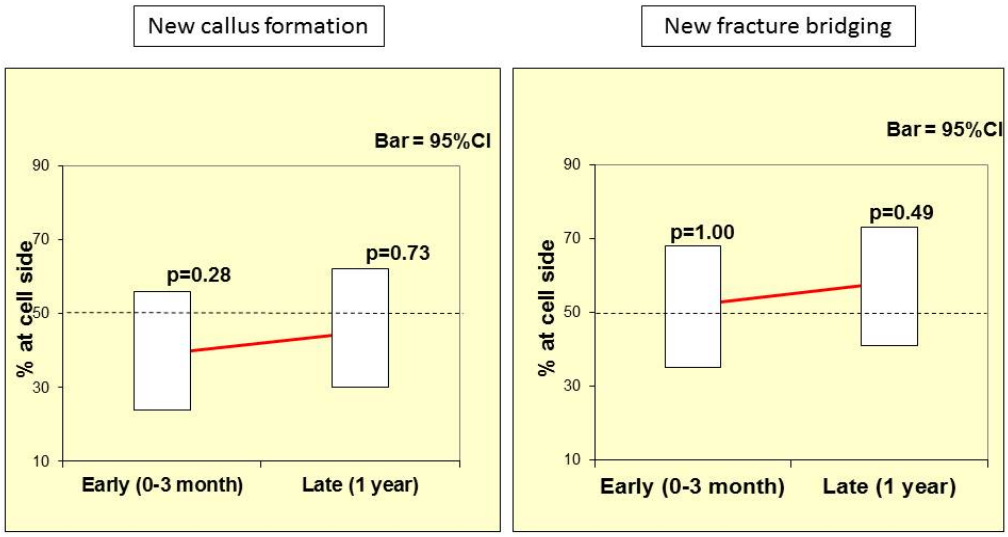

Figure3.6 New callus and fracture bridge formation at early and late time points from cell implantation

(The red bar represents the mean, and the horizontal hashed line represents 50% distribution. The vertical bar represents 95% confidence interval)

3.3.4 Secondary outcomes

3.3.4.1 Fracture union: A total of 21 out of 35 patients (60%; 95% CI 44-75%) achieved radiological fracture union at a mean follow-up of 2.6 years after cell implantation (range-0.24-8.24). The vast majority of categorical independent variables, among which the type of carrier used, had a small and non-significant effect on the union rate (Table 3.3). The only exception was having diabetes, the effect of which was not significant (p=0.06) yet it reduced the odds of achieving union by over 8-fold (Table 3). Among the continuous predictors, the number of previous operations and the cell doubling time during *in-vitro* culture of BMSCs were significant predictors of the union (Table 3.4).

In the multiple penalized logistic regression analysis, we used four univariable factors with $p<0.25$ as potential predictors, namely having diabetes, number of previous surgical interventions, age at cell implantation and cell doubling time. Age at accident and years since accident were excluded due to their strong correlation with age at implantation (Spearman's rho = 0.86; $p<0.001$) and number of previous operations (Spearman's rho = 0.60; $p<0.001$), respectively. According to the regression model, the chance of union was larger in patients with a lower age at cell implantation, fewer previous surgical interventions, cells with a shorter doubling time and non-diabetic patients (Table 3.5). The model explained 90% of the variation in outcome (Nagelkerke's $R^2=0.90$).

Factor	OR (95% CI)	p-value*
Gender (Male)	1.4 (0.27-7.0)	**0.73**
Fracture site (tibia)	1.7 (0.35-9.2)	**0.50**
Type of fracture (open)	0.82 (0.15-4.4)	**1.0**
Type of nonunion (hypertrophic)	3.6 (0.34-192)	**0.37**
Infection at insertion	7.46 (0.43 to 129)	**0.48**
Alcohol	1.1 (0.16-7.1)	**1.0**
Diabetes	0.12 (0.0022-1.4)	**0.06**
Smoking	0.39 (0.046-2.8)	**0.39**
Previous bone graft treatment	0.40 (0.06 to 2.3)	**0.27**
Previous BMP treatment	0.60 (0.06 to 2.3)	**1.0**
Carrier type	-	**0.61**

* p-values determined using Fisher's exact test

Table3.3 Univariable analysis of categorical predictors of union (OR-Odds Ratio)

Factor	OR (95% CI)*	Nagelkerke's R^{2*}	p-value*
Age at accident	0.97 (0.91 to 1.02)	**0.06**	0.25
Years since accident to implantation	0.92 (0.63 to 1.03)	**0.08**	0.17
Number of previous operations	0.58 (0.29 to 0.95)	**0.22**	0.02
Age at cell implantation	0.96 (0.89 to 1.01)	**0.11**	0.12
Cell number (10^6)	1.1 (0.78 to 1.6)	**0.01**	0.56
Cell doubling time (hrs)	0.87 (0.68 to 0.99)	**0.20**	0.04

OR and their 95% CI, Nagelkerke's R2 and p-values determined using penalized logistic regression

Table 3.4 Univariable analysis of continuous predictors of healing (OR-Odds Ratio)

Factors	Coeff. (95% CI)*	OR (95% CI) *	p-value*
Age at implantation	-0.15 (-0.36 to -0.02)	0.86 (0.69 to 0.98)	0.02
Number previous interventions	-0.48 (-2.3 to -0.11)	0.62 (0.097 to 0.90)	0.008
Doubling time	-0.19 (-0.63 to 0.01	0.82 (0.53 to 1.01)	0.07
Diabetes	-4.9 (-11 to -1.5)	0.008 ($3{\cdot}10^{-5}$ to 0.24)	0.003

* Coefficients, ORs and p-values determined using penalized logistic regression. For the mode, Nagelkerke's R^2 was 0.90.

Table3.5 Results of the multiple logistic regression analysis (OR-Odds Ratio)

3.3.4.2 Health-related quality of life

The mean preoperative EQ-5D index was very low (0.09; Table 3.6). Despite increasing significantly by 0.34 points, it was still low one year after the trial intervention (Table 3.6). A detailed sub-group analysis of the five dimensions of the EQ-5D showed noticeable improvement in scores relating to anxiety/depression, pain/discomfort and usual activity, minimal differences in mobility and no changes in self-care at 12 months (Fig 3.7).

Outcome	Mean pre-op (SD)	Mean post-op (SD)	Difference* (95% CI)	p-value
EQ-5D index	0.09 (0.45)	0.32 (0.41)	0.34 (0.11 to 0.58)	0.01

* Difference calculated using random intercept multilevel model. This difference does not equal the difference between the pre-op and post-op columns but does provide a better estimate by properly accounting for repeated measures.

Table 3.6 Change in Eq5D at one year from the trial

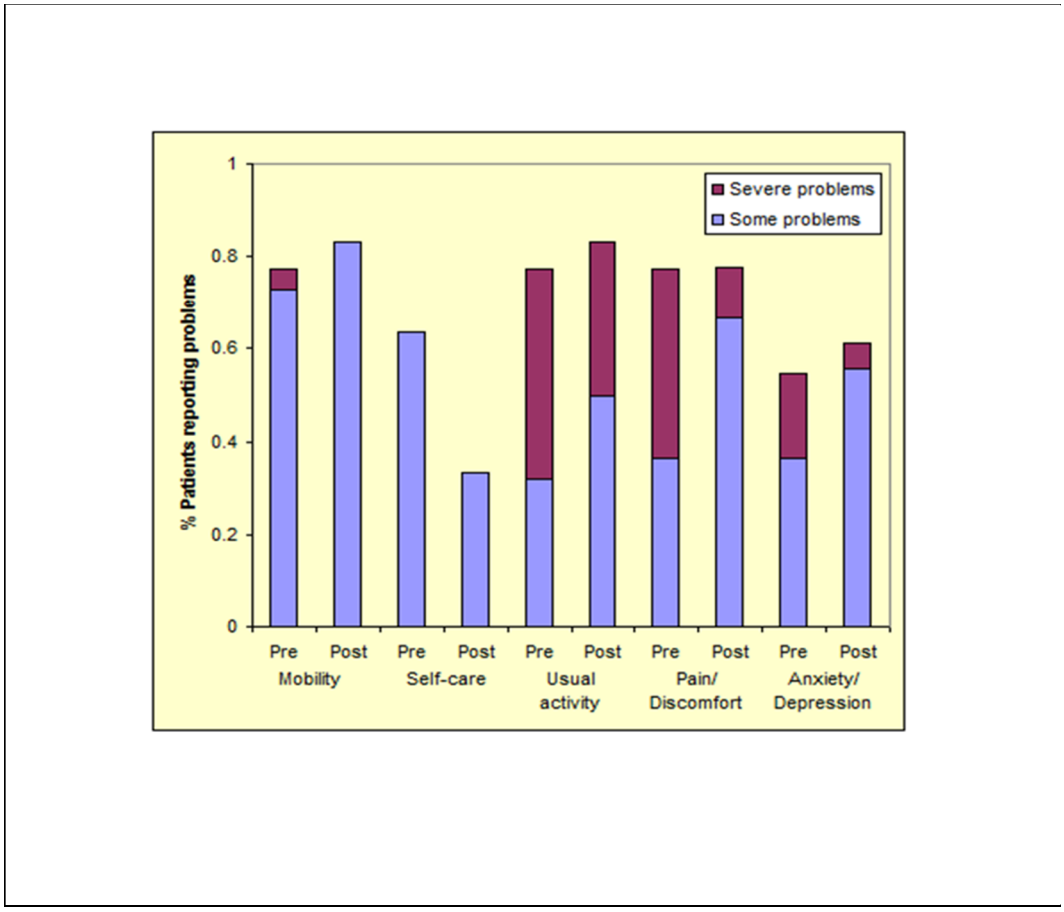

Figure 3.7 Self-reported health outcome according to five dimensions of the EQ-5D index

(pre- and 1-year post-intervention)

3.3.5 Adverse events

One patient developed sepsis following the trial intervention, requiring intensive hospital care. The patient recovered uneventfully without overt residual infection. Two patients died before final follow-up. One died within three months of the intervention due to an aorto-enteric fistula, and the other died three years after the intervention due to heart failure on a background of tricuspid regurgitation. One patient was reported to have a benign gastric tumour six years after the BMSC insertion. The patient was doing well at three years follow-up after the surgical excision of the tumour.

3.4 Discussion

This study reports the results of the first randomised controlled trial reporting the efficacy of *in vitro* culture expanded BMSCs in new bone formation in fracture nonunions. It is a self-controlled trial that minimises the confounding effects of fracture configuration and biology. This trial design, common in dentistry, maxillofacial surgery ("split-mouth design") and dermatology (Machin et al.) has been used in spinal fusion trials in orthopaedics (Alexander et al., 2001, Cammisa FP Jr et al., 2004, Machin et al.). To our knowledge, this is its first use in a trial of fracture nonunions.

The current work failed to demonstrate a significant difference in radiological new callus formation or fracture bridging between 'test' and 'control' sides at early (3-6 months) and late (6-12months) time points. The trial also presents with patient characteristics which represent a group of 'recalcitrant' nonunions of fracture. The cohort of patients in this study had nonunion for at least one year (median duration of 2.9 years) with at least one surgical intervention (median of 4 surgical interventions) before insertion of BMSC to achieve fracture union. Such a background of patients included in the study reflects the resistance to progress to a bony union or new bone formation in these patients from the outset. However, failure in demonstrating new callus or fracture bridging on the 'test' side in the trial can be potentially due to ineffective cell implantation, carry-across effects by the implanted cells to the control sides, or failure to identify the side with most new callus and bridging radiologically. Nevertheless, one of the novel findings of the study is the identification of *in-vitro* autologous BMSC doubling time in these patients as a predictor of fracture union.

At the onset of the trial, evidence on the choice of osteoconductive material as the carrier was inconclusive, with HA and other calcium phosphate ceramics regarded the most

promising(Cancedda R et al., 2007). Combining BMSCs with an osteoconductive carrier, used in most cases in our study, is supported in the literature (Cancedda R et al., 2007, Meijer et al., 2007). The cell implantation method involved mixing cells in serum with a carrier, resting the mixture and placing the mixture at the fracture site. A total of eight patients received cells with serum (no other specific carriers were used) on the 'test' side and only serum on the 'control' side to avoid any confounding effect on the primary outcome from the choice of the carrier material. However, the analysis of the influence of carrier material on the primary outcome when restricted to the commonest carrier in our study (β-TCP with calcium sulphate) showed no conclusive evidence to support its impact on the formation of new callus or bridging in comparison to the control side. The choice of carriers was also found to have no influence in fracture union amongst these patients. Nonetheless, a recent study comparing bone formation by BMSCs on four different ceramic scaffold materials suggests that coral may be preferable over β-TCP (Viateau V and Manassero, 2013(in press)), indicating carriers can potentially influence the outcome although such a finding is not discernible in the present study.

Carry-across effects from the cell implantation to the control side of the fracture could reduce the validity of the self-control trial design in this study (Machin et al.). The carry-across effect in self-controlled spinal fusion trials in the literature is due to the influence of one healing side on the other by altering the mechanical conditions (Alexander et al., 2001). The faster healing side stiffens the fracture, affecting the healing process on the other side. However, the frequency of radiological follow-up in the trial would have potentially allowed the assessors to identify any faster healing side. A second carry-across effect is the mechanism by which BMSCs are now known to exert their influence. At the trial onset, donor MSCs were considered to repair damaged tissues by replacing the function of

damaged cells (Tolar et al., 2010). However, since 2009 it has been observed that MSCs secrete large volumes of bioactive molecules in response to injury, which recruits immune and reparative cells at the recipient sites (Tolar et al., 2010). This secretory effect is likely to carry across from the implantation to the control side, diminishing any side to side differences.

Callus size, cortical continuity and persistence of fracture gap are the three most commonly used parameters to assess fracture union (Bhandari M et al., 2002). Callus size and fracture bridging (cortical continuity) were chosen as the primary outcome measures in this work. Defining the fracture gap from plain radiographs was deemed unreliable, especially in hypertrophic nonunions. Preintervention radiographs were included on each assessment slide for assessors to identify new bone formation in the post-intervention radiographs accurately. Inter-observer agreement on defining the side with most new callus or bridging was, however, low (κ=0.43-0.46). Having multiple assessors judging each radiograph or CT scan independently and using their combined opinion is known to increase reliability (Kraemer, 1979). Moreover, having four assessors increased the reliability to 0.75-0.77, implying excellent inter-observer agreement(Fleiss et al., 2003). The GLAD algorithm, which is more reliable than 'majority-voting', further improved on this number by taking into account the agreement of each assessor with the others and the quality of each image(Whitehill et al., 2009b). Hence, inaccurate radiological assessment does not explain the lack of difference between 'test' and 'control' sides in this trial.

Since carry-across effects threaten the validity of the primary outcomes of this study, its secondary outcomes are probably more relevant. The overall union rate in the trial was 60%, which is low compared to union rates in other studies of lower limb fracture nonunions. A systematic review of biologic enhancement remedies for nonunion (bone

autograft and/or BMP-7) found thirteen studies with a pooled healing rate of 94% (Pneumaticos SG et al., 2013). Several case series reports the results of percutaneous injection of concentrated bone marrow with a typical union rate of around 90% (Connolly JF et al., 1991, Hernigou et al., 2005). The difference in union rates between the present work and the other studies may be related to case severities. Patients in the trial were defined as having recalcitrant nonunions, they had a higher mean age, a larger median number of previous treatments and included a larger proportion of diabetic patients in comparison to patients in other studies (Pneumaticos SG et al., 2013, Hernigou et al., 2005, Connolly JF et al., 1991). Moreover, the results of the study demonstrated these three factors were important determinants of healing and hence can explain the lower union rate in these patients.

Diabetes and age are well-known risk factors contributing to nonunions (Calori GM et al., 2007) and perhaps, to their persistence. The number of previous treatments characterises the persistence of a nonunion, and therefore, its emergence as a risk factor for failure to heal is expected. The injury mechanism or type of fracture (open versus closed) were not significant predictors of nonunion, in agreement with the findings of the SPRINT trial for tibial fractures (Fong K et al., 2013).

A longer cell doubling time during passage one reduced the likelihood of achieving union whereas the number of implanted cells was inconsequential. Doubling time was reported important in a study comparing osteogenic potentials of culture expanded human BMSCs (Janicki P and Boeuf, 2011). The study found considerable donor variations of *in-vivo* osteogenic potential and identified a longer cell doubling time during *in vitro* expansion as the best predictor of poor osteogenicity. This suggests that weak osteogenic capacity of the patients BMSCs may have been an additional factor explaining the relatively low union rates

in this study. The data from this study might help define future quality criteria for BMSCs in bone regeneration. The irrelevance of cell numbers seems to contradict a study of percutaneous bone marrow grafting in which larger numbers of injected cells increased the odds of fracture union (Hernigou et al., 2005). However, the smallest number of implanted cells in the reported trial (2 million) vastly exceeds even the largest number in that study (70,000). Cell numbers may be important, but unlikely within the range in the present study (2 to 10 million).

The two deaths reported in this study were due to heart failure and a bleeding aorto-enteric fistula, unrelated to BMSC implantation. One case of benign gastric tumour was reported six years after BMSC implantation and was also considered unrelated to the implantation. The tumour was surgically excised, and no recurrence was reported at final follow-up. A report on the safety of stem cells for orthopaedic regeneration also reported a tumour (liver), likewise considered unrelated (Centeno CJ et al., 2010). The lack of related serious adverse events in the study highlights the safety of using autologous *in vitro* expanded BMSCs to treat nonunions. BMSCs in this study were grown for a maximum of three passages to minimise the risk of genetic changes associated with long-term culture and expansion (Wang et al., 2012). These cells were cultured in autologous serum, removing risks of prion or virion transmission from bovine-derived serum (Wang et al., 2012). Finally, the cells were implanted locally rather than administered intravenously, reducing risks of aberrant remote proliferation (Goldring et al., 2011).

Twelve months after cell implantation, the EQ-5D index had improved significantly by 0.34 points, suggesting substantial overall improvement. Despite such improvement, the EQ-5D index remained low at twelve months; such observations were highlighted in a previous study of patients with fracture nonunions (Zeckey C and Mommsen, 2011). This lack of a

direct relationship can be explained by factors such as age, education, psychological state and clinically important distress (Whynes, 2008).

Although the current study failed to demonstrate new bone formation at the site of cell insertion in fracture nonunions, it is imperative to highlight the areas potential weakness which can influence the outcome of the present study. The study has been designed to be randomised, and self-controlled i.e. cells were randomly inserted in the 'test' side. However, we cannot rule out the migration of BMSC to the 'control' side of the non-union neither can the paracrine effect of BMSC to the 'control' side be dismissed. This phenomenon can essentially nullify the differences in the primary outcome observed between the test and control arms of the study. The further pitfall in the methodology was the use of multiple carrier types in different patients for cell insertion making the results difficult to be compared due to the differences in the osteoconductive properties of the carrier material. The primary outcome was assessed mainly on plain radiographs which limits to the two-dimensional interpretation of the change in new bone formation in postoperative films. Moreover, the time points for the radiographic assessment were early (3-6 months) and late (6-12 months). Radiographic interpretation of change in new bone formation during these time scales can be conceived as wide particularly in identifying subtle differences between the 'test' and the 'control' side. Nevertheless, the study uniquely highlights a positive correlation between shorter *in vitro* cell doubling time with fracture union. More importantly, it has demonstrated the safety of using autologous BMSC in patients with no untoward adverse events. The results also confirm the previous findings to support diabetes, increasing age and a higher number of previous surgeries to be detrimental to the healing of nonunions.

Future studies to assess the potential of cell therapy in fracture nonunion should have defined patients receiving the BMSC and the controls receiving none. Moreover, all the patients should receive single carrier material for cell delivery so that the outcome between patients can be compared. An important aspect would be to study the *in-vitro* characteristics of the BMSC of these patient groups to identify any potential risk factors including genetic markers that can influence the outcome of the cell therapy in non-union. Further studies should also account for regular high-definition CT scans at much more frequent intervals to perform volumetric analysis of the change in new bone formation if any.

In conclusion, the current work showed no significant difference in new bone formation at the site of cell insertion in cases with recalcitrant fracture nonunion. However, this study has demonstrated that a faster cell doubling during *in vitro* culture and three patient characteristics (lower age, the absence of diabetes and a smaller number of previous operations) were strongly correlated with fracture healing. Further studies are required to identify subtle differences in new bone formation following cell therapy in nonunion. An emphasis on *in vitro* characterising BMSCs from patients with nonunion should also be undertaken to identify any risk factors to the successful outcome of such treatments.

Chapter 4: AUTOLOGOUS BONE PLUG SUPPLEMENTED WITH AUTOLOGOUS CHONDROCYTE IMPLANTATION IN OSTEOCHONDRAL DEFECTS OF THE KNEE

4.1 Introduction

Treating full-thickness cartilage loss associated with an underlying subchondral bone defect in young patients can be challenging. The most commonly reported aetiology which represents such a situation is osteochondritis dissecans (OD), a condition that primarily affects the subchondral bone before progressing to the overlying cartilage (Edmonds and Polousky, 2013). High-grade OD (ICRS Grade 3 and 4) can lead to full thickness cartilage loss extending to the subchondral bone, potentially beyond 10 mm in depth. Isolated osteochondral defects (OCDs) can also extend below the subchondral bone plate into the cancellous bone (ICRS Grade 4, severely abnormal cartilage) and are usually observed after trauma (Brittberg and Winalski, 2003). It has been suggested that such defects, with underlying 'cavitation' of the bone, are amenable to bone graft during cartilage repair surgery including Autologous Chondrocyte Implantation(ACI) (Brittberg and Winalski, 2003). Different operative techniques have been described including drilling (Kocher et al., 2001, Edmonds et al., 2010) or fixation (Kouzelis et al., 2006, Makino et al., 2005) and the excision of the fragment (Wright et al., 2004) in OD. Restoration of the articular surface with osteochondral autograft (OAT) (Laprell and Petersen, 2001) or microfracture (MF) (Gudas et al., 2006, Gudas et al., 2012) are other techniques and both have resulted in significant clinical improvement, although results after OAT were better than after MF in patients with OD or isolated osteochondral defects. A 'sandwich' technique with bone graft and ACI has also been described in seven patients with OD, specifically used to treat defects deeper than 10mm by using a bilayer periosteal patch. The technique places one patch over the bone graft with the other being anchored to the adjacent cartilage with chondrocytes

injected between the layers although results from this procedure were not reported separately (Peterson et al., 2003).

A subsequent modification of the 'sandwich' technique with matrix-induced ACI (MACI) and autologous cancellous bone graft, termed the bilayer collagen membrane technique (BCMT), reported encouraging results in patients with OD and OCD (Bartlett et al., 2005, Vijayan et al., 2012). The benefit of using ACI as a restorative surgery in such cases lies in its ability to address defects larger than 2.5cm² (Erickson et al., 2013) and deeper than 8-10mm by employing a concurrent autologous bone graft (Peterson et al., 2003, Vijayan et al., 2012). A further technique of autologous cancellous graft and single layer MACI has also been described to treat ICRS Grade 3 and Grade 4 OD (Ochs et al., 2011, Steinhagen et al., 2010). Progressive remodelling of the subchondral lamina and filling of the cartilage defect following the use of this particular technique was demonstrated on serial MRI scans from 26 patients. Remodelling and filling were observed to be positively correlated with the functional outcome (Ochs et al., 2011). However, none of the previous reports describes the structural result of the subchondral bone graft and its potential clinical implications. Additionally, a striking paucity of information exists with regards to the structural integration of the grafted bone and repair cartilage interface.

In the current study, we describe the 'Osplug' technique of using a single precise monocortical autologous bone cylinder graft with first or second generation ACI to simultaneously restore the subchondral bone and cartilage defect in patients with OD (ICRS Grade 3 and 4) and isolated OCD (ICRS Grade 4) of the knee joint. Additionally, we report the clinical, arthroscopic, MRI and histological outcome of patients treated with this technique.

4.2 Materials and Methods

The present study was approved by the Audit Committee of our hospital with regards to the clinical and imaging review. The histological analyses of the biopsies were approved by the local research ethics committee as part of the Retrospective Assessment of ACI (REACT) study (REC number: 09/H1203/90). All cases were operated by the senior author (JBR) from 2003-2008. All patients had preoperative MRI scans to confirm the presence of cartilage and subchondral bone defects. Patients with a minimum of 5mm of defect depth were included in the study. Radiographs were undertaken to ascertain the absence of malalignment in the knee. Previous surgeries to treat the condition were recorded, excluding the first stage of ACI. Failure was defined as a Lysholm score below the preoperative value, requirement of further surgical interventions (except one-year arthroscopy used to assess the repair site) or total knee replacement (TKR). An overview of the technique is illustrated in Figure 4.1.

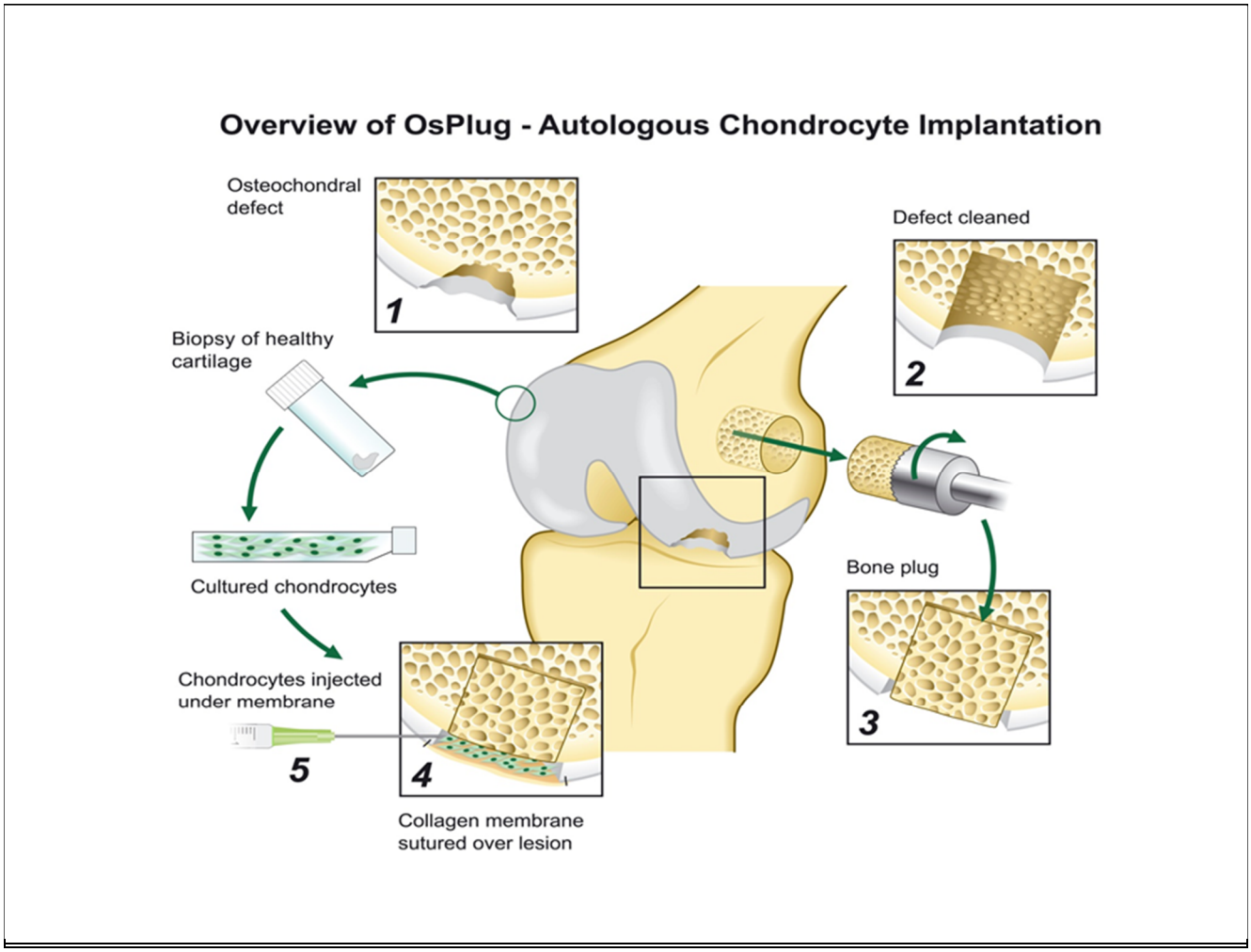

Figure 4.1 The 1st stage (as in standard ACI) is shown with the anticlockwise arrows while the steps involved in the 2nd stage are shown in the numbered boxes in a clockwise arrangement

4.2.1 Surgical Technique

The surgical technique had two stages. The first stage comprised an arthroscopy and cartilage biopsy to harvest the chondrocytes. The second stage involved insertion of a unicortical autologous bone graft in the subchondral bone defect and implantation of the autologous chondrocytes in the articular cartilage defect under a secured periosteum (first-generation ACI) or collagen patch (second generation ACI). The second stage was performed approximately three weeks after the first stage (Figure 4.1).

4.2.1.1 First stage: During the first stage of the procedure, patients underwent a diagnostic arthroscopy to evaluate the site and extent of the defect. A cartilage biopsy was undertaken at this stage from the lesser weight-bearing area of the knee. The chondrocytes generated from the harvested cartilage were expanded *in vitro* for approximately three weeks in the Good Manufacturing Practice (GMP) standard 'Oscell' cell production facility in our centre (Harrison, 2000).

4.2.1.2 Second stage: An arthrotomy was performed to access the cartilage and subchondral defect. The defect was debrided to healthy articular cartilage laterally and down to the healthy bone. The size of the defect was measured with Vernier callipers, and the exact location was recorded using the validated Oswestry Knee Map (Talkhani and Richardson, 1999). A cylindrical cortico-cancellous bone plug was then harvested from the non-articular part of the femoral condyle with a dowel drill. A site above the origin of the collateral ligament of either condyle was chosen and an osteoperiosteal flap raised. Care was taken to leave a 1cm margin from all weight-bearing joint surfaces. A fine osteotome was inserted to facilitate the release of the donor plug. This bone plug with the cortex side facing up was subsequently impacted into the defect to restore the subchondral bone plate and

underlying cancellous bone defect. A slight over-sized graft was used to ensure tight fit although the excess bone was trimmed with a high-speed burr. This was subsequently impacted into the defect with the cortex-side facing up to restore the subchondral plate and the underlying cancellous bone defect (Figure 3.2). The remaining chondral defect was then covered with a periosteal patch from the proximal tibia (5 cases) or a collagen membrane (Chondro-Gide®; Geistlich Sons Ltd, Manchester, UK) (12 cases), which was sutured with 6-0 Vicryl (Ethicon, Livingston, UK) to the adjacent cartilage. The edges were subsequently sealed using fibrin glue (TISSEEL; Baxter, Newbury, UK). Saline was injected under the patch to test for water tightness ('leak-test') and subsequently aspirated. Cultured autologous chondrocytes suspended in autologous serum were implanted beneath the patch through a 20 gauge Yale Spinal Needle (Becton Dickinson, Oxford, UK). This novel method of concurrent monocortical cylinder graft with first or second generation ACI was termed the Osplug technique. This technique of concurrent bone graft with ACI was undertaken to simultaneously restore the subchondral bone plate and repair the overlying cartilage. The principle of dealing with these types of osteoarticular defects was first described by Peterson et al, (2003) in treating ICRS Grade 4 defects extending to 10mm of the subchondral bone using first-generation ACI (described as 'sandwich technique'). Subsequently, a modification of the technique with MACI and cancellous bone graft was also undertaken (Bartlett et al., 2005, Vijayan et al., 2012). Use of multiple small bone cylinder grafts to address subchondral bone defects is also described in conjunction with MACI (Ochs et al., 2011). However, using second generation ACI and a tailored monocortical autologous bone graft is described in the current work. The technique conceives use of precisely measured bone cylinder graft to achieve a stable per-operative reconstruction of the subchondral bone plate and minimised the donor site morbidity from harvesting multiple

small bone cylinder grafts. Following bone graft, a standard second-generation ACI is undertaken with a periosteal or collagen patch.

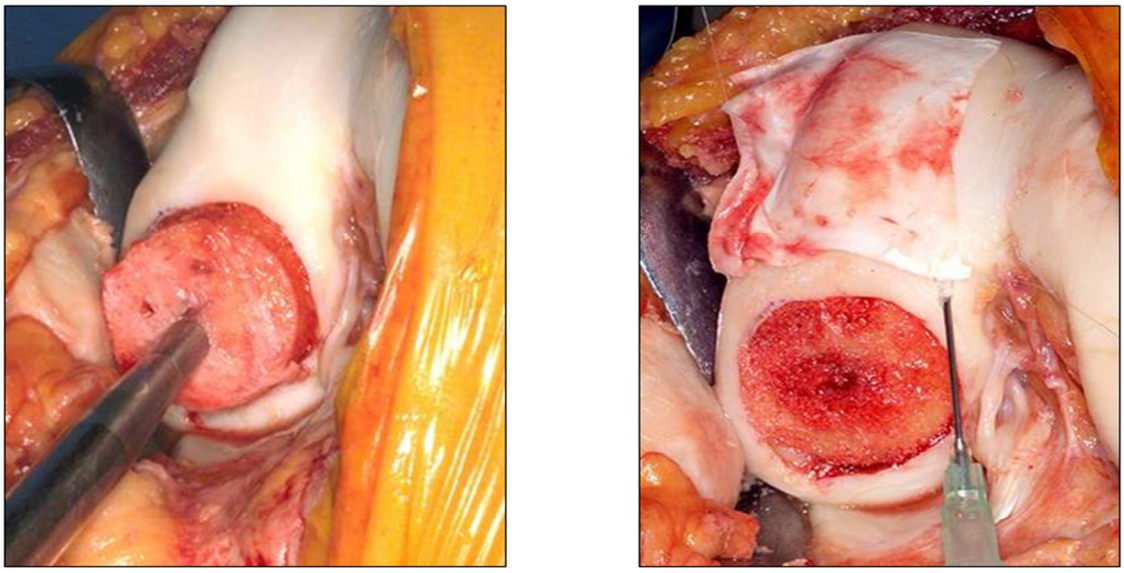

a b

Figure 4.2 (a) Insertion of 'Osplug' in the osteochondral defect of the medial femoral condyle. (b) Second generation ACI on the restored subchondral bone.

4.2.2 Rehabilitation

A standardised rehabilitation protocol was followed for all patients undergoing surgery (Bailey et al., 2003). This includes initial immobilisation of the knee for 6 hours allowing early cell adherence during the postoperative period (Minas and Peterson, 1999). Subsequently, continuous passive movement from full extension of the knee to 45 degrees of flexion for the first 48 hours after surgery was instituted to restore passive movement, particularly full extension of the knee to prevent adhesion and stiffness and achieve superior clinical outcome (Alfredson and Lorentzon, 1999). Patients were subsequently allowed to partially weight-bear with a hinged knee brace for 6-8 weeks to allow proprioception of the joint in addition to the concentric and eccentric loading of the joint. The eccentric loading improved the shock absorbing capacity of quadriceps during walking and converted the potential energy to forceful concentric contraction (this forms the basis of plyometric-type-work) (Bailey et al., 2003). Patients returned to full activity under the supervision of physiotherapist after 6-8 weeks although they refrained from sporting activities. Cycling was encouraged initially to allow dynamic strengthening of the muscles with the progressive proprioceptive conditioning of the joint, then swimming and running by six months. The total period of rehabilitation was tailored according to individual progress at this stage and can extend up to 12 months.

4.2.3 Outcome assessment

- *4.2.3.1 Primary clinical outcome*: Functional outcome in this study was assessed using the patient reported modified Lysholm scale for the assessment of cartilage defects (Smith et al., 2009) preoperatively, one year and five years after the surgery. All three scores were collected prospectively by the Oswestry Outcome Centre.
- *4.2.3.2 Arthroscopic assessment*: Patients had an arthroscopic assessment of the repair site documented in the knee map using the validated Oswestry Arthroscopy Score (OAS; (Smith et al., 2005)) approximately one year after the second stage of the procedure. Five parameters were assessed: the level of the treated articular surface compared to the surrounding cartilage (0-2), integration with the surrounding cartilage (0-2), the appearance of the surface (0-2), the colour of the graft (0-2), and stiffness of the graft on probing (0-2). The total score ranges from 0-10, with higher values indicating a better quality of repair tissue.
- *4.2.3.3 Histological assessment*: Biopsies of the repair tissue at the treated site were obtained during follow-up arthroscopic assessment of the knee. This was not routine and only performed if patients consented to the additional procedure. The Oswestry Knee Map, which recorded the site of the defect during the second stage, was used to ascertain the location of the graft. A core biopsy was taken with a Jamshidi needle close to the centre of the treated defect and included both the chondral and the underlying subchondral bone repair tissue. Biopsies were snap-frozen in liquid nitrogen-cooled hexane, embedded in OCT compound (Tissue-Tek, Zoeterwoude, Netherlands) and cryosectioned to produce 7 mm thick sections which were collected onto poly-L-lysine coated slides. These were then stained with either

haematoxylin and eosin (H&E) or toluidine blue for histological assessment of the general morphology of the repair tissue and glycosaminoglycan content, respectively, as per standard protocols (Roberts and Menage, 2004). The biopsy was assessed with bright light and polarised light microscopy for the morphology and collagen organisation. Sections were scored semi-quantitatively using the International Cartilage Repair Score II (ICRS II; (Mainil-Varlet et al., 2010)), assessing the quality of the repair tissue. This has 14 parameters, each with a range of 0-10 with higher values indicating better quality. One parameter, the 'overall score', assesses the full biopsy.

- 4.2.3.4 *MRI Scans*: MRI scans were also used to determine the quality of repair following the surgery. All MRIs were scored by a single musculoskeletal radiologist, with expertise in cartilage imaging, in conjunction with an orthopaedic surgeon inclined towards cartilage repair surgery.

  The MRI acquisition was composed of coronal and sagittal spin echo T1, and gradient echo T2 weighted sequences; axial dual echo (proton density and T2 weighting), and 3D fat-suppressed FLASH and 3D DESS sequences were also acquired. A 1.5 Tesla unit with 25mT/m gradient strength (Siemens Vision, Erlangen, Germany) and a standard Siemens viewing station and software (VB33A) were used. The parameters for the five sequences were:

  1) SE T1: Flip angle 90°, TR 722, TE 20, FOV 200, matrix 336x512.

  2) GRE T2: Flip angle 30°, TR 608, TE 18, FOV 200, matrix 224x512 matrix.

  3) Axial dual echo images: Turbo spin echo flip angle 180°, echo train length 5, spectral fat saturation, TR 3500, TE 16/98, FOV 175x200, matrix 210x256.4) 3D FLASH: Spectral fat saturation. Flip angle 30°, TR 50 ms, TE 11 ms, TA 9:38 min, FOV

180x180 mm, matrix 192x256, slab=90mm displayed as 60 continuous sagittal images of 1.5mm thickness.

5) 3D DESS: Spectral fat saturation and magnetisation transfer. Flip angle 40°, TR 58.6 ms, TE 9 ms, TA 12:01 min, FOV 180x180 mm, matrix 192x256, slab=96mm displayed as 64 continuous sagittal images of 1.5mm thickness.

The cartilage repair site was semi-quantitatively assessed with magnetic resonance observation of cartilage repair tissue (MOCART) parameters (Marlovits et al., 2006, Marlovits et al., 2004, Welsch et al., 2010). Also, particular attention was paid to determine if a subchondral lamina had reformed post-treatment (referred to as a 'neo-lamina') and also to the underlying autologous bone graft. The presence of a 'neo-lamina', indicating remodelling, was assessed along the whole dimension of the bony defect. This was categorised as described by Ochs et al., i.e., Grade-1 (0-25% of defect diameter), Grade-2 (26-50% defect diameter), Grade-3 (51-75% defect) and Grade-4 (>76% defect diameter) (Ochs et al., 2011).

Lateral integration of the cylindrical bone graft was assessed in both the coronal and sagittal planes at the graft and the host bone junction on the MRI scans. The presence of continuous trabeculae along this whole interface indicated 100% integration while the persistence of trabecular discontinuity indicated a lack of integration. The lateral integration was semi-quantitatively classified into four categories: Grade-1 (<25%), Grade-2 (26-50%), Grade-3 (51-75%) and Grade-4 (76-100%). The morphology of the central subchondral grafted bone was assessed according to the type of trabecular architecture and presence of cysts within the graft and was graded from completely remodelled graft to disorganised bone graft or bone graft with the presence of a cyst(s). Scans performed at least 12 months

after the second stage of the surgery were evaluated to appraise the longer-term quality of the repair, presence of the neo-lamina and the integration of the monocortical bone cylinder graft.

4.2.4 Statistics

A Shapiro-Wilk test was used to ascertain the normality of the data. The paired Wilcoxon Signed Rank test was used to demonstrate the difference between Lysholm scores at different time points. Rank-biserial and bivariate rank (Spearman) correlation analysis were used to investigate the relation between the Lysholm score and various categorical or continuous predictors and outcomes. IBM SPSS Statistics vs. 22 (IBM UK Ltd, Portsmouth, UK) was used for the analysis of the data.

4.3 Results

4.3.1 Patient characteristics

A total of 12 cases of OD (ICRS grade 3 and 4) and 5 cases of isolated OCD (ICRS grade 4) were included in this study. Their mean age at the time of surgery was 27 years ±7SD (range 17-40). Fifteen patients had the defect on the medial femoral condyle and two on the lateral femoral condyle. Ten patients had a lesion in the right knee and seven in the left knee. The mean defect size was 4.5 cm^2 ±2.6SD (range 1-9). The mean defect depth was 11.3 mm ±5SD (range 5-18). Twelve patients had a collagen patch (Chondro-Gide®; Geistlich Sons Ltd, Manchester, UK) and five patients had a periosteal patch from the proximal tibia to cover the defect. Each patient had received at least one previous surgery with a mean of 1.6 operations (range 1-4) to treat the defect; not including the 1^{st} stage of the ACI. There was no association between the number of previous surgeries and one-year Lysholm scores (p=0.47, Spearman's rho -0.214) or 5 years Lysholm scores (p=0.96, Spearman's rho -0.16). One patient was lost to follow-up at one year, and a further two patients were lost to follow-up at 5 years.

Pt. No.	Previous surgeries
1	Arthroscopy + removal of loose body + drilling
2	Arthroscopy + removal of loose body; Arthroscopy + debridement +drilling; Arthroscopy +microfracture
3	Arthroscopy + Smiles's pin fixation; Arthroscopy +debridement +drilling
4	Arthroscopy+ removal of loose bodies +debridement + drilling
5	Arthroscopy+ removal of loose bodies +debridement
6	Arthroscopy+ removal of loose bodies+ debridement
7	Arthroscopy+ removal of loose bodies+ debridement
8	Arthroscopy+ removal of loose bodies +microfracture
9	Arthroscopy+ removal of loose bodies; Arthroscopy +drilling
10	Arthroscopy+ removal of loose bodies +debridement
11	Arthroscopy+ removal of loose bodies+ debridement
12	Arthroscopy+ removal of loose bodies, 3x Arthroscopy + debridement
13	Arthroscopy+ removal of loose bodies +debridement
14	Arthroscopy+ removal of loose bodies+ debridement; Arthroscopy + debridement
15	Arthroscopy+ removal of loose bodies +microfracture
16	Arthroscopy+ pin fixation; Arthroscopy +removal of loose bodies+ debridement
17	Arthroscopy+ removal of loose bodies +microfracture; Arthroscopy + debridement

Table 4.1 Details of previous surgeries in patients treated with 'Osplug' technique

4.3.2 Clinical outcome

A Shapiro-Wilk test confirmed that the Lysholm scores did not follow a normal distribution (p=0.01). The median preoperative Lysholm score was 45 (IQR 24, range 16-79). The median Lysholm score increased to 77 (IQR 28, range 41-100) at 1 year and was 70 (IQR 35, range 33-91) 5 years after the surgery. A Wilcoxon Signed Rank test showed a statistically significant improvement in Lysholm scores at 1 year (p-value 0.001) and 5 years (p-value 0.009) in comparison to preoperative scores. The difference in Lysholm scores between 1 and 5 years was not statistically significant (p=0.50).

No association was found between the type of patch used (periosteum/collagen) and Lysholm score at 1 year (p-value = 0.86, point-biserial correlation-0.05) and 5 years (p-value = 0.95, point-biserial correlation-0.02). The clinical outcome was not related to the size (at one year, p=0.8 and five years, p=0.3) or depth (at one year, p=0.7 and five years, p=0.2) of the defect. A total of three patients had treatment failure with one requiring TKR and the other two required further surgical intervention, but none of these patients had their Lysholm score below the preoperative level.

The patient requiring TKR had a Lysholm score of 33 before failure at 5 years after the Osplug procedure; this score improved from 16 preoperatively to 41 at one year. Two patients required further surgical intervention, one at 2 years and one at 4 years because of persistent symptoms. Both had a Lysholm score of 45 prior to subsequent surgery, but in both cases, this was higher than their score before the Osplug procedure.

4.3.3 Arthroscopic assessment

Eleven patients had an arthroscopic assessment of the repair site at a mean of 1.3 years (range 0.7-2) postoperatively. The mean OAS was 6.2 (range 0-9). A statistically significant correlation was noted between OAS and Lysholm score at both 1 year (p=0.008, Spearman's rho 0.78) and 5 years (p-value=0.046, Spearman's rho 0.64). Furthermore, a significant association between the OAS and failure of the Osplug technique was observed (p-value = 0.001, point-biserial correlation-0.865).

4.3.4 Histological assessment

The mean value of the ICRS II 'overall score' for the repair tissue biopsies analysed was 5.2±1.6SD (range 2.3-7.4; Table 4.2). Of the 10 biopsies obtained (from 8 patients), 9 were found to be fibrocartilage, and one was a mixture of fibrocartilage and hyaline cartilage. Matrix metachromasia was very variable between different biopsies, with scores ranging from 2.7 to 8.9, being nearly normal (with a maximum of 10) for 2 biopsies. The surface architecture was generally good to excellent. Integration of the repair cartilage to the underlying subchondral bone was also good, with the tidemark being visible in more than half of the biopsies (Figure 4.3). Cell morphology was variable throughout the biopsies, with some being fibroblastic in shape, while others were more rounded and of chondrocyte morphology; clustering of cells was rare. Three biopsies contained evidence of ectopic calcification. One of these was a second biopsy from patient 1 taken 13 months after the first biopsy when no evidence of calcification was observed. One biopsy (from patient 9) showed quite an extensive calcification. There was no evidence of either vascularisation or inflammation in any of the biopsies examined. One patient (Patient 3) with sequential biopsies taken at 13 and 37 months after the Osplug procedure demonstrated an interesting

histological feature. Under polarised light, the 13 month biopsy showed collagen fibres running predominantly parallel between the cartilage and subchondral bone along the cartilage/bone graft interface; at 37 months, the orientation of the fibres in the bone had changed from being parallel to much more oblique, integrating the cartilage into the bone (Figure 4.4). In addition, the latest biopsy demonstrated an improvement in the individual ICRS II parameters for tissue morphology, cell morphology, subchondral bone, as well as the overall score, compared to the earlier biopsy.

Pt. No.	Months post ACI	Tissue Morphology	Staining	Cell Morphology	Clusters	Surface	Integration	Tidemark	SCB	Inflammation	Calcification	Vasc.	Superficial zone	Mid/deep zone	Overall
1	11	5.45	2.7	0.45	10	6.75	7.85	7.8	6.35	10	10	10	3.9	3.7	3.8
1	24	5.35	3.55	0.7	10	7.75	9.5	0.05	9.9	10	8.7	10	4.3	4.75	4.35
2	24	1.9	4.8	8.9	6.7	9.9	9.9	8.9	9	10	10	10	7.7	6.1	7.4
3	13	3.9	5.8	7.8	10	8.4	9.8	8.2	4.5	10	10	10	6.4	5.4	5.5
3	37	6.5	5.7	9.5	10	8.4	10	8.5	8	10	10	10	7.6	7.6	7.2
4	12	5.55	8.9	5.5	9.95	9.55	9.95	1.1	8	10	10	10	7.2	6.65	6.75
7	13	5.4	2.25	2.55	9.95	8.6	n/a	n/a	2.95	10	10	10	5.8	3.65	4.7
9	22	4.1	2.7	5.1	10	n/a	n/a	n/a	n/a	10	1.4	10	2.7	n/a	2.3
12	18	5.15	6.55	9.1	10	9.45	9.2	0.55	2.2	10	2.75	10	5.75	4.15	5.2
14	16	4.8	8.85	1.4	10	n/a	n/a	n/a	n/a	10	10	10	n/a	4.95	4.65

Table 4.2 Individual scores for the 14 parameters assessed with the ICRS II Histology Score (Mainil-Varlet et al., 2010) for each biopsy

(SCB-subchondral bone, Vasc-vascularisation

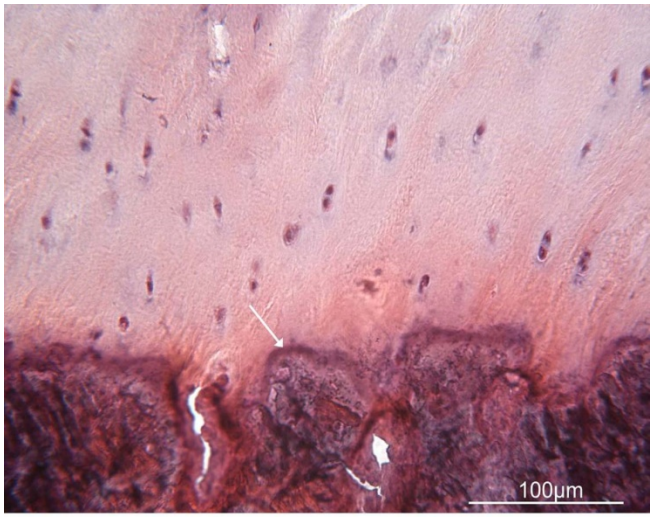

Figure 4.3 Representative image of a tidemark (arrow) in one of the repair tissue biopsies analysed (Scale bar represents 100µm)

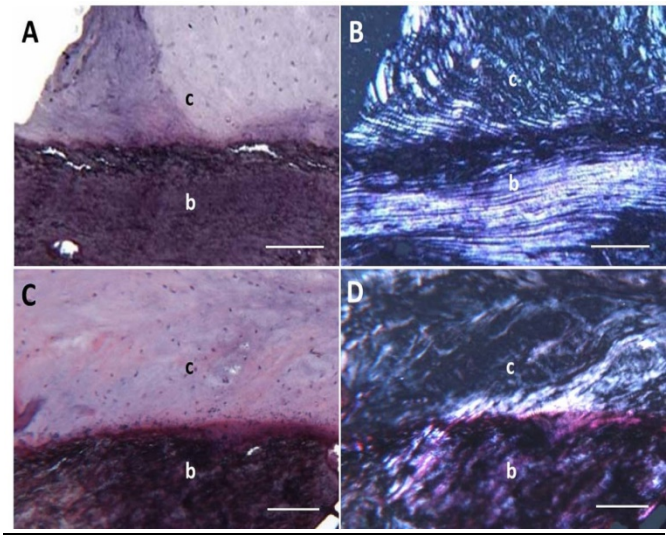

Figure 4.4 Sequential biopsy specimens at 13 months (A, B) and 37 months (C, D) after autologous chondrocyte implantation from patient 3. Under polarised light (images B and D are polarised light images of the hematoxylin and eosin–stained sections in A and C, respectively), collagen fibres in the 13-month biopsy specimen can be seen running parallel in the bone to the cartilage-bone interface. By 37 months, these fibres within the bone can be seen to be more oblique and integrate between the cartilage and bone. Scale bars = 500 mm. b, bone; c, cartilage.

4.3.5 MRI assessment

MRI scans were available for eleven patients, at a mean of 2.6 years ±1.8SD (range 1-6) after surgery. The overall MOCART score was 61±22SD (range 20-85) out of a total score of 100 with higher score implying better quality of cartilage repair (Table4.3). The degree of defect fill with the repair tissue was noted to be complete in 4 patients. Two patients had exposed subchondral bone. In one patient (patient 2) the repair cartilage was hypertrophic for more than 50% of the defect diameter and showed incomplete fill (to a level of >50% of the thickness of the adjacent cartilage) in the rest of the defect. Complete integration of the repair cartilage with adjacent healthy cartilage, represented by the isointense signal intensity of the repair tissue compared to the adjacent cartilage, was noted in 8 patients (73%). The neo-lamina was observed to be intact in only 3 patients; however, it was seen to be partially formed in the rest indicating a continuous process of remodelling in the subchondral lamina. The subchondral bone was not intact in 10 patients, with cysts in 5 patients (Figure 4.5) and disorganised bone graft with inhomogeneous signals in comparison to the adjacent bone in another 5 patients (Figure 4.6).

Figure 4.5 Sagittal image with proton density turbo spin echo spectral fat saturation MRI sequence of the knee demonstrating cyst within the bone graft.

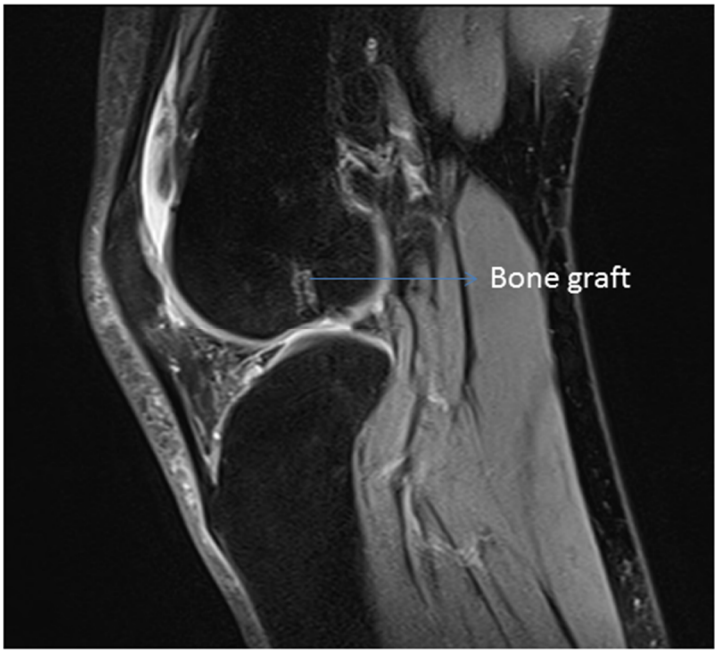

Figure 4.6 Sagittal image with proton density turbo spin echo spectral fat saturation MRI sequence of the knee demonstrating inhomogenous signal within the bone graft In comparison to the adjacent subchondral bone

Marginal integration of the 'Osplug' was classified as Grade 4 (76-100%) in the orthogonal plane of the bone graft in 8 out of 11 patients (73%; Figure 4.7). Interestingly, the three patients who failed had poor integration of the bone graft suggesting this to be a significant predictor of failure of the Osplug technique (Spearman's rho 0.8, p=0.003). Lateral integration seen on the MRI scans had a significant positive correlation with a good clinical outcome at 1 year (p-value=0.007, Spearman's rho 0.75) although it failed to reach statistical significance at 5 years (p-value=0.08, Spearman's rho 0.55). The grade of neo-lamina evident in MRI scans had a significant positive correlation to time of the scan since surgery (p-value=0.001, Spearman's rho 0.86). However, grade of neo-lamina had no significant correlation with the lateral integration of the bone graft (p=0.15), MOCART scores (p=0.8), one-year Lysholm scores (p=0.43) or five years Lysholm scores (p=0.5) (Table4.4).

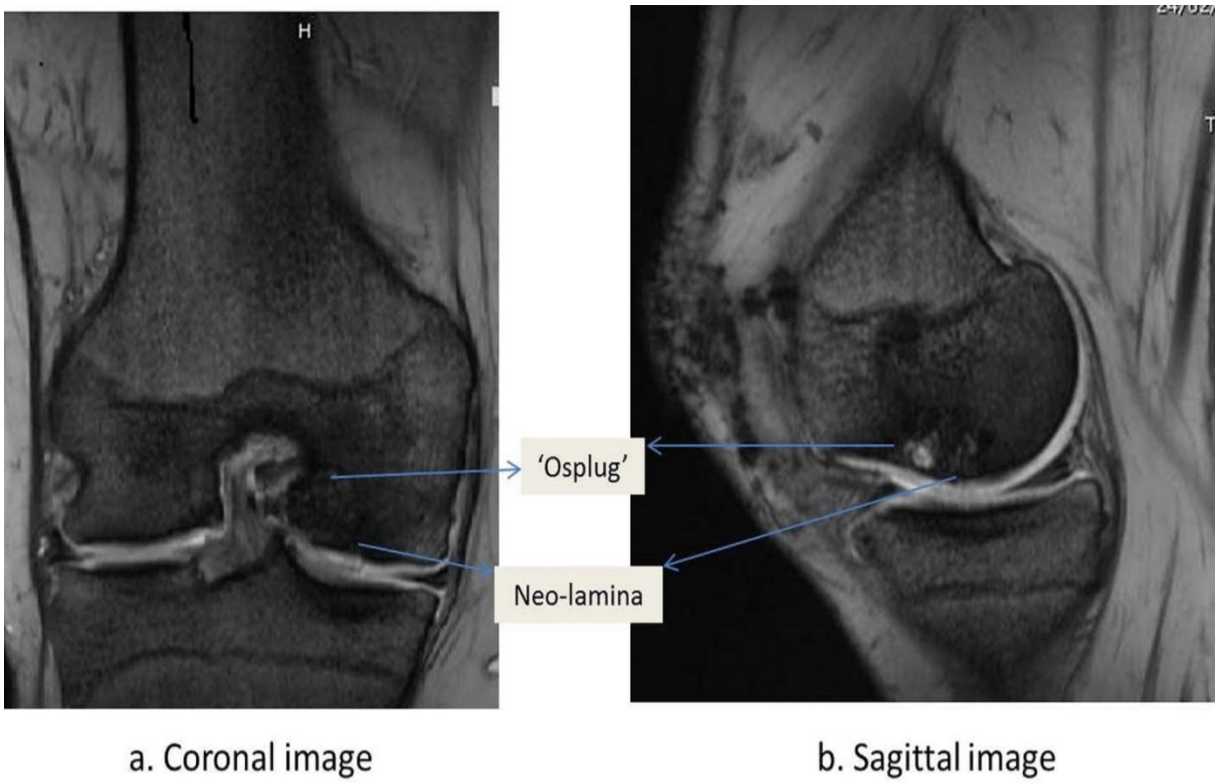

Figure 4.7 Representative image of lateral integration of the 'Osplug' in T2 weighted MRI sequence with continuous trabecular pattern representing Grade 4 (76-100%) marginal integration of the subchondral bone

Pt. No.	Time of MRI (years) post-ACI	Degree of repair + filling of defect	Integration of border of repair & native cartilage?	Surface of the repair cartilage	Structure of the repair	Signal intensity of repair cartilage? (DT2FSE/3D-GE-FS)	Subchondral lamina	Subchondral bone	Adhesion	Effusion	Total MOCART Score		Neo-lamina (Grade-1=0-25%, Gr 2=26-50%, Gr 3=51-75%, Gr 4=76-100%)	'Osplug' lateral integration (Gr 1=0-25%, Gr2=26-50%, Gr 3=51-75%,Gr4=76-100%)
2	2	10	15	5	0	30	5	0	5	0	75		4.00	4.00
3	6	10	15	5	5	30	5	5	5	5	85		4.00	4.00
5	3	5	15	0	5	30	0	0	5	0	60		3.00	4.00
9	1	20	10	5	5	30	0	0	5	0	75		1.00	3.00
10	4	0	0	0	0	15	5	0	5	0	25		4.00	4.00
11	1	20	15	5	5	30	0	0	5	0	80		1.00	4.00
12	3	20	15	5	0	15	0	0	5	0	60		3.00	3.00
14	2	20	15	5	0	30	0	0	5	0	75		3.00	4.00
15	3	5	0	0	0	30	0	0	5	0	40		3.00	4.00
16	1	15	15	5	0	30	0	0	5	0	70		1.00	4.00
17	1	0	0	0	0	15	0	0	5	0	20		1.00	2.00

Table 4.3 MRI characteristics of the cartilage in the repair site according to the MOCART scale. Two other bone properties were also assessed: the remodelling of the neo-lamina and the lateral integration of the monocortical cylinder graft

Scores ascertained to MOCART parameters are represented below (Welsch et al., 2010)-

a. The degree of defect fill and repair-Complete-20, Hypertrophy-15, Incomplete (>50% of adjacent cartilage)-10, Incomplete (<50% of adjacent cartilage)-5, Subchondral bone exposed-0.
b. Integration of the border-Complete-15, Incomplete(split like border visible)-10, Defect visible <50% of length-5, Defect visible >50% of length-0
c. Surface of the repair tissue-Surface intact-10, Surface damaged <50% of depth-5, Surface damaged >50% of depth-0
d. Structure of the repair-Homogenous-5, Inhomogenous-0
e. Signal intensity of the repair tissue-Normal(identical to the adjacent cartilage)-30, Nearly normal-15, Abnormal-0
f. Subchondral lamina-Intact-5, Not intact-0
g. Subchondral bone-Intact-5, Not intact-0
h. Adhesion-No-5, Yes-0
i. Effusion-No-5, Yes

j.

Variables		p-value	Correlation coefficient
1 year Lysholm score	Lateral integration of bone graft	0.007*	0.75
	OAS	0.008*	0.78
	Neo-lamina	0.43	0.27
5 year Lysholm score	Lateral integration of bone graft	0.08	0.55
	OAS	0.046*	0.64
	Neo-lamina	0.54	0.23
Failure	Lateral integration of bone graft	0.003*	0.8
	OAS	0.001*	0.86
	Neo-lamina	0.54	0.20
Time of MRI from surgery	Neo-lamina	0.004*	0.8
	Lateral integration	0.27	0.36

(p-value <0.05 (2-tailed) considered significant (marked with *), point-biserial and Spearman's correlation analysis was used to investigate the relation between the Lysholm score and various categorical or continuous predictors and outcome)

Table 4.4 Correlation matrix between variables

4.4 Discussion

This current work demonstrates that significant clinical and functional improvement can result for up to 5 years from the novel Osplug technique if patients have more severe OCD (ICRS 4) or OD (ICRS 3 and 4). The mean age of patients included in this study is 27 years with a mean defect size of 4.5 cm^2 (range 1-9) and an average depth of 11.3 mm (range 5-18). These parameters are comparable to previous reports of treatment with simultaneous ACI and bone graft (Peterson et al., 2003, Steinhagen et al., 2010, Vijayan et al., 2012, Ochs et al., 2011). Moreover, all patients in the current study had, at least, one previous surgical procedure (mean-1.6, range 1-4) which is comparable to an earlier study (Vijayan et al., 2012). However, such techniques have been described as a primary procedure in a proportion of their patients in two other series describing MACI with bone graft (Steinhagen et al., 2010, Ochs et al., 2011). Interestingly, these two studies of MACI and bone graft described a significant clinical and functional improvement at 12 months, which was maintained subsequently with no further significant rise or fall for a total follow-up of 36-39 months (Steinhagen et al., 2010, Ochs et al., 2011, Peterson et al., 2003). The present study noted a similar finding of a significant rise in Lysholm score at 1 year which was retained for at least 5 years of follow-up, with no further significant change in functional outcome in a patient group in which this technique was used as a salvage procedure after at least one failed procedure.

The validated arthroscopy score (Smith et al., 2005) for the repair site at 1.3 years was seen to have a significant positive correlation with the one and five-year clinical outcome. This is the first report demonstrating an association of the functional outcome with the macroscopic quality of the repair site after simultaneous ACI and bone graft technique,

where a poor arthroscopy score, indicative of suboptimal graft, was linked with a higher rate of treatment failure. A further unique finding was the low grade of bone plug integration seen in MRI scans which had a significant correlation with poor clinical outcome in one year and failure of the procedure, requiring reintervention or TKR. These findings indicate the contribution of the richly innervated subchondral bone as a potential source of pain and functional limitation, especially if it occurs in association with loss of overlying cartilage (Suri and Walsh, 2012). The current evidence suggests that in such cases the definition between articular cartilage and the subchondral bone is lost leading to the invasion of the articular cartilage by sensory nerves and blood vessels forming the basis of pain and progression of OA (Yuan et al., 2014). These promotes 'cross-talk' between the cartilage and subchondral bone which is primarily regulated by β-NGF (Nerve Growth Factor) and VEGF, specific antagonists to these growth factors also lead to clinical and functional improvement in patients reinstating their in role symptomatic and functional deterioration (Nagai et al., 2010, Spierings et al., 2013).

There are several reports in the literature of subchondral bone graft techniques in conjunction with cell therapy for cartilage repair. Impaction of loose cancellous bone was described by the proponents of the original 'sandwich' technique (Peterson et al., 2003) and kept unchanged in BCMT (Bartlett et al., 2005, Vijayan et al., 2012). Two studies described using a diamond core drill to harvest a monocortical graft (Ochs et al., 2011, Steinhagen et al., 2010), although the cortical layer was removed in one study, actually rendering those grafts to be cancellous bone cylinders (Steinhagen et al., 2010). A press-fit was attempted in these two studies by using more than one graft, with one study using fibrin glue between the grafts to ensure an adequate seal (Ochs et al., 2011) whilst the other one used an under-

sized core drill on the host bone to provide a tight fit (Steinhagen et al., 2010). Both of these studies had uniform patient characteristics (OD of ICRS grade 3 and 4) and used a single layer of MACI with the cylindrical bone graft. Both studies reported a significant clinical improvement at a mean follow-up of approximately 3 years (Steinhagen et al., 2010, Ochs et al., 2011). However, a poor clinical outcome was reported in defects larger than 6cm² with the use of cancellous bone cylinder grafts (Steinhagen et al., 2010, Ochs et al., 2011). The Osplug technique was developed to address large osteoarticular lesions in the knee as multiple bone plugs were found to be unstable in our experience. Moreover, large numbers of bone plugs may also lead to donor site morbidity. The Osplug technique advocates using a single monocortical bone graft which is tailored to the dimension of the defect. In the present study, it has been demonstrated that a similar functional outcome can be achieved using this technique at a longer follow-up of 5 years. The outcome does not depend on defect area or depth or whether a first or second generation ACI was used. The present study also demonstrates Grade 4 (76-100%) lateral integration of the monocortical graft in 8 of 11 patients using the novel technique, which had a significant positive correlation with the functional outcome at 1 year.

The only published study of patients with OD, which were treated with bone graft and ACI reported MOCART scores of consecutive MRI scans from 26 patients treated with cortico-cancellous bone graft and single layer MACI (Ochs et al., 2011). This study found a mean value of 62±19SD, comparable to the mean results of 61±22SD at 2.6 years from the present work (Ochs et al., 2011). A larger presence of a neo-lamina in this study was positively correlated with the duration between the surgery and the scan reinstating the previously hypothesised time-dependent process of remodelling in the subchondral lamina (Ochs et al.,

2011). There was no relationship between the grade of neo-lamina seen in MRI scans to the clinical outcome, overall MOCART score or lateral integration of the bone graft. This lack of correlation can be related to the small sample size in the current work, causing type-2 errors. Nevertheless, the findings in earlier work (Ochs et al., 2011) and the present work consistently demonstrate the presence of the subchondral neo-lamina at the interface of repair cartilage and bone graft following the concurrent use of cortico-cancellous cylinder grafts with ACI.

This is the first report of the histological assessment of the repair tissue following simultaneous bone graft and ACI using the ICRS II score (Mainil-Varlet et al., 2010). The most striking and structurally relevant microscopic finding in these samples was the consistent integration of the repair cartilage and the underlying subchondral bone, implying interfacial bonding between the grafted bone and overlying repair cartilage. Interestingly, two patients had a biopsy taken at two time-points, both demonstrating an increase over time in scores for tissue morphology, cell morphology, subchondral bone and overall score. This suggests a slow remodelling and maturation of the repair cartilage, as had previously been shown (McCarthy and Roberts, 2013, Roberts et al., 2009), in addition to a similar process occurring within the transplanted bone.

However, the present study has a small sample size of seventeen patients. To detect a large effect of the intervention (correlation coefficient of 0.5) we should ideally have 26 patients for the point-biserial correlation coefficient and 29 patients for Spearman's rank coefficient. This highlights the relative rarity of the condition from a single centre which is also evident from other published series (Bartlett et al., 2005, Maus et al., 2008, Vijayan et al., 2012).

In summary, the Osplug technique, combining a tailored monocortical autologous bone plug with ACI, shows promising early and mid-term functional outcomes with first or second generation ACI, irrespective of the size of the defect. A low arthroscopic score and poor integration of the monocortical bone graft assessed with MRI is associated with a poor clinical outcome and subsequent failure of the intervention. Establishing proper integration between the implanted cells and bone core appears critical to the long-term success of the procedure. Once this is established, there appears to be improvement and maturation with time, both in the quality of the cartilage repair histologically and also the remodelling of the subchondral neo-lamina of the bone, particularly in those patients who go on to benefit clinically.

Chapter 5: Combining osteotomy with autologous chondrocyte implantation to treat early osteoarthritis of the knee

5.1 Introduction

In the last decade, the rate of primary total knee replacements (TKRs) has doubled annually in the United States with a decrease in the average age of patients due to a growing incidence of knee injuries and an expanding indication for the surgery (Losina et al., 2012). Such a remarkable increase in primary TKR among a younger population with increased life expectancy implies that a higher proportion of the community will live with TKRs for longer (Weinstein et al., 2013). Despite the success in improving symptoms with knee arthroplasty, several studies have demonstrated functional limitations. Approximately 17 percent of patients with primary TKRs and 41 percent patients with revision TKRs remain dissatisfied with the outcome of the surgery (Dunbar et al., 2013). Given the rate of the sub-optimal outcome, it is not surprising to propose that TKRs should be reserved as a final option after first having tried alternatives (Dieppe et al., 2011).

Commonly used alternative procedures for cartilage repair are ACI (Bhosale et al., 2009), microfracture (Steadman et al., 2003) and Osteochondral Autologous Transplantations (OATS) (Hangody et al., 2004). The treatment of symptomatic articular cartilage defects is, however, more challenging if it co-exists with malalignment of the mechanical axis in the lower limb. Alternative techniques for biological restoration of the joint in such cases must include realignment osteotomy around the knee joint to correct the mechanical axis, alongside methods to repair the articular cartilage (Franceschi et al., 2008, Bauer et al., 2012, Sterett et al., 2010). A 10-year follow-up of a randomised controlled trial comparing ACI with OATS has shown better graft survival and significant clinical improvements after ACI (Bentley et al., 2012). Moreover, ACI was also shown to produce a better quality of repair tissue at 1 year in comparison to mosaicplasty during arthroscopic and histological

assessment (Bentley et al., 2003). Furthermore, the microscopic quality of repair tissue was also demonstrated to be superior in comparison to microfracture at 1 year (Saris et al., 2008). Furthermore, ACI has been demonstrated to be superior to other cartilage repair techniques for cartilage defects greater than 4 cm^2(Gomoll and Minas, 2012).

According to the Finnish Registry, High Tibial Osteotomy (HTO) for medial compartment osteoarthritis has an 89% survival at 5 years and 73% survival at 10 years, with failure defined as conversion to TKR (Niinimäki et al., 2012). Similarly, opening Distal Femoral Varus Osteotomy (DFVO) for lateral compartment OA has an estimated 79% survival at 5 years (Saithna et al., 2014).

Significant clinical improvement has been reported by combining HTO with ACI for repairing chondral defects in the medial compartment of the knee joint with varus malalignment at a mean follow-up of 28 months (Franceschi et al., 2008) and 5 years (Bauer et al., 2012). A non-randomised retrospective case-series confirmed that combining ACI with HTO imparts clinically significant improvement in outcomes in comparison to ACI in isolation. The same study also demonstrated a decreased rate of reintervention at 6 years follow-up in patients with ACI and HTO compared to ACI alone in patients with less than 5º of varus malalignment (Bode et al., 2013). A retrospective study showed significantly better clinical outcome at 11 years after HTO or HTO with ACI compared to HTO with microfracture (Ferruzzi et al., 2014). An evaluation of ACI highlighted that corrective osteotomy around the knee (for both varus and valgus malalignment) significantly improved survivorship of the cartilage repair for up to 15 years (Minas et al., 2014).

In this study, we prospectively evaluated the effectiveness of augmenting osteotomy with simultaneous ACI in knee joints with idiopathic varus or valgus malalignment and

symptomatic chondral defects in the medial or lateral compartments respectively. The primary outcome assessed was the change in Lysholm scores at final follow-up in comparison to the preoperative scores. The secondary outcomes were an objective assessment of chondral repair in the knee with arthroscopies and histological evaluation of the quality of the repair in patients where biopsies were available. Accurate assessment of the degree of correction achieved after realignment osteotomies were evaluated with standard weight-bearing knee radiographs.

5.2 Methods

The present study was approved by the hospital's audit and quality assurance board for review of outcome. Data was collected prospectively by the Oswestry Outcome Centre, an independent body within the hospital. All patients were operated by the senior author (JBR) between 1999 and 2010.

Patient inclusion criteria for combined treatment of osteotomy and ACI were:

1. Symptomatic cartilage defect(s) confirmed by knee arthroscopy in the lateral or medial compartment of the knee joint.
2. Established idiopathic malalignment of the lower limb identified on a standard weight-bearing radiograph.
3. Simultaneous ACI and osteotomy are done during the second stage of the procedure.

Patient exclusion criteria were:

1. Skeletally immature patients with open physis in the distal femur or proximal tibia.
2. Fixed flexion deformity of the knee.
3. Inflammatory arthritis.

The degree of preoperative malalignment was determined from standard weight-bearing knee radiographs (Colebatch et al., 2009). Functional outcomes were assessed by modified Lysholm scores validated for evaluation of the knee joint with underlying cartilage defects (Smith et al., 2009). 'Failure' was defined as conversion to TKR before the end of follow-up in this study. In these cases, the Lysholm score immediately before the TKR was considered as the final score.

5.2.1 Surgical Technique

The technique had two stages; the first stage comprised of a diagnostic knee arthroscopy and cartilage biopsy and the second stage involved corrective osteotomy of the knee and ACI. The second stage was performed three weeks after the first stage.

First stage: This includes diagnostic arthroscopy to evaluate the site and extent of the chondral defect. Cartilage biopsy was taken at this stage from an unaffected, less-weight-bearing area of the knee. The chondrocytes generated from the harvested cartilage were expanded *in vitro* for 3 weeks in the Good Manufacturing Practice (GMP) standard cell production facility in our centre. The number of chondrocytes from each patient was recorded in the laboratory before cell implantation at the second stage.

Second stage: The corrective osteotomy was combined with ACI at this stage. The deformity and planned degree of correction were determined preoperatively using weight-bearing knee radiographs. This was verified during the operation with an image intensifier and confirmed postoperatively. Varus alignment was defined as ≥2° towards varus, and valgus alignment was defined as ≥2° towards valgus from the neutral alignment of 180 ± 2° (Issa et al., 2007). Restoration of the neutral alignment (180 ± 2°) at the knee was considered to be the gold standard for correction which was ascertained with weight-bearing knee radiographs (Colebatch et al., 2009, Issa et al., 2007). DFVO was undertaken for correction of the mechanical axis in valgus knees and HTO for varus knees. One patient with a chondral defect in the lateral tibial plateau was treated with a lateral closing wedge high tibial osteotomy for the valgus knee.

a. Lateral Opening Wedge Distal Femoral Varus Osteotomy

Patients were positioned supine with their knee flexed to approximately 30º using sand bags. An image intensifier was used to confirm the site of the osteotomy. A skin incision was made laterally, starting distal to the lateral epicondyle and extending proximally up to 15-18 cm. A guidewire was inserted to ascertain the direction and level of the osteotomy. The osteotomy was performed 5cm proximal to the knee joint line with a Tuke saw aiming towards the medial epicondyle but maintaining a medial hinge on the cortex. The osteotomy site was gently opened to achieve the desired correction and the position secured with two conical absorbable composite screws (Bonejack™; Biocomposites Ltd., Keele, UK) or with cancellous bone grafts (Precision Bone Grafting System, Kaltec, Edwardstown, SA, Australia). A titanium plate was used to fix the osteotomy site (TomoFix®; Synthes Ltd, Welwyn Garden City, UK).

b. Medial Opening Wedge High Tibial Osteotomy

Patients were placed in supine position with their knees flexed to 90 º to allow full extension permitting an intra-operative check of the alignment. An anteromedial approach to the proximal tibia was used for HTO extending approximately 7-8 cm from the joint line. Insertion of the patellar tendon and its medial edge were exposed. The point of insertion of the patellar tendon was marked relative to the proximal tibia. The plane underneath the tendon was developed, followed by gentle placement of retractors for the osteotomy. The osteotomy level was 5cm distal to the joint line directed towards the proximal tibiofibular joint ensuring sufficient cortical contact laterally to form an effective hinge. A guidewire was placed with the extended knee directed towards the planned hinge point under an image-intensifier. The osteotomy was performed with a Tuke saw, and the continuity of the lateral

cortex was maintained. The osteotomy was then opened with the sequential use of increasing sizes of an osteotome to achieve the desired correction. Cancellous bone or two absorbable osteoconductive conical composite screws were used at the osteotomy site. A further vertical cut was made behind the patellar tendon insertion exiting through the anterior tibial cortex approximately 3 cm distal to the level of the osteotomy. The patellar-tendon-bone block was subsequently secured with a screw at the level of the patellar tendon marked initially before the osteotomy. This prevented the alteration of the height of patella following an opening wedge osteotomy (LaPrade et al., 2010). A titanium plate was used to stabilise the osteotomy site.

c. Autologous Chondrocyte Implantation

An arthrotomy was performed to access the articular cartilage defect and debride it to healthy adjacent articular cartilage and down to the subchondral bone plate, but without penetrating it. The size of the articular cartilage defect was recorded at this stage. Next, the defect was covered by a periosteal patch, harvested from the proximal medial tibia or by a collagen membrane (Chondro-Gide®; Geistlich Sons Ltd, Manchester, UK). The patch was sutured with 6-0 Vicryl (Ethicon, Livingston, United Kingdom) to the adjacent cartilage and the edges were sealed using fibrin glue (Tisseal; Baxter, Newbury, UK). A 'water-leak' test was performed to identify and seal any leak that might result in chondrocytes escaping from the enclosed space. The autologous chondrocyte suspension was subsequently injected into the defect before closing the patch. The outline of the defect was finally recorded on a knee map (Talkhani and Richardson, 1999).

5.2.2 Rehabilitation protocol

Patients received continuous passive movement from full extension to 30° flexion for the first 24-48 hours. They were subsequently mobilised allowing weight bearing as tolerated by the patient. A hinged knee brace was used to support the knee from full extension to flexion. The range of movement exercises was started on the first postoperative day. Mobilisation and weight bearing was restricted from 4-8 weeks to enable low strain consolidation of bone healing at the osteotomy site (Jagodzinski and Krettek, 2007).

5.2.3 Outcome assessment

5.2.3.1 Clinical follow-up

Patients were followed up at 2 and 6 months with a radiograph to ensure that the osteotomy had healed and also to check the final alignment. Subsequently, all patients were followed up annually to assess their clinical progress. The Lysholm scores were collected during each clinic visit by an independent member of the Oswestry Outcome Centre.

5.2.3.2 Arthroscopy

Patients had an arthroscopy of the knee at 1 year after the second stage of the procedure to assess the repair site. The repair site was evaluated with the validated OAS, in all cases by the senior author (Smith et al., 2005). The six scoring parameters were: graft level with surrounding cartilage (0-2), integration with surrounding cartilage (0-2), the appearance of the surface (0-2), the colour of the graft (0-2), and stiffness of the graft on probing (0-2). A higher score implied better quality of the cartilage repair tissue at the treated site.

5.2.3.3 Histology

Biopsies of the repair tissue at the treated site were obtained during follow-up arthroscopic assessment of the knee. This was not routine and subject to patients consenting to the additional procedure. A Jamshidi needle was used to take core-biopsies close to the centre of the treated defect and included both the repair tissue and the underlying subchondral bone (where possible). The cartilage repair site was ascertained from the knee-map used during the second stage of the procedure. The biopsy was snap-frozen in liquid nitrogen-cooled hexane before cryosectioning at 7um thickness onto poly-L-lysine coated slides. The sections were stained with haematoxylin and eosin to assess the general morphology of the

repair tissue and with toluidine blue to determine the metachromasia and proteoglycan content. Sections were scored for histological analysis using the International Cartilage Repair Score II (Mainil-Varlet et al., 2010) and the OsScore scoring systems (Roberts et al., 2003) for objective assessment of the quality of the repair tissue.

5.2.4 Statistics

A Shapiro-Wilks test and Q-Q plot were used to ascertain the distribution of the Lysohm scores. The data was not found to be normally distributed, and hence, non-parametric tests were used for the analysis. A paired Wilcoxon signed-rank test was used to evaluate the difference between pre- and postoperative Lysholm scores. A Mann-Whitney U test was used to determine the influence of gender, varus or valgus osteotomies, femoral or tibial osteotomies or type of patch used (periosteum or collagen), on the change of Lysholm scores. A univariable linear regression analysis was used to find if age, BMI, defect size or number of implanted chondrocytes of the studied cohort influenced the change in Lysholm scores. Additionally, a logistic regression analysis was used to ascertain the influence of the OAS on the failure of the procedure. A linear regression model was used to analyse the impact of corrected mechanical alignment on the change in the functional scores. A Kaplan-Meier cumulative survival analysis was done to estimate the time to failure. A Log-Rank test was used to determine the difference in estimated survival probability for varus and valgus osteotomies done for correction of mechanical alignment. All analyses were done using SPSS software (Version 22.0.0.0, IBM United Kingdom Ltd, Portsmouth, UK). For all analyses, a two-tailed p-value of 0.05 or below was assumed to denote significance.

5.3 Results

5.3.1 Patient Demographics

Fifteen patients with idiopathic malalignment and underlying chondral defects were treated with concurrent osteotomy and ACI (Table 5.1). The mean age at the time of surgery was 41.5 ± 11.2(SD) years (range 25.4-65.6), and the mean BMI was 28.8 ±4.3 (range 23.1-40.8). Five patients had a femoral osteotomy, and 10 patients had a tibial osteotomy; 4 patients had a periosteal patch and 11 patients a collagen membrane patch to cover the chondral defect. The average duration of follow-up was 5.7 years (range 1.7-10.3). No patients were lost to follow-up. A total of 4 patients had a 'failure' and required conversion to TKR. The average follow-up for these patients was 3.2 years (range 1.3-5).

Patient No.	*Gender*	*Age (years)*	*Chondral Defect Size (cm^2)*	*Cells ($x10^6/cm^2$)*	*Osteotomy Site*	*Osteotomy Type*	*Follow-up (years)*	*Failures*
1	F	50.3	13.75	0.655	Femur	Varus	1.7	Yes
2	M	45.1	7.71	0.519	Femur	Varus	9.6	No
3	M	29.7	6.6	1.030	Femur	Varus	5	Yes
4	M	25.4	6.6	0.803	Femur	Varus	5.6	No
5	M	38.5	5.5	1.441	Femur	Varus	4.6	Yes
6	F	36.3	1	6.875	Tibia	Varus	9.9	No
7	F	46.1	13.75	0.291	Tibia	Valgus	10	No
8	M	53.1	13.75	0.296	Tibia	Valgus	10.3	No
9	F	43.4	17.5	0.457	Tibia	Valgus	9	No
10	F	65.6	9.4	0.532	Tibia	Valgus	1.3	Yes
11	M	52.9	13.2	0.152	Tibia	Valgus	4.1	No
12	M	40.2	3.32	1.596	Tibia	Valgus	4	No
13	M	28.6	13.25	0.090	Tibia	Valgus	2.8	No
14	M	33.0	4	1.5	Tibia	Valgus	5.7	No
15	M	34.3	8	1.188	Tibia	Valgus	2.3	No

Table 5.1 Patient characteristics receiving osteotomy with ACI in addition to follow-up and failures

5.3.2 Functional outcome

The median Lysholm score before treatment was 42 (IQR of 25-54) and was 65 (IQR 36-84) at latest follow-up. The median change in Lysholm score was 29 (IQR of-6 to 37). This change was statistically significant (Wilcoxon signed-rank test, p=0.03). The median change in Lysholm scores was 36 points larger in patients receiving valgus osteotomies than those receiving varus osteotomies (Mann-Whitney U test, p=0.03; Table 2). The median change was 35 points greater in patients with tibial than in patients with femoral osteotomies (Mann-Whitney U test, p=0.02; Table 4.2). None of the other categorical parameters (gender or patch type) significantly influenced the change in outcome (Table 2). No significant influence was found in the continuous variables (age, BMI, size of the chondral defects and the cell number) on the change in Lysholm scores.

Patient grouping variables	*Median change in Lysholm Scores (95% CI)*	*Mann-Whitney U test (p-value)*
Gender	Male: 27 (-4.6 to 55.4)	0.6
	Female: 27 (-3.9 t0 32.1)	
Type of osteotomy	Varus: -4 (-22.5 to 24.8)	0.03*
	Valgus: 32 (13.6-44.3)	
Site of osteotomy	Femur: -6 (-29.9 to 21.9)	0.02*
	Tibia: 29 (15.3-42.2)	
Patch type	Collagen: 29 (1.7to 35.3)	0.85
	Periosteum: 16.4 (-27.1 to 59.1)	

Table 5.2 Change in the Lysholm scores between pre-and post-treatment for different patient grouping variables

(*significance considered at p<0.05)

5.3.3 Final alignment of the knee

The mean preoperative alignment from neutral was 7.5° for the 6 valgus knees and 6.8° for the 9 varus knees (Table 4.3). There was a significant change in the corrected postoperative alignment in comparison to the preoperative alignment following the osteotomy (Table 4.3). A linear regression analysis showed that the final alignment in this cohort did not influence the change in Lysholm scores (p-value 0.31, adjusted R^2-0.03).

Alignment	Preoperative (Mean±SD)	Postoperative (Mean±SD)	p-value
Valgus(n=6)	7.5° ± 3.8° (range 4-13)	2.25° ±1.5° (range 0-5)	0.046
Varus(n=9)	6.8° ±1.6° (range 5-10)	1.75° ±1.5° (range 0-4)	0.0001

Table 5.3 Pre and Postoperative alignment of the knee (measured from neutral 180°)

5.3.4 Arthroscopic Assessment

Twelve patients had an arthroscopic assessment of the repair site at an average interval of 13.2 months (range 5.2-31) from the second stage of the intervention. The mean OAS in these patients was 4.3 (range 0-10). In 4 out of 12 patients, the score was 0. The procedure failed in these four patients, and they eventually required TKR. Three patients scored 9 and above on the scale of 10, implying the excellent macroscopic quality of the graft. Logistic regression analysis demonstrated that OAS significantly predicted failure (p-value-0.004 and Nagelkerke's R^2= 1). Three patients did not have an arthroscopic intervention, and their mean Lysholm score was 61 (range 25-87) at 14 months follow-up.

5.3.5 Histology

Eight biopsies from 8 patients were obtained at a mean interval of 11.5 months ±2.7 SD (range 8-16). Histological assessments revealed 2 biopsies to be predominantly hyaline cartilage; 1 was a mixture of hyaline cartilage and fibrocartilage, and 5 were predominantly fibrocartilage. All 6 of the 8 biopsies that included the underlying subchondral bone had good or very good integration between the repair tissue and the underlying bone. There was only one case of ectopic vascularisation within the repair tissue. The tissue metachromasia indicating proteoglycan content was found to be good or very good in 7 repair biopsies and poor in 1 biopsy. Cellular morphology was found to be very good across all but 2 samples, where the cells had a less rounded chondrocyte-like appearance. A representative histological section from the repair site is illustrated in Figure 5.1 to show the tissue morphology and hyaline type cartilage at 13 months from surgery. The relationship between arthroscopic and histological scores with the outcome is shown in Table 5.4.

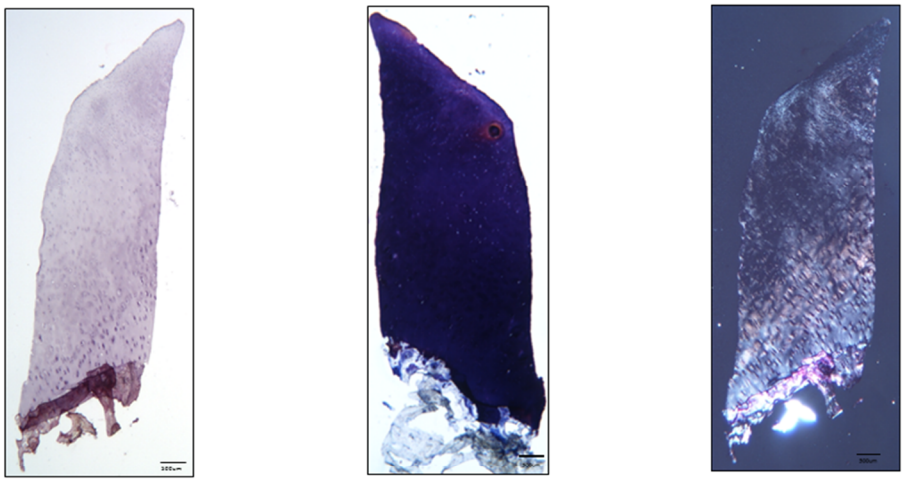

Figure 5.1 Histology of the repair tissue after 13 months of surgery from the same patient: (a) Haematoxylin & Eosin staining showing tissue morphology (b) Toluidine blue staining showing proteoglycan content (c) Polarised light microscopy showing hyaline type repair cartilage (Scale bar represents 500 um)

Patient No.	*OAS*	*ICRS II*	*OS score*	*Change in Lysholm*	*Outcome*
1	0	2.9	6.3	-6	Failed
3	0	NA	NA	-22	Failed
5	0	7.2	8.4	-2	Failed
6	9	7.25	7.5	27	Not failed
7	5	8.9	9.5	34	Not failed
8	4	5.2	6.5	29	Not failed
9	4	6.9	7.5	59	Not failed
10	0	NA	NA	-12	Failed
12	10	1.5	6.25	25	Not failed
13	5	3.65	6.75	37	Not failed
14	5	NA	NA	12	Not failed
15	10	NA	NA	32	Not failed

Table 5.4 Relationship between histological scores (ICRS II & OsScore), arthroscopic scores and outcome (NA-Not Available)

5.3.6 Survival analysis

A Kaplan-Meier survival analysis of the 15 patients showed that the estimated cumulative survival probability was 87% (±9 SE) at 5 years and 67% (±14 SE) at 10 years. The estimated survivorship after high tibial valgus osteotomy for correction of the varus deformity of the knee was 89% (±11 SE) at 5 years and 10 years. Survival after lateral opening wedge DFVO done for correction of the valgus deformity of the knees was 67% (±19 SE) at 5 years and 50% (±20 SE) at 10 years. A Log Rank test (Mantel-Cox) showed no significant difference in survival probability in the two groups (p-value 0.26,). A group of six patients receiving distal femoral varus osteotomy for valgus deformity in addition to five patients treated with high tibial osteotomy for varus deformity of the knee by the same surgeon was identified outside the study to ascertain the survival probability in patients receiving osteotomy in isolation. These patients did not receive ACI during their realignment surgery because no underlying chondral defect was identified on pre-operative imaging. However, a comparison of the population-based cumulative survival probability of the four groups (HTO with and without ACI & DFO with and without ACI) by a log-rank test revealed no significant difference amongst the group (p-value 0.27). An interesting observation, when compared with patients receiving osteotomy in isolation, is a complete absence of failure in HTO group when not complemented with ACI(i.e. no underlying chondral damage) and similarly, only one patient in the DFO group without ACI failed to highlight the propensity of failures in these patients when presenting with underlying chondral damage. The Kaplan-Meier graph demonstrating the cumulative survival in these four groups is illustrated in Fig 5.2.

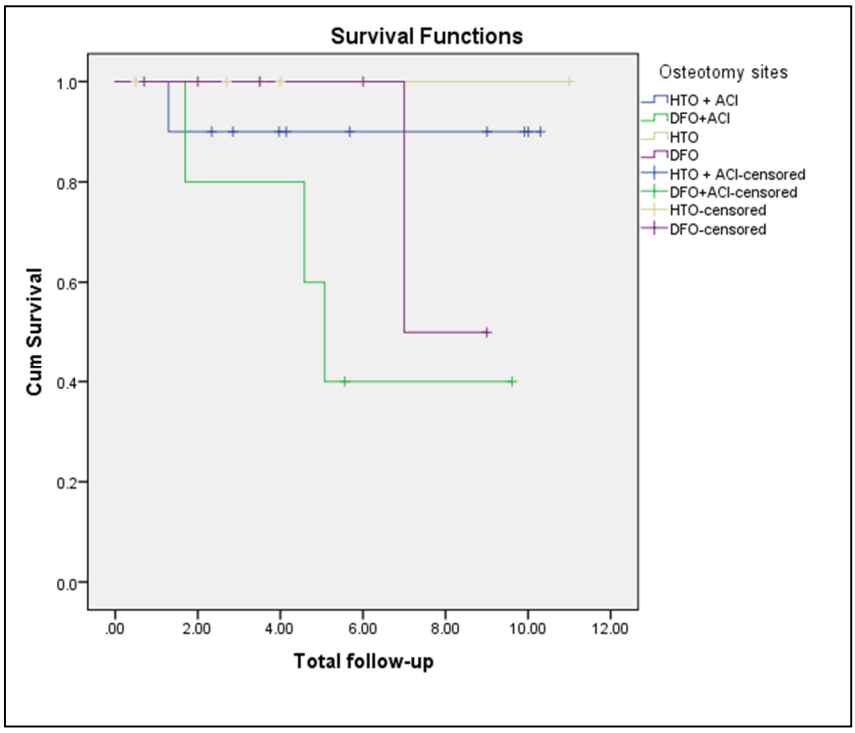

Figure 5.2 Kaplan-Meier survival curves comparing the cumulative survival probability of patients receiving High Tibial Osteotomy (HTO) or Distal Femoral Osteotomy (DFO) with/without ACI

5.4 Discussion

This is the first study that reports augmenting osteotomy with ACI for both medial and lateral compartment chondral defects with idiopathic varus and valgus malalignment of the knee respectively. The present work shows significant clinical improvement in median Lysholm scores after an average follow-up of 5.7 years, with no patients lost to follow-up. At the end of the latest follow-up, 11 patients had a well-functioning native knee, and 4 patients had failures which required TKR.

The median change in Lysholm score of 29 in this study is comparable to the mean improvement of 29 points following ACI with concurrent HTO used to treat chondral defects with varus malalignments of the knee (Franceschi et al., 2008). The present study showed significantly better clinical outcomes in cases treated with opening wedge valgus osteotomy in the proximal tibia (valgus HTO) for varus knee compared to opening wedge varus osteotomy in the distal femur (DFVO) for the valgus knee. This result is comparable to an earlier series of 12 patients, which reported the poor clinical outcome in 5 patients evaluated by Lysholm score at 74 months following opening wedge DFVO (Das et al., 2008). The present study also confirms the absence of any significant influence of age, BMI, defect size or number of implanted chondrocytes on the final clinical outcome, which is in agreement with larger studies of patients undergoing only ACI (Jungmann et al., 2012, Gooding et al., 2006).

The current study shows an estimated probability of retaining the native knee with improved functional outcome after combined osteotomy with ACI of 87% at 5 years and 73% at 10 years. The survivorship of knees receiving high tibial valgus osteotomy with ACI in the present series was 89% at 5 years and can be compared to recent reports of HTO that

also suggest an estimated survival of 89% at 5 years (Niinimäki et al., 2012, Saithna et al., 2014). Moreover, the 10 year survival probability was the same as the 5-year probability. This maintenance of short-term results over longer time periods is in line with results from ACI alone, where clinical outcomes are maintained over periods up to 9.3 years (Bhosale et al., 2009). This would be in contrast to HTO alone, for which the Finnish registry reports a survival probability of 73 % (Niinimäki et al., 2012).

The opening wedge lateral DFVO in the present study had survivorship of 67% at 5 years, less than previously reported series suggesting estimated survival probabilities of 79% at 5 years (Saithna et al., 2014) and 82% at 7 years (Dewilde et al., 2013). However, it is important to note that one of these previous studies, in which the same implant was used for opening wedge DFVO as in the current study, does acknowledge a lack of statistically significant clinical improvement in Lysholm score at 4.5 years follow-up (Saithna et al., 2014). A recent report has also described complications associated with friction and irritation of the iliotibial band following opening wedge DFVO using an identical fixation device (Jacobi et al., 2011) which is reflected by the poor functional outcome at follow-up (Das et al., 2008). Moreover, the lateral opening wedge DFVO tightens the iliotibial band and can increase the lateral compartment load. The tightening may also contribute to the reported high incidence of friction and irritation between the plate and the iliotibial band, in a similar way that a taut band can cause iliotibial band friction (Richards et al., 2003). The tautness leading to friction and irritation of the iliotibial band and an increased lateral load could explain the poorer clinical outcome in patients who had a combined varus osteotomy with ACI for valgus knee and lateral compartment chondral defects. It is also noteworthy that patients from the same centre with no underlying chondral damage and hence

necessitating no concurrent ACI treatments had lower rate of failures for both distal femoral varus osteotomies and high tibial valgus osteotomies in comparison to patients with underlying chondral damage requiring ACI, however no statistically significant difference in cumulative survival probability was noted in these groups. The postoperative alignments measured on standard knee radiographs were significantly improved in comparison to the preoperative alignment for both varus and valgus knees. The corrected alignment did not significantly correlate with the change in final Lysholm scores at follow-up.

The OAS was used to evaluate the quality of the repair site for 12 patients at an average interval of 13.2 months was a significant predictor of failure at final follow-up in the present work (Smith et al., 2005). Moreover, this is the first report of the histological outcome at the graft site following concurrent realignment and ACI. The ICRS II and the OsScores for histological evaluation of the repair site did not significantly relate to the functional outcome, but this can be due to the small sample size in this study (Roberts et al., 2003, Mainil-Varlet et al., 2010). The presence of good to very good subchondral integration, high proteoglycan content in addition to a cellular morphology consistent with chondrocytes in the majority of the biopsies demonstrates a promising structural outcome of the underlying surgical principle.

The clinical result of the current study supports the principle of combining osteotomy with ACI to treat chondral defects associated with idiopathic malalignment of the knee. In particular, the combination of opening wedge medial HTO and ACI is promising in addressing medial compartment cartilage defects in varus knees. However, the combination of opening wedge DFO to treat lateral compartment cartilage defects in valgus knees seems

disappointing. The OAS can be used to assess the quality of the graft, which can predict early failures.

However, there are limitations to the current work, and future studies are required. The number of patients in the study is small making it liable to Type-II errors. A control group was lacking in the present study to compare the outcome of osteotomy with ACI to that of osteotomy in isolation. Histology and OAS were not available for all patients. Furthermore, there was no uniform protocol in ascertaining the extent of correction of the varus and valgus deformity with standardised weight-bearing long leg alignment radiographs. However, the encouraging results of our study and earlier studies (Bode et al., 2013, Bauer et al., 2012, Franceschi et al., 2008) suggest that a randomised controlled trial to compare this treatment with other available options is justified. Such studies should be adequately powered to identify the differences between groups and ideally conducted in multiple units to improve the external validity. It should not only focus on OAS and histology of repair site in patients with clinically successful treatment but also have a detailed cellular and histological analysis of the treated knees which have failed and required joint replacement surgery.

To conclude, this study suggests that the combination of ACI and osteotomy can be used successfully in selected cases of large symptomatic cartilage defects, especially in cases of idiopathic varus malalignment of the knee. In contrast, a lateral opening wedge distal femoral osteotomy to treat lateral compartment cartilage lesions in a valgus knee showed relatively high failure rates in this series. The structural outcome of the repair site assessed by the OAS and histology reinforces the benefits of the underlying principles of the technique.

Chapter 6: Conclusion

This thesis covers subjects from bench to bedside. Work spans from an *in vitro* technique for cell therapy to the assessment of clinical effectiveness following applications of cell therapy in orthopaedics for bone and cartilage repair.

The *in vitro* research in the present thesis explores the potential of the umbilical cord as an alternate allogeneic source of cells to engineer cartilage and/or bone defects in orthopaedics. The novel technique of dissecting the four discrete regions of UC with subsequent explant culture of the four separate tissues to isolate cells is described in the work. All four cell preparations derived from the four regions of UC (PA, PV, CL, and WJ) express the surface markers prescriptive of MSC (Dominici et al., 2006). These cells showed tri-lineage differentiation capability to varying degrees; particularly the WJ-derived cells appeared to have weaker osteogenicity in comparison to cells from the other three locations. Cells from each of the four regions also expressed pluripotency markers, further indicating their differentiation potential and self-renewing capacity. Additionally, these four types of cell preparations were demonstrated to be non-immunogenic and expressed MHC Class I molecule (HLA-ABC) in the absence of HLA-DR or co-stimulatory molecules CD40, CD80 and CD86. These features observed in the cell populations obtained from four UC locations are suggestive of their potential for allogeneic transplantation in regenerative medicine.

The *in vivo* research focussed on assessing the potential of cultured autologous BMSC in new bone formation at nonunion fracture sites. This was ascertained by a randomised self-control trial designed with BMSC being inserted at one side of the non-united fracture ('test' side) with 'control' being on the opposite side of the nonunion, which precluded the

confounding variables exclusive to each patient's biology. The results of this study highlighted the lack of statistically significant rise in new bone formation at the side of BMSC insertion in comparison to their respective controls. However, a novel observation in the study was the direct correlation of shorter cell doubling time during *in vitro* culture with successful fracture union in these patients. Patient-related factors such as diabetes, multiple previous surgeries, and higher age group were observed to be negatively influencing bony union. A probabilistic model is used for the first time to ascertain the primary radiological outcome of increased bone formation at the nonunion site following BMSC insertion. This technique takes into account the difficulty of image analysis and experience of the independent assessors to achieve more sensitive outcome data in comparison to the conventional majority vote system (Whitehill et al., 2009b).

Clinical outcome of the novel 'Osplug' technique for treating ICRS Grade-4 cartilage defects or ICRS Grade 3 or 4 osteochondritis dissecans has been described in the current work. This method is shown to produce significant clinical improvement in patients for up to 5 years. A scoring parameter to assess the subchondral bone graft integration with the remodelling of the lamina (termed 'neo-lamina') as seen on MRI scans was devised and used for the first time in conjunction with conventional MOCART scoring criteria (Marlovits et al., 2006), to evaluate the osteoarticular repair. A low arthroscopic score (assessed with OAS) and poor integration of the monocortical bone graft (evaluated with the improvised criteria) at one year has been associated with a poor clinical outcome and subsequent failure of the surgical technique. Such observations highlight the importance of establishing proper integration between the implanted cells and bone core to be critical for long-term success of the procedure. The present work also reports the outcome of combining osteotomy with ACI to

treat chondral defects associated with malalignment of the knee. The results of the case-series treated with this method demonstrated favourable clinical outcome in cases with large chondral defects in varus knees. The structural outcome of the graft site evaluated arthroscopically with OAS and microscopically with ICRS II scoring parameters showed the benefits of the surgical technique. A cumulative probability estimate demonstrated 87% chance of retaining the native knee for five years; the macroscopic features of the graft assessed with OAS at one year was observed to be predictive of long-term failure. However, valgus knees requiring distal femoral opening wedge osteotomy had relatively poor results, with early failure. No studies on the outcome of treating valgus knees with combined osteotomy and ACI have previously been reported.

Future work:

UC-derived cells: Further work is required to demonstrate the immunological profile of UC-derived cells *in vitro* to investigate the allogeneic transplantation potential of these cells. Additionally, differentiation potential of these cells after being primed with pro-inflammatory cytokines needs to be undertaken, and the efficacy of different tissues (PA, PV, WJ, and CL) compared to develop insights of the best cell source if any. The safety profile of the UC-derived cells must be evaluated before animal and human clinical translation. Extensive animal studies to assess the *in vivo* efficacy should follow but pre-date the human application of these cells in orthopaedics regenerative medicine.

BMSC for fracture non-union: Future RCTs to determine the *in vivo* efficacy of autologous BMSCs for long bone nonunions are required, with separately matched control and a test group of patients. This will avoid the carry across effects of cells inserted in the 'test' side to the 'control' side, which can potentially influence the outcome of a self-controlled trial. Use

of a single carrier type is also recommended for a future trial to allow comparison of outcome between patients and avoid bias on the outcome due to the influence of the carriers themselves. Autologous BMSCs in these patients with non-union need to be characterised, especially with respect to their *in vitro* osteogenic performance and paracrine effects that can affect *in vivo* new bone formation in nonunions.

Clinical studies of ACI in special cases: Further follow-up with ten-year reports of the 'Osplug' technique mainly focussing on the clinical outcome and structural repair needs to be assessed with additional MRI scans to identify the long-term efficacy of this technique. Repair site biopsies at subsequent follow-up will improve our understanding of the interaction of the implanted chondrocytes in the cartilage repair tissue with the grafted bone in these cases. The potential use of biphasic scaffolds in such situations will need to transcend for human applications following successful use in larger animal models.

Encouraging preliminary results by implementing concurrent realignment osteotomy with ACI needs to be evaluated with further robust clinical studies and larger sample size. Patients in this study need to be randomised to treatment with ACI and osteotomy versus osteotomy in isolation. Further information on the repair site ought to be assessed with serial MRI scans, diagnostic arthroscopy, and biopsy.

To summarise, the thesis sheds light on the promising results of using cells derived from the umbilical cord to be a potential universal donor source that can be used 'off-the-shelf' for cell therapies in orthopaedics. Such findings form the basis for further *in vitro* characterisation of these cells particularly with respect to its immunogenicity in different inflammatory settings followed by large animal model studies to identify its *in vivo* efficacies. The present work also highlights the critical importance of *in vitro* doubling time

of autologous BMSC in predicting fracture union in patients with recalcitrant nonunions. This observation indicates towards the importance of *in vitro* characterisation of autologous BMSCs in patients with nonunions to identify potential correlations with clinical outcome and the *in vivo* performance of these cells in patients with nonunion. The outcome of the 'Osplug' technique described in the present work focusses the integral role of bone plug integration in treating osteoarticular defects when complemented with ACI. It also features successful preliminary results of combining ACI with osteotomy around maligned varus knees. Such positive clinical outcomes will complement the future use of biphasic scaffolds in treating osteoarticular defects in addition to the use of MSCs in the setting of cartilage regeneration in the knee.

References

ABZHANOV, A. & TABIN, C. J. 2004. Shh and Fgf8 act synergistically to drive cartilage outgrowth during cranial development. *Dev BioI,* 273**,** 134-48.

ADESIDA, A. B., MULET-SIERRA, A. & JOMHA, N. M. 2012. Hypoxia mediated isolation and expansion enhances the chondrogenic capacity of bone marrow mesenchymal stromal cells. *Stem Cell Res Ther,* 3**,** 9.

AKIYAMA, H. 2008. Control of chondrogenesis by the transcription factor Sox9. *Mod Rheumatol,* 18**,** 213-9.

ALEXANDER, D. I., MANSON, N. A. & MITCHELL, M. J. 2001. Efficacy of calcium sulfate plus decompression bone in lumbar and lumbosacral spinal fusion: preliminary results in 40 patients. *Canadian Journal of Surgery,* 44**,** 262-66.

ALFREDSON, H. & LORENTZON, R. 1999. Superior results with continuous passive motion compared to active motion after periosteal transplantation. A retrospective study of human patella cartilage defect treatment. *Knee Surg Sports Traumatol Arthrosc,* 7**,** 232-8.

ARUFE, M. C., DE LA FUENTE, A., FUENTES, I., TORO, F. J. & BLANCO, F. J. 2011. Umbilical cord as a mesenchymal stem cell source for treating joint pathologies. *World J Orthop,* 2**,** 43-50.

BAILEY, A., GOODSTONE, N., ROBERTS, S., HUGHES, J., ROBERTS, S., NIEKERK, L., RICHARDSON, J. & REES, D. 2003. Rehabilitation After Oswestry Autologous-Chondrocyte Implantation: The OsCell Protocol. *J Sport Rehabilitation,* 12**,** 104-8.

BAJADA, S., HARRISON, P., ASHTON, B., CASSAR-PULLICINO, V., ASHAMMAKHI, N. & RICHARDSON, J. 2007. Successful treatment of refractory tibial nonunion using calcium sulphate and bone marrow stromal cell implantation. *Journal of Bone and Joint Surgery Br,* 89**,** 1382-86.

BAJADA, S., MARSHALL, M. J., WRIGHT, K. T., RICHARDSON, J. B. & JOHNSON, W. E. 2009. Decreased osteogenesis, increased cell senescence and elevated Dickkopf-1 secretion in human fracture non union stromal cells. *Bone,* 45**,** 726-35.

BAKHSHI, T., ZABRISKIE, R. C., BODIE, S., KIDD, S., RAMIN, S., PAGANESSI, L. A., GREGORY, S. A., FUNG, H. C. & CHRISTOPHERSON, K. W., 2ND 2008. Mesenchymal stem cells from the Wharton's jelly of umbilical cord segments provide stromal support for the maintenance of cord blood hematopoietic stem cells during long-term ex vivo culture. *Transfusion,* 48**,** 2638-44.

BAKSH, D., YAO, R. & TUAN, R. S. 2007. Comparison of Proliferative and Multilineage Differentiation Potential of Human Mesenchymal Stem Cells Derived from Umbilical Cord and Bone Marrow. *Stem Cells* 25**,** 1384-92.

BARTLETT, W., GOODING, C. R., CARRINGTON, R. W., SKINNER, J. A., BRIGGS, T. W. & BENTLEY, G. 2005. Autologous chondrocyte implantation at the knee using a bilayer collagen membrane with bone graft. A preliminary report. *J Bone Joint Surg Br,* 87**,** 330-2.

BAUER, S., KHAN, R. J., EBERT, J. R., ROBERTSON, W. B., BREIDAHL, W., ACKLAND, T. R. & WOOD, D. J. 2012. Knee joint preservation with combined neutralising high tibial osteotomy (HTO) and Matrix-induced Autologous Chondrocyte Implantation (MACI) in younger patients with medial knee osteoarthritis: a case series with prospective clinical and MRI follow-up over 5 years. *Knee,* 19**,** 431-9.

BENTLEY, G., BIANT, L., VIJAYAN, S., MACMULL, S., SKINNER, J. & CARRINGTON, R. 2012. Minimum ten-year results of a prospective randomised study of autologous chondrocyte implantation versus mosaicplasty forsymptomatic articular cartilage lesions of the knee. *J Bone Joint Surg (Br),* 94**,** 504-9.

BENTLEY, G., BIANT, L. C., CARRINGTON, R. W., AKMAL, M., GOLDBERG, A., WILLIAMS, A. M., SKINNER, J. A. & PRINGLE, J. 2003. A prospective, randomised comparison of autologous chondrocyte implantation versus mosaicplasty for osteochondral defects in the knee. *J Bone Joint Surg Br,* 85**,** 223-30.

BHANDARI M, GUYATT GH, SWIONTKOWSKI MF, TORNETTA P, SPRAGUES & EH, S. 2002. A Lack of Consensus in the Assessment of Fracture Healing Among Orthopaedic Surgeons. *Journal of Orthopaedic Trauma,* 16**,** 562–66.

BHOSALE, A. M., KUIPER, J. H., JOHNSON, W. E., HARRISON, P. E. & RICHARDSON, J. B. 2009. Midterm to long-term longitudinal outcome of autologous chondrocyte implantation in the knee joint: a multilevel analysis. *Am J Sports Med,* 37 Suppl 1**,** 131S-8S.

BHOSALE, A. M. & RICHARDSON, J. B. 2008. Articular cartilage: structure, injuries and review of management. *Br Med Bull,* 87**,** 77-95.

BODE, G., SCHMAL, H., PESTKA, J. M., OGON, P., SUDKAMP, N. P. & NIEMEYER, P. 2013. A non-randomized controlled clinical trial on autologous chondrocyte implantation (ACI) in cartilage defects of the medial femoral condyle with or without high tibial osteotomy in patients with varus deformity of less than 5 degrees. *Arch Orthop Trauma Surg,* 133**,** 43-9.

BOER, B., KOPP, J., MALLANNA, S., DESLER, M., CHAKRAVARTHY, H., WILDER, P. J., BERNADT, C. & RIZZINO, A. 2007. Elevating the levels of Sox2 in embryonal carcinoma cells and embryonic stem cells inhibits the expression of Sox2:Oct-3/4 target genes. *Nucleic Acids Res,* 35**,** 1773-86.

BORA, F. W., JR. & MILLER, G. 1987. Joint physiology, cartilage metabolism, and the etiology of osteoarthritis. *Hand Clin,* 3**,** 325-36.

BOWERS, R. R. & LANE, M. D. 2008. Wnt signaling and adipocyte lineage commitment. *Cell Cycle,* 7**,** 1191-6.

BRADLEY, E. W. & DRISSI, M. H. 2011. Wnt5b regulates mesenchymal cell aggregation and chondrocyte differentiation through the planar cell polarity pathway. *J Cell Physiol,* 226**,** 1683-93.

BREZDEN, C. B. & RAUTH, A. M. 1996. Differential cell death in immortalized and non-immortalized cells at confluency. *Oncogene,* 12**,** 201-6.

BRIGHTON, C. T. & HEPPENSTALL, R. B. 1971a. Oxygen tension in zones of the epiphyseal plate, the metaphysis and diaphysis. An in vitro and in vivo study in rats and rabbits. *J Bone Joint Surg Am,* 53**,** 719-28.

BRIGHTON, C. T. & HEPPENSTALL, R. B. 1971b. Oxygen tension of the epiphyseal plate distal to an arteriovenous fistula. *Clin Orthop Relat Res,* 80**,** 167-73.

BRITTBERG, M. & WINALSKI, C. S. 2003. Evaluation of cartilage injuries and repair. *J Bone Joint Surg Am,* 85-A Suppl 2**,** 58-69.

BUCKWALTER, J. A. & MANKIN, H. J. 1998. Articular cartilage: tissue design and chondrocyte-matrix interactions. *Instr Course Lect,* 47**,** 477-86.

BURKHART, D. L. & SAGE, J. 2008. Cellular mechanisms of tumour suppression by the retinoblastoma gene. *Nat Rev Cancer,* 8**,** 671-82.

BUSIJA, L., BUCHBINDER, R. & OSBORNE, R. H. 2013. A grounded patient-centered approach generated the personal and societal burden of osteoarthritis model. *J Clin Epidemiol,* 66**,** 994-1005.

CALO, E., QUINTERO-ESTADES, J. A., DANIELIAN, P. S., NEDELCU, S., BERMAN, S. D. & LEES, J. A. 2010. Rb regulates fate choice and lineage commitment in vivo. *Nature,* 466**,** 1110-4.

CALORI GM, ALBISETTI W, AGUS A, IORI S & L., T. 2007. Risk factors contributing to fracture non-unions. *Injury,* 38 S11-18.

CAMMISA FP JR, LOWERY G, GARFIN SR, GEISLER FH, KLARA PM, MCGUIRE RA, SASSARD WR, STUBBS H & JE., B. 2004. Two-year fusion rate equivalency between Grafton DBM gel and autograft in posterolateral spine fusion: a prospective controlled trial employing a side-by-side comparison in the same patient. *Spine,* 29**,** 660-6.

CANCEDDA R, GIANNONI P & M., M. 2007. A tissue engineering approach to bone repair in large animal models and in clinical practice. *Biomaterials,* 28**,** 4240-50.

CAPLAN, A. L. 1991. Mesenchymal stem cells. *J Orthop Res.,* 9**,** 641-50.

CARLEVARO, M. F., CERMELLI, S., CANCEDDA, R. & DESCALZI CANCEDDA, F. 2000. Vascular endothelial growth factor (VEGF) in cartilage neovascularization and chondrocyte differentiation: auto-paracrine role during endochondral bone formation. *J Cell Sci,* 113 (Pt 1)**,** 59-69.

CARLIN, R., DAVIS, D., WEISS, M., SCHULTZ, B. & TROYER, D. 2006. Expression of early transcription factors Oct-4, Sox-2 and Nanog by porcine umbilical cord (PUC) matrix cells. *Reprod Biol Endocrinol,* 4**,** 8.

CARNES, J., STANNUS, O., CICUTTINI, F., DING, C. & JONES, G. 2012. Knee cartilage defects in a sample of older adults: natural history, clinical significance and factors influencing change over 2.9 years. *Osteoarthritis Cartilage,* 20**,** 1541-7.

CELIL, A. B. & CAMPBELL, P. G. 2005. BMP-2 and insulin-like growth factor-I mediate Osterix (Osx) expression in human mesenchymal stem cells via the MAPK and protein kinase D signaling pathways. *J Biol Chem,* 280**,** 31353-9.

CENTENO CJ, SCHULTZ JR, CHEEVER M, ROBINSON B, FREEMAN M & W., M. 2010. Safety and complications reporting on the re-implantation of culture-expanded mesenchymal stem cells using autologous platelet lysate technique. *Curr Stem Cell Res Ther. ,* 5**,** 81-93.

CHANG, Z., HOU, T., XING, J., WU, X., JIN, H., LI, Z., DENG, M., XIE, Z. & XU, J. 2014. Umbilical cord Wharton's jelly repeated culture system: a new device and method for obtaining abundant mesenchymal stem cells for bone tissue engineering. *PLoS One,* 9**,** e110764.

CHAO, Y. H., WU, H. P., CHAN, C. K., TSAI, C., PENG, C. T. & WU, K. H. 2012. Umbilical cord-derived mesenchymal stem cells for hematopoietic stem cell transplantation. *J Biomed Biotechnol,* 2012**,** e759503.

CHO, H. H., KYOUNG, K. M., SEO, M. J., KIM, Y. J., BAE, Y. C. & JUNG, J. S. 2006. Overexpression of CXCR4 increases migration and proliferation of human adipose tissue stromal cells. *Stem Cells Dev,* 15**,** 853-64.

CHO, T. J., GERSTENFELD, L. C. & EINHORN, T. A. 2002. Differential temporal expression of members of the transforming growth factor beta superfamily during murine fracture healing. *J Bone Miner Res,* 17**,** 513-20.

CHOUDHERY, M. S., BADOWSKI, M., MUISE, A. & HARRIS, D. T. 2013. Comparison of human mesenchymal stem cells derived from adipose and cord tissue. *Cytotherapy,* 15**,** 330-43.

CHRISTODOULOU, I., KOLISIS, F. N., PAPAEVANGELIOU, D. & ZOUMPOURLIS, V. 2013. Comparative Evaluation of Human Mesenchymal Stem Cells of Fetal (Wharton's Jelly) and Adult (Adipose Tissue) Origin during Prolonged In Vitro Expansion: Considerations for Cytotherapy. *Stem Cells Int,* 2013**,** e246134.

CHUI, K., JEYS, L. & SNOW, M. 2015. Knee salvage procedures: The indications, techniques and outcomes of large osteochondral allografts. *World J Orthop,* 6**,** 340-50.

CLEARY, M. A., VAN OSCH, G. J., BRAMA, P. A., HELLINGMAN, C. A. & NARCISI, R. 2015. FGF, TGFbeta and Wnt crosstalk: embryonic to in vitro cartilage development from mesenchymal stem cells. *J Tissue Eng Regen Med,* 9**,** 332-42.

COLEBATCH, A. N., HART, D. J., ZHAI, G., WILLIAMS, F. M., SPECTOR, T. D. & ARDEN, N. K. 2009. Effective measurement of knee alignment using AP knee radiographs. *Knee,* 16**,** 42-5.

CONNOLLY JF, GUSE R, TIEDEMAN J & R., D. 1991. Autologous marrow injection as a substitute for operative grafting of tibial nonunions. *Clin Orthopaedics Related Research***,** 259-70.

COURT-BROWN, C., AITKEN, S. & FORWARD, D. E. A. 2010. The epidemiology of adult fractures. *In:* BUCHOLZ, R., COURT-BROWN, C., HECKMAN, J. & TORNETTA, P. (eds.) *Rockwood and Green's fractures in adults.* 7th ed. Philidelphia: Lippincott Williams & Wilkins.

COVAS, D. T., SIUFI, J. L., SILVA, A. R. & ORELLANA, M. D. 2003. Isolation and culture of umbilical vein mesenchymal stem cells. *Braz J Med Biol Res,* 36**,** 1179-83.

CUNNINGHAM, F. & WILLIAMS, J. W. 2010. Williams Obstetrics. *In:* CUNNINGHAM, F. G. E. A. (ed.). New York McGraw-Hill, Medical.

CURL, W. W., KROME, J., GORDON, E. S., RUSHING, J., SMITH, B. P. & POEHLING, G. G. 1997. Cartilage injuries: a review of 31,516 knee arthroscopies. *Arthroscopy,* 13**,** 456-60.

DAS, D. H., SIJBESMA, T., HOEKSTRA, H. J. & LEEUWEN, W. M. V. 2008. Distal femoral opening-wedge osteotomy for lateral compartment osteoarthritis of the knee. *Open Access Surgery,* 1**,** 25-29.

DAVIS, L. A. & ZUR NIEDEN, N. I. 2008. Mesodermal fate decisions of a stem cell: the Wnt switch. *Cell Mol Life Sci,* 65**,** 2658-74.

DECKELBAUM, R. A., CHAN, G., MIAO, D., GOLTZMAN, D. & KARAPLIS, A. C. 2002. Ihh enhances differentiation of CFK-2 chondrocytic cells and antagonizes PTHrP-mediated activation of PKA. *J Cell Sci,* 115**,** 3015-25.

DEUSE, T., STUBBENDORFF, M., TANG-QUAN, K., PHILLIPS, N., KAY, M. A., EIERMANN, T., PHAN, T. T., VOLK, H. D., REICHENSPURNER, H., ROBBINS, R. C. & SCHREPFER, S. 2011. Immunogenicity and immunomodulatory properties of umbilical cord lining mesenchymal stem cells. *Cell Transplant,* 20**,** 655-67.

DEWILDE, T. R., DAUW, J., VANDENNEUCKER, H. & BELLEMANS, J. 2013. Opening wedge distal femoral varus osteotomy using the Puddu plate and calcium phosphate bone cement. *Knee Surg Sports Traumatol Arthrosc,* 21**,** 249-54.

DIEPPE, P., LIM, K. & LOHMANDER, S. 2011. Who should have knee joint replacement surgery for osteoarthritis? *Int J Rheum Dis,* 14**,** 175-80.

DOMINICI, M., LE BLANC, K., MUELLER, I., SLAPER-CORTENBACH, I., MARINI, F., KRAUSE, D., DEANS, R., KEATING, A., PROCKOP, D. & HORWITZ, E. 2006. Minimal criteria for defining multipotent mesenchymal stromal cells. The International Society for Cellular Therapy position statement. *Cytotherapy,* 8**,** 315-7.

DRAPER, J. S. & FOX, V. 2003. Human embryonic stem cells: multilineage differentiation and mechanisms of self-renewal. *Arch Med Res,* 34**,** 558-64.

DUNBAR, M. J., RICHARDSON, G. & ROBERTSSON, O. 2013. I can't get no satisfaction after my total knee replacement:Rhymes and Reasons. *The Bone & Joint Journal,* 95-B, Supple**,** 148–52.

EDMONDS, E. W., ALBRIGHT, J., BASTROM, T. & CHAMBERS, H. G. 2010. Outcomes of extra-articular, intra-epiphyseal drilling for osteochondritis dissecans of the knee. *J Pediatr Orthop,* 30**,** 870-8.

EDMONDS, E. W. & POLOUSKY, J. 2013. A review of knowledge in osteochondritis dissecans: 123 years of minimal evolution from Konig to the ROCK study group. *Clin Orthop Relat Res,* 471**,** 1118-26.

ERICKSON, B. J., CHALMERS, P. N., YANKE, A. B. & COLE, B. J. 2013. Surgical management of osteochondritis dissecans of the knee. *Curr Rev Musculoskelet Med,* 6**,** 102-14.

FAJAS, L., EGLER, V., REITER, R., HANSEN, J., KRISTIANSEN, K., DEBRIL, M. B., MIARD, S. & AUWERX, J. 2002. The retinoblastoma-histone deacetylase 3 complex inhibits PPARgamma and adipocyte differentiation. *Dev Cell,* 3**,** 903-10.

FERRUZZI, A., BUDA, R., CAVALLO, M., TIMONCINI, A., NATALI, S. & GIANNINI, S. 2014. Cartilage repair procedures associated with high tibial osteotomy in varus knees: clinical results at 11 years' follow-up. *Knee,* 21**,** 445-50.

FLEISS, J. L., LEVIN, B. & PAIK, M. 2003. The Measurement of Interrater Agreement. *Statistical Methods for Rates and Proportions, Third Edition***,** 598-626.

FONG, C. Y., RICHARDS, M., MANASI, N., BISWAS, A. & BONGSO, A. 2007. Comparative growth behaviour and characterization of stem cells from human Wharton's jelly. *Reprod Biomed Online,* 15**,** 708-18.

FONG, C. Y., SUBRAMANIAN, A., BISWAS, A., GAUTHAMAN, K., SRIKANTH, P., HANDE, M. P. & BONGSO, A. 2010. Derivation efficiency, cell proliferation, freeze-thaw survival, stem-cell properties and differentiation of human Wharton's jelly stem cells. *Reprod Biomed Online,* 21**,** 391-401.

FONG, C. Y., SUBRAMANIAN, A., GAUTHAMAN, K., VENUGOPAL, J., BISWAS, A., RAMAKRISHNA, S. & BONGSO, A. 2012. Human umbilical cord Wharton's jelly stem cells undergo enhanced chondrogenic differentiation when grown on nanofibrous scaffolds and in a sequential two-stage culture medium environment. *Stem Cell Rev,* 8**,** 195-209.

FONG K , TRUONG, V., FOOTE C, PETRISO B , WILLIAMS D, RISTEVSKI B, SPRAGUE S & M., B. 2013. Predictors of nonunion and reoperation in patients with fractures of the tibia: an observational study. *BMC Musculoskeletal Disorders,* 14.

FRANCESCHI, F., LONGO, U. G., RUZZINI, L., MARINOZZI, A., MAFFULLI, N. & DENARO, V. 2008. Simultaneous arthroscopic implantation of autologous chondrocytes and high tibial osteotomy for tibial chondral defects in the varus knee. *Knee,* 15**,** 309-13.

FREIDENSTEIN, A., PIATEZKY-SHAPIRO, I. I. & PETRAKOVA, K. 1966. Osteogenesis in transplants of bone marrow cells. *Journal of Embryology & Experimental Morphology* 16**,** 381-90.

FUJITA, T., AZUMA, Y., FUKUYAMA, R., HATTORI, Y., YOSHIDA, C., KOIDA, M., OGITA, K. & KOMORI, T. 2004. Runx2 induces osteoblast and chondrocyte differentiation and enhances their migration by coupling with PI3K-Akt signaling. *J Cell Biol,* 166**,** 85-95.

GANG, E. J., BOSNAKOVSKI, D., FIGUEIREDO, C. A., VISSER, J. W. & PERLINGEIRO, R. C. 2007. SSEA-4 identifies mesenchymal stem cells from bone marrow. *Blood,* 109**,** 1743-51.

GENIN, O., HASDAI, A., SHINDER, D. & PINES, M. 2008. Hypoxia, hypoxia-inducible factor-1alpha (HIF-1alpha), and heat-shock proteins in tibial dyschondroplasia. *Poult Sci,* 87**,** 1556-64.

GERBER, H. P., VU, T. H., RYAN, A. M., KOWALSKI, J., WERB, Z. & FERRARA, N. 1999. VEGF couples hypertrophic cartilage remodeling, ossification and angiogenesis during endochondral bone formation. *Nat Med,* 5**,** 623-8.

GERSTENFELD, L. C., ALKHIARY, Y. M., KRALL, E. A., NICHOLLS, F. H., STAPLETON, S. N., FITCH, J. L., BAUER, M., KAYAL, R., GRAVES, D. T., JEPSEN, K. J. & EINHORN, T. A. 2006. Three-dimensional reconstruction of fracture callus morphogenesis. *J Histochem Cytochem,* 54**,** 1215-28.

GERSTENFELD, L. C., CULLINANE, D. M., BARNES, G. L., GRAVES, D. T. & EINHORN, T. A. 2003. Fracture healing as a post-natal developmental process: molecular, spatial, and temporal aspects of its regulation. *J Cell Biochem,* 88**,** 873-84.

GIANNOTTI, S., TROMBI, L., BOTTAI, V., GHILARDI, M., D'ALESSANDRO, D., DANTI, S., DELL'OSSO, G., GUIDO, G. & PETRINI, M. 2013. Use of autologous human mesenchymal stromal cell/fibrin clot constructs in upper limb non-unions: long-term assessment. *PloS One,* 8**,** e73893.

GOLDRING, C. E., DUFFY, P. A., BENVENISTY, N., ANDREWS, P. W., BEN-DAVID, U., EAKINS, R., FRENCH, N., HANLEY, N. A., KELLY, L., KITTERINGHAM, N. R., KURTH, J., LADENHEIM, D., LAVERTY, H., MCBLANE, J., NARAYANAN, G., PATEL, S., REINHARDT, J., ROSSI, A., SHARPE, M. & PARK, B. K. 2011. Assessing the safety of stem cell therapeutics. *Cell Stem Cell,* 8**,** 618-28.

GOMOLL, A. & MINAS, T. 2012. How to Treat Cartilage Lesions in Patients with Osteoarthritis? *In:* BRITTBERG M, G. A., IMHOFF AB, KON E, MADRY H (ed.) *Cartilage Repair - Clinical Guidelines.* DJO Publishers.

GONZALEZ, R., GRIPARIC, L., UMANA, M., BURGEE, K., VARGAS, V., NASRALLAH, R., SILVA, F. & PATEL, A. 2010. An efficient approach to isolation and characterization of pre- and postnatal umbilical cord lining stem cells for clinical applications. *Cell Transplant,* 19**,** 1439-49.

GOODING, C. R., BARTLETT, W., BENTLEY, G., SKINNER, J. A., CARRINGTON, R. & FLANAGAN, A. 2006. A prospective, randomised study comparing two techniques of autologous chondrocyte implantation for osteochondral defects in the knee: Periosteum covered versus type I/III collagen covered. *Knee,* 13**,** 203-10.

GRANERO-MOLTO, F., WEIS, J. A., MIGA, M. I., LANDIS, B., MYERS, T. J., O'REAR, L., LONGOBARDI, L., JANSEN, E. D., MORTLOCK, D. P. & SPAGNOLI, A. 2009. Regenerative effects of transplanted mesenchymal stem cells in fracture healing. *Stem Cells,* 27**,** 1887-98.

GROGAN, S. P., OLEE, T., HIRAOKA, K. & LOTZ, M. K. 2008. Repression of chondrogenesis through binding of notch signaling proteins HES-1 and HEY-1 to N-box domains in the COL2A1 enhancer site. *Arthritis Rheum,* 58**,** 2754-63.

GRUBER, R., VARGA, F., FISCHER, M. B. & WATZEK, G. 2002. Platelets stimulate proliferation of bone cells: involvement of platelet-derived growth factor, microparticles and membranes. *Clin Oral Implants Res,* 13**,** 529-35.

GUDAS, R., GUDAITE, A., POCIUS, A., GUDIENE, A., CEKANAUSKAS, E., MONASTYRECKIENE, E. & BASEVICIUS, A. 2012. Ten-year follow-up of a prospective, randomized clinical study of mosaic osteochondral autologous transplantation versus microfracture for the treatment of osteochondral defects in the knee joint of athletes. *Am J Sports Med,* 40**,** 2499-508.

GUDAS, R., STANKEVICIUS, E., MONASTYRECKIENE, E., PRANYS, D. & KALESINSKAS, R. J. 2006. Osteochondral autologous transplantation versus microfracture for the treatment of articular cartilage defects in the knee joint in athletes. *Knee Surg Sports Traumatol Arthrosc,* 14**,** 834-42.

HAIGH, J. J., GERBER, H. P., FERRARA, N. & WAGNER, E. F. 2000. Conditional inactivation of VEGF-A in areas of collagen2a1 expression results in embryonic lethality in the heterozygous state. *Development,* 127**,** 1445-53.

HAN, Y. F., TAO, R., SUN, T. J., CHAI, J. K., XU, G. & LIU, J. 2013. Optimization of human umbilical cord mesenchymal stem cell isolation and culture methods. *Cytotechnology,* 65**,** 819-27.

HANDORF, A. M. & LI, W. J. 2011. Fibroblast growth factor-2 primes human mesenchymal stem cells for enhanced chondrogenesis. *PLoS One,* 6**,** e22887.

HANGODY, L., RATHONYI, G. K., DUSKA, Z., VASARHELYI, G., FULES, P. & MODIS, L. 2004. Autologous osteochondral mosaicplasty. Surgical technique. *J Bone Joint Surg Am,* 86-A Suppl 1**,** 65-72.

HARRISON, P. E., ASHTON, K., JOHNSON,W.E.B., TURNER, S.L., RICHARDSON, J.B., ASHTON, B.A. 2000. The in vitro growth of human chondrocytes. *Cell And Tissue Banking* 1**,** 255-60

HARTMANN, I., HOLLWECK, T., HAFFNER, S., KREBS, M., MEISER, B., REICHART, B. & EISSNER, G. 2010. Umbilical cord tissue-derived mesenchymal stem cells grow best under GMP-compliant culture conditions and maintain their phenotypic and functional properties. *J Immunol Methods,* 363**,** 80-9.

HEIR, S., NERHUS, T. K., ROTTERUD, J. H., LOKEN, S., EKELAND, A., ENGEBRETSEN, L. & AROEN, A. 2010. Focal cartilage defects in the knee impair quality of life as much as severe osteoarthritis: a comparison of knee injury and osteoarthritis outcome score in 4 patient categories scheduled for knee surgery. *Am J Sports Med,* 38**,** 231-7.

HERNBORG, J. S. & NILSSON, B. E. 1977. The natural course of untreated osteoarthritis of the knee. *Clin Orthop Relat Res***,** 130-7.

HERNIGOU, P., POIGNARD, A., BEAUJEAN, F. & ROUARD, H. 2005. Percutaneous autologous bone-marrow grafting for nonunions. Influence of the number and concentration of progenitor cells. *The Journal of Bone and Joint Surg Am,* 87**,** 1430-1437.

HILL, P. A., TUMBER, A. & MEIKLE, M. C. 1997. Multiple extracellular signals promote osteoblast survival and apoptosis. *Endocrinology,* 138**,** 3849-58.

HILTUNEN, M. O., RUUSKANEN, M., HUUSKONEN, J., MAHONEN, A. J., AHONEN, M., RUTANEN, J., KOSMA, V. M., MAHONEN, A., KROGER, H. & YLA-HERTTUALA, S. 2003. Adenovirus-mediated VEGF-A gene transfer induces bone formation in vivo. *FASEB J,* 17**,** 1147-9.

HOFMANN, A., RITZ, U., HESSMANN, M. H., SCHMID, C., TRESCH, A., ROMPE, J. D., MEURER, A. & ROMMENS, P. M. 2008. Cell viability, osteoblast differentiation, and gene expression are altered in human osteoblasts from hypertrophic fracture non-unions. *Bone,* 42**,** 894-906.

HOPEWELL, S., CLARKE, M., MOHER, D., WAGER, E. & MIDDLETON, P., ET AL. 2008. CONSORT for Reporting Randomized Controlled Trials in Journal and Conference Abstracts: Explanation and Elaboration. *PLoSMed,* 5**,** e20.

HORWITZ, E. M., LE BLANC, K., DOMINICI, M., MUELLER, I., SLAPPER-COTENBACH, I., MARINI, F., DEANS, R., KRAUSE, D. & KEATING, A. 2005. Clarification of the nomenclasture for MSC: te International Society of Cellular Therapy position statement. *Cytotherapy,* 7**,** 393-395.

HOSMER, D. & LEMESHOW, S. 2000. Applied Logistic Regression (2nd Edition). *John Wiley & Sons. Inc*.

HUANG, H. Y., HU, L. L., SONG, T. J., LI, X., HE, Q., SUN, X., LI, Y. M., LU, H. J., YANG, P. Y. & TANG, Q. Q. 2011. Involvement of cytoskeleton-associated proteins in the commitment of C3H10T1/2 pluripotent stem cells to adipocyte lineage induced by BMP2/4. *Mol Cell Proteomics,* 10**,** M110 002691.

IKEDA, T., KAMEKURA, S., MABUCHI, A., KOU, I., SEKI, S., TAKATO, T., NAKAMURA, K., KAWAGUCHI, H., IKEGAWA, S. & CHUNG, U. I. 2004. The combination of SOX5, SOX6, and SOX9 (the SOX trio) provides signals sufficient for induction of permanent cartilage. *Arthritis Rheum,* 50**,** 3561-73.

ISHIGE, I., NAGAMURA-INOUE, T., HONDA, M. J., HARNPRASOPWAT, R., KIDO, M., SUGIMOTO, M., NAKAUCHI, H. & TOJO, A. 2009. Comparison of mesenchymal stem cells derived from arterial, venous, and Wharton's jelly explants of human umbilical cord. *Int J Hematol,* 90**,** 261-9.

ISSA, S. N., DUNLOP, D., CHANG, A., SONG, J., PRASAD, P. V., GUERMAZI, A., PETERFY, C., CAHUE, S., MARSHALL, M., KAPOOR, D., HAYES, K. & SHARMA, L. 2007. Full-limb and knee radiography assessments of varus-valgus alignment and their relationship to osteoarthritis disease features by magnetic resonance imaging. *Arthritis Rheum,* 57**,** 398-406.

IZADIFAR, Z., CHEN, X. & KULYK, W. 2012. Strategic design and fabrication of engineered scaffolds for articular cartilage repair. *J Funct Biomater,* 3**,** 799-838.

JACOBI, M., WAHL, P., BOUAICHA, S., JAKOB, R. P. & GAUTIER, E. 2011. Distal femoral varus osteotomy: problems associated with the lateral open-wedge technique. *Arch Orthop Trauma Surg,* 131**,** 725-8.

JAGODZINSKI, M. & KRETTEK, C. 2007. Effect of mechanical stability on fracture healing--an update. *Injury,* 38 Suppl 1**,** S3-10.

JAISWAL, N., HAYNESWORTH, S. E., CAPLAN, A. I. & BRUDER, S. P. 1997a. Osteogenic differentiation of purified, culture-expanded human mesenchymal stem cells in vitro. *J Cell Biochem,* 64**,** 295-312.

JAISWAL, N., HAYNESWORTH, S. E., CAPLAN, A. I. & BRUDER, S. P. 1997b. Osteogenic differentiation of purified, culture-expanded human mesenchymal stem cells in vitro. *Journal of Cell Biochem***,** 295-312.

JAMES, A. W., LEUCHT, P., LEVI, B., CARRE, A. L., XU, Y., HELMS, J. A. & LONGAKER, M. T. 2010. Sonic Hedgehog influences the balance of osteogenesis and adipogenesis in mouse adipose-derived stromal cells. *Tissue Eng Part A,* 16**,** 2605-16.

JANICKI P & BOEUF, S., STECK E, EGERMANN M, KASTEN P, RICHTER W 2011. Prediction of in vivo bone forming potency of bone marrow-derived human mesenchymal stem cells. *European Cells and Materials,* 21**,** 488-507.

JESCHKE, M. G., GAUGLITZ, G. G., PHAN, T. T., HERNDON, D. N. & KITA, K. 2011. Umbilical Cord Lining Membrane and Wharton's Jelly-Derived Mesenchymal Stem Cells: the Similarities and Differences *The Open Tissue Engineering and Regenerative Medicine Journal,* 4.

JO, C. H., KIM, O. S., PARK, E. Y., KIM, B. J., LEE, J. H., KANG, S. B., HAN, H. S., RHEE, S. H. & YOON, K. S. 2008. Fetal mesenchymal stem cells derived from human umbilical cord sustain primitive characteristics during extensive expansion. *Cell Tissue Res,* 334**,** 423-33.

JOHNSON, P. D. & BESSELSEN, D. G. 2002. Practical aspects of experimental design in animal research. *ILAR J,* 43**,** 202-6.

JOHNSTONE, B., HERING, T. M., CAPLAN, A. I., GOLDBERG, V. M. & YOO, J. U. 1998. In vitro chondrogenesis of bone marrow-derived mesenchymal progenitor cells. *Exp Cell Res,* 238**,** 265-72.

JORDAN, D. & SMITH, P. 1997. Mathematical techniques:An introduction for the engineering,physical and mathematical sciences. *Oxford: Oxford University Press,* 2nd Edition.

JORDAN, D. W. & SMITH, P. 2nd edition, 2000. *Mathematical Techniques: An Introduction For the Engineering, Physical and Mathematical Sciences,* Oxford, UK, , Oxford University Press.

JUNGMANN, P. M., SALZMANN, G. M., SCHMAL, H., PESTKA, J. M., SUDKAMP, N. P. & NIEMEYER, P. 2012. Autologous chondrocyte implantation for treatment of cartilage defects of the knee: what predicts the need for reintervention? *Am J Sports Med,* 40**,** 58-67.

KADAM, S. S., TIWARI, S. & BHONDE, R. R. 2009. Simultaneous isolation of vascular endothelial cells and mesenchymal stem cells from the human umbilical cord. *In Vitro Cell Dev Biol Anim,* 45**,** 23-7.

KAGEYAMA, R., OHTSUKA, T. & KOBAYASHI, T. 2007. The Hes gene family: repressors and oscillators that orchestrate embryogenesis. *Development,* 134**,** 1243-51.

KALLALA, R. F., VANHEGAN, I. S., IBRAHIM, M. S., SARMAH, S. & HADDAD, F. S. 2015. Financial analysis of revision knee surgery based on NHS tariffs and hospital costs: does it pay to provide a revision service? *Bone Joint J,* 97-B**,** 197-201.

KANCZLER, J. M. & OREFFO, R. O. 2008. Osteogenesis and angiogenesis: the potential for engineering bone. *Eur Cell Mater,* 15**,** 100-14.

KANNAGI R, COCHRAN N A, ISHIGAMI F , HAKOMORI S, ANDREWS P W, KNOWLESB B & SOLTER., D. 1983. Stage-specific embryonic antigens (SSEA-3 and -4) are epitopes of a unique globo-series ganglioside isolated from human teratocarcinoma cells. *Journal of European Molecular Biology Organization,* 2**,** 2355–2361.

KARAHUSEYINOGLU, S., CINAR, O., KILIC, E., KARA, F., AKAY, G. G., DEMIRALP, D. O., TUKUN, A., UCKAN, D. & CAN, A. 2007. Biology of stem cells in human umbilical cord stroma: in situ and in vitro surveys. *Stem Cells,* 25**,** 319-31.

KE, Q. & COSTA, M. 2006. Hypoxia-inducible factor-1 (HIF-1). *Mol Pharmacol,* 70**,** 1469-80.

KELPKE, S. S., REIFF, D., PRINCE, C. W. & THOMPSON, J. A. 2001. Acidic fibroblast growth factor signaling inhibits peroxynitrite-induced death of osteoblasts and osteoblast precursors. *J Bone Miner Res,* 16**,** 1917-25.

KERAMARIS, N. C., CALORI, G. M., NIKOLAOU, V. S., SCHEMITSCH, E. H. & GIANNOUDIS, P. V. 2008. Fracture vascularity and bone healing: a systematic review of the role of VEGF. *Injury,* 39 Suppl 2**,** S45-57.

KETENJIAN, A. Y. & ARSENIS, C. 1975. Morphological and biochemical studies during differentiation and calcification of fracture callus cartilage. *Clin Orthop Relat Res***,** 266-73.

KHAN, W. S., ADESIDA, A. B. & HARDINGHAM, T. E. 2007. Hypoxic conditions increase hypoxia-inducible transcription factor 2alpha and enhance chondrogenesis in stem cells from the infrapatellar fat pad of osteoarthritis patients. *Arthritis Res Ther,* 9**,** R55.

KIJOWSKI, R., BLANKENBAKER, D. G., SHINKI, K., FINE, J. P., GRAF, B. K. & DE SMET, A. A. 2008. Juvenile versus adult osteochondritis dissecans of the knee: appropriate MR imaging criteria for instability. *Radiology,* 248**,** 571-8.

KIM, H. S., YUN, J. W., SHIN, T. H., LEE, S. H., LEE, B. C., YU, K. R., SEO, Y., LEE, S., KANG, T. W., CHOI, S. W., SEO, K. W. & KANG, K. S. 2015. Human umbilical cord blood mesenchymal stem cell-derived PGE2 and TGF-beta1 alleviate atopic dermatitis by reducing mast cell degranulation. *Stem Cells,* 33**,** 1254-66.

KIM, S. J., SHIN, Y. W., YANG, K. H., KIM, S. B., YOO, M. J., HAN, S. K., IM, S. A., WON, Y. D., SUNG, Y. B., JEON, T. S., CHANG, C. H., JANG, J. D., LEE, S. B., KIM, H. C. & LEE, S. Y. 2009. A multi-center, randomized, clinical study to compare the effect and safety of autologous cultured osteoblast(Ossron) injection to treat fractures. *BMC Musculoskelet Disord,* 10**,** 20.

KIRTON, J. P., CROFTS, N. J., GEORGE, S. J., BRENNAN, K. & CANFIELD, A. E. 2007. Wnt/beta-catenin signaling stimulates chondrogenic and inhibits adipogenic differentiation of pericytes: potential relevance to vascular disease? *Circ Res,* 101**,** 581-9.

KITA, K., GAUGLITZ, G. G., PHAN, T. T., HERNDON, D. N. & JESCHKE, M. G. 2010. Isolation and characterization of mesenchymal stem cells from the sub-amniotic human umbilical cord lining membrane. *Stem Cells Dev,* 19**,** 491-502.

KITOH, H., KAWASUMI, M., KANEKO, H. & ISHIGURO, N. 2009. Differential effects of culture-expanded bone marrow cells on the regeneration of bone between the femoral and the tibial lengthenings. *J Pediatr Orthop,* 29**,** 643-9.

KOAY, E. J. & ATHANASIOU, K. A. 2008. Hypoxic chondrogenic differentiation of human embryonic stem cells enhances cartilage protein synthesis and biomechanical functionality. *Osteoarthritis Cartilage,* 16**,** 1450-6.

KOCHER, M. S., MICHELI, L. J., YANIV, M., ZURAKOWSKI, D., AMES, A. & ADRIGNOLO, A. A. 2001. Functional and radiographic outcome of juvenile osteochondritis dissecans of the knee treated with transarticular arthroscopic drilling. *Am J Sports Med,* 29**,** 562-6.

KOESTENBAUER, S., ZECH, N. H., JUCH, H., VANDERZWALMEN, P., SCHOONJANS, L. & DOHR, G. 2006. Embryonic stem cells: similarities and differences between human and murine embryonic stem cells. *Am J Reprod Immunol,* 55**,** 169-80.

KON, T., CHO, T. J., AIZAWA, T., YAMAZAKI, M., NOOH, N., GRAVES, D., GERSTENFELD, L. C. & EINHORN, T. A. 2001. Expression of osteoprotegerin, receptor activator of NF-kappaB ligand (osteoprotegerin ligand) and related proinflammatory cytokines during fracture healing. *J Bone Miner Res,* 16**,** 1004-14.

KOUZELIS, A., PLESSAS, S., PAPADOPOULOS, A. X., GLIATIS, I. & LAMBIRIS, E. 2006. Herbert screw fixation and reverse guided drillings, for treatment of types III and IV osteochondritis dissecans. *Knee Surg Sports Traumatol Arthrosc,* 14**,** 70-5.

KRAEMER, H. C. 1979. Ramifications of a population model for κ as a coefficient of reliability. . *Psychometrika,* 44**,** 461-472.

KRAMPERA, M., GALIPEAU, J., SHI, Y., TARTE, K. & SENSEBE, L. 2013. Immunological characterization of multipotent mesenchymal stromal cells-The International Society for Cellular Therapy (ISCT) working proposal. *Cytotherapy,* 15**,** 1054-61.

KUBOTA, K., SAKIKAWA, C., KATSUMATA, M., NAKAMURA, T. & WAKABAYASHI, K. 2002. Platelet-derived growth factor BB secreted from osteoclasts acts as an osteoblastogenesis inhibitory factor. *J Bone Miner Res,* 17**,** 257-65.

KWON, T. G., ZHAO, X., YANG, Q., LI, Y., GE, C., ZHAO, G. & FRANCESCHI, R. T. 2011. Physical and functional interactions between Runx2 and HIF-1alpha induce vascular endothelial growth factor gene expression. *J Cell Biochem,* 112**,** 3582-93.

LA ROCCA, G., ANZALONE, R., CORRAO, S., MAGNO, F., LORIA, T., LO IACONO, M., DI STEFANO, A., GIANNUZZI, P., MARASA, L., CAPPELLO, F., ZUMMO, G. & FARINA, F. 2009. Isolation and characterization of Oct-4+/HLA-G+ mesenchymal stem cells from human umbilical cord matrix: differentiation potential and detection of new markers. *Histochem Cell Biol,* 131**,** 267-82.

LAFONT, J. E., TALMA, S. & MURPHY, C. L. 2007. Hypoxia-inducible factor 2alpha is essential for hypoxic induction of the human articular chondrocyte phenotype. *Arthritis Rheum,* 56**,** 3297-306.

LAPRADE, R. F., ORO, F. B., ZIEGLER, C. G., WIJDICKS, C. A. & WALSH, M. P. 2010. Patellar height and tibial slope after opening-wedge proximal tibial osteotomy: a prospective study. *Am J Sports Med,* 38**,** 160-70.

LAPRELL, H. & PETERSEN, W. 2001. Autologous osteochondral transplantation using the diamond bone-cutting system (DBCS): 6-12 years' follow-up of 35 patients with osteochondral defects at the knee joint. *Arch Orthop Trauma Surg,* 121**,** 248-53.

LEE, M. H., KIM, Y. J., KIM, H. J., PARK, H. D., KANG, A. R., KYUNG, H. M., SUNG, J. H., WOZNEY, J. M. & RYOO, H. M. 2003. BMP-2-induced Runx2 expression is mediated by Dlx5, and TGF-beta 1 opposes the BMP-2-induced osteoblast differentiation by suppression of Dlx5 expression. *J Biol Chem,* 278**,** 34387-94.

LEMAOULT, J., ROUAS-FREISS, N. & CAROSELLA, E. D. 2005. Immuno-tolerogenic functions of HLA-G: relevance in transplantation and oncology. *Autoimmun Rev,* 4**,** 503-9.

LEUNG, V. Y., GAO, B., LEUNG, K. K., MELHADO, I. G., WYNN, S. L., AU, T. Y., DUNG, N. W., LAU, J. Y., MAK, A. C., CHAN, D. & CHEAH, K. S. 2011. SOX9 governs differentiation stage-specific gene expression in growth plate chondrocytes via direct concomitant transactivation and repression. *PLoS Genet,* 7**,** e1002356.

LI, D. R. & CAI, J. H. 2012. Methods of isolation, expansion, differentiating induction and preservation of human umbilical cord mesenchymal stem cells. *Chin Med J (Engl),* 125**,** 4504-10.

LIDDLE, A. D., JUDGE, A., PANDIT, H. & MURRAY, D. W. 2014. Determinants of revision and functional outcome following unicompartmental knee replacement. *Osteoarthritis Cartilage,* 22**,** 1241-50.

LIPSITCH, M., TCHETGEN TCHETGEN, E. & COHEN, T. 2010. Negative controls: a tool for detecting confounding and bias in observational studies. *Epidemiology,* 21**,** 383-8.

LOH, Y. H., WU, Q., CHEW, J. L., VEGA, V. B., ZHANG, W., CHEN, X., BOURQUE, G., GEORGE, J., LEONG, B., LIU, J., WONG, K. Y., SUNG, K. W., LEE, C. W., ZHAO, X. D., CHIU, K. P., LIPOVICH, L., KUZNETSOV, V. A., ROBSON, P., STANTON, L. W., WEI, C. L., RUAN, Y., LIM, B. & NG, H. H. 2006. The Oct4 and Nanog transcription network regulates pluripotency in mouse embryonic stem cells. *Nat Genet,* 38**,** 431-40.

LOSINA, E., THORNHILL, T. S., ROME, B. N., WRIGHT, J. & KATZ, J. N. 2012. The dramatic increase in total knee replacement utilization rates in the United States cannot be fully explained by growth in population size and the obesity epidemic. *J Bone Joint Surg Am,* 94**,** 201-7.

MACDOUGALD, O. A. & LANE, M. D. 1995. Transcriptional regulation of gene expression during adipocyte differentiation. *Annu Rev Biochem,* 64**,** 345-73.

MACHIN, D., DAY, S. & GREEN, S. B. E. (eds.) 2004. *Textbook of clinical trials,* Chichester: Wiley

MAINIL-VARLET, P., VAN DAMME, B., NESIC, D., KNUTSEN, G., KANDEL, R. & ROBERTS, S. 2010. A new histology scoring system for the assessment of the quality of human cartilage repair: ICRS II. *Am J Sports Med,* 38**,** 880-90.

MAJORE, I., MORETTI, P., HASS, R. & KASPER, C. 2009. Identification of subpopulations in mesenchymal stem cell-like cultures from human umbilical cord. *Cell Commun Signal,* 7**,** 6.

MAJORE, I., MORETTI, P., STAHL, F., HASS, R. & KASPER, C. 2011. Growth and differentiation properties of mesenchymal stromal cell populations derived from whole human umbilical cord. *Stem Cell Rev,* 7**,** 17-31.

MAKINO, A., MUSCOLO, D. L., PUIGDEVALL, M., COSTA-PAZ, M. & AYERZA, M. 2005. Arthroscopic fixation of osteochondritis dissecans of the knee: clinical, magnetic resonance imaging, and arthroscopic follow-up. *Am J Sports Med,* 33**,** 1499-504.

MANDUCA, P., PALERMO, C., CARUSO, C., BRIZZOLARA, A., SANGUINETI, C., FILANTI, C. & ZICCA, A. 1997. Rat tibial osteoblasts III: propagation in vitro is accompanied by enhancement of osteoblast phenotype. *Bone,* 21**,** 31-9.

MANKANI, M. H., KUZNETSOV, S. A., WOLFE, R. M., MARSHALL, G. W. & ROBEY, P. G. 2006. In vivo bone formation by human bone marrow stromal cells: reconstruction of the mouse calvarium and mandible. *Stem Cells,* 24**,** 2140-9.

MANSUKHANI, A., BELLOSTA, P., SAHNI, M. & BASILICO, C. 2000. Signaling by fibroblast growth factors (FGF) and fibroblast growth factor receptor 2 (FGFR2)-activating mutations blocks mineralization and induces apoptosis in osteoblasts. *J Cell Biol,* 149**,** 1297-308.

MARCACCI, M., KON, E., MOUKHACHEV, V., LAVROUKOV, A., KUTEPOV, S., QUARTO, R., MASTROGIACOMO, M. & CANCEDDA, R. 2007. Stem cells associated with macroporous bioceramics for long bone repair: 6- to 7-year outcome of a pilot clinical study. *Tissue Eng,* 13**,** 947-55.

MARIE, P. J. 2003. Fibroblast growth factor signaling controlling osteoblast differentiation. *Gene,* 316**,** 23-32.

MARLOVITS, S., SINGER, P., ZELLER, P., MANDL, I., HALLER, J. & TRATTNIG, S. 2006. Magnetic resonance observation of cartilage repair tissue (MOCART) for the evaluation of autologous chondrocyte transplantation: determination of interobserver variability and correlation to clinical outcome after 2 years. *Eur J Radiol,* 57**,** 16-23.

MARLOVITS, S., STRIESSNIG, G., RESINGER, C. T., ALDRIAN, S. M., VECSEI, V., IMHOF, H. & TRATTNIG, S. 2004. Definition of pertinent parameters for the evaluation of articular cartilage repair tissue with high-resolution magnetic resonance imaging. *Eur J Radiol,* 52**,** 310-9.

MARMOTTI, A., MATTIA, S., BRUZZONE, M., BUTTIGLIERI, S., RISSO, A., BONASIA, D. E., BLONNA, D., CASTOLDI, F., ROSSI, R., ZANINI, C., ERCOLE, E., DEFABIANI, E., TARELLA, C. & PERETTI, G. M. 2012. Minced umbilical cord fragments as a source of cells for orthopaedic tissue engineering: an in vitro study. *Stem Cells Int,* 2012**,** e326813.

MARSELL, R. & EINHORN, T. A. 2011. The biology of fracture healing. *Injury,* 42**,** 551-5.

MATHIEU, M., RIGUTTO, S., INGELS, A., SPRUYT, D., STRICWANT, N., KHARROUBI, I., ALBARANI, V., JAYANKURA, M., RASSCHAERT, J., BASTIANELLI, E. & GANGJI, V. 2013. Decreased pool of mesenchymal stem cells is associated with altered chemokines serum levels in atrophic nonunion fractures. *Bone,* 53**,** 391-8.

MATSUNAGA, D., AKIZUKI, S., TAKIZAWA, T., YAMAZAKI, I. & KURAISHI, J. 2007. Repair of articular cartilage and clinical outcome after osteotomy with microfracture or abrasion arthroplasty for medial gonarthrosis. *Knee,* 14**,** 465-71.

MAUS, U., SCHNEIDER, U., GRAVIUS, S., MULLER-RATH, R., MUMME, T., MILTNER, O., BAUER, D., NIEDHART, C. & ANDEREYA, S. 2008. Clinical results after three years use of matrix-associated ACT for the treatment of osteochondral defects of the knee. *Z Orthop Unfall,* 146**,** 31-7.

MCCARTHY, H. S. & ROBERTS, S. 2013. A histological comparison of the repair tissue formed when using either Chondrogide((R)) or periosteum during autologous chondrocyte implantation. *Osteoarthritis Cartilage,* 21**,** 2048-57.

MCELREAVEY, K. D., IRVINE, A. I., ENNIS, K. T. & MCLEAN, W. H. 1991. Isolation, culture and characterisation of fibroblast-like cells derived from the Wharton's jelly portion of human umbilical cord. *Biochem Soc Trans,* 19**,** 29S.

MEGAS, P. 2005. Classification of non-union. *Injury,* 36 Suppl 4**,** S30-7.

MEIJER, G., DE BRUIJN, J., KOOLE, R. & VAN BLITTERSWIJK, C. 2007. (2007) Cell-Based Bone Tissue Engineering. . *PLoS Med,* 4**,** e9.

MENNAN, C., WRIGHT, K., BHATTACHARJEE, A., BALAIN, B., RICHARDSON, J. & ROBERTS, S. 2013. Isolation and characterisation of mesenchymal stem cells from different regions of the human umbilical cord. *Biomed Res Int,* 2013**,** e916136.

MILLS, L. A. & SIMPSON, A. H. R. W. 2013. The relative incidence of fracture non-union in the Scottish population (5.17 million): a 5-year epidemiologicalstudy. *BMJ Open***,** e002276

MINAS, T., GOMOLL, A. H., SOLHPOUR, S., ROSENBERGER, R., PROBST, C. & BRYANT, T. 2010. Autologous chondrocyte implantation for joint preservation in patients with early osteoarthritis. *Clin Orthop Relat Res,* 468**,** 147-57.

MINAS, T. & PETERSON, L. 1999. Advanced techniques in autologous chondrocyte transplantation. *Clin Sports Med,* 18**,** 13-44, v-vi.

MINAS, T., VON KEUDELL, A., BRYANT, T. & GOMOLL, A. H. 2014. The John Insall Award: A minimum 10-year outcome study of autologous chondrocyte implantation. *Clin Orthop Relat Res,* 472**,** 41-51.

MONTERO, A., OKAD, Y., TOMITA, M., ITO M, TSURUKAMI H, NAKAMURA T, DOETSCHMAN T, COFFIN JD & MM., H. 2000. Disruption of the fibroblast growth factor-2 gene results in decreased bone mass and bone formation. *The Journal of Clinical Investigation,* 105**,** 1085-1093.

MOUNTZIARIS, P. M. & MIKOS, A. G. 2008. Modulation of the inflammatory response for enhanced bone tissue regeneration. *Tissue Eng Part B Rev,* 14**,** 179-86.

MURTAUGH, L. C., CHYUNG, J. H. & LASSAR, A. B. 1999. Sonic hedgehog promotes somitic chondrogenesis by altering the cellular response to BMP signaling. *Genes Dev,* 13**,** 225-37.

NAGAI, T., SATO, M., KUTSUNA, T., KOKUBO, M., EBIHARA, G., OHTA, N. & MOCHIDA, J. 2010. Intravenous administration of anti-vascular endothelial growth factor humanized monoclonal antibody bevacizumab improves articular cartilage repair. *Arthritis Res Ther,* 12**,** R178.

NAGELKERKE, N. 1991. A Note on a General Definition of the Coefficient of Determination. *Biometrika,* 78**,** 691-92.

NG, F., BOUCHER, S., KOH, S., SASTRY, K. S., CHASE, L., LAKSHMIPATHY, U., CHOONG, C., YANG, Z., VEMURI, M. C., RAO, M. S. & TANAVDE, V. 2008. PDGF, TGF-beta, and FGF signaling is important for differentiation and growth of mesenchymal stem cells (MSCs): transcriptional profiling can identify markers and signaling pathways important in differentiation of MSCs into adipogenic, chondrogenic, and osteogenic lineages. *Blood,* 112**,** 295-307.

NIEHOF, M., MANNS, M. P. & TRAUTWEIN, C. 1997. CREB controls LAP/C/EBP beta transcription. *Mol Cell Biol,* 17**,** 3600-13.

NIINIMÄKI, T. T., ESKELINEN, A., MANN, B. S., JUNNILA, M., OHTONEN, P. & LEPPILAHTI, J. 2012. Survivorship of high tibial osteotomy in the treatment of osteoarthritis of the knee-Finnish Registry based study of 3195 knees. *Journal of Bone Joint Surg Br,* 94-B**,** 1517-21.

NIWA, H., MIYAZAKI, J. & SMITH, A. G. 2000. Quantitative expression of Oct-3/4 defines differentiation, dedifferentiation or self-renewal of ES cells. *Nat Genet,* 24**,** 372-6.

NJR 2014. National Joint Registry for England, Wales and Northern Ireland. *11th Annual Report*

OCHS, B. G., MULLER-HORVAT, C., ALBRECHT, D., SCHEWE, B., WEISE, K., AICHER, W. K. & ROLAUFFS, B. 2011. Remodeling of articular cartilage and subchondral bone after bone grafting and matrix-associated autologous chondrocyte implantation for osteochondritis dissecans of the knee. *Am J Sports Med,* 39**,** 764-73.

PANEPUCCI, R. A., SIUFI, J. L., SILVA, W. A., JR., PROTO-SIQUIERA, R., NEDER, L., ORELLANA, M., ROCHA, V., COVAS, D. T. & ZAGO, M. A. 2004. Comparison of gene expression of umbilical cord vein and bone marrow-derived mesenchymal stem cells. *Stem Cells,* 22**,** 1263-78.

PENG, H., WRIGHT, V., USAS, A., GEARHART, B., SHEN, H. C., CUMMINS, J. & HUARD, J. 2002. Synergistic enhancement of bone formation and healing by stem cell-expressed VEGF and bone morphogenetic protein-4. *J Clin Invest,* 110**,** 751-9.

PEREIRA, W. C., KHUSHNOOMA, I., MADKAIKAR, M. & GHOSH, K. 2008. Reproducible methodology for the isolation of mesenchymal stem cells from human umbilical cord and its potential for cardiomyocyte generation. *J Tissue Eng Regen Med,* 2**,** 394-9.

PETERSON, L., MINAS, T., BRITTBERG, M. & LINDAHL, A. 2003. Treatment of osteochondritis dissecans of the knee with autologous chondrocyte transplantation: results at two to ten years. *J Bone Joint Surg Am,* 85-A Suppl 2**,** 17-24.

PITTENGER, M., MACKAY, A., BECK, S., JAISWAL, R. K., DOUGLAS, R. & MOSCA, J. D. 1999. Multilinege potential of human mesenchymal cells. *Science,* 284**,** 143-47.

PIZETTE, S. & NISWANDER, L. 2000. BMPs are required at two steps of limb chondrogenesis: formation of prechondrogenic condensations and their differentiation into chondrocytes. *Dev Biol,* 219**,** 237-49.

PNEUMATICOS SG, PANTELI, M., T, RIANTAFYLLOPOULOS GK, PAPAKOSTIDIS C & PV., G. 2013. Management and outcome of diaphyseal aseptic non-unions of the lower limb: A systematic review. *Surgeon,* 12**,** 166-75.

PRASANNA, S. J., GOPALAKRISHNAN, D., SHANKAR, S. R. & VASANDAN, A. B. 2010. Pro-inflammatory cytokines, IFNgamma and TNFalpha, influence immune properties of human bone marrow and Wharton jelly mesenchymal stem cells differentially. *PLoS One,* 5**,** e9016.

QIAO, C., XU, W., ZHU, W., HU, J., QIAN, H., YIN, Q., JIANG, R., YAN, Y., MAO, F., YANG, H., WANG, X. & CHEN, Y. 2008. Human mesenchymal stem cells isolated from the umbilical cord. *Cell Biol Int,* 32**,** 8-15.

QUARTO, R., MASTROGIACOMO, M., CANCEDDA, R., KUTEPOV, S., MUKHACHEV, V., LAVROUKOV, A., KON, E. & MARCACCI, M. 2001. Repair of large bone defects with the use of autologous bone marrow stromal cells. *New England Journal of Medicine,* 344**,** 385-386.

REED, A. A., JOYNER, C. J., BROWNLOW, H. C. & SIMPSON, A. H. 2002. Human atrophic fracture non-unions are not avascular. *J Orthop Res,* 20**,** 593-9.

REED, A. A., JOYNER, C. J., ISEFUKU, S., BROWNLOW, H. C. & SIMPSON, A. H. 2003. Vascularity in a new model of atrophic nonunion. *J Bone Joint Surg Br,* 85**,** 604-10.

REZA, H., NG, B., PHAN, T., TAN, D., BEUERMAN, R. & ANG, L. 2011. Characterization of a novel umbilical cord lining cell with CD227 positivity and unique pattern of P63 expression and function. *Stem Cell Rev,* 7**,** 624-638.

RICHARDS, D. P., ALAN BARBER, F. & TROOP, R. L. 2003. Iliotibial band Z-lengthening. *Arthroscopy,* 19**,** 326-9.

RIZZINO, A. 2013. Concise review: The Sox2-Oct4 connection: critical players in a much larger interdependent network integrated at multiple levels. *Stem Cells,* 31**,** 1033-9.

ROBERTS, S., MCCALL, I. W., DARBY, A. J., MENAGE, J., EVANS, H., HARRISON, P. E. & RICHARDSON, J. B. 2003. Autologous chondrocyte implantation for cartilage repair:monitoring its success by magnetic resonance imaging and histology. *Arthritis Research & Therapy,* 5**,** R60.

ROBERTS, S. & MENAGE, J. 2004. Microscopic methods for the analysis of engineered tissues. *Methods Mol Biol,* 238**,** 171-96.

ROBERTS, S., MENAGE, J., SANDELL, L. J., EVANS, E. H. & RICHARDSON, J. B. 2009. Immunohistochemical study of collagen types I and II and procollagen IIA in human cartilage repair tissue following autologous chondrocyte implantation. *Knee,* 16**,** 398-404.

ROMANOV, Y. A., SVINTSITSKAYA, V. A. & SMIRNOV, V. N. 2003. Searching for alternative sources of postnatal human mesenchymal stem cells: candidate MSC-like cells from umbilical cord. *Stem Cells,* 21**,** 105-10.

ROSS, S. E., HEMATI, N., LONGO, K. A., BENNETT, C. N., LUCAS, P. C., ERICKSON, R. L. & MACDOUGALD, O. A. 2000. Inhibition of adipogenesis by Wnt signaling. *Science,* 289**,** 950-3.

SAITHNA, A., KUNDRA, R., GETGOOD, A. & SPALDING, T. 2014. Opening wedge distal femoral varus osteotomy for lateral compartment osteoarthritis in the valgus knee. *Knee,* 21**,** 172-5.

SALEHINEJAD, P., ALITHEEN, N. B., ALI, A. M., OMAR, A. R., MOHIT, M., JANZAMIN, E., SAMANI, F. S., TORSHIZI, Z. & NEMATOLLAHI-MAHANI, S. N. 2012. Comparison of different methods for the isolation of mesenchymal stem cells from human umbilical cord Wharton's jelly. *In Vitro Cell Dev Biol Anim,* 48**,** 75-83.

SARIS, D., PRICE, A., WIDUCHOWSKI, W., BERTRAND-MARCHAND, M., CARON, J., DROGSET, J. O., EMANS, P., PODSKUBKA, A., TSUCHIDA, A., KILI, S., LEVINE, D. & BRITTBERG, M. 2014. Matrix-Applied Characterized Autologous Cultured Chondrocytes Versus Microfracture: Two-Year Follow-up of a Prospective Randomized Trial. *Am J Sports Med,* 42**,** 1384-94.

SARIS, D. B., VANLAUWE, J., VICTOR, J., ALMQVIST, K. F., VERDONK, R., BELLEMANS, J. & LUYTEN, F. P. 2009. Treatment of symptomatic cartilage defects of the knee: characterized chondrocyte implantation results in better clinical outcome at 36 months in a randomized trial compared to microfracture. *Am J Sports Med,* 37 Suppl 1**,** 10S-19S.

SARIS, D. B., VANLAUWE, J., VICTOR, J., HASPL, M., BOHNSACK, M., FORTEMS, Y., VANDEKERCKHOVE, B., ALMQVIST, K. F., CLAES, T., HANDELBERG, F., LAGAE, K., VAN DER BAUWHEDE, J., VANDENNEUCKER, H., YANG, K. G., JELIC, M., VERDONK, R., VEULEMANS, N., BELLEMANS, J. & LUYTEN, F. P. 2008. Characterized chondrocyte implantation results in better structural repair when treating symptomatic cartilage defects of the knee in a randomized controlled trial versus microfracture. *Am J Sports Med,* 36**,** 235-46.

SARUGASER, R., LICKORISH, D., BAKSH, D., HOSSEINI, M. M. & DAVIES, J. E. 2005. Human umbilical cord perivascular (HUCPV) cells: a source of mesenchymal progenitors. *Stem Cells,* 23**,** 220-9.

SCHEDLICH, L. J., FLANAGAN, J. L., CROFTS, L. A., GILLIES, S. A., GOLDBERG, D., MORRISON, N. A. & EISMAN, J. A. 1994. Transcriptional activation of the human osteocalcin gene by basic fibroblast growth factor. *J Bone Miner Res,* 9**,** 143-52.

SCHOPPERLE, W. M. & DEWOLF, W. C. 2007. The TRA-1-60 and TRA-1-81 human pluripotent stem cell markers are expressed on podocalyxin in embryonal carcinoma. *Stem Cells,* 25**,** 723-30.

SECCO, M., ZUCCONI, E., VIEIRA, N. M., FOGACA, L. L., CERQUEIRA, A., CARVALHO, M. D., JAZEDJE, T., OKAMOTO, O. K., MUOTRI, A. R. & ZATZ, M. 2008. Multipotent stem cells from umbilical cord: cord is richer than blood! *Stem Cells,* 26**,** 146-50.

SEEBACH, C., HENRICH, D., TEWKSBURY, R., WILHELM, K. & MARZI, I. 2007. Number and proliferative capacity of human mesenchymal stem cells are modulated positively in multiple trauma patients and negatively in atrophic nonunions. *Calcif Tissue Int,* 80**,** 294-300.

SESHAREDDY, K., TROYER, D. & WEISS, M. L. 2008. Method to isolate mesenchymal-like cells from Wharton's Jelly of umbilical cord. *Methods Cell Biol,* 86**,** 101-19.

SHARMA, L., ECKSTEIN, F., SONG, J., GUERMAZI, A., PRASAD, P., KAPOOR, D., CAHUE, S., MARSHALL, M., HUDELMAIER, M. & DUNLOP, D. 2008. Relationship of meniscal damage, meniscal extrusion, malalignment, and joint laxity to subsequent cartilage loss in osteoarthritic knees. *Arthritis Rheum,* 58**,** 1716-26.

SILVA, J., NICHOLS, J., THEUNISSEN, T. W., GUO, G., VAN OOSTEN, A. L., BARRANDON, O., WRAY, J., YAMANAKA, S., CHAMBERS, I. & SMITH, A. 2009. Nanog is the gateway to the pluripotent ground state. *Cell,* 138**,** 722-37.

SMITH, G. D., TAYLOR, J., ALMQVIST, K. F., ERGGELET, C., KNUTSEN, G., GARCIA PORTABELLA, M., SMITH, T. & RICHARDSON, J. B. 2005. Arthroscopic assessment of cartilage repair: a validation study of 2 scoring systems. *Arthroscopy,* 21**,** 1462-7.

SMITH, H. J., RICHARDSON, J. B. & TENNANT, A. 2009. Modification and validation of the Lysholm Knee Scale to assess articular cartilage damage. *Osteoarthritis Cartilage,* 17**,** 53-8.

SON, M. Y., CHOI, H., HAN, Y. M. & CHO, Y. S. 2013. Unveiling the critical role of REX1 in the regulation of human stem cell pluripotency. *Stem Cells,* 31**,** 2374-87.

SPEERIN, R., SLATER, H., LI, L., MOORE, K., CHAN, M., DREINHOFER, K., EBELING, P. R., WILLCOCK, S. & BRIGGS, A. M. 2014. Moving from evidence to practice: Models of care for the prevention and management of musculoskeletal conditions. *Best Pract Res Clin Rheumatol,* 28**,** 479-515.

SPIERINGS, E. L., FIDELHOLTZ, J., WOLFRAM, G., SMITH, M. D., BROWN, M. T. & WEST, C. R. 2013. A phase III placebo- and oxycodone-controlled study of tanezumab in adults with osteoarthritis pain of the hip or knee. *Pain,* 154**,** 1603-12.

SPINELLA-JAEGLE, S., RAWADI, G., KAWAI, S., GALLEA, S., FAUCHEU, C., MOLLAT, P., COURTOIS, B., BERGAUD, B., RAMEZ, V., BLANCHET, A. M., ADELMANT, G., BARON, R. & ROMAN-ROMAN, S. 2001a. Sonic hedgehog increases the commitment of pluripotent mesenchymal cells into the osteoblastic lineage and abolishes adipocytic differentiation. *J Cell Sci,* 114**,** 2085-94.

SPINELLA-JAEGLE, S., ROMAN-ROMAN, S., FAUCHEU, C., DUNN, F. W., KAWAI, S., GALLEA, S., STIOT, V., BLANCHET, A. M., COURTOIS, B., BARON, R. & RAWADI, G. 2001b. Opposite effects of bone morphogenetic protein-2 and transforming growth factor-beta1 on osteoblast differentiation. *Bone,* 29**,** 323-30.

STANDRING, S. 2005. Gray's anatomy : the anatomical basis of clinical practice *In:* STANDRING, S. (ed.) *Anatomy : the anatomical basis of clinical practice.* 39 ed. New York Elsevier Limited.

STEADMAN, J. R., BRIGGS, K. K., RODRIGO, J. J., KOCHER, M. S., GILL, T. J. & RODKEY, W. G. 2003. Outcomes of microfracture for traumatic chondral defects of the knee: average 11-year follow-up. *Arthroscopy,* 19**,** 477-84.

STEINHAGEN, J., BRUNS, J., DEURETZBACHER, G., RUETHER, W., FUERST, M. & NIGGEMEYER, O. 2010. Treatment of osteochondritis dissecans of the femoral condyle with autologous bone grafts and matrix-supported autologous chondrocytes. *Int Orthop,* 34**,** 819-25.

STERETT, W. I., STEADMAN, J. R., HUANG, M. J., MATHENY, L. M. & BRIGGS, K. K. 2010. Chondral resurfacing and high tibial osteotomy in the varus knee: survivorship analysis. *Am J Sports Med,* 38**,** 1420-4.

STEVENS, M. M., MARINI, R. P., MARTIN, I., LANGER, R. & PRASAD SHASTRI, V. 2004. FGF-2 enhances TGF-beta1-induced periosteal chondrogenesis. *J Orthop Res,* 22**,** 1114-9.

STUDENT, A. K., HSU, R. Y. & LANE, M. D. 1980. Induction of fatty acid synthetase synthesis in differentiating 3T3-L1 preadipocytes. *J Biol Chem,* 255**,** 4745-50.

SUBRAMANIAN, A., FONG, C. Y., BISWAS, A. & BONGSO, A. 2015. Comparative Characterization of Cells from the Various Compartments of the Human Umbilical Cord Shows that the Wharton's Jelly Compartment Provides the Best Source of Clinically Utilizable Mesenchymal Stem Cells. *PLoS One,* 10**,** e0127992.

SURI, S. & WALSH, D. A. 2012. Osteochondral alterations in osteoarthritis. *Bone,* 51**,** 204-11.

TAGHIZADEH, R. R., CETRULO, K. J. & CETRULO, C. L. 2011. Wharton's Jelly stem cells: future clinical applications. *Placenta,* 32 Suppl 4**,** S311-5.

TALKHANI, I. & RICHARDSON, J. 1999. Knee diagram for the documentation of arthroscopic findings of the knee - cadaveric study. *The Knee* 6**,** 95-101.

TANG, Q. Q., GRONBORG, M., HUANG, H., KIM, J. W., OTTO, T. C., PANDEY, A. & LANE, M. D. 2005. Sequential phosphorylation of CCAAT enhancer-binding protein beta by MAPK and glycogen synthase kinase 3beta is required for adipogenesis. *Proc Natl Acad Sci U S A,* 102**,** 9766-71.

TANG, Q. Q. & LANE, M. D. 2012. Adipogenesis: from stem cell to adipocyte. *Annu Rev Biochem,* 81**,** 715-36.

TANG, Q. Q., OTTO, T. C. & LANE, M. D. 2003. Mitotic clonal expansion: a synchronous process required for adipogenesis. *Proc Natl Acad Sci U S A,* 100**,** 44-9.

TAWONSAWATRUK T, KELLY MB & H, S. 2013. Evaluation of Native Mesenchymal Stem Cells from Bone Marrow and Local Tissue in an Atrophic Non-union Model. *Tissue Engineering Part-C Methods,* 20

524-32.

TECIC, T., LEFERING, R., ALTHAUS, A., RANGGER, C. & NEUGEBAUER, E. 2013. Pain and quality of life 1 year after admission to the emergency department: factors associated with pain. *Eur J Trauma Emerg Surg,* 39**,** 353-61.

THOMAS, D. M., CARTY, S. A., PISCOPO, D. M., LEE, J. S., WANG, W. F., FORRESTER, W. C. & HINDS, P. W. 2001. The retinoblastoma protein acts as a transcriptional coactivator required for osteogenic differentiation. *Mol Cell,* 8**,** 303-16.

TOLAR, J., LE BLANC, K., KEATING, A. & BLAZAR, B. R. 2010. Concise review: hitting the right spot with mesenchymal stromal cells. *Stem Cells,* 28**,** 1446-55.

TONG, C. K., VELLASAMY, S., TAN, B. C., ABDULLAH, M., VIDYADARAN, S., SEOW, H. F. & RAMASAMY, R. 2011. Generation of mesenchymal stem cell from human umbilical cord tissue using a combination enzymatic and mechanical disassociation method. *Cell Biol Int,* 35**,** 221-6.

TSAGIAS, N., KOLIAKOS, I., KARAGIANNIS, V., ELEFTHERIADOU, M. & KOLIAKOS, G. G. 2011. Isolation of mesenchymal stem cells using the total length of umbilical cord for transplantation purposes. *Transfus Med,* 21**,** 253-61.

TUFAN, A. C., DAUMER, K. M., DELISE, A. M. & TUAN, R. S. 2002. AP-1 transcription factor complex is a target of signals from both WnT-7a and N-cadherin-dependent cell-cell adhesion complex during the regulation of limb mesenchymal chondrogenesis. *Exp Cell Res,* 273**,** 197-203.

TUFAN, A. C. & TUAN, R. S. 2001. Wnt regulation of limb mesenchymal chondrogenesis is accompanied by altered N-cadherin-related functions. *FASEB J,* 15**,** 1436-8.

TULI, R., TULI, S., NANDI, S., HUANG, X., MANNER, P. A., HOZACK, W. J., DANIELSON, K. G., HALL, D. J. & TUAN, R. S. 2003. Transforming growth factor-beta-mediated chondrogenesis of human mesenchymal progenitor cells involves N-cadherin and mitogen-activated protein kinase and Wnt signaling cross-talk. *J Biol Chem,* 278**,** 41227-36.

UNDALE, A., FRASER, D., HEFFERAN, T., KOPHER, R. A., HERRICK, J., EVANS, G. L., LI, X., KAKAR, S., HAYES, M., ATKINSON, E., YASZEMSKI, M. J., KAUFMAN, D. S., WESTENDORF, J. J. & KHOSLA, S. 2011. Induction of fracture repair by mesenchymal cells derived from human embryonic stem cells or bone marrow. *J Orthop Res,* 29**,** 1804-11.

USFDA 1998. Guidance Document for Industry and CDRH Staff for the Preparation of Investigational Device Exemptions and Premarket Approval Applications for Bone Growth Stimulator Devices. *In:* DIVISION OF GENERAL AND RESTORATIVE DEVICES (ed.). Bone Growth Stimulator Devices (http://www.fda.gov/cdrh/ode/bgsguide.html): Food and Drug Administration, US Department of Health and Human Services

VANLAUWE, J., SARIS, D. B., VICTOR, J., ALMQVIST, K. F., BELLEMANS, J. & LUYTEN, F. P. 2011. Five-year outcome of characterized chondrocyte implantation versus microfracture for symptomatic cartilage defects of the knee: early treatment matters. *Am J Sports Med,* 39**,** 2566-74.

VELLET, A. D., MARKS, P. H., FOWLER, P. J. & MUNRO, T. G. 1991. Occult posttraumatic osteochondral lesions of the knee: prevalence, classification, and short-term sequelae evaluated with MR imaging. *Radiology,* 178**,** 271-6.

VIATEAU V & MANASSERO, M., SENSÉBÉ L, LANGONNÉ A, MARCHAT D, LOGEART-AVRAMOGLOU D, PETITE H, BENSIDHOUM M 2013(in press). Comparative study of the osteogenic ability of four different ceramic constructs in an ectopic large animal model. *J Tissue Eng Regen Med*.

VIJAYAN, S., BARTLETT, W., BENTLEY, G., CARRINGTON, R. W., SKINNER, J. A., POLLOCK, R. C., ALORJANI, M. & BRIGGS, T. W. 2012. Autologous chondrocyte implantation for osteochondral lesions in the knee using a bilayer collagen membrane and bone graft: a two- to eight-year follow-up study. *J Bone Joint Surg Br,* 94**,** 488-92.

WAN, C., GILBERT, S. R., WANG, Y., CAO, X., SHEN, X., RAMASWAMY, G., JACOBSEN, K. A., ALAQL, Z. S., EBERHARDT, A. W., GERSTENFELD, L. C., EINHORN, T. A., DENG, L. & CLEMENS, T. L. 2008. Activation of the hypoxia-inducible factor-1alpha pathway accelerates bone regeneration. *Proc Natl Acad Sci U S A,* 105**,** 686-91.

WANG, H. S., HUNG, S. C., PENG, S. T., HUANG, C. C., WEI, H. M., GUO, Y. J., FU, Y. S., LAI, M. C. & CHEN, C. C. 2004. Mesenchymal stem cells in the Wharton's jelly of the human umbilical cord. *Stem Cells,* 22**,** 1330-7.

WANG, Y., HAN, Z. B., SONG, Y. P. & HAN, Z. C. 2012. Safety of mesenchymal stem cells for clinical application. *Stem Cells International,* 2012**,** 652034.

WEBER, B. G. & CECH, O. 1976. Pseudoarthrosis, Pathology, Biomechanics, Therapy, Results. Bern: Hans Huber.

WEINSTEIN, A. M., ROME, B. N., REICHMANN, W. M., COLLINS, J. E., BURBINE, S. A., THORNHILL, T. S., WRIGHT, J., KATZ, J. N. & LOSINA, E. 2013. Estimating the burden of total knee replacement in the United States. *J Bone Joint Surg Am,* 95**,** 385-92.

WEISS, M. L., ANDERSON, C., MEDICETTY, S., SESHAREDDY, K. B., WEISS, R. J., VANDERWERFF, I., TROYER, D. & MCINTOSH, K. R. 2008. Immune properties of human umbilical cord Wharton's jelly-derived cells. *Stem Cells,* 26**,** 2865-74.

WELSCH, G. H., MAMISCH, T. C., ZAK, L., BLANKE, M., OLK, A., MARLOVITS, S. & TRATTNIG, S. 2010. Evaluation of cartilage repair tissue after matrix-associated autologous chondrocyte transplantation using a hyaluronic-based or a collagen-based scaffold with morphological MOCART scoring and biochemical T2 mapping: preliminary results. *Am J Sports Med,* 38**,** 934-42.

WHITEHILL, J., RUVOLO, P., WU, T., BERGSMA, J. & MOVELLAN, J. 2009a. Whose Vote Should Count More:Optimal Integration of Labels from Labelers of Unknown Expertise. *Advances in Neural Information Processing Systems 22*.

WHITEHILL, J., RUVOLO, P., WU, T., BERGSMA, J. & MOVELLAN, J. 2009b. Whose Vote Should Count More:Optimal Integration of Labels from Labelers of Unknown Expertise. *Advances in Neural Information Processing Systems* 2035-2043.

WHYNES, D. 2008. *RE: & The TOMBOLA Group.Correspondence between EQ-5D health state classifications and EQ VAS scores.*

WIDUCHOWSKI, W., WIDUCHOWSKI, J. & TRZASKA, T. 2007. Articular cartilage defects: study of 25,124 knee arthroscopies. *Knee,* 14**,** 177-82.

WILLIAMS, R., KHAN, I. M., RICHARDSON, K., NELSON, L., MCCARTHY, H. E., ANALBELSI, T., SINGHRAO, S. K., DOWTHWAITE, G. P., JONES, R. E., BAIRD, D. M., LEWIS, H., ROBERTS, S., SHAW, H. M., DUDHIA, J., FAIRCLOUGH, J., BRIGGS, T. & ARCHER, C. W. 2010. Identification and clonal characterisation of a progenitor cell sub-population in normal human articular cartilage. *PLoS One,* 5**,** e13246.

WRIGHT, K. T., MASRI, W. E., OSMAN, A., ROBERTS, S., TRIVEDI, J., ASHTON, B. A. & JOHNSON, W. E. 2008. The cell culture expansion of bone marrow stromal cells from humans with spinal cord injury: implications for future cell transplantation therapy. *Spinal Cord,* 46**,** 811-7.

WRIGHT, R. W., MCLEAN, M., MATAVA, M. J. & SHIVELY, R. A. 2004. Osteochondritis dissecans of the knee: long-term results of excision of the fragment. *Clin Orthop Relat Res***,** 239-43.

WU, C. C. & CHEN, W. J. 2000. A revised protocol for more clearly classifying a nonunion. *J Orthop Surg (Hong Kong),* 8**,** 45-52.

WU, K., CHAN, C., TSAI, C., CHANG, Y., SIEBER, M., CHIU, T., HO, M., PENG, C., WU, H. & HUANG, J. 2011. Effective treatment of severe steroid-resistant acute graft-versus-host disease with umbilical cord-derived mesenchymal stem cells. *Transplantation,* 27**,** 1412-16.

WU, K., SHEU, J., WU, H., TSAI, C., SIEBER, M., PENG, C. & CHAO, Y. 2013. Cotransplantation of umbilical cord-derived mesenchymal stem cells promote hematopoietic engraftment in cord blood transplantation: a pilot study. *Transplantation,* 15**,** 773-77.

YOON, B. H., ROMERO, R., PARK, J. S., KIM, M., OH, S. Y., KIM, C. J. & JUN, J. K. 2000. The relationship among inflammatory lesions of the umbilical cord (funisitis), umbilical cord plasma interleukin 6 concentration, amniotic fluid infection, and neonatal sepsis. *Am J Obstet Gynecol,* 183**,** 1124-9.

YOON, J. H., ROH, E. Y., SHIN, S., JUNG, N. H., SONG, E. Y., CHANG, J. Y., KIM, B. J. & JEON, H. W. 2013. Comparison of explant-derived and enzymatic digestion-derived MSCs and the growth factors from Wharton's jelly. *Biomed Res Int,* 2013**,** e428726.

YUAN, X. L., MENG, H. Y., WANG, Y. C., PENG, J., GUO, Q. Y., WANG, A. Y. & LU, S. B. 2014. Bone-cartilage interface crosstalk in osteoarthritis: potential pathways and future therapeutic strategies. *Osteoarthritis Cartilage,* 22**,** 1077-89.

ZECKEY C & MOMMSEN, P., ANDRUSZKOW H, MACKE C, FRINK M, STÜBIG T, HÜFNER T, KRETTEK C, HILDEBRAND F. 2011. The Aseptic Femoral and Tibial Shaft Non-Union in Healthy Patients – An Analysis of the Health-Related Quality of Life and the Socioeconomic Outcome. *The Open Orthopaedics Journal,* 5**,** 193-197.

ZENG, L., KEMPF, H., MURTAUGH, L. C., SATO, M. E. & LASSAR, A. B. 2002. Shh establishes an Nkx3.2/Sox9 autoregulatory loop that is maintained by BMP signals to induce somitic chondrogenesis. *Genes Dev,* 16**,** 1990-2005.

ZHANG, J. W., KLEMM, D. J., VINSON, C. & LANE, M. D. 2004. Role of CREB in transcriptional regulation of CCAAT/enhancer-binding protein beta gene during adipogenesis. *J Biol Chem,* 279**,** 4471-8.

ZHANG, Y. Y., LI, X., QIAN, S. W., GUO, L., HUANG, H. Y., HE, Q., LIU, Y., MA, C. G. & TANG, Q. Q. 2011. Transcriptional activation of histone H4 by C/EBPbeta during the mitotic clonal expansion of 3T3-L1 adipocyte differentiation. *Mol Biol Cell,* 22**,** 2165-74.

ZHAO, W., JI, X., ZHANG, F., LI, L. & MA, L. 2012. Embryonic stem cell markers. *Molecules,* 17**,** 6196-236.

ZHENG, Q., ZHOU, G., MORELLO, R., CHEN, Y., GARCIA-ROJAS, X. & LEE, B. 2003. Type X collagen gene regulation by Runx2 contributes directly to its hypertrophic chondrocyte-specific expression in vivo. *J Cell Biol,* 162**,** 833-42.

ZHOU, G., ZHENG, Q., ENGIN, F., MUNIVEZ, E., CHEN, Y., SEBALD, E., KRAKOW, D. & LEE, B. 2006. Dominance of SOX9 function over RUNX2 during skeletogenesis. *Proc Natl Acad Sci U S A,* 103**,** 19004-9.

ZHOU, J., MENG, J., GUO, S., GAO, B., MA, G., ZHU, X., HU, J., XIAO, Y., LIN, C., WANG, H., DING, L., FENG, G., GUO, X. & HE, L. 2007. IHH and FGF8 coregulate elongation of digit primordia. *Biochem Biophys Res Commun,* 363**,** 513-8.

Appendices

A. Literature search strategy for UC derived cells in orthopaedics

A review of the literature was undertaken using Pubmed, Embase and Ovid Medline in addition to hand searching of bibliographies of relevant articles to identify pertinent literature in this area.

Search strategy: The following search terms were used-*cord lining, Wharton's jelly, umbilical cord artery, umbilical cord vein, umbilical cord stroma, sub-amnion, umbilical cord lining, peri-vascular, stem cell, MSC, umbilical cord, umbilical cord matrix and orthopaedic regeneration*. The search terms were combined with 'AND'/'OR' Boolean operators to refine the results. Studies describing UC-derived stem cells tested for non-orthopaedic regeneration or UC from non-human sources were excluded. Only articles published in the English language were considered for the literature review.

B. Literature search strategy for the potential of BMSC in new bone formation in human fractures and nonunion

A review of medical literature from the electronic databases of Ovid MEDLINE, EMBASE and PubMed, was supplemented by hand searching of bibliographies of relevant articles.

Search strategy: The following search terms were used-*nonunion, bone defects, bone marrow stromal cells, bone marrow derived cells, stem cells and MSC*. The search terms were combined with 'AND'/'OR' Boolean operators to refine the results. Studies describing the treatment of human long bone nonunions or bone defects with autologous bone marrow derived cultured cells were included for the purpose of this review. Articles published in the English language only were included for review.

C. Literature search strategy for the use of ACI with concurrent bonegraft for treating osteoartcular defects:

Hand searching of bibliographies supplemented a review of medical literature from the electronic databases of Ovid MEDLINE, EMBASE and PubMed of the relevant articles.

Search strategy: The following search terms were used: *osteochondral defects, osteoarticular defects, Autologous Chondrocyte Implantation, bone graft, Osteochondritis dissecans and knee joint*. The search terms were combined with 'AND'/'OR' Boolean operators to refine the results. All types of ACI (first generation to the third generation) with autologous bone grafts in human knees were included. Studies describing other forms of treatment and treatment of other joints were excluded.

D. Literature search strategy for treating chondral defect with malaligned knee with ACI and osteotomy

Hand-searching of bibliographies supplemented a review of medical literature from the electronic databases of Ovid MEDLINE, EMBASE and PubMed.

Search strategy: The following search terms were used-*Autologous Chondrocyte Implantation, High Tibial Osteotomy (HTO), Femoral osteotomy, Valgus osteotomy, Varus osteotomy and knee*. The search terms were combined with 'AND'/'OR' Boolean operators to refine the results. Studies describing the treatment of cartilage defects of knee joint were only included for the review. A comparative study evaluating the outcome of ACI + osteotomy, ACI in isolation and microfracture with/without realignment were included for the purpose of this review. Only articles published in the English language were considered.